MATERIALS AND CHEMISTRY LABORATORY, INC. STUDIES

THIS PAGE WAS INTENTIONALLY LEFT BLANK

MATERIALS & CHEMISTRY LABORATORY, INC.

"Linking Technology to Solutions"

Estimation of Site-Specific Penetrator Weathering and Corrosion Rate and DU Migration for Jefferson Proving Ground Site

MCLinc Project: EMP002105/SAI002726
SAIC Purchase Order: 23900-BA-SO887/10147178

Prepared for:

Joseph N. Skibinski, Program Manager for SAIC

Compiled by:
William D. Bostick, Ph.D.
Materials and Chemistry Laboratory, Inc. (MCLinc)
400 Heritage Center Boulevard
Oak Ridge, Tennessee 37830-1702
(865) 576-4138 www.MCL-inc.com

July 2013

William Bostick	Date
Robert J. Stevenson	Date
Earl B. Munday	Date

TABLE OF CONTENTS

TABLE OF TABLES

TABLE OF FIGURES

ACRONYMS

Δ	difference
Σ	standard deviation
%	percent
°C	degrees Celsius
AC	Avonsburg/Cobbsfork
AEPI	US Army Environmental Policy Institute
Al	aluminum
APHA	American Public Health Association
ASTM	American Society of Testing and Materials
C	carbon
Ca	calcium
$CaCl_2$	calcium chloride
$CaCO_3$	calcite
calc.	calculated
$Ca(UO_2)_6O_4(OH)_6H2O)_8$	becquerelite
CEC	CATOPM EXCCJAMGE CA[ACOTU
CFR	Code of Federal Regulation
cm	centimeter(s) – unit of area
cm^2	square centimeter(s) – unit of area
cm^3	cubic centimeter(s) – unit of area
CO_2	carbon dioxide
COC	Chain of Custody
CR	Cincinnati/Rossmoyne
d	day(s)
DoD	US Department of Defense
DU	Depleted Uranium (< 0.7 weight percent isotope U-235)
DUP	duplicate
DIW	de-ionized water
EDS	energy-dispersive X-ray spectroscopy (adjunct to SEM)
Eh	redox potential (a measurement of how easily a substance gains or loses electrons in a redox reaction.)
EPA	U.S. Environmental Protection Agency
Fe	iron
g	gram(s)
$g\ cm^{-2}y^{-1}$	gram(s) per square centimeter year
g/d	gram(s) per day
g-U	gram(s) uranium
GR	Grayford/Rker
h	hour(s)
H_2O_2	hydrogen peroxide
ICP-MS	inductively coupled plasma with mass spectroscopic detection

ICP-OES	inductively coupled plasma with optical emission spectroscopic detection
ID	identification
JPG	Jefferson Proving Ground, Indiana
K	potassium
Kd	partition coefficient
Kg	kilogram(s)
kV	kilovolts
L	liter
L/min	liter(s) per minute
LCS	laboratory control sample
MBq/g-U	megaBecquerel(s) per gram of uranium
MCLinc	Materials and Chemistry Laboratory, Inc.
meq	milliequivalent
Mg	magnesium
mg/Kg	milligrams(s) per kilogram
mg/L	milligram(s) per liter
µg	microgram(s)
µg/L	microgram(s) per liter
mm	millimeter(s)
mm^2	square millimeter(s)
Mn	manganese
mol/L	mole(s) per liter
MS	matrix spike
N	normal
n	An integer
N/A	not applicable
Na	sodium
NaCl	sodium chloride
NIST	US National Institute of Standards and Technology
NOM	naturally-occurring organic matter
NRC	U.S. Nuclear Regulatory Commission
O	oxygen
P	phosphorus
PAC	JPG soil type Avonsburg/Cobbsfork
pCi	picoCurie(s) (unit of radioactivity)
pCi/L	picoCurie(s) per liter
pCi/µg-U	picoCurie(s) per microgram of uranium
pCO_2	partial pressure of dissolved carbon dioxide
PCR	JPG soil type Cincinnati/Rossmoyne
PGR	JPG soil type Grayford/Ryker
pH_{IEP}	isoelectrical point
ppm	parts per million (mg/L)

pzc	point of zero charge
QA	quality assurance
R^2	linear regression squared correlation coefficient
redox	*red*uction-*ox*idation
S	sulfur
SA	specific activity
SAIC	Science Applications International Corporation
SE	sequential extraction (testing protocol)
SEM	scanning electron microscopy
Si	silicon
TC	total carbon
Ti	titanium
TOC	total organic carbon
^{234}U	uranium-234
^{235}U	uranium isotope 235
^{238}U	uranium-238
U	uranium
U(IV)	reduced forms of uranium
U(VI)	oxidized forms of uranium
UNEP	United Nations Environment Programme
UO_2	uraninite
UO_2^{+2}	uranyl ion
UO_2CO_3	rutherfordine
$UO_3 \cdot nH_2O$	schoepite
$UO_4 \cdot 4H_2O$	studtite
U_{total}	total uranium
UXO	(conventional) unexploded ordinance
Wt.%	weight percent (percentage composition by mass)
XPS	X-ray photoelectron spectroscopy
XRD	X-ray diffraction
y	year
y^{-1}	per year

ABSTRACT

This report summarizes extensive testing performed in a laboratory setting, using depleted uranium (DU) penetrator dart segments retrieved from the Jefferson Proving Ground (JPG) in southeastern Indiana, as well as Site soil and rainwater. These media were used in conjunction with a laboratory weathering procedure (American Society of Testing and Materials [ASTM] D 5744) that (1) enhances reaction-product transport in the aqueous leach of a solid sample, and (2) measures rates of weathering product release.

In this testing, the penetrator dart segments are shown to very slowly corrode; the corrosion products subsequently partially dissolve and then leach through a thin soil column under the accelerated weathering test conditions. After 22 accelerated leach intervals, representing over one year of real-time leaching, the *maximum* cumulative mass fraction of DU draining from the shallow soil column with implanted penetrator segment is estimated to be less than or equal to 8E-05 (less than or equal to 0.008 percent, by mass). The *maximum* concentration of dissolved uranium in the soil column leachate toward the end of the testing period (presumably after saturation of uranium bound to soil minerals) approaches approximately 10 milligrams per liter (mg/L) (approximately 4E+03 picoCurie per liter [pCi/L]). This is consistent with formation of schoepite (nominally $UO_3 \bullet 2H_2O$) as the long-term solubility-limiting surface alteration product (Jang et al., 2006). Schoepite was determined to be a major mineral phase in both the original and induced weathering dart corrosion rinds. Hold-up (retardation) of dissolved uranium by sorption to the site soil minerals and/or formation of relatively insoluble secondary uranium compounds, appears to be significant and controls the near-field migration of uranium species.

At the termination of the accelerated leaching protocol, the DU dart segments were removed, and the environmentally-available uranium inventory in the soil was estimated. After twenty-three cycles of accelerated leaching (representing actual experimental elapsed time 1.27 years [y]), the *fractional DU mass loss* to near-field soil and eluted water averaged approximately 0.002 per year (y^{-1}). Of this total, only a small proportion of inventory had partitioned to the aqueous eluent, the balance remained bound within the soil. Based on the DU-exposed soil and water mass balance, the average computed DU corrosion rate in our experiment is approximately 0.02 gram(s) per centimeter squared year [$g\ cm^{-2}y^{-1}$]). This value is well within the range of similar estimates cited by Handley-Sidhu et al. (2010) for corrosion rates for DU under oxic conditions in a non-marine environment (reported range approximately 0.01 to 0.8 $g\ cm^{-2}y^{-1}$). At these low corrosion rates, the DU material from largely intact penetrator darts would require many decades to corrode completely.

There is considerable hold-up of uranium within the near-field soil. Many soil phases, including hydrous oxide minerals and soil organic matter can interact with the soluble uranyl ion (UO_2^{2+}) to retard its migration. To further assess this expectation, aliquots of drained, DU-exposed soil were assessed by a modified Tessier Sequential Extraction (SE) procedure. The premise of the Tessier-type SE protocol is that a progressively more aggressive series of lixiviates are used to extract the soil matrix, in order to assess the risk of ground water contamination and the subsequent migration of contaminant into the environment. These SE methods recognize that total soil metal inventory is of limited use in understanding bioavailability or metal mobility, and that it is useful to estimate the amount of metal

present in different solid-phase forms. Despite some drawbacks, the SE method can provide a valuable tool to distinguish among trace element fractions of different solubility related to mineral phases. Uranium was found to be associated predominantly with the relatively more refractory "carbonate" and "hydrous metal oxide" (operationally-defined) geochemical fractions.

1. INTRODUCTION AND SUMMARY

The JPG in southeastern Indiana was established in 1941 as a proving ground for the test firing of a wide variety of munitions. DU projectiles were tested here between 1983 and 1994. These tests were intended to be nondestructive in nature (i.e., without the formation of DU aerosol from striking hard targets), although some of the rounds may have partially fragmented upon impact. It is estimated that approximately 154,000 pounds (70,000 kilograms [Kg]) of DU remain in the DU Impact Area (SAIC 2007). The DU impact area (approximately 2000 acres) is under U.S. Nuclear Regulatory Commission (NRC) license and is contaminated with both conventional unexploded ordinance (UXO) and DU.

The purpose of the present investigation is to better address the request for information by the NRC for potential decommissioning and modification to a possession-only radiological license for the JPG site. Concerns expressed by the NRC (and by the local community) include the site-specific corrosion rate of the DU armor-piercing projectile darts (kinetic energy "penetrators") and potential subsequent transport of toxic uranium U to the local groundwater system.

The data from these investigations describe a net release rate of DU, produced by corrosion of the penetrator dart segment and subsequent migration through a thin Site soil segments induced by drainage of Site rain water, in accordance with a laboratory weathering procedure (ASTM D 5744) that (1) enhances reaction-product transport in the aqueous leach of a solid sample, and (2) measures rates of weathering product release.

As Hilton (2000) observes, there is no simple correlation between corrosion rate data and release rate data. The corrosion rate is the rate at which a material physically degrades. It is based on the total amount of material reacted. The release rate is the rate that material is transported away from the sample. The release rate is related to the corrosion rate, but it depends on a number of other factors, including structural adherence of oxide, solubility of the corrosion products formed, colloid formation in aqueous phase, and sequestration of radionuclides in the soil matrix and alteration products that may be formed.

Figure 1 illustrates a prepared cross-sectional view of a typical surface-corroded DU projectile dart. It shows a thin (approximately 1 millimeter [mm]) corrosion rind comprised of gray-colored, sparingly-soluble reduced uranium oxide (UO_x, where x is less than or equal to 2.67) immediately adjacent to the metal alloy. Near the interface with oxic soil media there is a yellow-colored, fluorescent phase, identified by X-ray diffraction as schoepite (nominally $UO_3 \cdot nH_2O$, where n is an integer), which appears to be the long-term uranium solubility-limiting phase; Jang et al. (2006) predict solubility of schoepite to be approximately 2 to 20 milligrams per liter (mg/L) at near-neutral (pH of 6 to 7.5) oxic groundwater. Overlaying the uranium oxide mineral phases is a layer of adherent soil phase, which may "armor" the corrosion products to some extent (by forming a physical barrier).

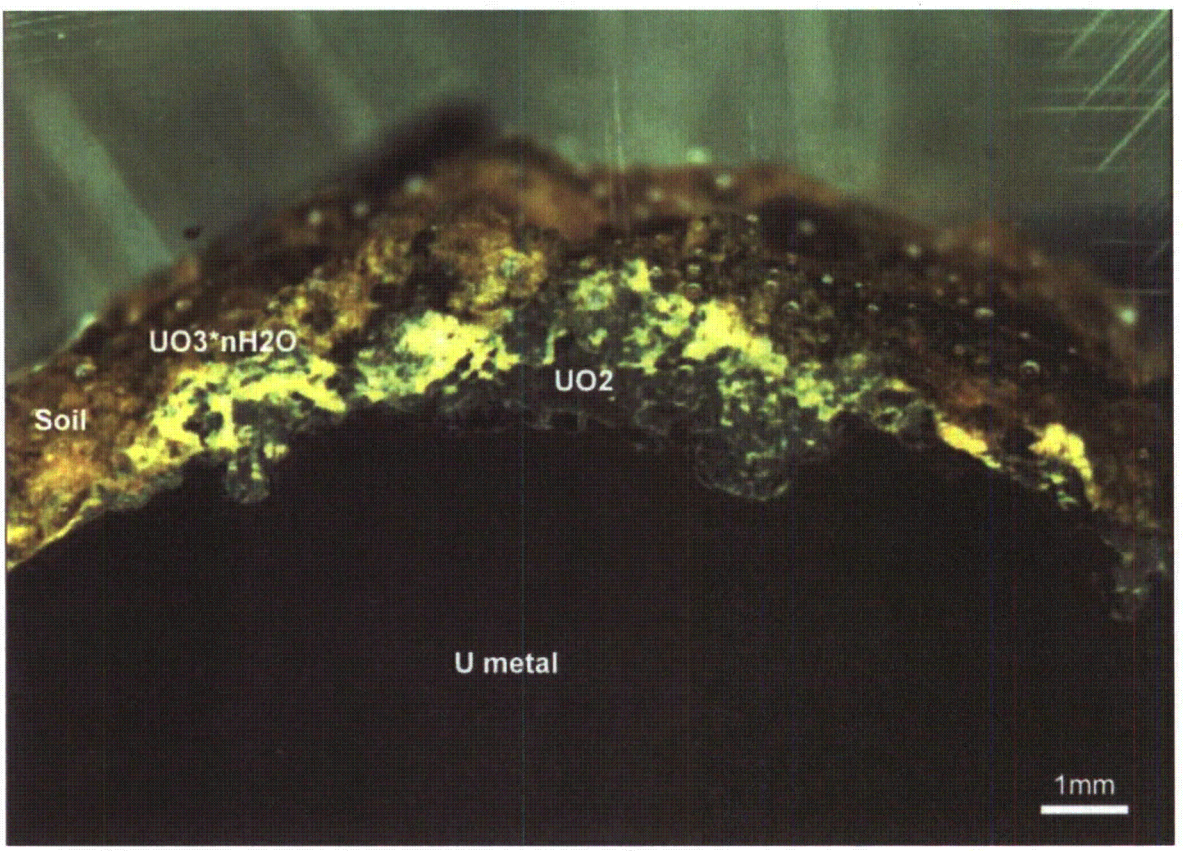

Figure 1. Optical Microscopic Image for a Polished Cross-section of a Dart Segment from As-received Specimen 08-2288 (Associated with Soil Type PAC).
Dart core diameter is approximately 25 mm.

Table 1 summarizes the estimated mass balance for DU after twenty-three cycles of accelerated leaching (actual experimental elapsed time 1.27 years). Normalized to the experimental elapsed time, the *fractional DU mass loss* to near-field soil and eluted water averaged (1.57 grams [g]/605.4-g)/(1.27-y) = 0.002 y^{-1}. Of this total, only about 2.5 percent of the DU "loss" inventory partitioned to the aqueous eluent, the balance remained bound within the soil.

Table 1. Mass Balance Summary: Partitioning of DU to Retained Soil and Eluted Aqueous Phases after 23 Cycles of Accelerated Leaching*

MCL ID	Soil Type	Description	Penetrator	Original Mass Penetrator (g)	End of Test: Mass Balance for U Loss			
					U Inventory (g)			Total % Mass Loss
					Aqueous	Soil	Total	
13-1663	PAC	Cell #1 Soil	Scraped	701.8	0.05	1.71	1.75	0.25%
13-1664	PAC	Cell #2 Soil	Unscraped	623.5	0.04	0.73	0.77	0.12%
13-1665	PCR	Cell #3 Soil	Scraped	577.1	0.04	1.43	1.47	0.26%
13-1666	PCR	Cell #4 Soil	Unscraped	620.2	0.04	1.49	1.54	0.25%
13-1667	PGR	Cell #5 Soil	Scraped	583.1	0.03	1.60	1.63	0.28%
13-1668	PGR	Cell #6 Soil	Unscraped	526.4	0.02	2.25	2.27	0.43%
13-1669	PAC	Cell #7 Soil	N/A		0.000	0.001	0.00	N/A
Average for Cells #1 through #6				605.4	0.04	1.54	1.57	0.26%

Notes:

* Total elapsed time = 463 days (actual experimental accelerated leach test interval).
% - percent
DU – depleted uranium
g – gram(s)
ID – identification
N/A – not applicable
PAC – soil type Avonsburg/Cobbsfork
PCR – soil type Cincinnati/Rossmoyne
PGR – soil type Grayford/Ryker
U - uranium

As shown in Appendix A2, Handley-Sidhu et al. (2010) have reviewed the few existing published corrosion rate estimates for DU under environmental conditions. Corrosion rates are normalized to the nominal (geometric) metal substrate surface area, as indicated in Equation (1):

$$\textbf{Corrosion Rate } (\mathbf{g\ cm^{-2}y^{-1}}) = \frac{\textbf{365 x Weight loss (g)}}{\textbf{Metal Surface Area (cm}^{\mathbf{2}}\textbf{) x Time (days)}} \qquad (1)$$

For data derived from the current investigation, based upon the mass balance estimates presented in Table 1, and the nominal DU penetrator segment geometric surface area derived in Appendix 2, a rough estimate for DU corrosion can be derived (Table 2). These estimates for corrosion rates are a simplistic linear extrapolation of the mass balance data over the actual duration of the experiment; data shown in Appendix A1 indicates that partitioning to the eluted aqueous phase is not constant over time, but that estimates for uranium concentration demonstrate considerable variability by collection interval.

Table 2. Estimates for DU Corrosion Rate Under Accelerated Leaching (Real Time Leach Duration 1.3 years)

Cell Number	Original dart mass (g)	Penetrator Dart Preparation	Nominal Dart Surface Area (cm^2) *	Aqueous Eluent		Total (Soil + Aqueous)	
				g-U lost	Rate g $cm^{-2}y^{-1}$ **	g-U lost	Rate g $cm^{-2}y^{-1}$ **
1	701.8	Scraped	80.18	0.047	4.64E-04	1.75	1.72E-02
2	623.5	Unscraped	72.35	0.040	4.33E-04	0.77	8.44E-03
3	557.1	Scraped	65.71	0.045	5.38E-04	1.47	1.77E-02
4	620.2	Unscraped	72.02	0.043	4.74E-04	1.54	1.68E-02
5	583.1	Scraped	68.31	0.026	3.03E-04	1.63	1.88E-02
6	526.4	Unscraped	62.64	0.022	2.73E-04	2.27	2.85E-02
Average	602		70.2	0.037	4.14E-04	1.57	(1.8 ± 0.6)E-2

Notes:

* From Appendix 3, Table A3-1 (Estimates for nominal geometric surface area)

** Computed using equation (1), with Time = 463 days (actual experimental accelerated leach test interval; the time equivalent for typical JPG field exposure (wet/dry cycles) has not been estimated).

% - percent

cm^2 – centimeters squared

DU – depleted uranium

g – gram(s)

g $cm^{-2}y^{-1}$ – gram(s) per centimeter squared year

g-U – gram(s) uranium

JPG – Jefferson Proving Ground, Indiana

Despite the limitations for the stated assumptions used for calculation of the corrosion rates summarized in Table 2, the average computed DU corrosion rate (approximately 0.02 g $cm^{-2}y^{-1}$) is well within the range of similar estimates cited by Handley-Sidhu et al. (2010) for corrosion rates for DU under oxic conditions in soil-moist oxic environment (reported range approximately 0.01 to 0.8 g $cm^{-2}y^{-1}$).

As noted previously (Table 1), there is considerable hold-up of uranium within the near-field soil. Many soil phases, including hydrous oxide minerals and soil organic matter, can interact with the soluble UO_2^{+2} to retard its migration. The physical properties summarized in Table 3 (i.e., relatively low pH value and relatively high total organic carbon) may favor such soil retention.

Table 3. Drained DU Exposed Soil: Select Physical Properties

Sample ID	Description	Drained Soil	Soil pH Value (ASTM D4972 *)		TOC (mg/Kg)		TC (mg/Kg)	
		% Moisture	DIW	0.01 N $CaCl_2$	As-Received Basis	Dry Weight Basis	As-Received Basis	Dry weight Basis
E-1	Cell #1 Soil	18.2%	4.48	4.24	6,780	8,270	8,520	10,400
E-1-DUP	Cell #1 Soil	17.9%						
E-2	Cell #2 Soil	16.7%	4.36	4.17	6,900	8,280	9,130	11,000
E-3	Cell #3 Soil	15.9%	3.92	3.68	6,970	8,290	10,100	12,000
E-4	Cell #4 Soil	15.3%	3.99	3.76	4,860	5740	9,340	11,000
E-5	Cell #5 Soil	14.9%	4.43	4.23	8,400	9,870	8,940	10,500
E-6	Cell #6 Soil	15.9%	4.55	4.33	8,380	9,960	9,630	11,500
E-7	Cell #7 Soil	19.2%	4.40	4.22	7,690	9520	7,850	9,720
E-7-DUP	Cell #7 Soil				6,110	7,560	7,990	9,890
Average		16.8%	4.30	4.09	7,010	8,440	8,940	10,750

Notes:

* ASTM Method D4972 (Standard Test Method for pH of Soils) calls for pH measurements on soil aliquots equilibrated with both de-ionized water (DIW) and with 0.01 N CaCl2 solutions.

% - percent
$CaCl_2$ – calcium chloride
DIW – deionized water
DU – depleted uranium
DUP – duplicate
ID – identification
mg/Kg – milligram(s) per kilogram
N – Normal
TC – total carbon
TOC – total organic carbon

To further assess this expectation, aliquots of drained, DU-exposed soil were assessed by a modified Tessier SE procedure. The premise of the Tessier-type SE protocol is that a progressively more aggressive series of lixiviates are used to extract the soil matrix, in order to assess the risk of ground water contamination and the subsequent migration of contaminant into the environment. These SE methods recognize that total soil metal inventory is of limited use in understanding bioavailability or metal mobility, and that it is useful to estimate the amount of metal present in different solid-phase forms. Despite some drawbacks, the SE method can provide a valuable tool to distinguish among trace element fractions of different solubility related to mineral phases.

U was found to be associated predominantly with the relatively more refractory "carbonate" and "hydrous metal oxide" (operationally-defined) geochemical fractions (*vide infra*). The soils contained plentiful iron (Fe), manganese (Mn), and aluminum (Al), which have mineral forms that can sorb and bind UO_2^{2+} (Krupka and Serne, 2002).

2. MATERIALS AND METHODS

2.1. Description of the Methodology for the Simulated Weathering of the Six Penetrator Segments

Initially, six penetrator dart segments were prepared, two each cut from three penetrators. Three segments were used "as is," without scraping the exterior surface, and three segments were scraped to remove bulk corrosion product from the exterior surface. Soils from three locations (designed PAC [JPG soil type Avonsburg/Cobbsfork], PCR [JPG soil type Cincinnati/Rossmoyne], PGR [JPG soil type Grayford/Ryker], see Table 1) were also received by Materials and Chemistry Laboratory, Inc (MCLinc). These soils were collected from areas outside of the DU impact areas, and were collected at near-surface (0 to 0.5 feet). Each soil was mixed separately to provide three homogeneous samples from each location. A scraped penetrator segment was placed in a Kg quantity of soil from each location in a humidity cell and an "unscraped " (as-received) segment was likewise placed in a Kg quantity of soil from each location resulting in six humidity cells that contained a penetrator segment and soil sample. A seventh humidity cell contained a 1-Kg sample of soil from location Avonsburg/Cobbsfork (AC) without a penetrator segment. This information is summarized in Table 4. The recorded initial mass of penetrator includes a relatively small contribution of adherent corrosion product, considered inconsequential for mass balance purposes.

Table 4. Test Cell Preparation

Cell No.	Soil Location *	Penetrator Segment ID No. (location/condition)	Initial Mass of Soil (g)	Initial Mass of Penetrator (g)
1	PAC	JP-PAC-005 (AC/Scraped)	1,000.1	701.8
2	PAC	JP-PAC-005 (AC/Un-scraped)	1,001.4	623.5
3	PCR	JP-PCR-008 (CR/Scraped)	1,000.2	577.1
4	PCR	JP-PCR-008 (CR/Un-scraped)	1,000.3	620.2
5	PGR	JP-PGR-001 (GR/Scraped)	1,000.5	583.1
6	PGR	JP-PGR-001 (GR/Un-scraped)	1,000.1	526.4
7	PAC	No penetrator segment	1,000.4	

Notes:

* PAC = soil type Avonsburg/Cobbsfork; PCR = soil type Cincinnati/Rossmoyne, PGR = soil type Grayford/Ryker.
g – gram(s)
ID – identification

The leachate sample identification numbers follow this designation scheme:

For example, 00-1-AC-005-S, where "00" is the initial leach that was done prior the first dry air or wet air cycles. The first leachate collection following the first dry air and wet air cycle was 01-1-AC-005-S. The

"1" is the cell number. The "005" is the penetrator segment number. The "S" means that the segment was scraped. A "U" instead of "S" would mean that the segment was un-scraped.

2.2. Description of the simulated weathering cycles

The simulated weathering cycles basically followed the ASTM Method D5744-96, *Standard Test Method for Laboratory Weathering of Solid Materials Using a Modified Humidity Cell*, (Reapproved 2001). This procedure (1) enhances reaction product transport in the aqueous leach of a solid material sample of specified mass, and (2) measures rates of weathering-product mass release. The weathering protocol selected simulates the effect of DU weathering in the vadose zone, including periodic intervals of short-term rainfall flooding, and is believed to be more aggressive than weathering induced by actual field metrological conditions. The native soil utilized in this testing includes viable indigenous microbes, so that it was unnecessary to inoculate the solids with *Thiobacillus ferroxidans* (as suggested in Appendix to D5744 for testing vs. barren rock ore).

The apparatus for this testing is illustrated in Figure 2. Following the ASTM D5744 method, the simulated weathering cycle starts with an initial water leach. That is, the very first activity after loading the penetrator segments and soil into the humidity cells is to add water to each cell so as to cover the surface of the soil several inches deep in water. In all cases, approximately 900-g of site rainwater was added to each cell for this purpose. The rain water used was collected and supplied to MCLinc by the client. The as-received rainwater had pH a value approximately 5.0 and correspondingly low total (bicarbonate) alkalinity (0.5 mg/L, expressed as $CaCO_3$ [calcite]). Complexation with carbonate ion often controls the mobility of UO_2^{+2} in groundwater (see, e.g., Curtis et al., 2006; Zhou and Gu, 2005). An increase in alkalinity in water drained from the test cells would likely suggest partial dissolution and depletion of $CaCO_3$ mineral phase from the test soil.

After adding the water to each cell, the water was allowed to remain in each cell for three hours, and then the plug was removed from the bottom of each cell to begin draining the water directly into tared (pre-weighed) and labeled collection bottles. The seven cells were allowed to drain for 69 hours (h) after opening the drain plugs. The collected water was sent to the designated lab for analyses under Chain-of-Custody (COC) seals with a COC sheet. Each cell was re-weighed to record a weight for each wet cell. Then the dry air manifold was connected to each cell and dry air was passed thru each cell at a rate of greater than1 liter per minute (L/min) for 9 days (d). Following the dry air cycle, each cell was removed again and re-weighed. All seven cells were then connected to the wet air manifold and wet air was flowed through each cell at greater than 1-L/min for 9-d. After 9-d of the wet air treatment, each cell was re-weighed and approximately 900- g of water was added to each cell to start the next leach cycle. This simulated weathering cycle was repeated numerous times resulting in 23 leachate sample sets. That is, the initial leachate collection was numbered "00" and the last leachate collection which followed 22 dry air, wet air, leach cycles were numbered "22" for a total of 23 leachate collection sets with seven water samples per each collection set.

Figure 2 illustrates a penetrator dart segment placed in an accelerated leach testing apparatus cell. The soil containment cell dimensions are approximately 11.7 centimeters (cm) (inside diameter) by approximately 20.5-cm (depth) (total volume about 2.2 liters [L]). The drained soil occupies approximately 860 cubic centimeters (cm^3), for a packed bed density of 1.16 g/cm^3.

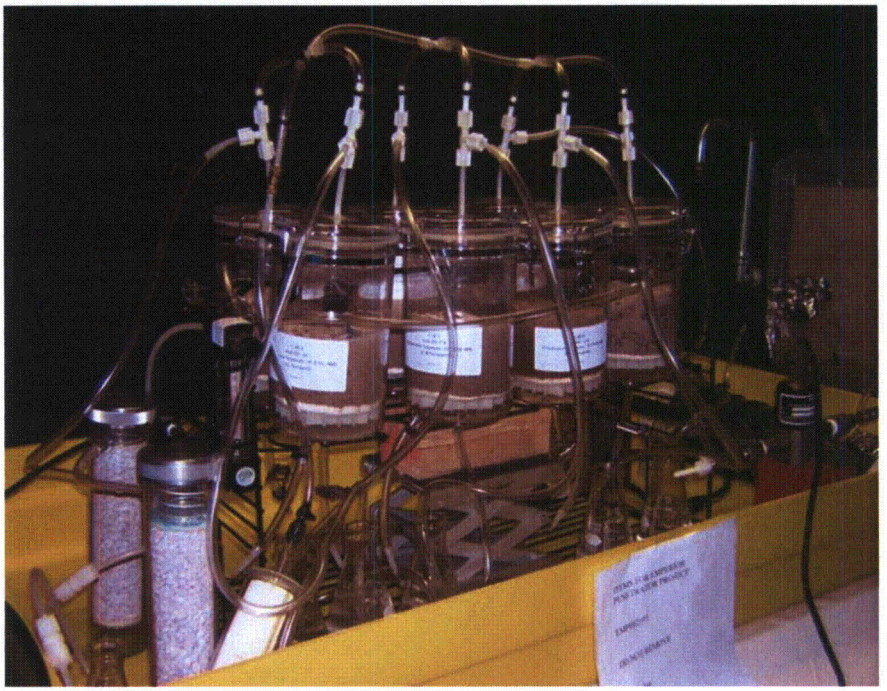

Figure 2. Illustration of the Modified Humidity Cell Apparatus, Constructed Consistent with ASTM D5744-96 Requirements

Figure 3. Embedded Penetrator Segment in Cell #1, Photographed After the Drying Cycle.

2.3. U Activity and Equivalent Mass Estimates

By request of the client, uranium isotopes in the leachate were monitored by alpha spectroscopy (subcontracted to Eberline Services, Oak Ridge, TN). All sample batch analytical quality assurance (QA) (blank, laboratory control sample [LCS], spike, minimum detection activity, duplicate [DUP] analyses) were within acceptable limits. For purposes of estimating uranium mass balance (e.g., mass fraction of original penetrator segment mass leached per sampling interval and cumulative over the duration of the experiment), it is useful to convert the measured isotopic activities to their mass equivalents, using the literature specific activities cited in Table 5.

Table 5. U Isotopic Specific Activity

Isotope	pCi/µg-U
U-234	6.23E+03
U-235	2.16E+00
U-236	6.51E+01
U-238	3.36E-01

Notes:
pCi/µg-U – picoCuries per microgram(s) uranium
U – uranium

Table 6 lists radiochemical attributes for natural and munitions-grade DU.

Table 6. Radiochemical Attributes for Natural and Munitions-grade DU

pCi/µg-U	Natural U		DU (Munitions)[1]	
	0.693		0.382	
Isotope	%Mass	%Activity	%Mass	%Activity
U-234	0.0055%	49.61%	0.0006%	9.70%
U-235	0.7111%	2.22%	0.2000%	1.13%
U-236	0.0000%	0.0003%	0.0003%	0.05%
U-238	99.2835%	48.17%	99.8000%	89.12%

Notes:
% - percent
DU – depleted uranium
pCi/µg-U – picoCuries per microgram(s) uranium
U – uranium

2.4. Alkalinity

Alkalinity, a significant contributor to uranyl mobility, was determined by titration versus standardized acid to an endpoint of pH 4.5 (bicarbonate endpoint), and results are expressed as mg/L $CaCO_3$

[1] ** http://www.informaworld.com/smpp/section?content=a714111273&fulltext=713240929. (See also Littleton, 2006).

(American Public Health Association [APHA], Standard Methods for the Examination of Water and Wastewater, Method 2320 B).

3. RESULTS

3.1. Characterization of original (as-found) penetrator corrosion rinds

Literature expectations for uranium at the *surface* of a DU penetrator are that it would slowly oxidize in wet oxic soil to initially form low-solubility UO_2 (uraninite), and ultimately (upon prolonged weathering), it would form more oxidized, relatively soluble phases such as schoepite (hydrated UO_3 - nominally $UO_3 \bullet 2H_2O$) or possibly other alteration phases (such as rutherfordine (UO_2CO_3) or becquerelite ($Ca(UO_2)_6O_4(OH)_6(H_2O)_8$), depending upon site-specific geochemical factors. These weathered phases are often the solubility-limiting phases for uranium in natural systems, but they can also be further transformed into other compounds.

Wagner and Stevenson (2009) report that the uranium oxide phases identified on as-found site corrosion rind were UO_2 (uraninite) and $UO_3 \bullet 2H_2O$ (schoepite) (major phases), and (minor) uranyl peroxide, $UO_4 \bullet 4H_2O$ (studtite). Whereas uraninite is relatively insoluble, the more oxidized species such as schoepite and studtite should exhibit moderate, pH-dependent, solubility in oxic water. Studtite (uranyl peroxide hydrate) and/or metastudtite (partially dehydrated studtite) are likely produced as very minor phases due to alpha radiolysis of water that forms the peroxide reagent; see Douglas et al. (2005), Rey, (2009). Studtite and metastudtite have been identified at other sites as an alteration product in casks of spent nuclear fuel (Douglas et al., 2005; Young et al., 2006).

These observations may be compared to those of Mellini and Riccobono (2005), who report that a DU penetrator, shot in 1999 at Djakovica, Western Kosovo, and there collected in June 2001, showed evident alteration processes, perceivable as black and yellow coatings. X-ray diffraction (XRD) indicates that the black coating mostly consists of uraninite, UO_2, with possible presence of other more oxidized uranium forms, such as U_3O_8. The yellow material is reported to be mostly amorphous, with variable weak diffraction lines, due to minor embedded uraninite grains, or possibly schoepite. Therefore, the Djakovica dart shows evident oxidation and leaching processes, progressively releasing mobile forms. [2]

The *maximum* solubility of oxidized uranium phases (surface layers on penetrators [e.g., schoepite]) at near-neutral pH (as found in the water in Kosovo) is about 10 mg/L (parts per million [ppm])[3]. However, there are many processes in nature that can retard the transport of uranium (sorption to hydrated metal oxide minerals and organic matter in the soil; co-precipitation with $CaCO_3$, etc., under certain conditions, the leached hexavalent soluble form of uranium may become reduced [if the soil contains iron-II-bearing minerals, bacteria, or organic matter], transforming to the tetravalent insoluble form [UO_2] – with crystalline material having low solubility at neutral pH, perhaps as low as 1 microgram per liter [µg/L],

[2] The darts recovered from Jefferson Proving Grounds show similar characteristics; see Travaglini (2008) and Wagner (2009).

[3] http://www.reliefweb.int/library/documents/2001/unep-duappendix5-12mar.pdf
(For DU, this stated maximum uranium solubility represents up to 4,000 pCi/L. This is approximately the maximum activity observed in this investigation; see Fig. 3.)

but oxidizing conditions, complexation and degree of crystallinity can significantly affect this property); see Casas et al (1998)., Kertes et al. (1985).

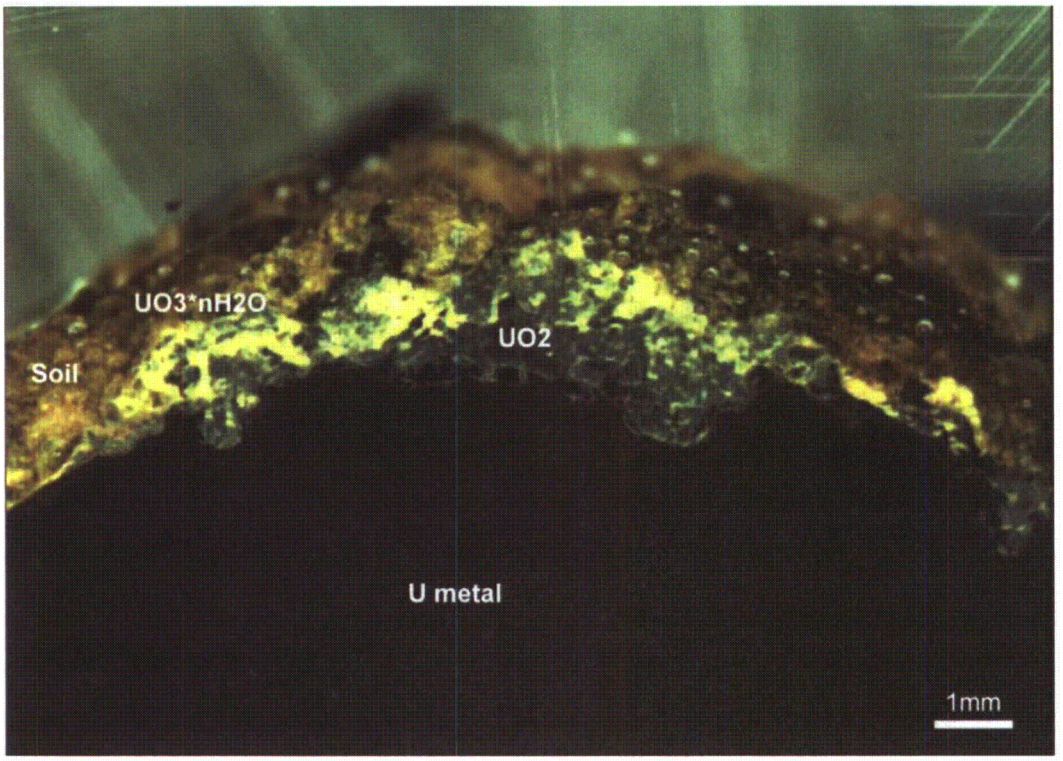

Figure 4. Optical Microscopic Image for a Polished Cross-section of a Dart Segment from As-received Specimen 08-2288 (Associated with Soil Type PAC). Dart core diameter is approximately 25 mm.

Figure 4 illustrates an optical image for a polished cross-section of an as-received penetrator dart segment, which has been embedded in epoxy resin (Stevenson, 2010A). It shows a thin (1 to 2 mm) rind of corrosion products – a dark gray, near-surface zone (assumed to be predominantly UO_2), overlain by a yellow, highly fluorescent material (schoepite). The corrosion products are also encased in a tenaciously adherent accretion of soil minerals, which likely also serve as a physical barrier to the corrosion and subsequent leaching phenomena. Brock (2003), and Buck and Brock (2004) conclude from a study of DU from an arid site that uranium precipitates as aggregates of tabular, hexagonal schoepite-metaschoepite crystals with silicate clay/silt particles, coated with amorphous silica, and so dissolved uranium does not move quickly and is probably inhibited by the adherent silicate coatings. The surface corrosion layer(s) illustrated in Figure 4 (and similar images presented by Stevenson, 2010A) appear far less than the estimates presented by Schimmack et al. (2007), who estimated that 7.9 percent of the initial DU mass was corroded after 3 years, based upon their laboratory column experiments.

3.2. Post-Leach Characterization of Corrosion Products

Examination of air-dried corrosion products on penetrator dart segments at the conclusion of the accelerated leach study identified meta-schoepite, equivalent to $UO_3 \cdot nH_2O$ (with n less than2), yellow, and trace UO_2, black, as the dominant uranium-bearing phases (Stevenson, 2010); see Figure 4. Thus the mineralogy of corrosion products induced during the accelerated weathering procedure is essentially the same as those identified as present on the as-received specimens.

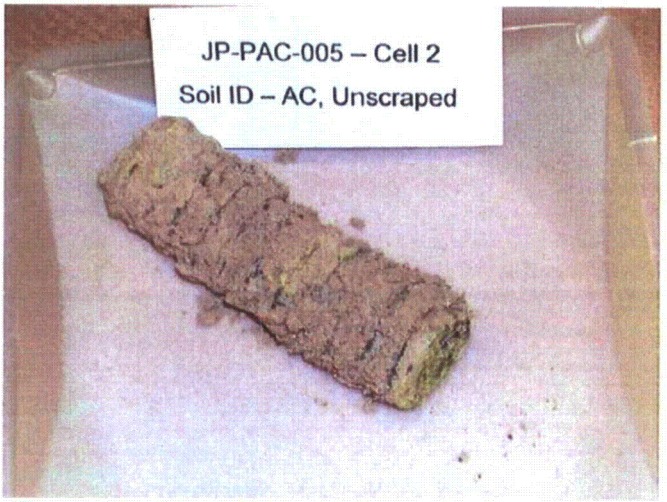

Figure 5. Side View Photograph of Unscraped JP-PAC-005 from Cell 2.

Figure 6. End View Photograph of Unscraped JP-PAC-005 from Cell 2.

Photographs of penetrator segment from Cell #2, retrieved at the conclusion of leach cycle #22. (From Stevenson, 2010).

3.3. Summary of X-ray Photoelectron Spectroscopy (XPS) Results

Samples of crushed corrosion products (as previously prepared for XRD analysis) were examined by the surface-selective technique of XPS. This technique can differentiate between reduced forms of uranium (U(IV)) and oxidized forms (U(VI)).

As Burns (1999) notes, UO_2 is probably always at least partially oxidized in nature, especially at the near-surface. Prepared specimens of corrosion scrapings were briefly subjected to argon ion milling, to clean the surfaces (e.g., removing the ubiquitous superficial oxidized uranium from reduced phases such as UO_2), so that the recorded composition more nearly approximates the bulk phase; see Nelson et al., (2003). Table 7 summarizes XPS data for numerous as-received penetrator darts. Table 8 summarizes data from post-leach retrieved segments, with comparison to the original (as-found) specimen from which the segment was prepared.

In general, the uranium valence state distributions for near-surface corrosion products are similar for as-received and post-weathering specimens (with approximately 2/3 as oxidized U(VI) and 1/3 as reduced U(IV)). The post-weathering estimates of uranium valance states show less variability than did the original (as-found) specimens.

Table 7. Summary of XPS Results (Percent Distribution of U(IV) and U(VI) for As-found Corrosion Products.

Soil Type PAC			Soil Type PCR			Soil Type PGR		
Specimen	**U(IV)**	**U(VI)**	**Specimen**	**U(IV)**	**U(VI)**	**Specimen**	**U(IV)**	**U(VI)**
08-2300	26.5	73.5	08-2294	33.2	66.8	**08-2296**	**61.1**	**38.9**
08-2301	30.4	69.6	08-2304	52.7	47.3	08-2297	20.4	79.6
08-2303	42.9	57.1	08-2305	48.0	52.0	08-2295	36.9	63.1
08-2285	35.9	64.1	08-2307	47.6	52.4	08-2298	30.3	69.7
08-2288	**44.2**	**55.8**	08-2291	15.2	84.8			
08-2302	29.0	71.0	08-2306	41.4	58.6			
08-2284	21.6	78.4	08-2289	45.1	54.9			
08-2287	35.1	64.9	**08-2290**	**60.4**	**39.6**			
08-2299	35.0	65.0	08-2292	47.7	52.3			
08-2286	25.0	75.0	08-2293	8.9	91.1			
Average ± σ	**32.6 ± 7.4**	**67.4 ± 7.4**	**Average ± σ**	**40.0 ± 16.4**	**60.0 ± 16.4**	**Average ± σ**	**37.2 ± 17.3**	**62.8 ± 17.3**

Notes: **Bolded** specimens are those selected for segmentation and use in accelerated leach tests.
± – plus or minus
σ – standard deviation
PAC – soil type Avonsburg/Cobbsfork
PCR – soil type Cincinnati/Rossmoyne
PGR – soil type Grayford/Ryker
U(IV) – reduced forms of uranium
U(VI) – oxidized forms of uranium

Table 8. Summary of XPS Results (Percent Distribution of U(IV) and U(VI) for Post-leach Corrosion Products.

Original	As-found (Pre-Leach)		Post-leach			
Segment MCLinc ID	% distribution		Post-Leach Cell #	Initial Condition	% distribution	
	U(IV)	U(VI)			U(IV)	U(VI)
08-2288	44.2	55.8	1	Scraped	32.8	67.2
			2	Unscraped	29.1	70.9
08-2290	60.4	39.6	3	Scraped	35.0	65.0
			4	Unscraped	35.4	64.6
08-2296	61.1	38.9	5	Scraped	29.7	70.3
			6	Unscraped	29.0	71.0
Average ± σ	**55.2 ± 9.6**	**44.8 ± 9.6**		**Average ± σ**	**31.8 ± 3.0**	**68.2 ± 3.0**

Notes:
% – percent
± – plus or minus
σ – standard deviation
ID – identification
MCLinc – Materials and Chemistry Laboratory, Inc.
U(IV) – reduced forms of uranium
U(VI) – oxidized forms of uranium

3.4. Leach Study Results

Leach study data are summarized in Appendix 1, and include graphical representations for the estimated cumulative mass fraction of uranium collected during the test leach intervals. The original mass of penetrator dart emplaced in the test soil is used as the operational uranium source term. This is a very good approximation for the mass source term, although it is recognized that:

1) the penetrator is an alloy (containing, e.g., approximately 0.4 weight percent [wt.%] titanium [Ti]);
2) there is a small amount of surface oxidation product(s) present on the segments (see "Characterization" Section above, and Figure 4); and
3) the native soils used have a small amount of uranium present (see data for Cell 7, with no penetration segment added).

The relatively large mass of the penetrator dart segment make the corrections for other surface-adherent phases and native soil sources negligible. For the purpose of mass balance estimate, uranium isotopic activities in the collected leachate are converted to their mass-equivalents (using the parameters from Table 2). Note that the density of metallic DU in the original penetrator darts is approximately 19.05

g/cm^3, with the relatively thin rind of adherent corrosion product and soil being much less dense (e.g., schoepite density about 4.8 g/cm^3).[4, 5]

Table 9 compares the initial mass of the dart segments used with the mass of the retrieved darts at the conclusion of the testing (note that estimates are for gently brushed dart segments, and include the contributions by tenaciously-adherent corrosion product and soil accretion). These measurements support the conclusion that changes in penetrator dart mass after accelerated weathering are minimal. Mass balance data presented in Appendix 1 also support this conclusion.

Table 9. Mass Estimates for Penetrator Dart Segments **

Cell	Initial Dart mass (g)	Final Dart mass (g)	Change Δ (g)	% Change %Δ
1	701.8	706.7	4.9	0.7%
2	623.5	626.5	3.0	0.5%
3	577.1	579.7	2.6	0.5%
4	620.2	622.6	2.4	0.4%
5	583.1	585.4	2.3	0.4%
6	526.4	525.5	-0.9	-0.2%

Notes:
** Estimates include associated adherent corrosion product and soil grains.
Δ – difference
% – percent
g – gram(s)

In general, the very first few leachate samples collected appear to have isotopic disequilibrium (i.e., activity is dominated by uranium – 234 [^{234}U], and are not in the isotopic proportions expected for bulk-phase DU; see Table 3 and Figure 5). Uranium isotopes in groundwater are often not in secular equilibrium (i.e., activity of ^{234}U "daughter" is not equal to the activity of the uranium – 238 [^{238}U] "parent"). General consensus is that the proportion of isotope ^{234}U can be elevated in groundwater in the presence of relatively "insoluble" uranium minerals, due to alpha recoil reactions that preferentially eject the (more active) ^{234}U at the mineral surface into a new chemical environment (e.g., groundwater), where the uranium is more soluble and hence more mobile (Sahoo, 2009; Pottorff, 2004; Abdul-Hadi et al., 2001). It is probable that the initial excess of ^{234}U activity in the leachate solution represents the dissolution of accumulated corrosion rind (which is relatively enriched in ^{234}U due to alpha recoil phenomena), and that by leach interval #6, there is an approach to steady-state for the rates of corrosion formation and subsequent leaching[6], as inferred by the ^{234}U contribution to total activity in the leachate approaching the expected value for ^{234}U activity ratio in the bulk phase of the DU in the penetrator.

[4] http://webmineral.com/data/Schoepite.shtml
[5] http://www.wolframalpha.com/entities/minerals/schoepite/dz/jv/qb/
[6] See discussion from http://home.datacomm.ch/ecoglobe/nuclear/duunepa5.htm: "This (steady-state leach rate) indicates that in soil solutions the rate of schoepite dissolution is about the same as the rate of oxidation of the penetrators."

By interval #10 (or sooner) the measured isotopic composition of uranium in the leachate is consistent with a steady-state leach of DU (Figure 6). In addition, the measured activity ratios for $^{234}U/^{238}U$ approximate the expectations for munitions DU (Table 3).

Handley-Sidhu et al. (2010) report that corrosion of unfired DU follows a latency period that depends on the specific geochemical conditions; they recommend that this latency be subtracted to give a more accurate estimate of steady-state corrosion rate.

At long-term, the cumulative mass fraction of uranium in the leachate converges for scraped and non-scraped penetrator segments (see Figure 7 for PAC soil), and the subsequent rate of leaching appears to approach a steady-state rate that may persist until the sorptive capacity of the thin soil column is exhausted.

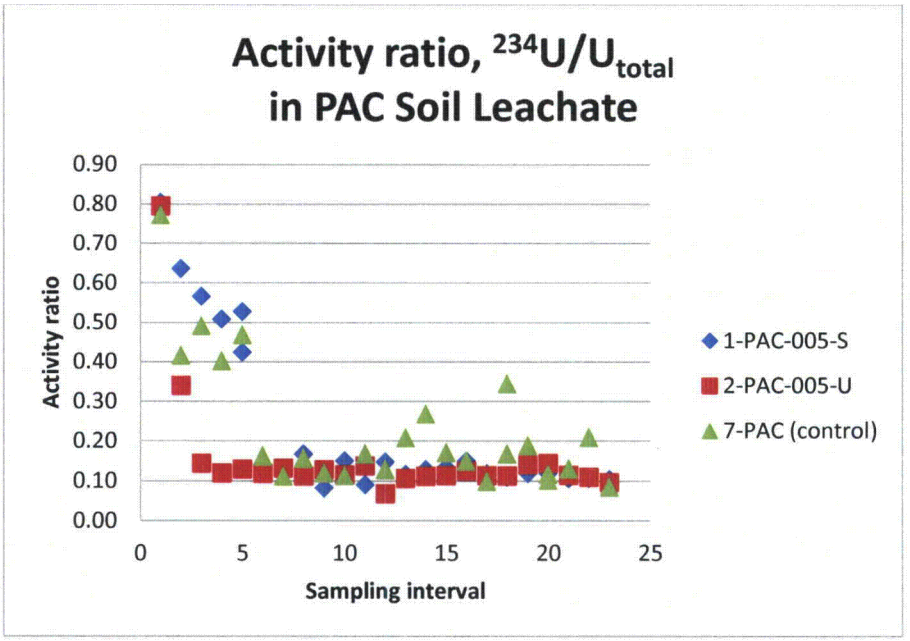

Figure 7. Estimates for the Ratio of Measured Activity, $^{234}U/U_{total}$, in PAC Soil Column Leachate.

By sampling interval 10 (or sooner), the activity ratio approaches the expected value for steady-state leaching from DU (activity, $^{234}U/U_{total}$ is approximately 0.10; see Table 3). (Data for control soil, 7-PAC, with no added penetrator dart segment, have low activity and hence high uncertainty for the calculated activity ratio estimate).

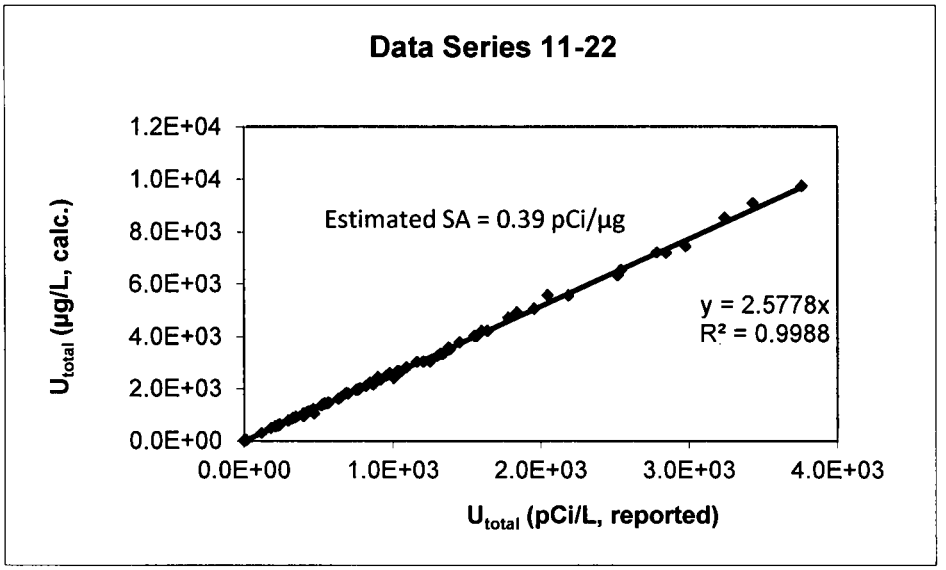

Notes:

calc. – calculated
µg/L – microgram(s) per liter
pCi/µg – 30icocurie(s) per microgram
R^2 – linear regression squared correlation coefficient
SA – specific activity
U_{total} – total uranium

Figure 8. Uranium in Leachate Solution (Data From All Soil Columns, Leach Intervals 11 through 22).

Uranium mass concentration is estimated from reported isotopic activities, using literature values for their individual specific activity (SA) (see Table 2). The estimated SA (SA is approximately 0.39 pCi/µg-U) in the leachate is approximately the same as the theoretical value for DU from munitions (see Table 3).

4. EXAMINATION OF DU-EXPOSED SOIL

The original configuration of the soil test cells was presented in Table 1. Soil specimens and associated DU penetrator dart segments (described in Table 1) were subjected to 22 accelerated leach intervals, in accordance with ASTM D 5744; this testing represented over one year of real-time leaching. At the end of this test cycle, soil columns remained in standby condition while awaiting Project review of the Interim Report (EMP002105), and/or requests for additional testing. The provenance of the soil specimens during this prolonged interval is given in Appendix 2.

A geological description of the DU impact area soil types is given in SAIC (2007). The field data indicate that the somewhat poorly drained Avonburg series may be grouped together with the poorly drained Cobbsfork series for the purpose of interpretation and future site characterization sampling tasks. Combined, these two soil series would comprise approximately 55 percent of the DU Impact Area. The well-drained Cincinnati and Rossmoyne series also may be grouped together, since both have a fragipan

subsurface diagnostic horizon, which tends to perch water during parts of the year, and this combination would account for another 32 percent of the DU Impact Area. The well-drained Grayford/Ryker, and somewhat poorly drained Holton series all have somewhat unique soil conditions and are proposed to be treated separately, and combined account for the remaining 13 percent of the DU Impact Area.

The soil samples originally supplied to MCLinc were collected at the JPG Site at a depth of 0 to 0.5 feet below ground surface, at select locations from outside of the DU Impact Area.

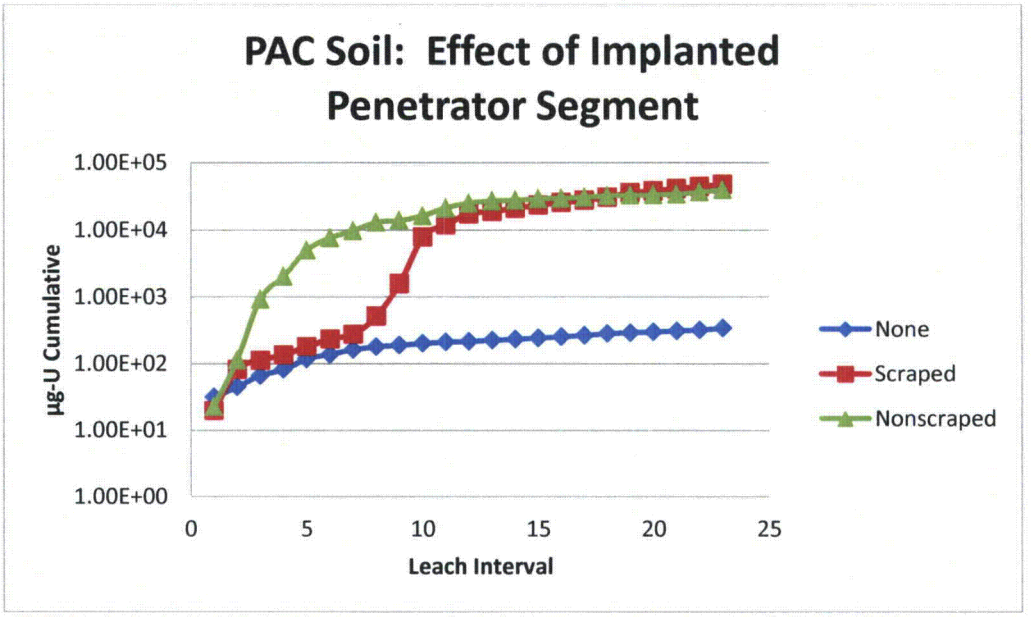

Notes:

µg-U – microgram(s) uranium
PAC – soil type Avonsburg/Cobbsfork

Figure 9. Estimates of Total uranium (µg), Cumulative, As Leached from Soil Type PAC: Effect of Added Penetrator Dart Segment.
Cell #7 has no added penetrator segment. (Note logarithmic chart ordinate).

4.1. Soil pH Estimates

Soil pH value is estimated using ASTM D4972-01, *Standard Test Method for pH of Soils*. By this method, pH measurements are made in both water and a dilute (0.01 Normal [N]) $CaCl_2$ solution (pH 5.15) because the calcium displaces some of the exchangeable aluminum. The low ionic strength counters the dilution effect on the exchange equilibrium by setting the salt concentration of the solution closer to that expected in the soil solution. The pH values obtained in the solution of $CaCl_2$ are slightly lower than those measured in water due to the release of more aluminum ions which then hydrolyze. Therefore, both measurements are required to fully define the character of the soil pH. Data are summarized in Table 10; soil pH values (for all specimens) are slightly acidic (pH 4.0 to 4.8), suggesting the occurrence of exchangeable Al and also minimal $CaCO_3$. High microbial respiration (producing weakly acidic dissolved carbon dioxide [CO_2]) can also contribute to soil acidity; McLean (1982) states

that soil water in a pore containing 10 percent CO_2 in the gaseous state would be at a pH value of 4.45 if it is not buffered at a higher pH by the soil or neutralized by basic substances.

Table 10. Soil pH Values

MCL ID	Soil Type *	Description	pH (in DIW)	pH (in 0.01 N $CaCl_2$)	Δ
13-1663	PAC	Cell #1 Soil	4.48	4.24	-0.24
13-1664	PAC	Cell #2 Soil	4.36	4.17	-0.19
13-1665	PAC	Cell #3 Soil	3.92	3.68	-0.24
13-1666	PCR	Cell #4 Soil	3.99	3.76	-0.23
13-1667	PCR	Cell #5 Soil	4.43	4.23	-0.2
13-1668	PGR	Cell #6 Soil	4.55	4.33	-0.22
13-1669	PGR	Cell #7 Soil	4.40	4.22	-0.18
13-1671	PAC	Soil Type PAC	4.79	4.49	-0.3
13-1672	PAC	Soil Type PCR	4.47	3.95	-0.52
13-1672-DUP	PCR	Soil Type PCR	4.46	3.91	-0.55
13-1673	PGR	Soil Type PGR	4.82	4.52	-0.3

Notes:

* PAC = soil type Avonsburg/Cobbsfork; PCR = soil type Cincinnati/Rossmoyne, PGR = soil type Grayford/Ryker.
Δ – the difference in pH vales estimated for soil contacted with DIW and with dilute $CaCl_2$ solution.
$CaCl_2$ – calcium chloride
DIW – deionized water equilibration
ID – identification
MCL – Materials and Chemistry Laboratory, Inc.
N – normality

Chen and Yiacoumi (2002) performed simulation calculations to show that DU mobilization from soil is a relatively slow process. Whenever possible, simulation results were compared with published experimental and field data. Precipitation, redox (*red*uction-*ox*idation reaction), and sorption reactions resulted in the immobilization of DU. Among these reactions, sorption played a major role, and the pH of soils was critical in the immobilization; higher pH in soils generally resulted in greater immobilization of DU.

Sorption of ions to mineral surfaces is strongly dependent upon the solution phase pH value, which affects the surface charge distribution on the sorptive substrate. As the pH value increases above the point of zero charge (pzc) for the substrate, the surface becomes more negatively charged and the sorption of cations generally increases. Conversely, sorption of anions is generally favored at pH values below the pzc of the substrate. For iron-containing minerals, the pzc is typically in the range of 6 to 8.5 (Silva & Nitche, 1995).

Sorption by iron oxides of uranyl carbonate anions is strongly affected by solution pH value, with an optimum specific sorption occurring at pH values near 5.5 to 6.5 (Farrell et al., 1999; Krupka and Serne, 2002; Jang et al., 2007), although removal of soluble uranium by all mechanisms (e.g., by sorption, ion-exchange and co-precipitation) may continue to be effective at elevated pH values. Barnett et al. (2002) had fair success modeling the sorption of soluble uranium to soil minerals, based upon a model independently developed for sorption of UO_2^{+2} to ferrihydrate; both experimental data and theoretical

prediction indicate maximum partition coefficient (Kd) values for UO_2^{+2} sorbed to soil minerals at pH values near 5 to 8.

4.2. Soil Moisture Estimates

Moisture in select soil samples was analyzed using MCLinc, *Operator Aid,* MCL-7756, Appendix MM, based on ASTM-D2216, *Standard Test Method for Laboratory Determination of Water (Moisture Content of Soil and Rock by Mass.* Results are summarized in Table 11.

Table 11. Soil Moisture Estimates

MCL ID	Soil Type *	Description	As-Prepared		As Retrieved (Drained) Soil		
			wet wt. (g)	Water (wt. %) **	wet wt. (g)	Water (wt. %)	Dry wt. (g)
13-1663	PAC	Cell #1 Soil	1000	13.3	1058	18.1	867
13-1664	PAC	Cell #2 Soil	1001	12.9	1047	16.7	872
13-1665	PCR	Cell #3 Soil	1000	14.1	1021	15.9	859
13-1666	PCR	Cell #4 Soil	1000	13.6	1020	15.3	864
13-1667	PGR	Cell #5 Soil	1000	15.1	998	14.9	849
13-1668	PGR	Cell #6 Soil	1000	14.8	1013	15.9	852
13-1669	PAC	Cell #7 Soil	1000	12.0	1089	19.2	880
13-1671	PAC	Background				2.6	
13-1672	PCR	Background				2.1	
13-1673	PGR	Background				9.0	

Notes:
* PAC = soil type Avonsburg/Cobbsfork; PCR = soil type Cincinnati/Rossmoyne, PGR = soil type Grayford/Ryker.
** Estimated value, based on the dry weight estimate from retrieved soil.
% – percent
g – gram(s)
ID – identification
MCL – Materials and Chemistry Laboratory, Inc.
wt. – weight

So-called "background" soil samples (13-1671, 13-1672, 13-173) were aliquots of stored original soils; these aliquots had dessicated considerably during storage.

4.3. TOC Estimates

Aliquots of wet soil were submitted to GEL Laboratories, LLC[7] for analysis of Total Carbon (TC) and TOC, using EPA SW846 Method 9060. Results (summarized in Table 4) are reported on as-received basis (see Table 11 for moisture estimates).

[7] GEL Laboratories, LLC, Charleston, SC, Work Order 329188, reported July 15, 2013.

Table 12. TC and TOC in Soil Samples*

MCL Sample ID	Soil Type	Description	TOC (mg/Kg)	TC (mg/Kg)	TOC/TC (%)
13-1663	PAC	Cell #1 Soil	6,780	8,520	80%
13-1664	PAC	Cell #2 Soil	6,900	9,130	76%
13-1665	PCR	Cell #3 Soil	6,970	10,100	69%
13-1666	PCR	Cell #4 Soil	4,860	9,340	52%
13-1667	PGR	Cell #5 Soil	8,400	8,940	94%
13-1668	PGR	Cell #6 Soil	8,380	9,630	87%
13-1669	PAC	Cell #7 Soil	7,690	7,850	98%
13-1669	PAC	Cell #7 Soil	6,110	7,990	76%
13-1671	PAC	Background	12,500	12,800	98%
13-1672	PCR	Background	9,030	10,700	84%
13-1673	PGR	Background	8,210	12,200	67%

Notes:

* Reported "as-received" basis.
% – percent
ID – identification
MCL – Materials and Chemistry Laboratory, Inc.
mg/Kg – milligram(s) per kilogram
PAC – soil type Avonsburg/Cobbsfork
PCR – soil type Cincinnati/Rossmoyne
PGR – soil type Grayford/Ryker
TC – total carbon
TOC – total organic carbon

Soil organic carbon is the main source of energy for soil microorganisms. TOC contains contributions from soil microbial biomass, decomposing plant matter, stable "humus" from organic decomposition residues, etc. For the soils described in Table 12, TOC is the predominant form of carbon. Minerals, such as $CaCO_3$ and dolomite, are the principal inorganic carbonate species in most soils.

4.4. Soil Analysis

Soils were analyzed for major elements (greater than 1.0 weight percent) and minor elements (from 1.0 to 0.1 weight percent) using a scanning electron microscope (SEM) and associated energy dispersive spectrometer (EDS). Samples were prepared by grinding to a fine powder in a SPEX mixer mill for three minutes using tungsten carbide lined grinding vials and a tungsten carbide ball. Preliminary examination of the powdered original soils (13-1671, 13-1672, and 13-1673) with a polarized light microscope showed the samples to consist primarily of quartz (near 70 percent by volume) and clay with minor amounts of plagioclase feldspar, and heavy mineral phases (e.g., pyroxene, titanite, rutile and other oxides).

Small portions of the powdered samples were placed on carbon dots mounted on Al disks. The powder was compacted by hand and carbon coated. A JEOL 840 SEM and an EDAX genesis EDS system were used for analyses. Analyses were performed using a 20 kilovolt (kV) beam

scanned over a 1.8 millimeter squared (mm^2) area, and counted for a period of 200 seconds. Representative EDS spectra are shown in the figures below. Figure 10 is from sample 13-1663, a post-leach sample for soil type PAC. Figure 11 is from sample 13-1671, an original, air-dried sample of soil type PAC.

Results for all samples are reported as oxide equivalents in Table 13 below. These data represent averages of two analyses per sample and are normalized to 100 percent by weight. Carbon was not included since no carbonate was noted under polarized light microscopy.

Table 13. Weight Percent of Oxides in Soils as Determined by Semi-quantitative EDS Analysis.

Oxides	Sample Numbers (in weight percent of oxides)									
	13-1663	13-1664	13-1665	13-1666	13-1337	13-1668	13-1669	13-1671	13-1672	13-1673
SiO_2	80.23	78.80	83.09	84.17	70.01	69.18	80.18	82.66	84.15	74.59
TiO_2	1.35	1.11	1.12	1.07	0.92	1.03	1.29	0.98	1.36	1.03
Al_2O_3	10.97	12.23	7.88	7.93	15.92	16.03	10.71	9.95	7.62	12.39
Fe_2O_3	4.19	4.21	4.45	3.64	8.28	8.92	4.47	3.40	3.55	7.12
MgO	0.55	0.59	0.38	0.35	0.94	1.03	0.50	0.49	0.38	0.75
CaO	0.44	0.59	0.27	0.28	0.53	0.52	0.45	0.40	0.29	0.60
K_2O	1.66	1.41	1.54	1.52	2.28	2.44	1.68	1.37	1.49	2.13
Na_2O	0.46	0.85	0.62	0.49	0.93	0.54	0.48	0.48	0.59	0.77
P_2O_5	0.08	0.11	0.05	0.07	0.09	0.09	0.04	0.08	0.06	0.12
SO_2	0.10	0.13	0.13	0.13	0.06	0.12	0.12	0.12	0.11	0.15
CuO	0.00	0.00	0.50	0.38	0.07	0.13	0.09	0.10	0.44	0.39
Total	100.0	100.0	100.0	100.0	100.0	100.0	100.0	100.0	100.0	100.0

Notes:
EDS – energy dispersive spectrometer

As a quality check, two internal standards from the National Institute of Standards and Technology (NIST) were analyzed along with the samples; NIST 2704 (Buffalo River Sediment) and NIST 2711 (Montana Soil). The published analyses for both standards, as well as the results of two analyses from this study are shown in Table 14. Note that the results for analyses from this study and the published results do show some differences. The published analyses, given as weight percent elements, were recast to weight percent oxides and normalized to 100 percent. This was the same treatment used for the results reported in the study. As reported, the original analyses were not normalized to 100 percent. However, given the semi-quantitative nature of the present study, the analyses compare favorably to the standards.

Table 14. Comparison of Standards Analyses.

Oxides	NIST Sample 2704 (Buffalo River Sediment) (in weight percent of oxides)			NIST Sample 2711 (Montana Soil) (in weight percent of oxides)		
	2704 published	2704-01	2704-02	2711 published	2711-01	2711-02
SiO_2	69.07	62.02	61.35	69.71	65.21	64.61
TiO_2	0.85	0.92	0.90	0.55	0.60	0.65
Al_2O_3	12.82	16.32	16.22	13.21	15.79	15.49
Fe_2O_3	6.52	9.26	9.85	4.42	5.55	6.14
MnO	0.00	0.13	0.11	0.88	0.30	ND
MgO	2.21	2.29	2.20	1.86	2.07	2.21
CaO	4.04	3.46	3.84	4.31	4.94	6.16
K_2O	2.67	3.36	3.44	3.16	3.30	3.54
Na_2O	0.82	0.61	0.67	1.65	1.96	1.20
SO_2	0.88	0.97	1.05	0.09	0.21	ND
CuO	0.12	0.25	0.29	0.15	ND	ND
Total	100	100	99.9	99.9	99.9	100

Notes:
NIST – National Institute of Standards and Technology

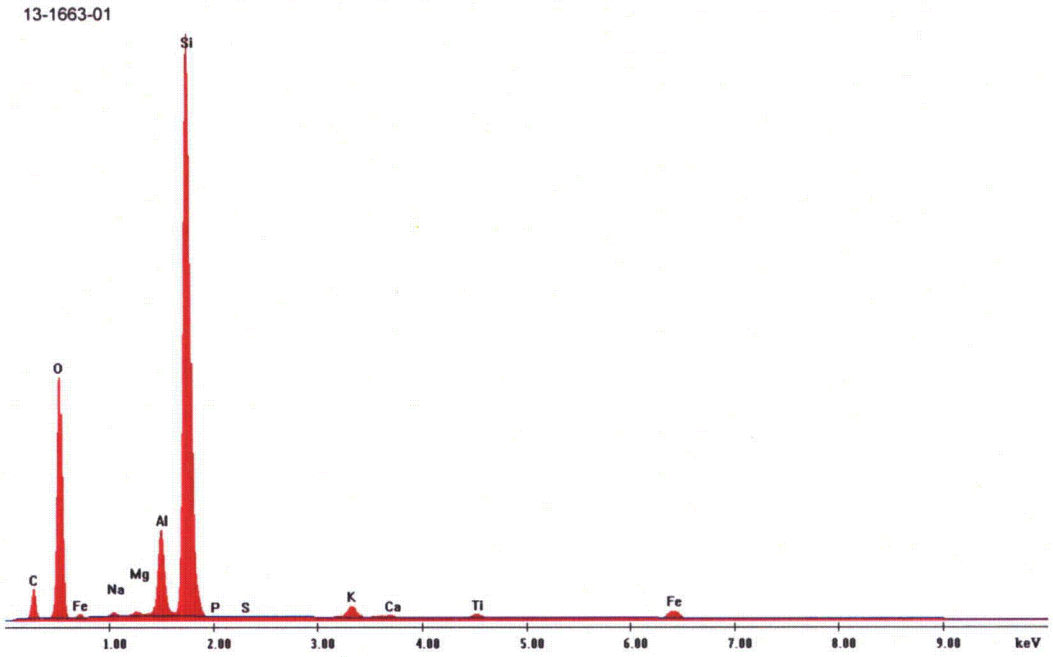

Notes: Al – aluminum
C – carbon
Ca – calcium
EDS – energy-dispersive X-ray spectroscopy
Fe – iron
K – potassium
keV – kilo electron volts
Mg – magnesium
Na – sodium
NIST – National Institute
O – oxygen
PAC – soil type Avonsburg/Cobbsfork
P – phosphorus
Si – silicon
S – sulfur
Ti – titanium

Figure 10. EDS Spectra for Sample 13-1663; Post leach Soil Type PAC.

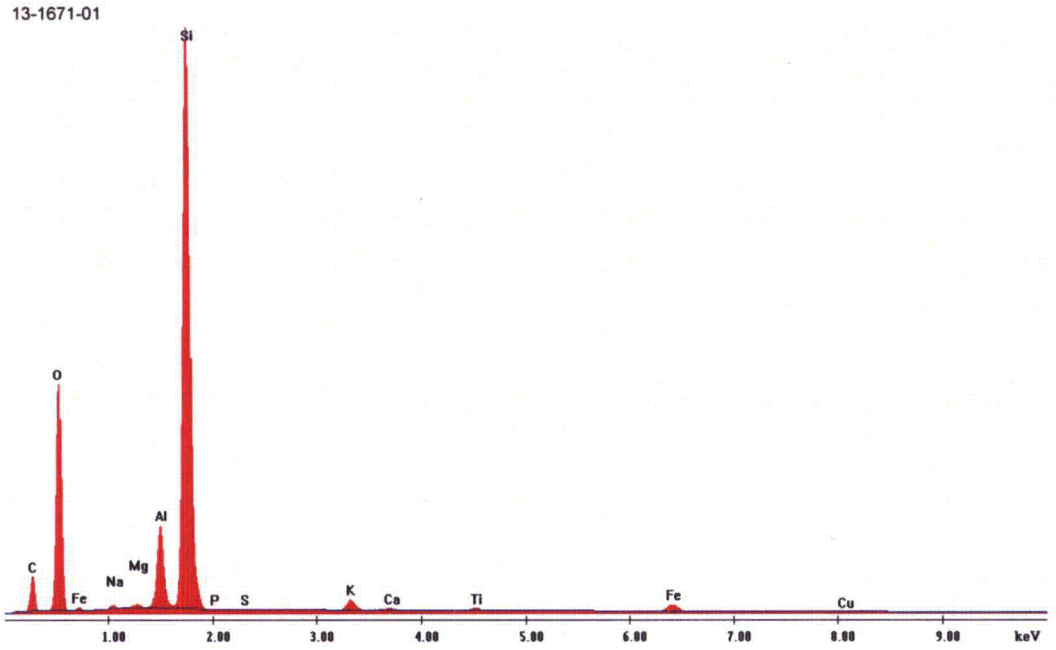

Notes: Al – aluminum
C – carbon
Ca – calcium
Cu – copper
EDS – energy-dispersive X-ray spectroscopy
Fe – iron
K – potassium
keV – kilo electron volts
Mg – magnesium
Na – sodium
NIST – National Institute
O – oxygen
PAC – soil type Avonsburg/Cobbsfork
P – phosphorus
Si – silicon
S – sulfur
Ti – titanium

Figure 11. EDS Spectra for Sample 13-1671; Original Pre-leach Soil Type PAC.

5. SEQUENTIAL EXTRACTION (SE) OF SOIL SPECIMENS

5.1. Background

Often, the technique of choice for evaluating low-level radionuclide partitioning in soils and sediments is the SE approach. This methodology applies operationally-defined chemical treatments to selectively dissolve specific classes of macro-scale soil or sediment components [e.g., Tessier et al. (1979); Phillips and Chappelle (1995)]. These methods recognize that total soil metal inventory is of limited use in

understanding bioavailability or metal mobility, and that it is useful to estimate the amount of metal present in different solid-phase forms. Despite some drawbacks, the SE method can provide a valuable tool to distinguish among trace element fractions of different solubility related to mineral phases.

Many recent studies published in the technical literature have used a selected sequence of extractions from the soil matrix, with each successive lixiviant solution increasing in its aggressiveness. The results of these SE (or "fractionation") often allow a comparison of how tenaciously different metal contaminants partition to different soil and sediment compositions. The partitioning of contaminants to different geochemical fractions is related to the contaminant speciation (or chemical form), as well as other physiochemical factors. Metals deemed least mobile in soil have a relatively small proportion of the total associated with the most readily accessible (or "exchangeable") fraction whilst having the greatest proportion associated with the most refractory (or "residual") fraction. Metals in the residual fraction are typically locked up within refractory crystalline mineral phases, and are not readily accessible to leach into the environment except on a geological time scale.

SE by modified Tessier protocol has attracted attention as an operational means to aid in the assessment for the potential risk of DU penetrator shards left in war zones, such as the Balkans and the Middle East (see, e.g., Oliver et al., [2008]; and Radenković et al.).

Details of the modified Tessier SE procedure performed at MCLinc are presented in Appendix 4. The sequence of extractions, and the attributed geochemical components affected, is briefly described below:

Fraction 1: Exchangeable Cations (Magnesium Chloride lixiviate, pH approximately 7);

Fraction 2: Carbonate-Bound Metals (Acetate Reagent, pH approximately 8.2);

Fraction 3: Metals Associated With Hydrous Iron- and Manganese Oxides (Hydroxylamine-Acetate Reagent);

Fraction 4: Bound to Organic Matter (Acid and hydrogen peroxide [H_2O_2] reagent).

For purpose of mass balance calculations, it is also necessary to determine the total environmentally-available metal inventory.

5.2. Total Environmentally-Available Metal (Extractable Inventory)

Aliquots of the selected soil samples (less than 2-mm size fraction) were extracted as described in MCL-7746, *Acid Digestion for Metals Based on EPA Method 3050B*. This digestion method (using strong nitric acid and H_2O_2) recovers most of the environmentally available heavy metal content, but it does not recover metals locked within a refractory silicate matrix.

5.3. Residual Fraction

Because the residual fraction is not considered to be available for release to the environment except on a geological time scale, it may not be necessary to quantitate this fraction unless the data is needed for mass balance closure. Total digestion is relatively difficult and expensive, and seldom used in environmental

analysis. More commonly used strong acid-based extractions such as EPA Methods 3050 and 3051 generally recover most of the available heavy metal content, but they cannot recover metals locked within a refractory silicate matrix. The proportion of residual metal may also be roughly estimated by mass balance, if an estimate of total constituent analysis is available for the original material. In the tabulations reported below, the residual fraction is defined as the computed difference between the total environmentally-available metal inventory and the sum of inventories from extraction Fractions 1 through 4.

5.4. Results

Inductively-coupled plasma – optical emission (ICP-OES) is used to quantitate uranium and select metals in soil extract. Inductively-coupled plasma – mass spectroscopy (ICP-MS) is used to determine the uranium enrichment (weight percent uranium-235 (^{235}U) isotope) in soil extracts. For extracts derived from soil from Cells 1 through 6, previously contacted with DU, the average uranium enrichment was determined to be (0.198 ± 0.004) percent ^{235}U isotope, consistent with the expected composition of United States DU munitions (see Table 3).[8]

Cell #7 was prepared using PAC-type soil collected outside of the DU impact area. This soil and its extracts had no detectable uranium content. An aliquot of Cell #7 was used for purposes of preparing a matrix spike (MS), by the addition of a small aliquot of natural uranium (0.71 percent ^{235}U isotope) as uranyl nitrate solution; leached aliquots from Cell #7-MS were determined to have an average uranium enrichment value (0.703 ± 0.006) percent ^{235}U isotope. The recovery of added uranium (at 248 mg/Kg) was 110 percent.

Results for the extraction of select metals in the test soil cells are summarized in Tables 15 through 21, and are presented in graphical form in Figures 12 through 18. By the end of the accelerated soil leaching procedure, the drained soils leached in the presence of penetrator dart segments (Cells 1 through 6) were in contact with aqueous phase containing soluble uranium at approximately 10 mg/L, consistent with formation of schoepite (nominally $UO_3 \bullet 2H_2O$) as the solubility-limiting surface alteration product (See Section 3.1). Thus, it is expected that the drained test soils from these cells would have a considerable inventory of exchangeable U, due to soluble uranium remaining in the pore water. However, most of the test cell soils had the greatest proportion of uranium in the more-refractory so-called carbonate and hydrous oxide fractions, with the latter usually predominant. This is consistent with other investigations of uranium contaminated soils.

The surface complexation reaction of uranyl with iron-containing minerals has been used as one means to model subsurface migration (Barnett et al., 2002; Payne and Waite, 1991; De Nero et al., 1999), used in conjunction with information on the site water chemistry and hydrology. The assessment of uranium

[8] The NRC defines DU as U in which the percentage of the ^{235}U isotope by weight is less than 0.711 percent (10 Code of Federal Regulations [CFR] 40.4). The military specifications designate that the DU used by U.S. Department of Defense (DoD) contain less than 0.3 percent ^{235}U (U.S. Army Environmental Policy Institute [AEPI], 1995). In actuality, DoD uses only DU that contains approximately 0.2 percent ^{235}U (AEPI, 1995). [See URL: http://www.gulflink.osd.mil/library/randrep/du/mr1018.7.chap1.html]

bound to hydrous metal oxides is one component of the operationally-defined partitioning by the SE methodology.

For modeling the retardation of the mobility of UO_2^{+2} in soil matrix, the fraction operationally associated with hydrous metal oxides has generally been the dominant concern. Bryan and Siegel (1998) go as far as to claim that such binding may be essentially irreversible under normal environmental conditions. However, the so-called "organic" geochemical compartment may also be important; for example, Oliver et al. (2006) used SE to identify the dominance of organic matter in controlling migration and bioavailability of DU in the near-field.

Table 15. SE of Cell #1 Soil (PAC)

MCLinc ID	Fraction	U *†		Mn *		Al *		Fe *	
		mg/Kg	%Total	mg/Kg	%Total	mg/Kg	%Total	mg/Kg	%Total
13-1675	Exchangeable	126	9%	14	6%	69	1%	4	0%
13-1676	Carbonate-Bound	439	30%	0.4	0%	6.3	0%	4	0%
13-1677	Hydrous Oxide	739	51%	137	63%	198	3%	1,060	16%
13-1678	Organic matter	80	6%	32	15%	777	13%	279	4%
(Calculated)	Residual	66	5%	34	16%	4800	82%	5333	80%
13-1663	Total	1,450	100%	217	100%	5,850	100%	6,680	100%

Notes: * Analysis of extracts by ICP-OES (inductively coupled plasma – optical emission spectroscopy)
† ICP-MS: Average wt.% ^{235}U isotope = (0.194 ± 0.004) – DU
% - percent
Al – aluminum
DU – depleted uranium
Fe – Iron
ICP-MS – inductively coupled plasma – mass spectroscopy
ID – identification
mg/Kg – milligram(s) per kilogram
Mn - manganese
PAC –soil type Avonsburg/Cobbsfork
SE – sequential extraction
U – uranium
^{235}U – uranium – 235
wt.% - weight percent

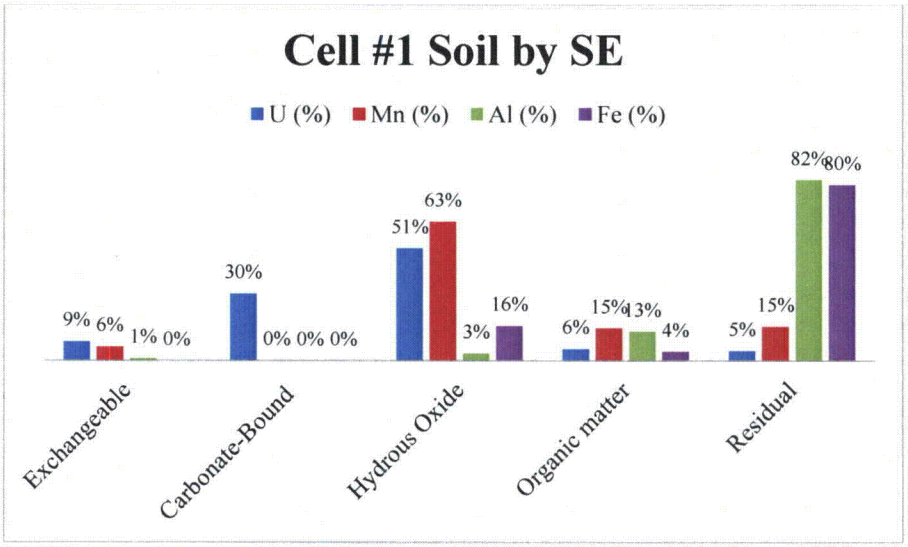

Figure 12. Partitioning of Select Metals to Aqueous SE Extract for Cell #1 Soil

Table 16. SE of Cell #2 Soil (PAC)

MCLinc ID	Fraction	U *†		Mn *		Al *		Fe *	
		mg/Kg	%Total	mg/Kg	%Total	mg/Kg	%Total	mg/Kg	%Total
13-1679	Exchangeable	34	4%	14	6%	81	1%	3.9	0%
13-1680	Carbonate-Bound	175	19%	0.4	0%	7	0%	3.9	0%
13-1681	Hydrous Oxide	324	36%	143	58%	226	4%	1,380	19%
13-1682	Organic matter	56	6%	35	14%	698	11%	283	4%
(Calculated)	Residual	313	35%	56	23%	5098	83%	5669	77%
13-1664	Total	902	100%	248	100%	6,110	100%	7,340	100%

Notes: * Analysis of extracts by ICP-OES (inductively coupled plasma – optical emission spectroscopy)
† ICP-MS: Average wt.% ^{235}U isotope = (0.193 ± 0.001) – DU
% - percent
Al – aluminum
DU – depleted uranium
Fe – Iron
ICP-MS – inductively coupled plasma – mass spectroscopy
ID – identification
mg/Kg – milligram(s) per kilogram
Mn - manganese
PAC –soil type Avonsburg/Cobbsfork
SE – sequential extraction
U – uranium
^{235}U – uranium – 235
wt.% - weight percent

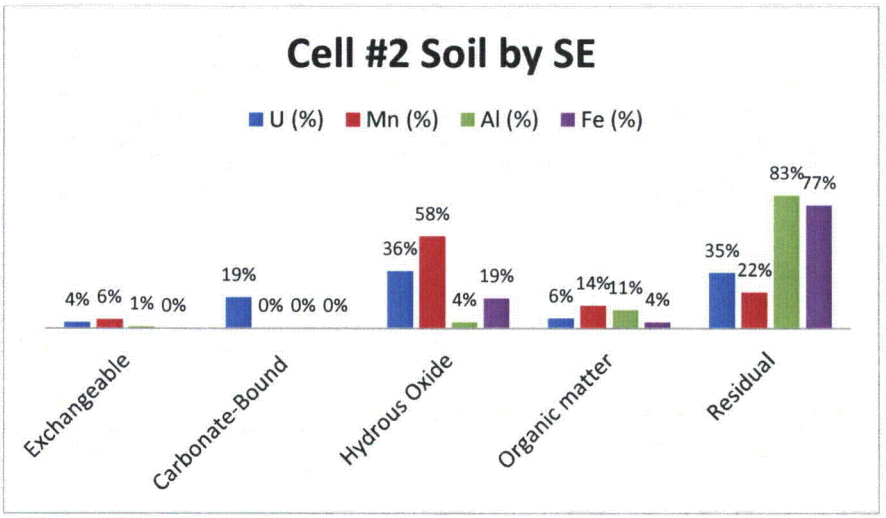

Figure 13. Partitioning of Select Metals to Aqueous SE Extract for Cell #2 Soil

Table 17. SE of Cell #3 Soil (PCR)

MCLinc ID	Fraction	U *†		Mn *		Al *		Fe *	
		mg/Kg	%Total	mg/Kg	%Total	mg/Kg	%Total	mg/Kg	%Total
13-1679	Exchangeable	211	13%	12	7%	175	4%	3.9	0%
13-1680	Carbonate-Bound	438	26%	0.4	0%	11	0%	3.9	0%
13-1681	Hydrous Oxide	115	7%	64	36%	160	4%	1,030	15%
13-1682	Organic matter	629	37%	25	14%	436	10%	345	5%
(Calculated)	Residual	287	17%	79	44%	3498	82%	5587	80%
13-1664	Total	1,680	100%	180	100%	4,280	100%	6,970	100%

Notes: * Analysis of extracts by ICP-OES (inductively coupled plasma – optical emission spectroscopy)
† ICP-MS: Average wt.% ^{235}U isotope = (0.200 ± 0.002) – DU
% - percent
Al – aluminum
DU – depleted uranium
Fe – Iron
ICP-MS – inductively coupled plasma – mass spectroscopy
ID – identification
mg/Kg – milligram(s) per kilogram
Mn - manganese
PCR –soil type Cincinnati/Rossmoyne
SE – sequential extraction
U – uranium
^{235}U – uranium – 235
wt.% - weight percent

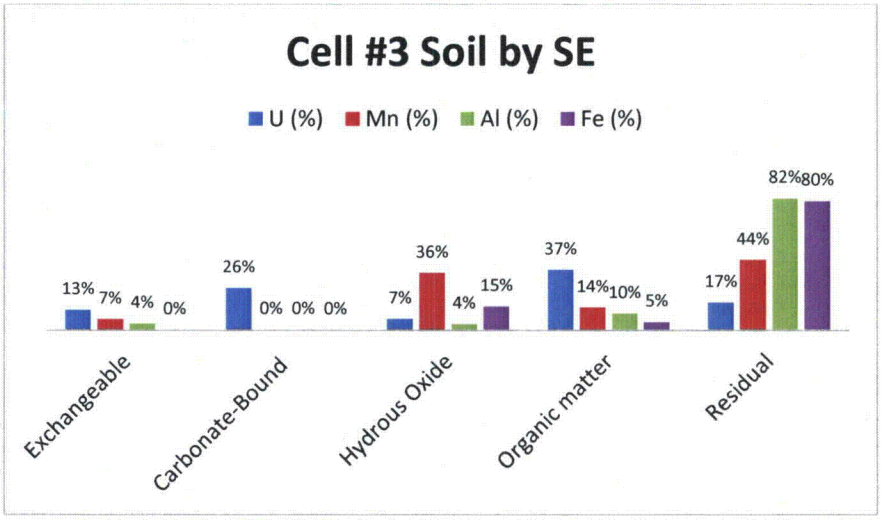

Figure 14. Partitioning of Select Metals to Aqueous SE Extract for Cell #3 Soil

Table 18. SE of Cell #4 Soil (PCR)

MCLinc ID	Fraction	U *†		Mn *		Al *		Fe *	
		mg/Kg	%Total	mg/Kg	%Total	mg/Kg	%Total	mg/Kg	%Total
13-1679	Exchangeable	212	11%	12	8%	170	4%	4	0%
13-1680	Carbonate-Bound	427	22%	0.4	0%	9	0%	4	0%
13-1681	Hydrous Oxide	629	32%	91	59%	181	4%	1,260	19%
13-1682	Organic matter	123	6%	21	14%	540	13%	338	5%
(Calculated)	Residual	569	29%	30	19%	3310	79%	5154	76%
13-1664	Total	1,960	100%	154	100%	4,210	100%	6,760	100%

Notes: * Analysis of extracts by ICP-OES (inductively coupled plasma – optical emission spectroscopy)
† ICP-MS: Average wt.% ^{235}U isotope = (0.198 ± 0.002) – DU
% - percent
Al – aluminum
DU – depleted uranium
Fe – Iron
ICP-MS – inductively coupled plasma – mass spectroscopy
ID – identification
mg/Kg – milligram(s) per kilogram
Mn - manganese
PCR –soil type Cincinnati/Rossmoyne
SE – sequential extraction
U – uranium
^{235}U – uranium – 235
wt.% - weight percent

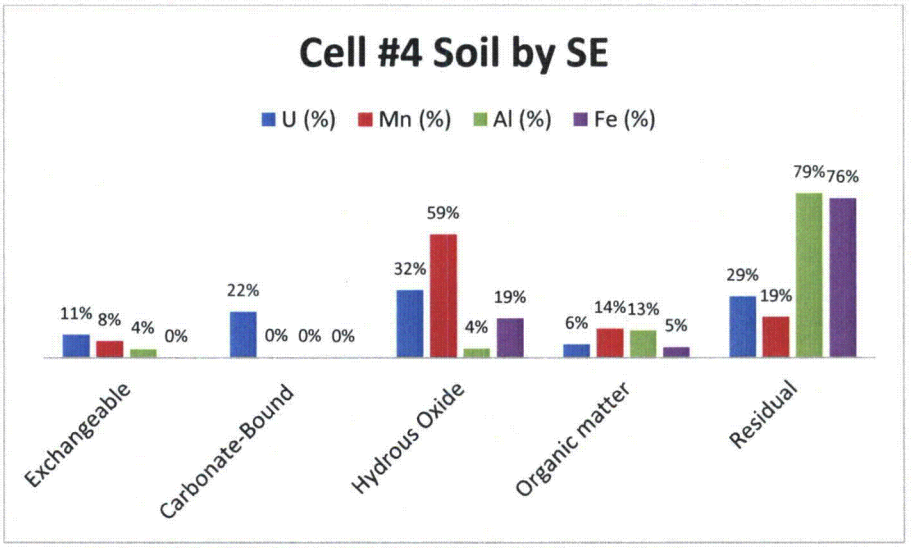

Figure 15. Partitioning of Select Metals to Aqueous SE Extract for Cell #4 Soil

Table 19. SE of Cell #5 Soil (PCR)

MCLinc ID	Fraction	U *†		Mn *		Al *		Fe *	
		mg/Kg	%Total	mg/Kg	%Total	mg/Kg	%Total	mg/Kg	%Total
13-1679	Exchangeable	140	10%	16	4%	159	2%	6.8	0%
13-1680	Carbonate-Bound	419	29%	0.4	0%	9	0%	3.9	0%
13-1681	Hydrous Oxide	712	48%	252	64%	369	4%	959	5%
13-1682	Organic matter	88	6%	49	12%	938	10%	174	1%
(Calculated)	Residual	111	8%	76	19%	7635	84%	18316	94%
13-1664	Total	1,470	100%	393	100%	9,110	100%	19460	100%

Notes: * Analysis of extracts by ICP-OES (inductively coupled plasma – optical emission spectroscopy)
† ICP-MS: Average wt.% ^{235}U isotope = (0.201 ± 0.004) – DU
% - percent
Al – aluminum
DU – depleted uranium
Fe – Iron
ICP-MS – inductively coupled plasma – mass spectroscopy
ID – identification
mg/Kg – milligram(s) per kilogram
Mn - manganese
PCR –soil type Cincinnati/Rossmoyne
SE – sequential extraction
U – uranium
^{235}U – uranium – 235
wt.% - weight percent

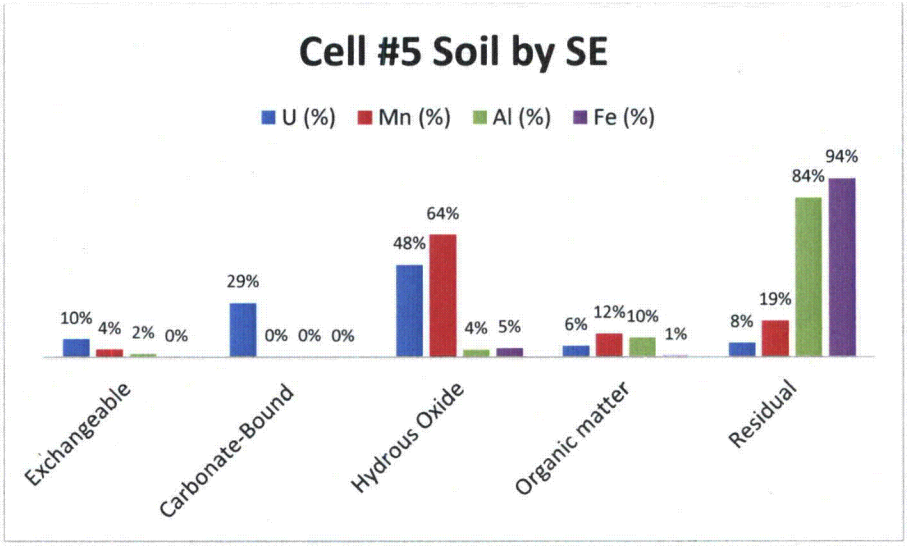

Figure 16. Partitioning of Select Metals to Aqueous SE Extract for Cell #5 Soil

Table 20. SE of Cell #6 Soil (PCR)

MCLinc ID	Fraction	U *†		Mn *		Al *		Fe *	
		mg/Kg	%Total	mg/Kg	%Total	mg/Kg	%Total	mg/Kg	%Total
13-1695	Exchangeable	133	5%	7	2%	111	1%	7.8	0%
13-1696	Carbonate-Bound	463	17%	0.4	0%	9	0%	4	0%
13-1697	Hydrous Oxide	982	36%	394	89%	463	5%	1,120	5%
13-1698	Organic matter	96	4%	98	22%	916	10%	177	1%
(Calculated)	Residual	1036	38%	-56	-13%	7701	84%	19081	94%
13-1667	Total	2,710	100%	444	100%	9,200	100%	20,390	100%

Notes: * Analysis of extracts by ICP-OES (inductively coupled plasma – optical emission spectroscopy)
† ICP-MS: Average wt.% ^{235}U isotope = (0.198 ± 0.003) – DU
% - percent
Al – aluminum
DU – depleted uranium
Fe – Iron
ICP-MS – inductively coupled plasma – mass spectroscopy
ID – identification
mg/Kg – milligram(s) per kilogram
Mn - manganese
PCR –soil type Cincinnati/Rossmoyne
SE – sequential extraction
U – uranium
^{235}U – uranium – 235
wt.% - weight percent

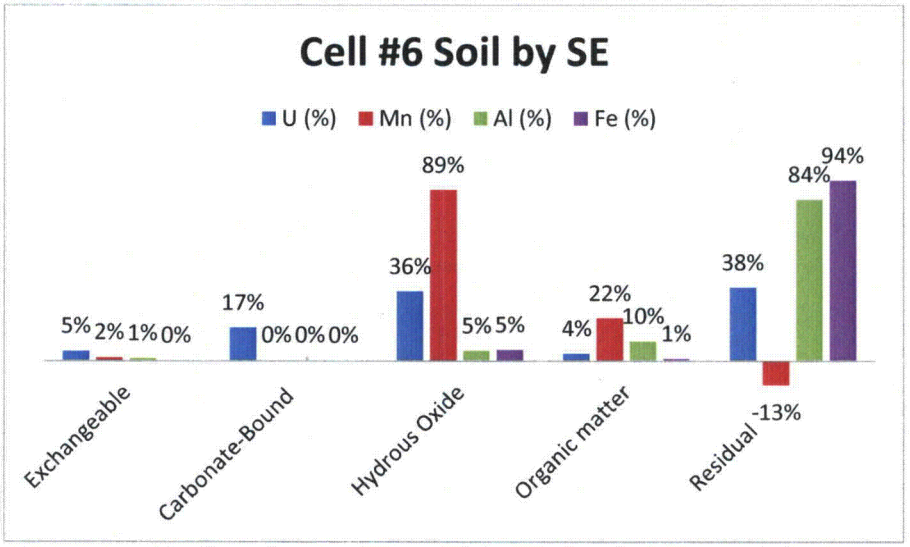

Figure 17. Partitioning of Select Metals to Aqueous SE Extract for Cell #6 Soil

Table 21. SE of Cell #7 Soil (7-PAC-MS)

MCLinc ID	Fraction	U *†		Mn *		Al *		Fe *	
		mg/Kg	%Total	mg/Kg	%Total	mg/Kg	%Total	mg/Kg	%Total
13-1695	Exchangeable	17	6%	20	9%	96	2%	3.9	0%
13-1696	Carbonate-Bound	86	32%	0.5	0%	10	0%	3.9	0%
13-1697	Hydrous Oxide	121	44%	136	62%	224	4%	1,360	19%
13-1698	Organic matter	18	7%	29	13%	678	12%	268	4%
(Calculated)	Residual	31	11%	33	15%	4502	82%	5634	77%
13-1667	Total	273	100%	218	100%	5,510	100%	7,270	100%

Notes: * Analysis of extracts by ICP-OES (inductively coupled plasma – optical emission spectroscopy)
† ICP-MS: Average wt.% ^{235}U isotope = (0.703 ± 0.0063) – U (natural)
% - percent
Al – aluminum
Fe – Iron
ICP-MS – inductively coupled plasma – mass spectroscopy
ID – identification
mg/Kg – milligram(s) per kilogram
Mn - manganese
MS – matrix spike
PCR –soil type Cincinnati/Rossmoyne
SE – sequential extraction
U – uranium
^{235}U – uranium – 235
wt.% - weight percent

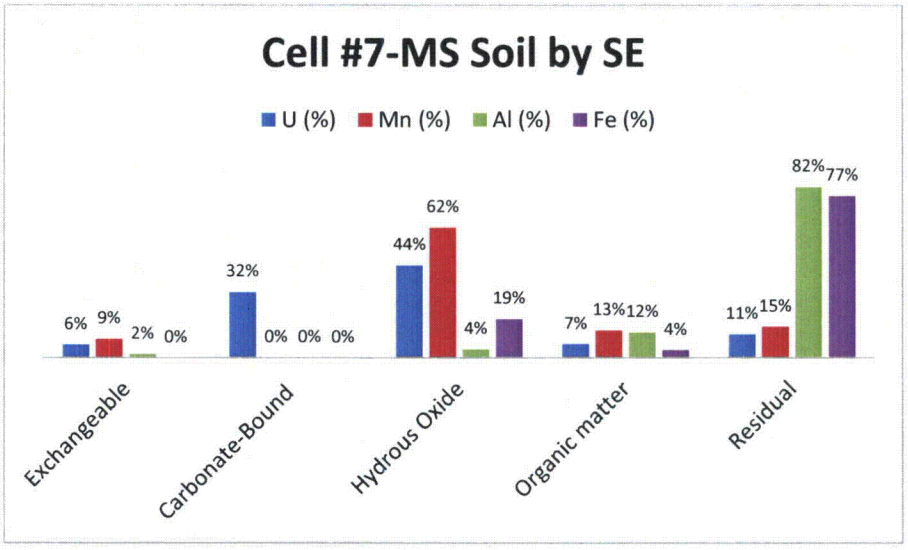

Figure 18. Partitioning of Select Metals to Aqueous SE Extract for Cell #7-MS Soil

6. MASS BALANCE SUMMARY – PERCENTAGES OF DU RETAINED IN SOIL AND ELUTED INTO COLLECTED WATER

Refer to Table 1 for the leach test logistics (i.e., original mass for as-received Site soil and inserted penetrator dart segment). For the soil test columns with inserted penetrator dart segments (*viz.*, Cells #1 through #6), the *average* mass of DU partitioning to soil and water, referenced to the original mass of penetrator dart, is only on the order of approximately 0.3 percent after about 1.3-y of accelerated leaching (Table 22). Of this small mass of DU "lost "from the dart specimen, 98 percent is retained in the near-field soil, and 2 percent is leached into the collected water (aqueous fraction).

Table 22. Partitioning of DU to Retained Soil and Eluted Aqueous Phases after 23 Cycles of Accelerated Leaching

MCL ID	Soil Type	Description	Penetrator	Original Mass Penetrator (g)	End of Test: Mass Balance for U Loss			
					Uranium Inventory (g)			Total % Mass Loss
					Aqueous	Soil	Total	
13-1663	PAC	Cell #1 Soil	Scraped	701.8	0.05	1.53	1.58	0.23%
13-1664	PAC	Cell #2 Soil	Unscraped	623.5	0.04	0.94	0.98	0.16%
13-1665	PCR	Cell #3 Soil	Scraped	577.1	0.04	1.72	1.76	0.30%
13-1666	PCR	Cell #4 Soil	Unscraped	620.2	0.04	2.00	2.04	0.33%
13-1667	PGR	Cell #5 Soil	Scraped	583.1	0.03	1.47	1.50	0.26%
13-1668	PGR	Cell #6 Soil	Unscraped	526.4	0.02	2.75	2.77	0.53%
13-1669	PAC	Cell #7 Soil	N/A	N/A	0.000	0.001	0.00	N/A
Average for Cells #1 through #6				605.4	0.04	1.73	1.77	0.30%

Notes: % - percent
g – gram(s)
ID – identification
MCL – Materials and Chemistry Laboratory, Inc.
mg/Kg – milligram(s) per kilogram
Mn - manganese
N/A – not applicable
PAC – soil type Avonsburg/Cobbsfork
PCR –soil type Cincinnati/Rossmoyne
PGR – soil type Grayford/Ryker
U – uranium

The average mass balance estimates in Table 22, for DU distributed to soil and water, are consistent with the rough estimates for differences in mass for the penetrator dart segments, before and after leaching, summarized in Table 6 (less than 0.5 weight percent). These mass balance estimates by the accelerated leaching procedure (approximately 0.30 percent of DU mass dissolved and/or detached after about 1.3-y) are far less than the laboratory column experiment estimates presented by Schimmack et al. (2007), who projected that 7.9 percent of the initial DU mass was corroded after 3-y.

7. CORROSION RATE ESTIMATES

Data for nominal metal corrosion rate is typically normalized to the substrate surface area, and expressed in units such as g $cm^{-2}y^{-1}$ (Handley-Sidhu et al. [2010]; Hilton [2000]) (Equation A2-2).

$$\textbf{Corrosion Rate } (g\ cm^{-2}y^{-1}) = \frac{365 \times \text{Weight loss (g)}}{\text{Metal Surface Area } (cm^2) \times \text{Time (days)}} \qquad (1)$$

Combined uranium mass partitioning to soil and water are presented in Table 22. Nominal geometric surface areas for the penetrator dart segment used are presented in Appendix A2. These estimates are used for the computations presented in Table 23.

Table 23. Estimates for DU Corrosion Rate under Accelerated Leaching (Real Time Leach Duration is 1.3-y)

Cell Number	Original Dart Mass (g)	Penetrator Dart Preparation	Nominal Dart Surface Area (cm^2) *	Aqueous Eluent		Total (Soil + Aqueous)	
				g-U Lost	Rate (g $cm^{-2}y^{-1}$) **	g-U Lost	Rate (g $cm^{-2}y^{-1}$) **
1	701.8	Scraped	80.18	0.05	4.64E-04	1.58	1.56E-02
2	623.5	Unscraped	72.35	0.04	4.33E-04	0.98	1.07E-02
3	557.1	Scraped	65.71	0.04	5.38E-04	1.76	2.10E-02
4	620.2	Unscraped	72.02	0.04	4.74E-04	2.04	2.23E-02
5	583.1	Scraped	68.31	0.03	3.03E-04	1.50	1.73E-02
6	526.4	Unscraped	62.64	0.020	2.73E-04	2.77	3.48E-02

Notes: * Appendix, Table A3-1, (Nominal geometric surface area)
** Computed using equation (1).
cm2 – square centimeter(s)
DU – depleted uranium
g – gram(s)
g $cm^{-2}y^{-1}$ – gram(s) per square centimeter year
g-U – gram(s) uranium
y – year(s)

From Table 23, the *nominal* average corrosion rate for DU penetrator dart segment, accounting for loss to residual soil and aqueous eluate, is approximately (2.0 ± 0.8)E-2 g-$cm^{-2}y^{-1}$. This estimate was computed using conservative estimates for the dart surface area and for the elapsed exposure time (i.e., accelerated leaching versus field conditions).

In a recent review, Handley-Sidhu et al. (2010) compiled estimates for the corrosion rates of DU-titanium (Ti) alloy; their summary table is reproduced below as Table 24. In general, for DU weathered under non-marine geological conditions, reported corrosion rates ranged from approximately 0.01 g $cm^{-2}y^{-1}$ (for waterlogged soil) to 0.8 g $cm^{-2}y^{-1}$ (for organic clay-rich soil). Our crude estimates for DU corrosion in soils exposed to oxic wet/dry accelerated leach conditions (approximately 0.02 g $cm^{-2}y^{-1}$) is toward the lower end of this literature range.

Table 24. Corrosion Rates of DU-Ti alloy, as Compiled by Handley-Sidhu et al. (2010).

Study	Environment	Geochemical Conditions	Rate ($g\ cm^{-2}y^{-1}$)	Comments	References
1	Air	Oxic	0.0012	Laboratory air (30 days)	Trzaskoma (1982)
2	H_2O	Oxic	0.072	Distilled water	Trzaskoma (1982)
3	3.5% NaCl	Oxic	0.40		Trzaskoma (1982)
4	5% NaCl	Oxic	1.5		McIntyre et al. (1988)
5	Seawater, Solway Firth	Oxic	2.6-3.1	In situ biogeochemical conditions and the level of physical disturbance were uncharacterised.	Toque and Baker (2007)
6	Marine sediment, Solway Firth	Not characterized	1.4-1.8	In situ biogeochemical conditions and the level of physical disturbance were uncharacterised.	Toque and Baker (2007)
7	Marine sediment microcosums simulating the Solway Firth	Progressively anoxic	0.056 ± 0.006	Salinities of 31.5 and 16.5; pH 6.4–8.0; 3.2% OC; CEC 4.0 meq/100 g and inorganic carbon 370 mg kg−1	Handley-Sidhu et al. (2009b)
8	Waterlogged sand (salinities of 31.5)	Nitrate-reducing	0.020 ± 0.003	(Salinity of 31.5; pH 7.6–7.9; 0.8% OC; CEC 1.3 meq/100 g and inorganic carbon 430 mg kg−1	Handley-Sidhu (2008)
9	Dune sand Eskmeals, Cumbria	Not characterized	0.080-0.17	pH 6.5–7.9	Toque and Baker (2006)
10	Dune sand simulating Eskmeals, Cumbria	Oxic	0.10 ± 0.01	pH 7.2–7.5; 0.8% OC; CEC 1.3 meq/100 g; inorganic carbon 430 mg kg−1 and sand moisture content of 13%	Handley-Sidhu et al (2009a)
11	Organic, clay-rich soil from Kirkcudbright	Not characterized	0.80-1.1	pH 5.8–6.0	Toque and Backer (2006)
12	Field-moist soil	Oxic	0.49 ± 0.06	pH 5.0–6.5; 12% OC; CEC 21 meq/100 g; inorganic carbon 80 mg kg−1 and soil moisture content of 22%	Handley-Sidhu et al (2009c)
13	Sandy-loamy and silty-loamy soil	Not characterized	0.19 ± 0.03	Two soils investigated; pH 5.6 and 5.7; 2.1% OC.	Schimmack et al. (2007)
14	Waterlogged soil	Nitrate-reducing	0.010-0.02*	pH 5.0 – 6.5; 12% OC; CEC 21 meq/100 g and inorganic carbon 80 mg kg^{-1}. *Corrosion ceased under anoxic conditions.	Handley-Sidhu et al (2009c)
15	Phosphate-fertilized waterlogged soil	Nitrate-reducing	0.00016-0.0044	Olsen phosphorus 27 – 45 mg kg^{-1}; pH 5.0 – 6.0; 12% OC; CEC 21 meq/100 g and inorganic carbon 80 mg kg^{-1}.	Unpublished;

Notes: * Corrosion ceased under anoxic conditions. % – percent
CEC – cation exchange capacity
DU – depleted uranium
g $cm^{-2}y^{-1}$ – gram(s) per centimeters squared year
H_2O – water
meq – milliequivalent of hydrogen
mg kg-1 – milligram(s) per kilogram
NaCl – sodium chloride
OC – organic carbon
Ti – titanium

8. SUMMARY DISCUSSION

The data reported here support the modeling of net uranium transport from a corroding DU penetrator dart segment emplaced in a relatively thin layer of Site soil, when subjected to a standardized accelerated leach protocol (ASTM Method D4646). In this scenario, a number of competing phenomena are occurring (dart corrosion, uranium oxide dissolution and leaching, subsequent partitioning of uranium to soil and aqueous phases, etc.), such that the data summarized in Appendix A-1 represent net uranium partition to the leachate under the defined test conditions (i.e., uranium release rate).

The mechanistic steps for penetrator dart corrosion after embedment in near-surface (oxic) soil, and the subsequent transport of relatively mobile uranyl species in soil and water phases, may be simplistically represented as follows:

A. Oxidation of uranium alloy to form solid corrosion rind:

$$x\text{U (metal)} + y\text{O}_2 + n\text{H}_2\text{O} \rightarrow (\text{UO}_2 + \text{UO}_3 \bullet n\text{H}_2\text{O})$$

B. Leaching/dissolution of schoepite-type (UO_3) corrosion rind:

$$\text{UO}_3 \cdot 2\text{H}_2\text{O}_{(s)} + 2\text{H}^+ \leftrightarrow \text{UO}_2^{2+} + 3\text{H}_2\text{O}_{(l)}$$

C. Complexation of leached uranyl ion (UO_2^{2+}):

$$\text{UO}_2^{2+} + 2\text{HCO}_3^- \leftrightarrow \text{UO}_2(\text{CO}_3)_2^{2-} + 2\text{H}^+$$

D. Retardation of leached uranyl ion by soil minerals (surface complexation):

$$\text{(e.g.) FeOH} + \text{UO}_2^{2+} + 2\text{CO}_3^{2-} + \text{H}^+ \leftrightarrow [\text{FeOH}_2^+ \text{UO}_2(\text{CO}_3)_2^{-2}]$$

E. Formation of secondary alteration minerals (potential long-term sinks for U)

Each of these mechanistic steps is discussed in more detail below.

8.1. Mechanistic A: Oxidation of Uranium Alloy to Form Solid Corrosion Rind (Analogy to Nuclear Fuel Element Corrosion)

At proposed disposal repository depths, ground waters are inevitably oxygen-free and any oxygen introduced during repository construction and operation prior to sealing will be rapidly consumed by mineral and biochemical reactions in the surrounding clays and by minor corrosion of the container (Shoesmith, 2007). These conditions are thus different than those for DU fragments located in the oxic vadose zone of soil, but they may be applicable to fragments in waterlogged anoxic soils.

High activity fuel element corrosion in anoxic water is driven reaction by radiolytically-produced H_2O_2; under conditions of lower alpha radiation fields (and with dissolved oxygen), corrosion by chemical reactions prevail, with transport of uranium being solubility-limited (Shoesmith, 2007); see Fig. 19 (from Shoesmith, 2007). The very low specific activity of depleted uranium UO_2 (0.017 mega Becquerel per

gram of UO_2 [MBq/g-UO_2]) place it within the regime of solubility control, with minimal accelerated corrosion due to radiolytic production of peroxide.

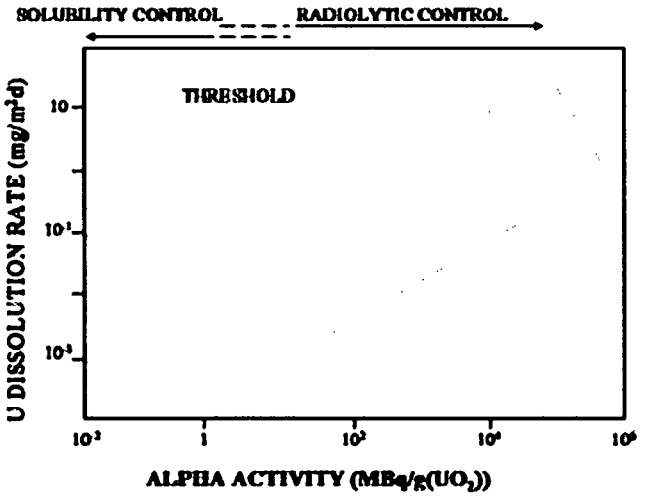

Figure 19. Illustration Showing the Concept of an Alpha Activity Threshold for the Onset of Radiolytically-controlled Fuel Corrosion.

Below the threshold, the fuel dissolution process is solubility-controlled. (From Shoesmith, 2007, Fig. 10).

Hilton (2000) and Delegard and Schmidt (2008) review the corrosion of uranium metal in *anoxic* humid environments. According to most technical literature on the subject, the net *anoxic* reaction of uranium metal with water is hyperstoichiometric, forming UO_{2+x}, with x being less than 0.1 (Hilton 2000). The technical literature also notes that the uranium oxide initially formed on the metal surface is not protective and periodically spalls from the surface. The initial UO_2 corrosion product will readily react with gaseous or dissolved atmospheric oxygen and is further oxidized to form phases such as metaschoepite, nominally $UO_3 \cdot 2H_2O$ (Sinkov et al. 2008):

$$UO_2 + 0.5\ x\ O_2 \rightarrow UO_{2+x}$$

$$UO_2 + 0.5\ O_2 + 2\ H_2O \rightarrow UO_3 \cdot 2H_2O$$

U metal corrosion in *anoxic* liquid water generally is uniform, and the corrosion rate is linear (proportional to time) or specifically paralinear (initially parabolic but becoming linear following cyclic spallation and re-generation of the non-adherent uranium oxide layer).

Reported measurements of the corrosion rates of uranium metal in aerated or oxic liquid water are much more limited than those in anoxic water, and available data show a great deal of variation (Delegard and Schmidt, 2008). According to the critical data review by Delegard and Schmidt , the projected uranium

metal corrosion rate at 15 degrees Celsius (°C) for anoxic water is approximately 260-times greater than the *oxic* water rate.

However, as Hilton (2000) observes, there is no simple correlation between corrosion rate data and release rate data. The corrosion rate is the rate at which a material physically degrades. It is based on the total amount of material reacted per unit surface area. The release rate is the rate that material is transported away from the sample. The release rate is related to the corrosion rate, but it depends on a number of other factors. Some of these factors include structural adherence of oxide, solubility, colloid formation and sequestration of radionuclides in alteration products.

Handley-Sidhu et al. (2010) present a summary table for literature estimates for corrosion rates of DU-Ti alloy. Rate estimates vary greatly (e.g., 0.0002 to 2 g $cm^{-2}y^{-1}$), but are generally lowest for nitrate-reducing, phosphate-fertilized waterlogged soil and highest in oxic brackish or marine (saline water) environments. Figure 20, from Handley-Sidhu et al. (2010), illustrates conceptually the metallic uranium corrosion component of the net uranium release mechanism. The tests described in this investigation predominantly represent "field-moist" (oxic) environment, with brief interludes of suboxic exposure (cell flooding during the exposure cycle; see Section 2.2). Uranium metal is observed to corrode more rapidly under field-moist than waterlogged exposure condition (Handley-Sidhu et al., 2010).

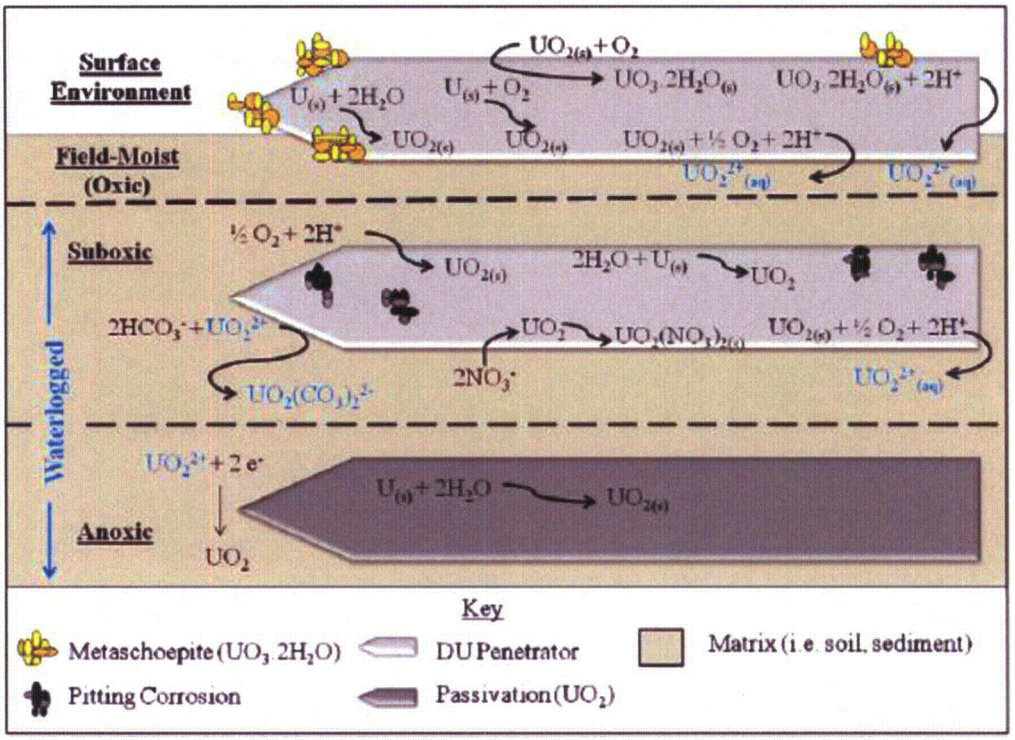

Figure 20. Conceptual Model of the Main Mechanisms of DU Penetrator Corrosion in the Terrestrial Environment (Figure 2 in Handley-Sidhu et al., 2010)

De Windt et al. (2003) have published model predictions for UO_2 oxidative dissolution and subsequent uranium transport. (In the data examples considered here, UO_2 is a primary corrosion product for uranium metal).

8.2. Mechanistic B: Leaching/Dissolution of Schoepite-type (UO_x) Corrosion Rind

Data presented in this report and elsewhere in the literature indicate that the near-surface corrosion products on weathered DU penetrator darts in oxic moist soil are similarly dominated by uraninite (UO_{2+x},) and schoepite-type minerals ($UO_3 \cdot nH_2O$, where n is less than or equal to 2).

Experimental and theoretical treatment by Jang et al. (2006) predicts solubility of schoepite to be approximately 1E-5 to 1E-6 moles per liter (mol/L) (2 to 20 ppm) at near-neutral (pH 6 to 7.5) oxic groundwater. In this investigation, leaching of corroded DU penetrator darts within shallow soil columns requires considerable time to approach these limiting levels of soluble uranium in the drained leachate solution, indicating that considerable uranium must be held up by minerals present in the soil prior to

saturation. The net mobility of the dissolved uranyl ions in groundwater is largely controlled by the bicarbonate anion in the aqueous phase and the presence of hydrous metal oxide phases in the soil.

8.3. Mechanistic C: Complexation of Leached Uranyl Ion (UO_2^{2+})

The potential off-site mobility of uranium thus depends on the partitioning of uranium between aqueous and solid (soil and sediment) phases. The aqueous speciation of actinides in low-temperature geochemical solutions is dictated primarily by the redox potential, the pH, and the total dissolved carbonate concentration (Murphy and Shock, 1999). Hexavalent uranium (as uranyl, UO_2^{2+}) may be relatively mobile, forming strong soluble complexes with ubiquitous (bi)carbonate ion which renders it appreciably soluble even under mild reducing conditions.

Figures 21 and 22 are published distribution estimates for uranium in modeled water compositions; it is strongly recommended that a theoretical distribution diagram be computed using the thermodynamic master parameters (redox potential [Eh], pH, and alkalinity), plus dissolved oxygen and complexation ligands such as fluoride and phosphate ions, that have been determined for authentic *in-situ* JPG groundwater (or porewater) composition. Established soil-water chemistry models, such as PHREEQC or MINTEQA, may be helpful.

Note in Appendix A-1 that near-field rainwater leachate has low total alkalinity (typically only a few mg/L as $CaCO_3$); this may help limit uranium transport in the near-field. Also note that many of the near-field leachate samples had pH values in the range of approximately 5.5 to 7.5, a favorable range for sorption to many types of soil minerals and mineral coatings (Fig. 23).

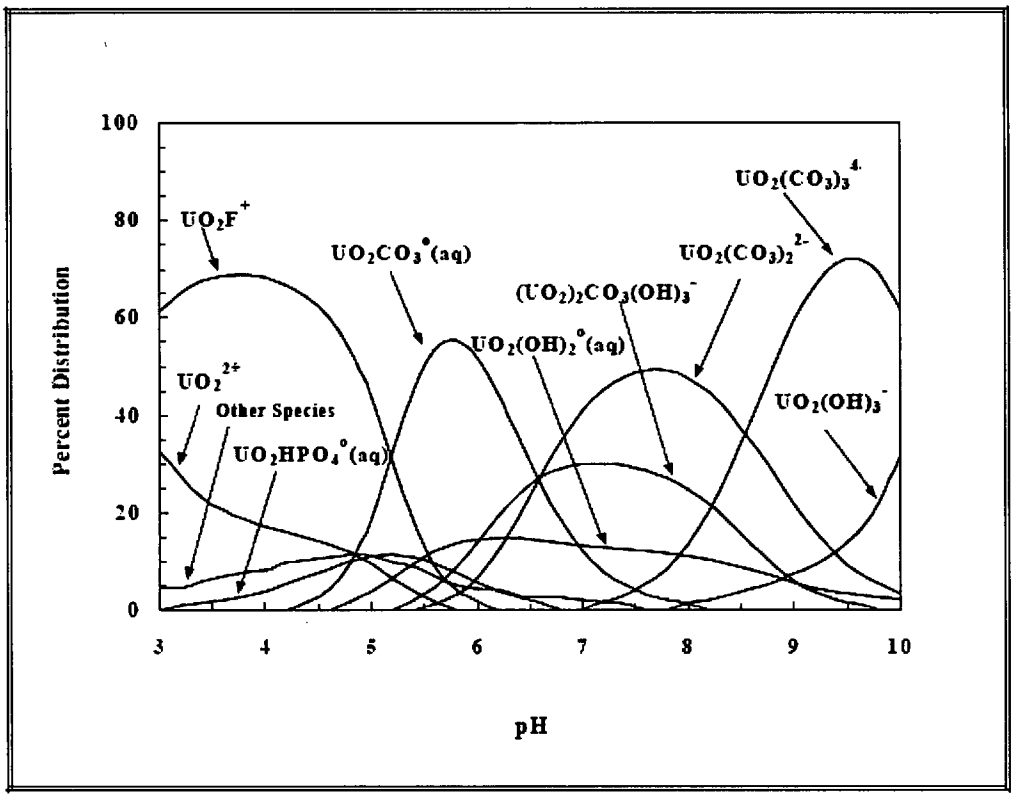

Figure 21. Calculated Distribution of U(VI) Hydrolytic Species as a Function of pH at 1,000 µg/L (4.2E-6 mol/L) Total Dissolved U(VI) in a Model Groundwater Composition Containing Bicarbonate Ion.
(From Fig. 5.7 in EPA 402-R-99-004B).

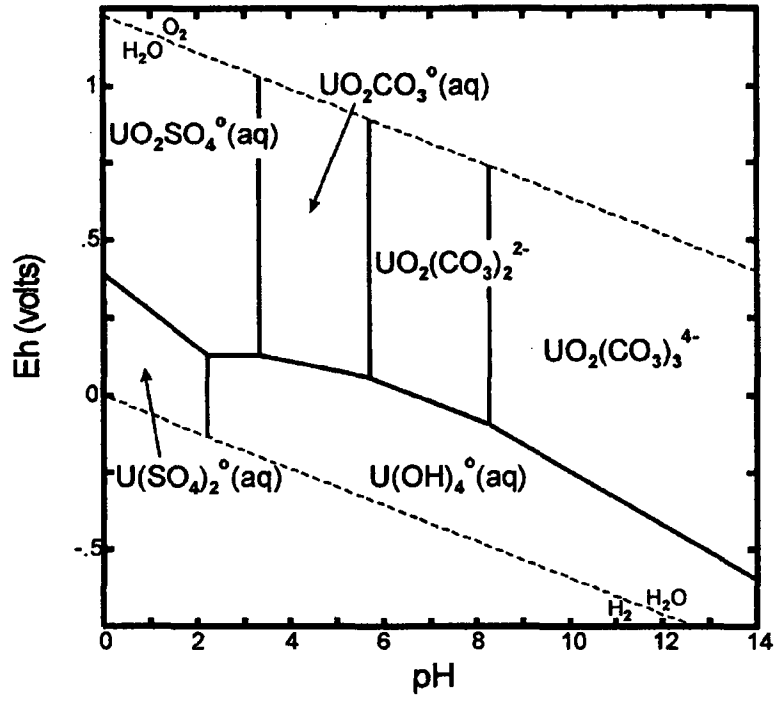

Figure 6.2. Eh-pH Diagram Showing the Dominant Aqueous Complexes of Uranium [Diagram was calculated at 25 °C and a concentration of 10^{-7} mol/L total dissolved uranium in the presence of dissolved chloride, nitrate, carbonate, and sulfate.]

Figure 22. Eh-pH Phase Diagram for Soluble Uranium (Figure 6.2 in Krupka and Serne, 2002).

8.4. Mechanistic D: Retardation of Leached Uranyl Ion by Soil Minerals (Surface Complexation)

Sorption of ions to mineral surfaces is strongly dependent upon the solution phase pH value, which affects the surface charge distribution on the sorptive substrate. As the pH value increases above the point of zero charge (pzc) for the substrate, the surface becomes more negatively charged and the sorption of cations generally increases. Conversely, sorption of anions is generally favored at pH values below the pzc of the substrate.

Quartz (pzc less than or equal to 3)[9] is typically the predominant mineral in soil; this is expected to give the soil matrix a net negative surface charge under most environmental pH conditions, which in turn attracts colloidal-sized iron oxide particles, the latter generally having a net positive surface charge under the same conditions (Puls and Powell, 1982). A double-layer effect occurs: silica would normally repel

[9] E. Papirer (Ed.) (2000), Adsorption on Silica Surfaces, Surfactant Science series, Vol. 90.

anions, such as complexed U; however, the silica does attract a layer of colloidal hydrous metal oxides, which can then surface complex with uranyl carbonate.

For iron-containing minerals, the pzc is typically in the range of 6 to 8.5 (Silva and Nitche, 1995). The isoelectrical point (pH_{IEP}) for metastable 2-line ferrihydrate (dominant Fe-colloid species in aquatic systems) is pH 8.7 (Shafer et al., 2003) (positive zeta potential [i.e., net positively-charged surface] at pH less than pH_{IEP}). Sorption by iron oxides of uranyl carbonate anions is strongly affected by solution pH value, with an optimum specific sorption occurring at pH values near 5.5 to 6.5 (Farrell et al., 1999; Krupka and Serne, 2002; Jang et al., 2007), although removal of soluble uranium by all mechanisms (e.g., by sorption, ion-exchange and co-precipitation) may continue to be effective at elevated pH values. Barnett et al. (2002) had fair success modeling the sorption of soluble uranium to soil minerals, based upon a model independently developed for sorption of uranyl ion to ferrihydrate; both experimental data and theoretical prediction indicate maximum Kd values for uranyl ion sorbed to soil minerals at pH values near 5 to 8 (see also Figure 14).

In the illustrative equations above, Mechanistic D represents surface sorption of soluble uranyl carbonate complex to solid hydrous iron oxide mineral substrate, such as goethite (Hsi and Langmuir, 1985). Other important uranium surface complexation agents in soil include clay and phosphate minerals and natural organic matter (NOM) (EPA 402-R-99-004B). Insoluble NOM may decrease the mobility of uranium by forming surface terinary complexes (Murphy et al., 1999); soluble NOM (e.g., fulvic acid) may increase the mobility of uranyl.

In the presence of (bi)carbonate, partition of uranyl to hydrous metal oxides and select other soil mineral phases is usually maximum in the near-neutral pH range of approximately 5 to 8 (USEPA 1999; Krupka and Serne, 2002; Ho and Miller, 1986; Meinrath et al., 1986; Koss, 1988); see Figure 14. The extent of uranium binding to soil minerals varies considerably with the Site-specific compositions of soil and groundwater constituents; see Figure 12. Soils containing larger percentages of iron oxide minerals and mineral coatings and/or clay minerals will exhibit higher sorption characteristics for uranium than soils dominated by quartz and feldspar minerals (Krupka and Serne, 2002).

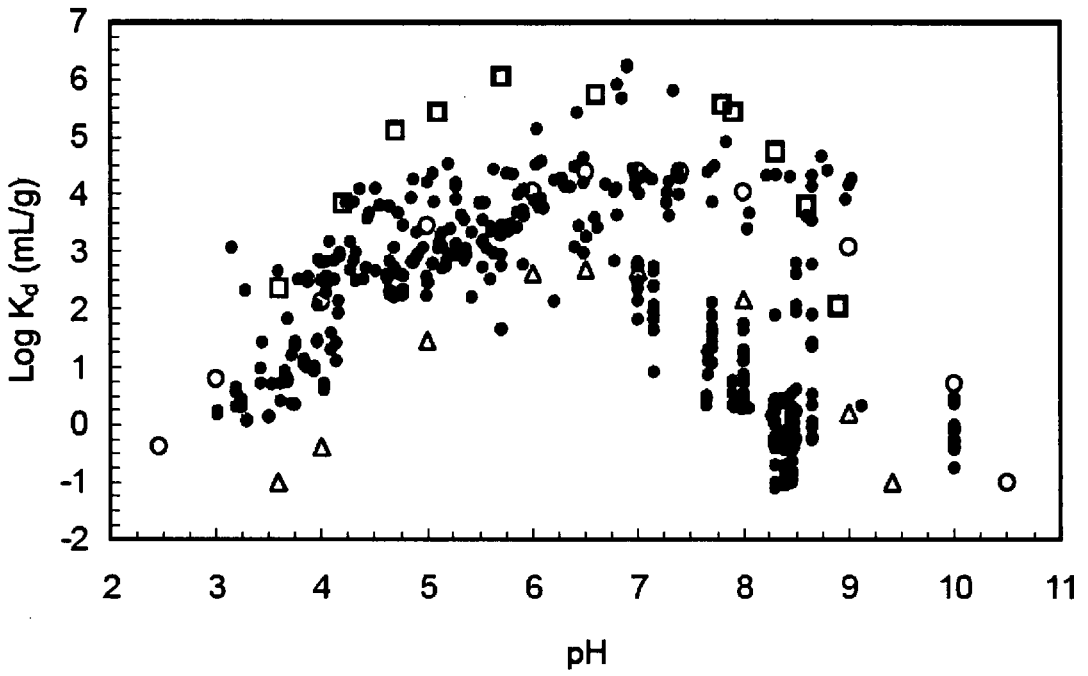

Figure 23. Distribution of U(VI) Kd Values for Sediments and Single-Mineral Phases as a Function of pH in Carbonate-Containing Aqueous Solutions.

[Filled circles represent U(VI) Kd values compiled from the literature for sediments, and listed in Table J.5 in EPA (1999b). Open symbols represent Kd maximum and minimum values estimated from uranium adsorption measurements plotted by Waite et al. (1992) for ferrihydrite (open squares), kaolinite (open circles), and quartz (open triangles).] This illustration is taken from Figure 6.4 in Krupka and Serne (2002).

8.5. Mechanistic E. Formation of Secondary Alteration Minerals (potential long-term sinks for U)

Finch and Murakami (1999) describe the phenomenon of uranium paragenesis, as noted at weathered natural uraninite deposits. First, uraninite slowly dissolves and uranyl oxyhydroxide minerals (e.g., schoepite) precipitate. Next is the near-surface replacement of earlier-formed uranyl oxyhydroxides by moderately insoluble uranyl silicates. In weakly complexing waters, some uranium is transported short distances to precipitate on the outer surfaces of corroding uraninite as a coarsely crystalline rind of uranyl oxyhydroxides, such as schoepite or (in calcium-rich systems) becquerelite. Monocarbonates such as (sparingly soluble) rutherfordine (UO_2CO_3) may precipitate where the partial pressure of dissolved carbon dioxide (pCO_2) values are sufficient (e.g., as produced by biological activity on natural organic matter). The early formed uranium oxyhydroxides may dissolve to form a soluble carbonate complex (e.g., $UO_2(CO_3)_3^{2-}$), or may be replaced by (e.g.) rutherfordine or becquerelite. Many other additional alteration products may be formed, depending upon local mineralogy and ground water composition, since approximately 200 uranium minerals are known to exist.

For the paragenesis of the initial corrosion product, some analogies may also be drawn from the studies performed to support the geologic disposal of spent nuclear fuel (Wonkiewicz and Buck, 1999), although the applicable conditions of ambient temperature and fugacity of dissolved gases (O_2, CO_2) are often quite different. Oxidative corrosion occurs along the grain boundaries of near-surface UO_{2+x}. Carbonate concentration has a strong effect on the dissolution rate of UO_2. Long-term (multi-year) studies with unirradiated UO_2 indicated precipitation of alteration products such as dehydrated schoepite within the corroded inter grain boundaries, with additional interactions of uranyl with silicon, sodium, potassium, calcium, etc., contributed from the synthetic ground water leachant solution, to form a variety of sparingly-soluble alteration phases. These alteration phases may limit the aqueous transport or diffusion of components near the surface interface between the reacting solid and the leachant solution. In natural geologic systems, uranyl oxide hydrate (schoepite-type) phases and alkali and alkaline earth uranyl silicate alteration phases may persist for very long times, thereby acting as relatively long-term sinks for U. Johnson et al. (2004) report that formation of uranium-silicate mineral aggregates appears to be the limiting factor in vertical vadose zone transport of DU at the arid site they investigated.

Formation of alteration products represents a variety of reactions between uranyl and other constituents in soil and ground water to precipitate relatively insoluble U-containing solids, such as uranyl silicates (e.g., uranophane $[Ca(UO_2)_2(SiO_3OH)_2 \cdot (H_2O)_5]$) or phosphates (a family of more than 40 minerals, represented by autunite $[Ca[(UO_2)(PO_4]2 \cdot (H_2O)_{10}]$ (Finch and Murakami, 1999). Figure 22 (from Finch and Murakami, 1999) shows some possible routes for formation of both soluble and insoluble uranium complexes.

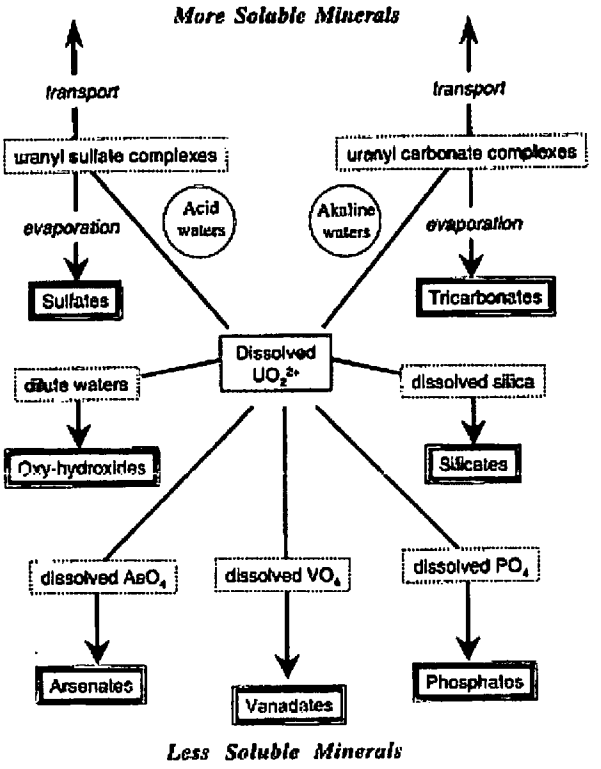

Figure 24. Select Reactions of Dissolved Uranyl Ion (Figure 2 from Finch and Murakami, 1999).

Delegard and Schmidt (2008), report that uranium species identified in sludge from Hanford K-basin, which was historically used for storage of irradiated spent fuel (including uranium metal), now shows the progression of phases arising from the corrosion of uranium metal and subsequent uranium oxidation and mineralization reactions. The identified phases include uraninites (UO_2, U_4O_9, U_3O_7), triuranium octaoxide (U_3O_8), various schoepites and metaschoepites (e.g., $UO_3 \cdot 2.25H_2O$, $UO_3 \cdot 2H_2O$), uranyl peroxides (studtite and metastudtite; respectively), and hexavalent sodium, potassium, and calcium uranium compounds, such as becquerelite and compreignecite [$K_2(UO_2)_6O_2(OH)_6 \cdot 8H_2O$], but no residual uranium metal itself.

9. COMPARISON LITERATURE DATA FOR THE DISSOLUTION RATE FOR DU PENETRATOR DARTS AND SUBSEQUENT MIGRATION OF URANIUM

Estimates of JPG uranium release rates and crude estimates for "corrosion rates" (to allow comparison to literature compilations; see Handley-Sidhu, 2010) are derived in Appendix 2. The calculated values are summarized in Table 25. The calculation for "corrosion rate" in Table 27 includes the cumulative mass balance for soil and water (see Table 22).

Table 25. Estimates for Mean DU Release Rate and Nominal DU "Corrosion Rate" for JPG Data

(Leach intervals #10-23, elapsed time interval 211-463-d)

Cell ID	DU Release Rate * (g-U/d)	Nominal DU "Corrosion Rate" ** ((g-U) $cm^{-2}y^{-1}$)
1-AC-S	(1.55 ± 0.68)E-04	1.56E-02
2-AC-U	(0.86 ± 0.69)E-04	1.07E-02
3-CR-S	(1.21 ± 0.72)E-04	2.10E-02
4-CR-U	(1.24 ± 1.02)E-04	2.23E-02
5-GR-S	(0.69 ± 0.27)E-04	1.73E-02
6-GR-U	(0.35 ± 0.20)E-04	3.48E-02
7-AC (no dart)	(5.16 ± 1.69)E-07	N/A

Notes:

* See discussion in Appendix 3.

** Estimates for nominal DU corrosion rate include mass balance of total DU Partitioned to soil and water for the duration of the testing.

AC – Avonsburg/Cobbsfork
CR – Cincinnati/Rossmoyne
ID – identification
GR – Grayford/Ryker
g-U/d – gram(s) uranium per day
(g-U) $cm^{-2}y^{-1}$ – gram(s) uranium per square centimeters year
JPG – Jefferson Proving Ground
N/A – not applicable

In a unique long-term study, German scientists investigated the behavior of armor piercing DU ammunition in soil, which was exposed to weathering and leaching.[10] These scientists noted that when uranium ammunition in organic-rich farm soil is exposed to simulated weathering under laboratory conditions (using synthetic rainwater leachant for a total duration of three years), secondary uranium minerals are formed, e.g., sabugalite [$HAl(UO_2)_4(PO_4)_4 \cdot 15H_2O$], in which toxic uranium is tightly bound. These scientists estimated that DU bullets could completely transform into minerals such as sabugalite within a time span of only 50 years (see also Schimmack et al., 2007). In this instance, it is likely that phosphate in the fertilized farm soil promoted stabilization of the leached uranyl ion; Bostick (2003) note that phosphate mineral soil amendment greatly retards the mobility of uranium by a combination of short-term surface sorption and longer-term precipitation and mineralization.

Handley-Sidhu and co-workers (2009, 2010) report that mechanism of corrosion of (DU) penetrator waste in the near-surface terrestrial environment and the corrosion products formed were highly dependent on the water status of the soil. Under field-moist (presumably oxic) conditions, DU corroded at a rate of 0.49 plus or minus 0.06 g cm^{-2} y^{-1} and the main uranium input to surrounding soil was large metaschoepite particles. However, under waterlogged (presumably less oxic) conditions the rate of corrosion was significantly slower at 0.01 to 0.02 g cm^{-2} y^{-1} and occurred with the release of dissolved species to the surrounding environment. These predictions differ qualitatively from those of Hilton (2000) and Delegard and Schmidt (2008), who state that corrosion of enriched uranium metal (with

[10] http://www.fzd.de/db/Cms?pNid=1770&pOid=26451 ; http://www.hzdr.de/db/Cms?pOid=24122&pNid=473

radiolysis generation of H_2O_2) is much greater under *anoxic* conditions (but also see Figure 10, which indicates that uranium dissolution rates are lower under solubility-limited conditions).

Handley-Sidhu and co-workers predict that, under sub-oxic conditions, complete corrosion of a 120 mm penetrator would take approximately 540-y. The water content and biogeochemistry of the soil had a marked effect on the corrosion rate of DU. Corrosion was reportedly 40 times faster under field moist conditions than in waterlogged soils, thus the authors predict complete corrosion of a 120 mm Charm penetrator was calculated to take 90-y and 3900-y, respectively.[11] Soil microbial activity is expected to affect both the corrosion and net transport of uranium. Among other effects, microbial activity contributes to elevated pCO_2 in soil pore water.

British investigators[12] report that DU projectile corrosion and subsequent seepage of leached uranium are very Site-specific, with projection of mean penetrator dissolution times of around 12-y and 90-y for two soil types and water flux conditions. Yet another published estimate[13] predicted that a DU penetrator can be fully oxidized to corrosion products (e.g., uranium oxides and carbonates) within 25-y to 35-y after impact. An earlier report had estimated that near-surface Charm-3 DU darts (initial mass 4500-g) could totally corrode within as little as 20 years; UNEP, 2002; other estimates for dissolution of this size dart range from 30-y to 60-y (Handley-Sidhu et al., 2010).

Johnson et al. (2004) assessed the solubility of corrosion and migration products from two DU kinetic energy penetrators exposed on the desert surface for a 22-y period. They note that as uranium leached from the penetrator migrates beyond several centimeters in depth, it forms insoluble aggregates with silicate minerals. The formation of uranium-silicate mineral aggregates appears to be the limiting factor in vertical vadose zone transport of DU at the site investigated.

The rate of corrosion of DU projectiles in the environment is sensitive to the oxygen fugacity (e.g., oxic near-surface deposition versus anoxic water-logged condition). The subsequent migration of leached uranium will also be very sensitive to water properties (e.g., pH and redox condition, ligands such as bicarbonate, etc.), as well soil parameters, such as microbial consortia, natural organic matter content, hydrous metal oxide minerals and mineral coatings), etc.

Consensus appears to be that corroding spent penetrator darts may persist in the environment for many decades, depending upon the Site-specific conditions that include dissolved gas fugacity (pO_2, pCO_2), water properties (e.g., alkalinity, salinity), soil organic matter and mineralogy (e.g., hydrous metal oxide, phosphate minerals), and the native soil microbial and fungi consortia. Longer-term protection of ground water may be reliant upon strong sorption of released uranyl, and/or subsequent formation of less-soluble alteration products, within the associated near-field soil zone.

[11] http://goldschmidt.info/2008/abstracts/finalPDFs/A350.pdf
[12] http://proceedings.ndia.org/jsem2007/4132_TOQUE.pdf
[13] http://www.mindfully.org/Nucs/2003/DU-UNEP-10mar03.htm

10. REFERENCES AND BIBLIOGRAPHY

Abdul-Hadi A, Alhassanieh O, Ghafar M., "Disequilibrium of uranium isotopes in some Syrian groundwater," *Applied Radiation and Isotopes*, Volume 55, Issue 1, July 2001, Pages 109-113.

AEPI (U.S. Army Environmental Policy Institute), *Health and Environmental Consequences of Depleted Uranium Use in the U.S. Army*, technical report, Atlanta, Ga.: U.S. Army Environmental Policy Institute, June 1995.

American Public Health Association (APHA), *Standard Methods for the Examination of Water and Wastewater*, Method 2320 B (Alkalinity/Titration Method).

ASTM Method D 4646-03, *Standard Test Method for 24-h Batch-Type Measurement of Contaminant Sorption by Soils and Sediments.*

ASTM Method D 5744, *Accelerated Weathering of Solid materials Using a Modified Humidity Cell.*

ASTM Method D2216, *Standard Test Method for Laboratory Determination of Water (Moisture Content of Soil and Rock by Mass).*

ASTM Method D4972-01, *Standard Test Method for pH of Soils,* (http://www.astm.org/Standards/D4972.htm)

Barnett, M. O.; Jardine, P. M.; and Brooks, S. C. (2002). "U (VI) adsorption to heterogeneous subsurface media: Application of a surface complexation model." *Environ. Sci. Technol.*, 36(5), 937-942.

Baumann, N.; Arnold, T.; Geipel, G.; Trueman, E.R.; Black, S.; Read, D; (2006), "Detection of U(VI) on the surface of altered depleted uranium by time-resolved laser-induced fluorescence spectroscopy (TRLFS)," *Science of the total environment*, 366, (2-3), pp. 905-909.

Bostick, W.D., *Uranium Transport Modeling*, ANS Topical Meeting, Decommissioning, Decontamination & Reutilization, Chattanooga, TN, Sept. 2007.

Bostick, W.D. (2003), *Use of Apatite for Chemical Stabilization of Subsurface Contaminants*, Final Report to U.S. Department of Energy, under contract DE-AC26-01NT41306. [http://www.osti.gov/dublincore/ecd/servlets/purl/820754-Fk9X7K/native/820754.pdf]

Brock, Amy L. (2003), *Corrosion of Depleted Uranium In An Arid Environment: Characterization With XRD, Sem/Eds And Microprobe Analyses*, Presented to The Geological Society of America, Annual Meeting (November 2–5, 2003) (http://gsa.confex.com/gsa/2003AM/finalprogram/abstract_58213.htm).

Bryan, C.R. and Siegel, M.D. (1998). *Irreversible adsorption of uranium onto iron oxides: a mechanism for natural attenuation at uranium contaminated sites*. In Eighth Annual West Coast Conference on Contaminated Soils and Groundwater, Abstracts and Supplemental Information, Association for the Environmental Health of Soils, Oxnard, CA, 201p.

Buck, B.J.; A.L. Brock (2004), "Corrosion of Depleted Uranium in an Arid Environment: Soil-Geomorphology, SEM/EDS, XRD, and Electron Microprobe Analyses," *Soil & Sediment Contamination*, 13:545–561. (http://www.rockmagnetism.ru/articles/415.pdf).

Burns, P.C.; Finch, R. (eds.), *Reviews in Mineralogy, Vol. 38, Uranium: Mineralogy, Geochemistry and the Environment*, Mineralogy Soc. of America (1999).

Burns, P.C. (1999), "The Crystal Chemistry of Uranium," Chapter 2 in Burns, P.C.; Finch, R. (eds.) Reviews in Mineralogy, Vol. 38, *Uranium: Mineralogy, Geochemistry and the Environment*, Mineralogy Soc. of America.

Casas, I; J. De Pablo; J. Gim´Enez; M.E. Torrero; J. Bruno; E. Cera; R.J. Finch, R.C. Ewing (1998), The role of pe, pH, and carbonate on the solubility of UO_2 and uraninite under nominally reducing conditions, *Geochimica et Cosmochimica Acta*, Vol. 62, No. 13, pp. 2223–2231.

Chen, J.P. and S. Yiacoumi (2002), "Modeling of Depleted Uranium Transport in Subsurface Systems," *Water, Air, & Soil Pollution*, **140** (1-4).

Curtis, G. P.; J. A. Davis; and D. L. Naftz (2006), "Simulation of reactive transport of uranium (VI) in groundwater with variable chemical conditions," *Water Resour. Res.*, **42**, (4).

Danesi, P.R.; Markowicz, A.; Chinea-Cano, E.; Burkart, W.; Salbu, B.; Donohue, D.; et al. (2003) "Depleted uranium particles in selected Kosovo samples." *J Environ Radioactiv*; **64**:143–54.

Del Nero, M.; S. Salah; T. Miura; A. Clement; F. Gauthier-Lafaye (1999), "Sorption/Desorption Processes of Uranium in Clayey Samples in the Bangome Natural Reactor Zone, Gabon," *Radiochim. Acta*, **87**, 135-149.

Delegard, C.H.; A.J. Schmidt (2008), *Uranium Metal Reaction Behavior in Water, Sludge, and Grout Matrices*, PNNL-17815 (http://www.pnl.gov/main/publications/external/technical_reports/PNNL-17815.pdf).

De Windt, L.; A. Burnol; P. Montarnal; J. van der Lee (2003), "Intercomparison of reactive transport models applied to UO2 oxidative dissolution and uranium migration," *J Contam Hydrol.*; **61** (1-4):303-12.

Douglas, M.; Clark, S.B.; Freise, J.L.; Arey, B.W.; Buck, E.C.; Hanson, B.D. (2005), "Neptunium(V) partitioning to uranium(VI) oxide solids," *Environ. Sci. Technol.*, **39**, 4117-4124.

Ebinger, E.H. and W.R. Hansen (1996), *Jefferson Proving Ground Data Summary and Risk Assessment*, LA-UR-96-835, (http://jpgbrac.com/documents%5Cadmin_record%5Cbase%20operations%20and%20closure%5Cjpg%20data%20summary%20and%20risk%20assessment.pdf).

Falck, W.E.; D. Read; S. Black; D. Thornley; M. Siitari-Kauppi (2009), *Uranium Migration in Crystalline Rocks*, EUR 23816 EN – 2009 (viewable at URL: http://publications.jrc.ec.europa.eu/repository/bitstream/111111111/5891/1/reqno_jrc50583_report_eur_23816_en-final.pdf%5B1%5D.pdf).

Farrell, J.; W.D. Bostick; R.J. Jarabek; J.N. Fiedor (1999), Uranium removal from ground water using zero valent iron media, *Ground Water*, **77**(4), 618-624.

Finch, R.; Murakami, T. (1999), "Systematics and Paragenesis of Uranium Minerals," Chapter 3 in Burns, P.C.; Finch, R. (eds.), *Reviews in Mineralogy*, Vol. 38, Uranium: Mineralogy, Geochemistry and the Environment, Mineralogy Soc. of America.

Gerstmann, U.C.; W. Szymczak; V. Höllriegl; W. Bo Li; P. Roth; P.Schramel; S. Takenaka and U. Oeh, "Investigations on the solubility of corrosion products on depleted uranium projectiles by simulated body fluids and the consequences on dose assessment," *Radiation and Environmental Biophysics*, Volume 47, Number 2, 205-212.

Giblin, A.M.; Batts, B.D.; Swayne, D.J. (1981). "Laboratory Simulation Studies of Uranium Mobility in Natural Waters," *Geochim. Cosmochim. Acta*, **45**, 699-709.

Gorman-Lewis, D.; J.B. Fein; P.C. Burns; J.E.S Szymanowski, and J. Converse (2008A), "Solubility measurements of the uranyl oxide hydrate phases metaschoepite, compreignacite, Na–compreignacite, becquerelite, and clarkeite," *J. Chem. Thermodynamics,* 40980–990.

Gorman-Lewis, D.; P.C. Burns; J.B. Fein (2008B), "Review of uranyl mineral solubility measurements," *J. Chem. Thermodynamics* **40**, 335–352.

Handley-Sidhu, S.; P.J. Worsfold; C. Boothman; J.R. Lloyd; R. Alvarez; F.R. Livens; D.J. Vaughan; M.J. Keith-Roach (2009a), "Corrosion and Fate of Depleted Uranium Penetrators under Progressively Anaerobic Conditions in Estuarine Sediment," *Environmental Science & Technology 43* (2), 350-355.

Handley-Sidhu, S.; P.J. Worsfold; F.R. Liven; D.J. Vaughan; J.R. Lloyd; C. Boothman; M. Sajih; R. Alvarez; M.J. Keith-Roach (2009b), "Biogeochemical Controls on the Corrosion of Depleted Uranium Alloy in Subsurface Soils", *Environmental Science & Technology*, **43** (16), 6177-6182.

Handley-Sidhu, S; Bryan, N.D.; Worsfold, P.J.; Vaughan, D.J.; Livens, F.R. and Keith-Roach, M.J. (2009c). "Corrosion and transport of depleted uranium in sand-rich environments." *Chemosphere*, 77, 1434-1439.

Handley-Sidhu, S.; Keith-Roach, M.J.; Lloyd, J.R.; Vaughan, D.J. (2010), "A review of the environmental corrosion, fate and bioavailability of munitions grade depleted uranium," *Sci Total Environ 408(23):5690-700.*

Hilton, B.A. (2000). *Review of Oxidation Rates of DOE Spent Nuclear Fuel Part 1: Metallic Fuel.*ANL-00/24, Argonne National Laboratory, Idaho Falls, ID. [text available at URL: http://www.osti.gov/bridge/product.biblio.jsp?osti_id=775264].

Hlavay, J.; Prohaska, T.; Weisz, M.; Wenzel, W.W.; Stingeder, G.J. (2004). "Determination of Trace Elements Bound to Soils and Sediment Fractions," *Pure Appl. Chem.*, **76**(2), 415-442.

Ho, C.H.; Miller, H.N. (1986) "Adsorption of Uranyl Species from Bicarbonate Solution onto Hematite Particles," *J. Colloid Interface Sci.*, **110**, 165-171.

Hsi, C.-K.; Langmuir, D. (1985), "Adsorption of Uranyl onto Ferric Oxyhydroxides: Application of the Surface Complexation Site-Binding Model," *Geochim. Cosmochem. Acta*, **49**, 1931-1941.

Jang, J.E.; B.A. Dempsey; W.D. Burgos (2006), "Solubility of schoepite: comparison and selection of complexation constants for U(VI)," *Water Research* **40** 2738-2746. (Viewable at URL: http://www.engr.psu.edu/ce/enve/burgos/new/publications/Jang%20et%20al%202006%20Wat%20Res%20schoepite%20solubility.pdf).

Jang, J.E.; B.A. Dempsey and W.D. Burgos (2007), "AModel-Based Evaluation of Sorptive Reactivities of Hydrous Ferric Oxide and Hematite for U(VI)," *Environ. Sci. Technol.* **2007**, 41, 4305-4310.

Johnson, W.H.; B.J. Buck; H. Brogonia; A.L. Brock (2004), "Variations in Depleted Uranium Sorption and Solubility with Depth in Arid Soils," Soil *and Sediment Contamination*, 13(6) 533 – 544.

Kertes, A.S.; Guillaumont, R. (1985) "Solubility of UO_2. A Comparative Review," *Nucl. & Chem. Waste Mgt.*, 5, 215.

Kohler, M.; Curtis, G.P.; Meece, D.E.; Davis, J.A. (2004), "Methods for Estimating Adsorbed Uranium(VI) and Distribution Coefficients of Contaminated Soil," *Environ. Sci. Technol.*, **38**, 240-247.

Koss, V. (1988), "Modeling of Uranium(VI) Sorption and Speciation in a Natural Sediment-Groundwater System," *Radiochim. Acta*, **44/45**, 403-406.

Krupka, K.M.; Serne, R.J. (2002), "Geochemical Factors Affecting the Behavior of Antimony, Cobalt, Europium, Technetium, and Uranium in Vadose Sediments," Report PNNL-14126. (Viewable at URL: http://www.pnl.gov/main/publications/external/technical_reports/PNNL-14126.pdf).

Littleton, B., "Depleted Uranium Technical Brief," EPA 402-R-06-011 (December 2006).

Manaka, M.; Y. Seki; K. Okuzawa; H. Kamioka and Y Watanabe, (2007) "Natural attenuation of dissolved uranium within a small stream of central Japan," *Limnology*, Volume 8, Number 2, 143-153.

McIntyre, J.G.; Lefeave, E.P.; Musselman, K.A., "Galvanic corrosion behaviour of depleted uranium in synthetic seawater coupled to aluminium, magnesium, and mild steal," *Corros Sci*, 1988; 44:502-10.

McLean, E.O. (1982). "Soil pH and Lime Requirement," Chapter 12 in A.L. Page (Editor), *Methods of Soil Analysis, Part 2: Chemical and Microbial Properties*, 2nd Ed., American Soc. Agronomy, Inc.

MCLinc, *Electron Microscopy Operation Guide*, MCL-7708.

MCLinc, *Acid Digestion for Metals Based on EPA Method 3050B*, MCL-7746.

MCLinc, *Inductively Coupled Plasma – Atomic Emission Spectrometry Metals Analysis*, MCL-7751.

MCLinc, *Acid Digestion of Aqueous Samples (EPA Method 3010A)*, MCL-7752.

MCLinc, *Modified Tessier Sequential Extraction Procedure for 2.5-g Soil or Sediment Sample*, MCL-7756, Appendix XX.

MCLinc, *Operator Aid for Determination of Water Content by Mass*, Operator Aid, MCL-7756, Appendix MM.

MCLinc, *ICP-MS Element/Metal Sample Preparation and Analysis (Based upon EPA Method 6020A and EPA ORD Method 200.8)*, MCL-7768.

MCLinc, *Determination of Isotopic Ratios by ICP-MS*, MCL-7769.

Meinrath, G.; Kato, K.; Kimura, T.; Yoshida, Z. (1996). "Solid-Aqueous Phase Equilibria of Uranium (VI) under Ambient Conditions," *Radiochimica Acta*, **75**, 159-167.

Mellini, M. and Riccobono, R. (2005), "Chemical and mineralogical transformations caused by weathering in anti-tank DU penetrators ("the silver bullets") discharged during the Kosovo war," *Chemosphere*, **60** (9), 1246-1252.

Moyes, L.N.; Parkman, R.H.; Charnock, J.M.; Vaughan, D.J.; Livens, F.R.; Hughes, C.R.; Braithwaite, A. (2000). "Uranium Uptake from Aqueous Solution by Interaction with Goethite, Lepidocrocite, Muscovite, and Mackinawite: An X-ray Absorption Spectroscopy Study." *Environ. Sci. Technol.*, **34**, 1062-1068.

Murakami, T.; Ohnuki, T.; Isobe, H.; Sato, T. (1997), "Mobility of uranium during weathering," *American Mineralogist* **82**, 888-899.

Murphy, W.M.; Shock, E.L. (1999), "Environmental Aqueous Geochemistry of Actinides," Chapter 5 in Burns, P.C.; Finch, R. (eds.) *Reviews in Mineralogy*, Vol. 38, Uranium: Mineralogy, Geochemistry and the Environment, Mineralogy Soc. of America.

Murphy, Richard. J.,;John. J. Lenhart and Bruce. D. Honeyman, 1999, "The Binding of Thorium and Uranium to Hematite in the Presence of Natural Organic Matter." *Colloids and Surfaces: A. Physicochemical and Engineering Aspects*, Vol. 157, pp. 47-62.

Nelson, A.J.l Meier, T.C.; Saw, C.K.; Griffith, L.V.; "Surface and bulk chemistry of calcined UO2 powders," *Journal of Vacuum Science & Technology A: Vacuum, Surfaces, and Films*, 21(3), 762-765 (2003).

Oliver, I.W.; A.B. Mackenzie; R.M. Ellam; M.C. Graham and J.G. Farmer; "Determining the extent of depleted uranium contamination in soils at a weapons test site: An isotopic investigation," *Geochimica et Cosmochimica Acta*, Volume 70, Issue 18, Supplement 1, August-September 2006, Page A457.

Oliver, I.W.; M.C. Graham; A.B. MacKenzie; R.M. Ellam and J.G. Farmer; "Distribution and partitioning of depleted uranium (DU) in soils at weapons test ranges – Investigations combining the BCR extraction scheme and isotopic analysis," *Chemosphere*, Volume 72, Issue 6, June 2008, Pages 932-939.

Payne, T.E.; P.L. Airey (2006), "Radionuclide migration at the Koongarra uranium deposit, Northern Australia – Lessons from the Alligator Rivers analogue project," *Physics and Chemistry of the Earth, Parts A/B/C*, Volume 31, Issues 10-14, 2006, Pages 572-586.

MIGRATION (2005), The 10th international conference on the chemistry and migration of actinides and fission products in the geosphere.

Payne, T.E.; Waite, T.D. (1991), "Surface Complexation Modeling of Uranium Sorption Data Obtained by Isotope Exchange Techniques," *Radiochim. Acta*, **52/53**, 487-493.

Phillips, I.; Chapple, L. (1995), "Assessment of a Heavy Metals-Contaminated Site Using Sequential Extraction, TCLP, and Risk Assessment Techniques," *J. Soil Contam.*, 4, 311-325.

Pottorff, E.T., (2004), *Distinguishing Anthropogenic Uranium at the Rocky Flats Environmental Technology Site, Golden, Colorado*, WM-4035.

Puls, R.W.; Powell, R.M. (1992). "Surface-Charge Repulsive Effects on the Mobility of Inorganic Colloids in Subsurface Systems," Chapter 4 in Sabatini, D.A. and Knox, R.C. (Eds.) *Transport and Remediation of Subsurface Contaminants*, ACS Symposium Series 491, American Chemical Society, Washington, DC., pp. 40-54.

Radenković, R.; D. Djordjević; J. Joksić; S. Djogo; P. Pfendt; and J. Raičević; *Uranium Mobility in Soils Contaminated with Depleted Uranium*, CEJOEM 2003, Vol.9. No.4.: 327–331.

Radenković, M.B.; S.A. Cupać; J.D. Joksić and D.J. Todorović, "Depleted uranium mobility and fractionation in contaminated soil (Southern Serbia)," *Environmental Science and Pollution Research*, Volume 15, Number 1, 61-67 (2008).

Relyea, J.F. (1982), "Theoretical and Experimental Considerations for the Use of the Column Method for Determining Retardation Factors," *Radioactive Waste Management and the Nuclear Fuel Cycle*, 3, 151-166.

Rey, A., et al. (2009), "Stability of uranium (VI) peroxide hydrates under ionizing radiation," *Amer. Mineralogist*, **94**, 229-235.

Sahoo, S.K. (2009), "Measurement of uranium and its isotopes at trace levels in environmental samples using mass spectrometry", *Indian Journal of Physics*, **83** (6), 787-797.

SAIC (2007), Well Location Selection Report. Depleted Uranium Impact Area Site Characterization: Soil Verification, Surface Water Gauge Installation, Fracture Trace Analysis, and Electrical Imaging Jefferson Proving Ground, Madison, Indiana (NRC Staff Exh. 26; Viewable at URL: http://pbadupws.nrc.gov/docs/ML0731/ML073100034.pdf).

Salbu, B.; K. Janssens; O.C. Lind; K. Proost; L. Gijsels; P.R. Danesi (2004), "Oxidation states of uranium in depleted uranium particles from Kuwait," *J. Environ. Radioactivity*.

Schimmack, W.; U. Gerstmann; W. Schultz and G. Geipel (2007)," Leaching of depleted uranium in soil as determined by column experiments," *Radiation and Environmental Biophysics*, 46, (3), 221-227.

Schäfer, T.; Artinger, R.; Dardenne, K.; Bauer, A.; Schuessler, W.; Kim, J.I. (2003), "Colloid-Borne Americium Migration in Gorlebe Groundwater: Significance of Iron Secondary Phase Transformation," *Environ. Sci. Technol.*, **37**, 1528-1534.

Shaw, S.; Baxter, A.C.; Jackman, S.A.; Thompson, I.P. (2007): Geochemical and microbiological controls on the corrosion and transport of depleted uranium in soil- Goldschmidt Conference Abstracts, **A925**: http://www.the-conference.com/2007/gold2007/abstracts/A925.pdf

Shoesmith, D.W., "Used Fuel and Uranium Dioxide Dissolution Studies – A Review," Report No.: NWMO-TR-2007-03 (July 2007). (http://www.nwmo.ca/uploads_managed/MediaFiles/8_NWMOTR-2007-03_UraniumReview_R0d.pdf).

Silva, R. J. and H. Nitsche (1995), "Actinide Environmental Chemistry," *Radiochim. Acta*, 70/71, 377.

Sinkov S.I.; C.H. Delegard; and A.J. Schmidt. 2008. *Preparation and Characterization of Uranium Oxidesin Support of the K Basin Sludge Treatment Project*. PNNL-17678, Pacific Northwest National Laboratory, Richland, WA.

Stevenson, R.J. (2010A), *Characterization of Two sections of Sample JP-PAC-05 (2288) by Scanning Electron Microscopy with Associated Energy Dispersive Spectroscopy (EDS)*, MCLinc Report to J. Skibinski, SAIC, dated January 22, 2010.

Stevenson, R.J. (2010B), *Characterization of six scraped penetrator by scanning electron microscopy with associated energy dispersive spectroscopy (EDS) and x-ray diffraction (XRD)*, MCLinc Report to J. Skibinski, SAIC, dated October 21, 2010.

Tessier, A.; Campbell, P.G.C.; Bisson, M. (1979), "Sequential Extraction Procedure for the Speciation of Particulate Trace Metals," *Anal. Chem.*, **51**, 844-851.

Toque, C.C.L.; Baker, A.C.; *MOD DU program: Report on the corrosion of depleted uranium in the Solway Firth*; 2007. DSTL/ CR11679 V1.0, Alverstoke.

Travaglini, S. (2008), *Corrosion study of 24 penetrator samples: Initial images*, MCLinc Report to J. Skibinski, SAIC, dated November 24, 2008.

Tricknor, K.V. (1994), "Uranium Sorption on Geological Minerals," *Radiochim. Acta*, **64**, 229-236.

Trueman, E.; Black, S.; Read, D. (2004) *Characterization of depleted uranium (DU) from an unfired CHARM-3 penetrator* - Sci. Tot. Env. **327**, 337-340.

Trueman, E.; Black, S.; Read, D.; Hodson, M. (2003). "Alteration of depleted uranium metal," *Geochim. Cosmochim. Acta*, **67**: A493.

Trzaskoma, P.P., "Corrosion rates and electrochemical studies of depleted uranium alloy tungsten fiber metal matrix composite," *J Electrochem Soc* 1982; 129:1398-402

UNEP. *Depleted uranium in Serbia and Montenegro: Postconflict environmental assessment in the Federal Republic of Yugoslavia. France: United Nations Environment Programme, Imprimerie Chirat; 2002.* (Viewable at URL: http://postconflict.unep.ch/publications/duserbiamont.pdf) .

U.S. Environmental Protection Agency, *National Primary Drinking Water Regulations: Analytical Method for Uranium,* Federal Register: August 25, 2004 (Volume 69, Number 164), pp. 52176-52181.

U.S. Environmental Protection Agency, *Total Organic Carbon (TOC) in Soil,* SW-846 Method 9060.

U.S. Environmental Protection Agency (1999), *Understanding Variation in Partition Coefficient, Kd, Values Volume II: Review of Geochemistry and Available Kd Values for Cadmium, Cesium, Chromium, Lead, Plutonium, Radon, Strontium, Thorium, Tritium and Uranium,* EPA 402-R-99-004B. [See link at URL: http://www.epa.gov/rpdweb00/cleanup/402-r-99-004.html#vol2]

Wagner, G.J. and R.J. Stevenson (2009), *Characterization of Twenty-four Uranium Samples by X-Ray Diffraction (XRD) and Scanning Electron Microscopy with Associated Energy Dispersive Spectroscopy (EDS),* MCLinc Report to J. Skibinski, SAIC, dated April 21, 2009.

Walenta, K. (1974), "On studtite and its composition," *American Mineralogist,* **59**, 166-171.

Wazne, M.; Korfiatis, G.P.; Meng, X. (2003), "Carbonate Effects on Hexavalent Uranium Adsorption by Iron Oxyhydroxide," *Environ. Sci. Technol.,* **37**, 3619-3624.

Wronkiewicz, D.J.; E.C. Buck (1999), "Uranium mineralogy and the geologic disposal of spent nuclear fuel," Chapter 10 in Burns, P.C.; Finch, R. (eds.), *Reviews in Mineralogy,* Vol. 38, Uranium: Mineralogy, Geochemistry and the Environment, Mineralogy Soc. of America.

Young, C.M.; K.A. Nelson; G.T. Stevens; V.J. Grassi (2006), *Occurrence of Metastudtite (Uranium Peroxide Dihydrate) at a FUSRAP Site,* WM'06 Conference, February 26-March 2, 2006, Tucson, AZ.

Zabielski, C.V.; M. Levy (1992), *Corrosion of high density kinetic energy penetrator materials,* US MTL TR 92-17 [URL: http://www.dtic.mil/cgi-bin/GetTRDoc?Location=U2&doc=GetTRDoc.pdf&AD=ADA249439].

Zhou, P.; Gu, B. (2005), "Extraction of Oxidized and Reduced Forms of Uranium from Contaminated Soils: Effect of Carbonate Concentration and pH," *Environ. Sci. Technol.,* **39**, 4435-4440.

Zickafoose, M.S (1997), ANALYSIS OF URANIUM OXIDE WEATHERING BY MOLECULAR SPECTROSCOPY (MS Thesis, AFIT).

ACKNOWLEDGEMENTS

The following staff members at MCLinc contributed significantly to this project:

Dr. W. Bostick

Dr. M. Colberg

J. Hall

M. Hall

R. Jarabek

E. Munday

M. Sanders

B. Stephenson

Dr. R. Stevenson

S. Travaglini

M. Tutor

Dr. G. Wagner

In addition, we thank our subcontractors:

GEL Laboratories, LLC (Charleston, SC) provided data on organic carbon in DU-exposed soils.

Eberline Services, Inc. (Oak Ridge, TN) performed aqueous uranium activity measurements by alpha spectroscopy.

APPENDIX 1. LEACH DATA SUMMARY

A1. SUMMARY OF LEACH SERIES

Table A1- 1. Leach Intervals and Duration

Series (cycle)	Leach Interval	Time elapsed (d)	Time elapsed (y)	Collection date
0	1	0	0.00	6/29/2009
1	2	22	0.06	7/20/2009
2	3	43	0.12	8/10/2009
3	4	64	0.18	8/31/2009
4	5	85	0.23	9/21/2009
5	6	106	0.29	10/12/2009
6	7	127	0.35	11/2/2009
7	8	148	0.41	11/23/2009
8	9	169	0.46	12/4/2009
9	10	190	0.52	1/4/2010
10	11	211	0.58	1/25/2010
11	12	232	0.64	2/15/2010
12	13	253	0.69	3/8/2010
13	14	274	0.75	3/29/2010
14	15	295	0.81	4/19/2010
15	16	316	0.87	5/10/2010
16	17	337	0.92	5/31/2010
17	18	358	0.98	6/21/2010
18	19	379	1.04	7/12/2010
19	20	400	1.10	8/2/2010
20	21	421	1.15	8/23/2010
21	22	442	1.21	9/13/2010
22	23	463	1.27	10/4/2010

Notes: d – day(s)
y – year(s)

Table A1- 2. Summary for Leach Series 1-AC-005-S
Scraped Penetrator (701.8-g), placed in PAC Soil (1000.1-g)

Series 1-AC-005-S		PAC-005-S Leachate					
Sample ID	Leach Interval	Leachate Volume (L)	Alkalinity (mg/L as $CaCO_3$) [Initial pH]	U_{total} (pCi/L ± %2σ) *	U_{total} (µg-U/L) **	U_{total} (pCi/µg-U)	Cumulative Mass Fraction Leached
00-1-AC-005-S	1	0.638	11.4 mg/L [pH_o 6.5]	6.51E+01 (±13%)	3.05E+01	2.13	2.77E-08
01-1-AC-005-S	2	0.600	54.8 mg/L [pH_o 6.5]	1.08E+02 (±12%)	1.03E+02	1.05	1.16E-07
02-1-AC-005-S	3	0.625	78.1 mg/L [pH_o 7.4]	8.59E+01 (±12%)	6.68E+01	1.29	1.60E-07
03-1-AC-005-S	4	0.625	7.2 mg/L [pH_o 6.9]	2.65E+01 (±13%)	3.70E+01	0.72	1.93E-07
04-1-AC-005-S	5	0.636	18.4 mg/L [pH_o 6.5]	4.46E+01 (±13%)	6.80E+01	0.66	2.56E-07
05-1-AC-005-S	6	0.655	6.4 mg/L [pH_o 6.9]	3.28E+01 (±15%)	8.50E+01	0.39	3.35E-07
06-1-AC-005-S	7	0.663	6.1 mg/L [pH_o 6.7]	2.38E+01 (±15%)	6.11E+01	0.39	3.93E-07
07-1-AC-005-S	8	0.687	3.4 mg/L [pH_o 6.2]	1.47E+02 (±28%)	3.54E+02	0.42	7.40E-07
08-1-AC-005-S	9	0.687	2.38 [pH_o 6.0]	5.93E+02 (±18%)	1.54E+03	0.38	2.25E-06
09-1-AC-005-S	10	0.698	3.1 mg/L [pH_o 5.3]	3.50E+03 (±16%)	8.80E+03	0.40	1.10E-05
10-1-AC-005-S	11	0.699	2.2 mg/L [pH_o 5.2]	2.19E+03 (±17%)	5.87E+03	0.37	1.69E-05
11-1-AC-005-S	12	0.733	2.5 mg/L [pH_o 5.1]	2.98E+03 (±17%)	7.45E+03	0.40	2.46E-05
12-1-AC-005-S	13	0.686	1.2 mg/L [pH_o 5.6]	7.78E+02 (±17%)	2.02E+03	0.39	2.66E-05
13-1-AC-005-S	14	0.688	2.4 mg/L [pH_o 5.6]	1.39E+03 (±15%)	3.51E+03	0.40	3.00E-05
14-1-AC-005-S	15	0.691	2.3 mg/L [pH_o 5.7]	1.32E+03 (±15%)	3.34E+03	0.40	3.33E-05
15-1-AC-005-S	16	0.689	2.8 mg/L [pH_o 6.0]	1.21E+03 (±17%)	3.04E+03	0.40	3.63E-05
16-1-AC-005-S	17	0.694	2.4 mg/L [pH_o 5.7]	1.09E+03 (±17%)	2.82E+03	0.39	3.91E-05
17-1-AC-005-S	18	0.706	2.8 mg/L [pH_o 5.8]	1.55E+03 (±15%)	4.02E+03	0.39	4.31E-05
18-1-AC-005-S	19	0.714	3.6 mg/L [pH_o 5.6]	2.79E+03 (±15%)	7.20E+03	0.39	5.05E-05
19-1-AC-005-S	20	0.699	2.35 [pH_o 5.5]	1.38E+03 (±16%)	3.58E+03	0.39	5.40E-05

Series 1-AC-005-S		PAC-005-S Leachate					
Sample ID	**Leach Interval**	**Leachate Volume (L)**	**Alkalinity (mg/L as $CaCO_3$) [Initial pH]**	**U_{total} (pCi/L ± %2σ) ***	**U_{total} (µg-U/L) ****	**U_{total} (pCi/µg-U)**	**Cumulative Mass Fraction Leached**
20-1-AC-005-S	21	0.701	2.8 mg/L [pH_o 5.7]	1.60E+03 (±16%)	4.17E+03	0.38	5.82E-05
21-1-AC-005-S	22	0.695	6.6 mg/L [pH 6.8]	1.60E+03 (±20%)	4.21E+03	0.38	6.24E-05
22-1-AC-005-S	23	0.694	6.2 mg/L [pH 6.9]	1.84E+03 (±17%)	4.90E+03	0.37	6.72E-05

Notes: * Result (± %2σ, propagated error), where %2σ = 100%* (2σ/Result)
** Estimated with use of isotopic specific activities
% – percent
σ – one standard deviation
AC – Avonsburg/Cobbsfork
$CaCO_3$ – calcite
g – gram(s)
ID – identification
L – liter
µg-U/L – microgram(s) uranium per liter
mg/L – milligram(s) per liter
PAC – soil type Avonsburg/Cobbsfork
pCi/L – picoCuries per liter
pCi/µg-U – picoCuries per microgram of uranium
pH_o – initial pH
U_{total} – total uranium

Table A1- 3. Summary for Leach Series 2-AC-005-U

Non-Scraped (As-Found) Penetrator (623.5-g), placed in PAC Soil (1001.4-g)

Series 1-AC-005-U		PAC-005-U Leachate					
Sample ID	**Leach Interval**	**Leachate Volume (L)**	**Alkalinity (mg/L as $CaCO_3$) [Initial pH]**	**U_{total} (pCi/L ± %2σ) ***	**U_{total} (µg-U/L) ****	**U_{total} (pCi/µg-U)**	**Cumulative Mass Fraction Leached**
00-2-AC-005-U	1	0.639	10.0 mg/L [pH_o 6.5]	6.90E+01 (±13%)	3.53E+01	1.95	3.62E-08
01-2-AC-005-U	2	0.612	53.3 mg/L [pH_o 6.8]	7.78E+01 (±13%)	1.49E+02	0.52	1.83E-07
02-2-AC-005-U	3	0.688	20.3 mg/L [pH_o 7.1]	4.77E+02 (±16%)	1.18E+03	0.40	1.49E-06
03-2-AC-005-U	4	0.688	4.5 mg/L [pH_o 6.4]	6.03E+02 (±16%)	1.57E+03	0.38	3.22E-06
04-2-AC-005-U	5	0.691	6.4 mg/L [pH_o 6.4]	1.65E+03 (±16%)	4.23E+03	0.39	7.90E-06
05-2-AC-005-U	6	0.695	5.3 mg/L [pH_o 6.3]	1.42E+03 (±15%)	3.69E+03	0.38	1.20E-05
06-2-AC-005-U	7	0.663	5.6 mg/L [pH_o 6.2]	1.23E+03 (±15%)	3.17E+03	0.39	1.54E-05
07-2-AC-005-U	8	0.687	4.1 mg/L [pH_o 6.1]	1.80E+03 (±15%)	4.75E+03	0.38	2.06E-05
08-2-AC-005-U	9	0.675	2.9 mg/L [pH_o 6.0]	5.26E+02 (±17%)	1.36E+03	0.39	2.21E-05
09-2-AC-005-U	10	0.718	3.4 mg/L [pH_o 6.0]	1.27E+03 (±17%)	3.32E+03	0.38	2.59E-05
10-2-AC-005-U	11	0.696	3.11 [pH_o 5.5]	2.76E+03 (±16%)	7.09E+03	0.39	3.38E-05
11-2-AC-005-U	12	0.720	3.1 mg/L [pH_o 5.4]	2.05E+03 (±18%)	5.57E+03	0.37	4.02E-05
12-2-AC-005-U	13	0.702	1.8 mg/L [pH_o 5.7]	9.60E+02 (±16%)	2.51E+03	0.38	4.31E-05
13-2-AC-005-U	14	0.672	2.2 mg/L [pH_o 5.8]	3.99E+02 (±17%)	1.04E+03	0.38	4.42E-05
14-2-AC-005-U	15	0.684	2.6 mg/L [pH_o 5.9]	8.88E+02 (±17%)	2.29E+03	0.39	4.67E-05
15-2-AC-005-U	16	0.677	2.8 mg/L [pH_o 6.2]	2.98E+02 (±17%)	7.63E+02	0.39	4.75E-05
16-2-AC-005-U	17	0.678	2.6 mg/L [pH_o 5.8]	5.23E+02 (±15%)	1.35E+03	0.39	4.90E-05
17-2-AC-005-U	18	0.697	2.8 mg/L [pH_o 5.8]	7.55E+02 (±17%)	1.94E+03	0.39	5.12E-05
18-2-AC-005-U	19	0.707	1.9 mg/L [pH_o 5.5]	4.01E+02 (±18%)	1.01E+03	0.40	5.23E-05

Series 1-AC-005-U		PAC-005-U Leachate					
Sample ID	**Leach Interval**	**Leachate Volume (L)**	**Alkalinity (mg/L as $CaCO_3$) [Initial pH]**	**U_{total} (pCi/L ± %2σ) ***	**U_{total} (µg-U/L) ****	**U_{total} (pCi/µg-U)**	**Cumulative Mass Fraction Leached**
19-2-AC-005-U	20	0.682	2.32 [pH_o 5.5]	4.12E+02 (±17%)	1.03E+03	0.40	5.34E-05
20-2-AC-005-U	21	0.682	1.85 mg/L [pH_o 5.6]	3.49E+02 (±16%)	9.01E+02	0.39	5.44E-05
21-2-AC-005-U	22	0.679	4.1 mg/L [pH_o 6.1]	1.45E+03 (±16%)	3.78E+03	0.38	5.86E-05
22-2-AC-005-U	23	0.682	5.9 mg/L [pH_o 5.9]	1.78E+03 (±17%)	4.72E+03	0.38	6.37E-05

Notes: * Result (± %2σ, propagated error), where %2σ = 100%* (2σ/Result)
** Estimated with use of isotopic specific activities
% – percent
σ – one standard deviation
AC – Avonsburg/Cobbsfork
$CaCO_3$ – calcite
g – gram(s)
ID – identification
L – liter
µg-U/L – microgram(s) uranium per liter
mg/L – milligram(s) per liter
PAC – soil type Avonsburg/Cobbsfork
pCi/L – picoCuries per liter
pCi/µg-U – picoCuries per microgram of uranium
pH_o – initial pH
U_{total} – total uranium

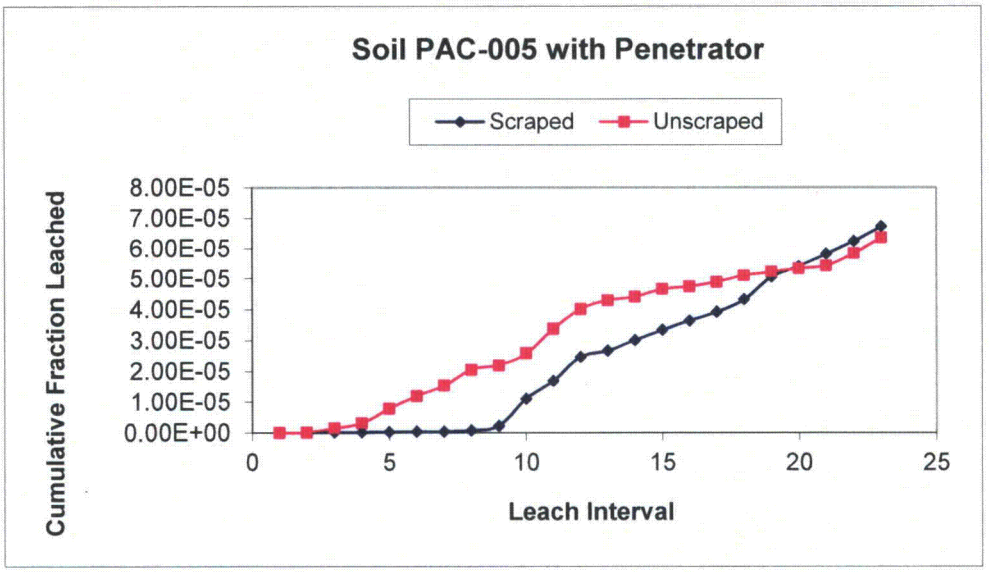

Notes: PAC – soil type Avonsburg/Cobbsfork

Figure A1- 1. Estimates of Fractional Leaching of Uranium from Penetrators in Soil for Specimens in PAC-005 Soil.

Data for Cell #1 represents "scraped" condition and Cell #2 represents "unscraped" condition.

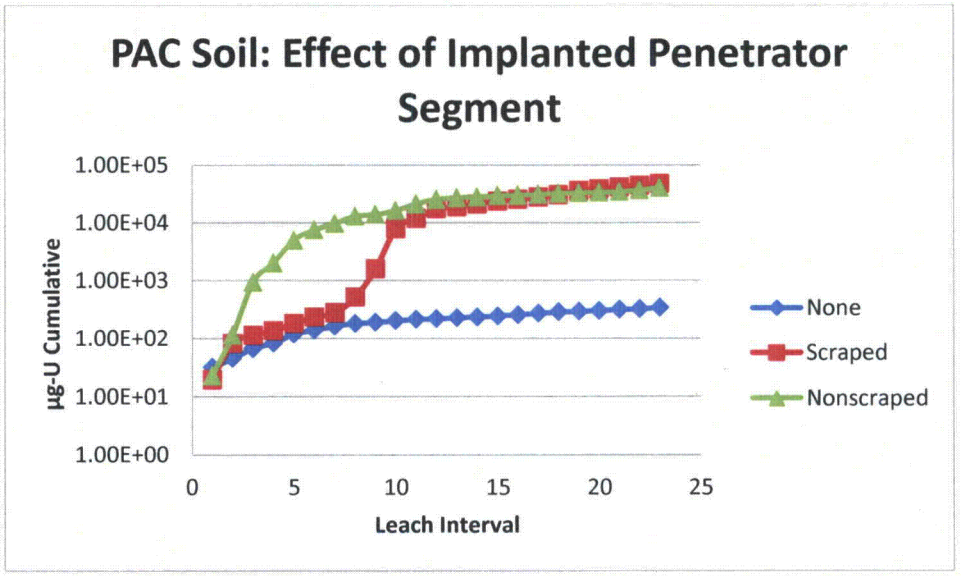

Notes: PAC – soil type Avonsburg/Cobbsfork
µg-U – microgram of uranium

Figure A1- 2. Estimates of Total Uranium (µg), Cumulative, as Leached from Soil Type PAC: Effect of Added Penetrator Dart Segment.

Cell #7 has no added penetrator segment. (Note logarithmic chart ordinate).

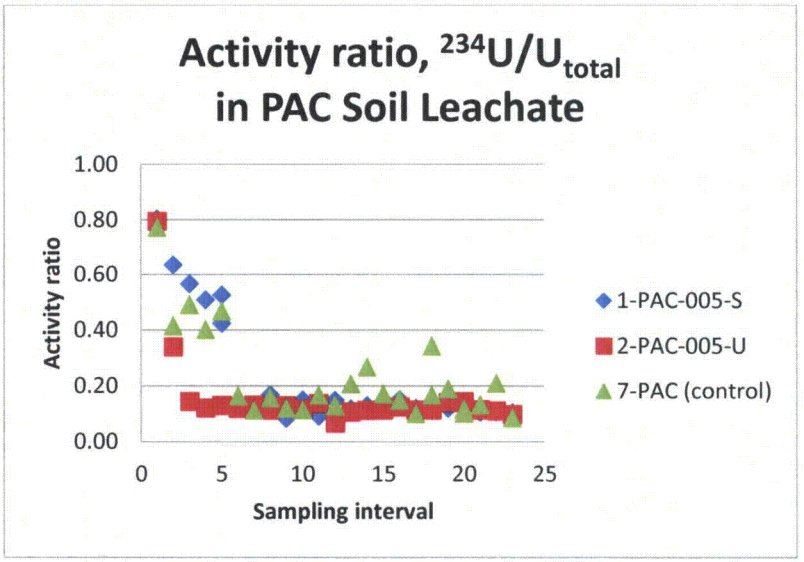

Notes: ^{234}U – uranium-234
PAC – soil type Avonsburg/Cobbsfork
U_{total} – total uranium

Figure A1- 3. Estimates for the Ratio of Measured Activity, $^{234}U/U_{total}$, in PAC Soil Column Leachate.

By sampling interval 10 (or sooner), the activity ratio approaches the expected value for steady-state leaching from DU (activity, $^{234}U/U_{total}$ of approximately 0.10; see Text Table 6). (Data for control soil, 7-PAC, with no added penetrator dart segment, have low activity and hence high uncertainty for the calculated activity ratio estimate).

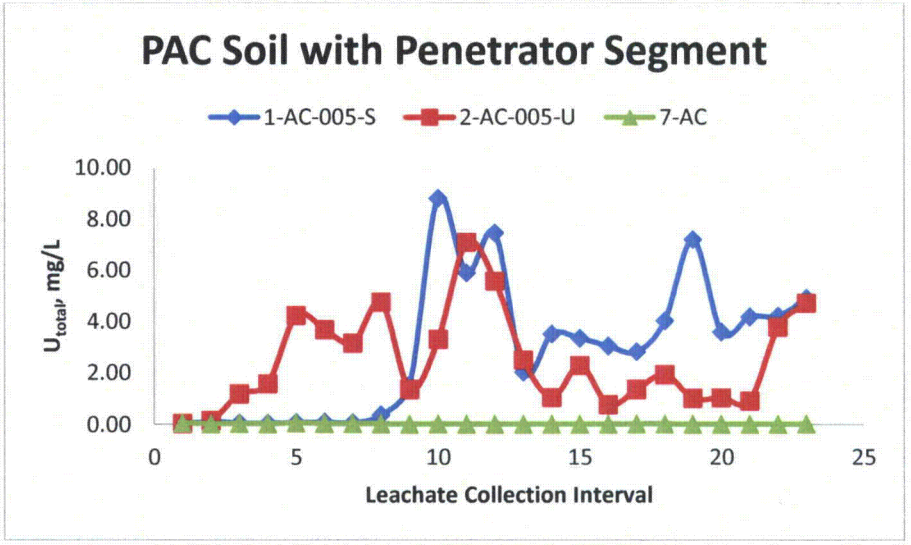

Notes: AC – Avonsburg/Cobbsfork
mg/L – milligram(s) per liter
PAC – soil type Avonsburg/Cobbsfork
U_{total} – total uranium

Figure A1- 4. Estimates of Total Uranium *Concentration* in Aqueous Eluate by Collection Interval for Soil Type PAC

Also included is data for Cell 7 (7-AC), which is a control cell with no added penetrator segment.

Table A1- 4. Summary for Leach Series 3-CR-008 S
Scraped Penetrator (577.1-g), placed in PCR Soil (1000.2-g)

3-CR-008-S		PCR-008-S Leachate					
Sample ID	**Leach Interval**	**Leachate Volume (L)**	**Alkalinity (mg/L as $CaCO_3$) [Initial pH]**	**U_{total} (pCi/L ± %2σ) ***	**U_{total} (µg-U/L) ****	**U_{total} (pCi/µg-U)**	**Cumulative Mass Fraction Leached**
00-3-CR-008-S	1	0.639	12.1 mg/L [pH_o 6.6]	2.53E+02 (±13%)	1.14E+02	2.22	1.26E-07
01-3-CR-008-S	2	0.674	0.00 mg/L [pH_o 2.8]	7.77E+01 (±16%)	1.77E+02	0.44	3.33E-07
02-3-CR-008-S	3	0.647	5.4 mg/L [pH_o 6.2]	3.31E+02 (±17%)	7.25E+02	0.46	1.15E-06
03-3-CR-008-S	4	0.631	1.70 mg/L [pH_o 5.3]	4.60E+02 (±16%)	1.09E+03	0.42	2.33E-06
04-3-CR-008-S	5	0.633	3.9 mg/L [pH_o 6.10	8.52E+02 (±14%)	2.07E+03	0.41	4.61E-06
05-3-CR-008-S	6	0.659	2.4 mg/L [pH_o 5.8]	7.29E+02 (±15%)	1.92E+03	0.38	6.80E-06
06-3-CR-008-S	7	0.689	2.7 mg/L [pH_o 5.8]	1.01E+03 (±16%)	2.60E+03	0.39	9.90E-06
07-3-CR-008-S	8	0.672	2.2 mg/L [pH_o 5.6]	8.50E+02 (±18%)	2.25E+03	0.38	1.25E-05
08-3-CR-008-S	9	0.692	1.7 mg/L [pH_o 5.2]	1.04E+03 (±17%)	2.75E+03	0.38	1.58E-05
09-3-CR-008-S	10	0.692	0.95 mg/L [pH_o 4.9]	1.24E+03 (±17%)	3.29E+03	0.38	1.97E-05
10-3-CR-008-S	11	0.694	0.05 mg/L [pH_o 4.6]	1.09E+03 (±15%)	2.78E+03	0.39	2.31E-05
11-3-CR-008-S	12	0.694	0.00 mg/L [pH_o 4.5]	8.20E+02 (±18%)	2.11E+03	0.39	2.56E-05
12-3-CR-008-S	13	0.680	0.42 mg/L [pH_o 4.7]	9.19E+02 (±18%)	2.35E+03	0.39	2.84E-05
13-3-CR-008-S	14	0.698	0.62 mg/L [pH_o 4.7]	1.04E+03 (±16%)	2.67E+03	0.39	3.16E-05
14-3-CR-008-S	15	0.699	0.37 mg/L [pH_o 4.6]	1.01E+03 (±16%)	2.39E+03	0.42	3.45E-05
15-3-CR-008-S	16	0.717	0.90 mg/L [pH_o 4.8]	1.25E+03 (±16%)	3.04E+03	0.41	3.83E-05
16-3-CR-008-S	17	0.712	2.6 mg/L [pH_o 4.8]	9.01E+02 (±19%)	2.45E+03	0.37	4.13E-05
17-3-CR-008-S	18	0.731	0.41 mg/L [pH_o 4.6]	1.03E+03 (±17%)	2.65E+03	0.39	4.47E-05
18-3-CR-008-S	19	0.727	0.90 mg/L [pH_o 4.8]	1.16E+03 (±16%)	3.03E+03	0.38	4.85E-05

3-CR-008-S		PCR-008-S Leachate					
Sample ID	**Leach Interval**	**Leachate Volume (L)**	**Alkalinity (mg/L as $CaCO_3$) [Initial pH]**	**U_{total} (pCi/L ± %2σ) ***	**U_{total} (µg-U/L) ****	**U_{total} (pCi/µg-U)**	**Cumulative Mass Fraction Leached**
19-3-CR-008-S	20	0.702	0.73 mg/L [pH_o 4.7]	1.57E+03 (±16%)	4.00E+03	0.39	5.33E-05
20-3-CR-008-S	21	0.712	0.52 mg/L [pH_o 4.6]	1.30E+03 (±16%)	3.27E+03	0.40	5.74E-05
21-3-CR-008-S	22	0.668	4.39 mg/L [pH_o 5.7]	2.85E+03 (±16%)	7.18E+03	0.40	6.57E-05
22-3-CR-008-S	23	0.710	2.1 mg/L [pH_o 4.9]	3.76E+03 (±18%)	9.73E+03	0.39	7.77E-05

Notes: * Result (± %2σ, propagated error), where %2σ = 100%* (2σ/Result)
** Estimated with use of isotopic specific activities
% – percent
σ – one standard deviation
$CaCO_3$ – calcite
CR – Cincinnati/Rossmoyne
g – gram(s)
ID – identification
L – liter
µg-U/L – microgram(s) uranium per liter
mg/L – milligram(s) per liter
PCR – soil type Cincinnati/Rossmoyne
pCi/L – picoCuries per liter
pCi/µg-U – picoCuries per microgram of uranium
pH_o – initial pH
U_{total} – total uranium

Table A1- 5. Summary for Leach Series 4-CR-008 U
Non-Scraped (As-Found) Penetrator (620.2-g), placed in PCR Soil (1000.3-g)

4-CR-008-U		PCR-008-U Leachate					
Sample ID	**Leach Interval**	**Leachate Volume (L)**	**Alkalinity (mg/L as $CaCO_3$) [Initial pH]**	**U_{total} (pCi/L ± %2σ) ***	**U_{total} (µg-U/L) ****	**U_{total} (pCi/µg-U)**	**Cumulative Mass Fraction Leached**
00-4-CR-008-U	1	0.620	8.0 mg/L [pH_o 6.3]	8.69E+01 (±12%)	7.22E+01	1.20	7.22E-08
01-4-CR-008-U	2	0.609	0.00 mg/L [pH_o 3.2]	3.52E+02 (±17%)	8.82E+02	0.40	9.39E-07
02-4-CR-008-U	3	0.694	2.7 mg/L [pH_o 5.8]	7.62E+02 (±17%)	1.55E+03	0.49	2.67E-06
03-4-CR-008-U	4	0.627	2.0 mg/L [pH_o 5.6]	6.10E+02 (±13%)	1.49E+03	0.41	4.18E-06
04-4-CR-008-U	5	0.641	2.0 mg/L [pH_o 5.4]	6.34E+02 (±15%)	1.43E+03	0.44	5.66E-06
05-4-CR-008-U	6	0.647	2.0 mg/L [pH_o 5.4]	6.43E+02 (±15%)	1.64E+03	0.39	7.37E-06
06-4-CR-008-U	7	0.663	1.7 mg/L [pH_o 5.3]	5.10E+02 (±15%)	1.38E+03	0.37	8.85E-06
07-4-CR-008-U	8	0.704	0.97 mg/L [pH_o 4.98	3.68E+02 (±16%)	9.55E+02	0.39	9.93E-06
08-4-CR-008-U	9	0.698	0.00 mg/L [pH_o 4.4]	4.84E+02 (±16%)	1.22E+03	0.40	1.13E-05
09-4-CR-008-U	10	0.681	0.00 mg/L [pH_o 4.5]	4.47E+02 (±16%)	1.15E+03	0.39	1.26E-05
10-4-CR-008-U	11	0.704	0.07 mg/L [pH_o 4.6]	3.80E+02 (±16%)	1.00E+03	0.38	1.37E-05
11-4-CR-008-U	12	0.681	0.00 mg/L [pH_o 4.4]	2.39E+02 (±17%)	5.92E+02	0.40	1.43E-05
12-4-CR-008-U	13	0.685	0.10 mg/L [pH_o 4.5]	4.02E+02 (±15%)	1.02E+03	0.40	1.55E-05
13-4-CR-008-U	14	0.681	0.00 mg/L [pH_o 4.5]	4.23E+02 (±15%)	1.00E+03	0.42	1.66E-05
14-4-CR-008-U	15	0.686	0.00 mg/L [pH_o 4.5]	4.72E+02 (±17%)	1.04E+03	0.45	1.77E-05
15-4-CR-008-U	16	0.695	0.84 mg/L [pH_o 4.8]	5.68E+02 (±17%)	1.46E+03	0.39	1.94E-05
16-4-CR-008-U	17	0.678	1.4 mg/L [pH_o 4.9]	1.64E+03 (±15%)	4.22E+03	0.39	2.40E-05
17-4-CR-008-U	18	0.695	0.70 mg/L [pH_o 4.7]	1.96E+03 (±17%)	5.06E+03	0.39	2.96E-05
18-4-CR-008-U	19	0.696	0.88 mg/L [pH_o 4.7]	2.19E+03 (±14%)	5.56E+03	0.39	3.59E-05

4-CR-008-U		PCR-008-U Leachate					
Sample ID	**Leach Interval**	**Leachate Volume (L)**	**Alkalinity (mg/L as $CaCO_3$) [Initial pH]**	**U_{total} (pCi/L ± %2σ) ***	**U_{total} (µg-U/L) ****	**U_{total} (pCi/µg-U)**	**Cumulative Mass Fraction Leached**
19-4-CR-008-U	20	0.693	1.3 mg/L [pH_o 4.8]	2.52E+03 (±19%)	6.31E+03	0.40	4.29E-05
20-4-CR-008-U	21	0.687	0.79 mg/L [pH_o 4.7]	2.54E+03 (±17%)	6.53E+03	0.39	5.39E-05
21-4-CR-008-U	22	0.694	1.9 mg/l [pH_o 4.9]	3.24E+03 (±15%)	8.53E+03	0.38	6.42E-05
22-4-CR-008-U	23	0.694	0.72 mg/L [pH_o 4.6]	3.43E+03 (±17%)	9.09E+03	0.38	7.51E-05

Notes: * Result (± %2σ, propagated error), where %2σ = 100%* (2σ/Result)
** Estimated with use of isotopic specific activities
% – percent
σ – one standard deviation
$CaCO_3$ – calcite
CR – Cincinnati/Rossmoyne
g – gram(s)
ID – identification
L – liter
µg-U/L – microgram(s) uranium per liter
mg/L – milligram(s) per liter
PCR – soil type Cincinnati/Rossmoyne
pCi/L – picoCuries per liter
pCi/µg-U – picoCuries per microgram of uranium
pH_o – initial pH
U_{total} – total uranium

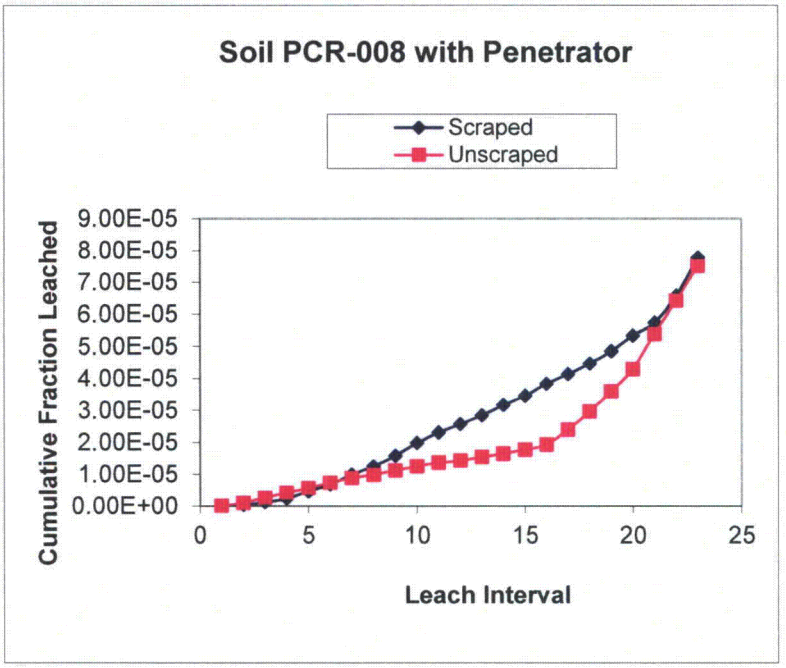

Notes: PCR – soil type Cincinnati/Rossmoyne

Figure A1- 5. Estimates of Fractional Leaching of Uranium from Penetrators in Soil for Specimens in PCR-008 Soil

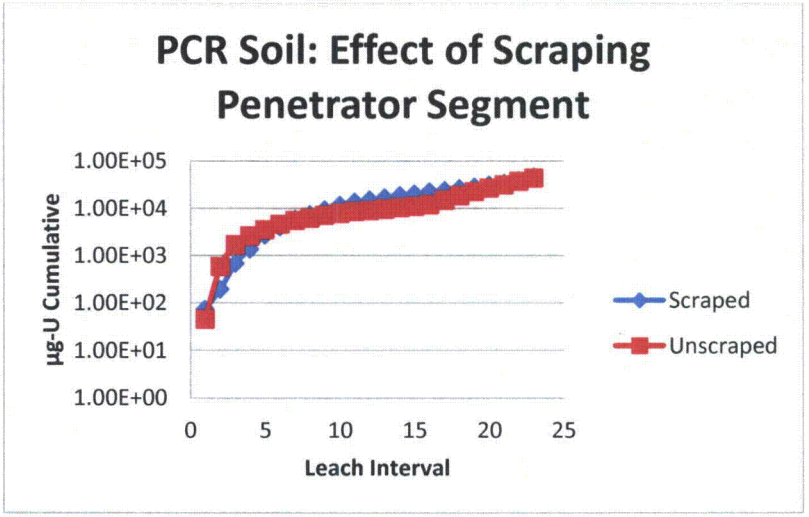

Notes: PCR – soil type Cincinnati/Rossmoyne
µg-U – microgram(s) uranium

Figure A1- 6. Data as in Figure A1-5, but with Logarithmic Chart Ordinate (to Emphasize Data for Initial Leach Intervals).

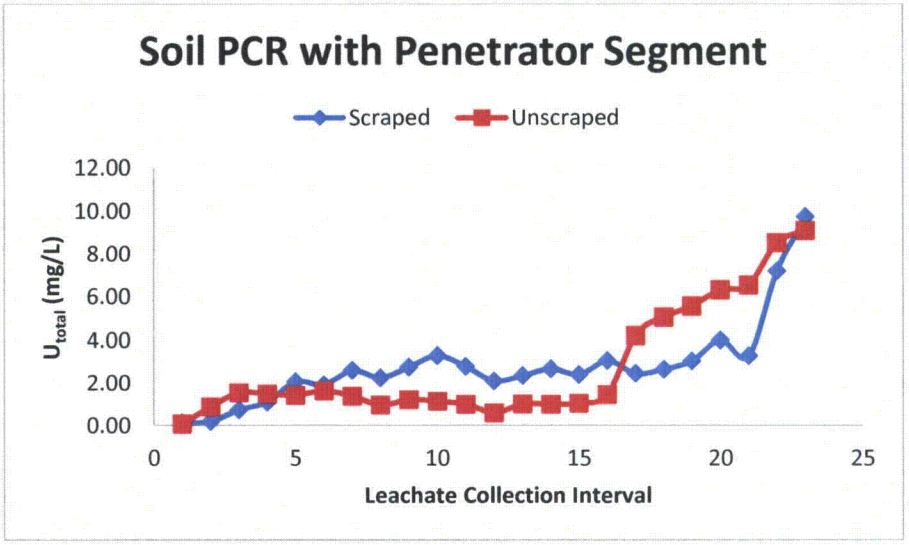

Notes: PCR – soil type Cincinnati/Rossmoyne
µg/L – microgram(s) per liter
U_{total} – total uranium

Figure A1- 7. Estimates of Total Uranium *Concentration* in Aqueous Eluate by Collection Interval for Soil Type PCR

Table A1- 6. Summary for Leach Series 5-GR-001 S
Scraped Penetrator (583.1-g), placed in PGR Soil (1000.5-g)

5-GR-001-S		PGR-001-S Leachate					
Sample ID	**Leach Interval**	**Leachate Volume (L)**	**Alkalinity (mg/L as $CaCO_3$) [Initial pH]**	**U_{total} (pCi/L ± %2σ) ***	**U_{total} (µg-U/L) ****	**U_{total} (pCi/µg-U)**	**Cumulative Mass Fraction Leached**
00-5-GR-001-S	1	0.690	19.4 mg/L [pH_o 6.8]	1.05E+02 (±13%)	5.67E+01	1.85	6.70E-08
01-5-GR-001-S	2	0.641	1.9 mg/L [pH_o 5.4]	4.10E+01 (±13%)	7.96E+01	0.51	1.55E-07
02-5-GR-001-S	3	0.682	2.9 mg/L [pH_o 6.0]	1.18E+02 (±14%)	2.35E+02	0.50	4.29E-07
03-5-GR-001-S	4	0.666	2.6 mg/L [pH_o 6.0]	1.70E+02 (±15%)	4.21E+02	0.41	9.09E-07
04-5-GR-001-S	5	0.681	3.7 mg/L [pH_o 6.3]	2.67E+02 (±14%)	6.38E+02	0.42	1.66E-06
05-5-GR-001-S	6	0.696	2.8 mg/L [pH_o 6.0]	6.47E+02 (±15%)	1.62E+03	0.40	3.58E-06
06-5-GR-001-S	7	0.684	2.7 mg/L [pH_o 5.8]	1.21E+03 (±15%)	3.16E+03	0.38	7.29E-06
07-5-GR-001-S	8	0.710	2.5 mg/L [pH_o 5.9]	6.11E+02 (±16%)	1.59E+03	0.39	9.22E-06
08-5-GR-001-S	9	0.695	2.7 mg/L [pH_o 6.8]	2.88E+02 (±16%)	7.75E+02	0.37	1.01E-05
09-5-GR-001-S	10	0.707	2.8 mg/L [pH_o 6.0]	1.35E+03 (±16%)	3.47E+03	0.39	1.43E-05
10-5-GR-001-S	11	0.725	2.9 mg/L [pH_o 6.2]	9.58E+02 (±17%)	2.58E+03	0.37	1.76E-05
11-5-GR-001-S	12	0.711	2.7 mg/L [pH_o 5.6]	1.05E+03 (±16%)	2.62E+03	0.40	2.07E-05
12-5-GR-001-S	13	0.707	1.7 mg/L [pH_o 5.8]	5.44E+02 (±15%)	1.41E+03	0.39	2.25E-05
13-5-GR-001-S	14	0.726	2.6 mg/L [pH_o 5.6]	6.54E+02 (±16%)	1.68E+03	0.39	2.45E-05
14-5-GR-001-S	15	0.724	2.6 mg/L [pH_o 5.8]	8.47E+02 (±15%)	2.23E+03	0.38	2.73E-05
15-5-GR-001-S	16	0.724	2.5 mg/L [pH_o 5.8]	6.88E+02 (±17%)	1.82E+03	0.38	2.96E-05
16-5-GR-001-S	17	0.726	2.4 mg/L [pH_o 5.7]	2.38E+02 (±19%)	5.90E+02	0.40	3.03E-05
17-5-GR-001-S	18	0.736	2.3 mg/L [pH_o 5.7]	7.67E+02 (±16%)	1.96E+03	0.39	3.28E-05
18-5-GR-001-S	19	0.733	2.0 mg/L [pH_o 5.5]	8.72E+02 (±19%)	2.16E+03	0.40	3.55E-05

5-GR-001-S		PGR-001-S Leachate					
Sample ID	**Leach Interval**	**Leachate Volume (L)**	**Alkalinity (mg/L as $CaCO_3$) [Initial pH]**	**U_{total} (pCi/L ± %2σ) ***	**U_{total} (µg-U/L) ****	**U_{total} (pCi/µg-U)**	**Cumulative Mass Fraction Leached**
19-5-GR-001-S	20	0.717	2.2 mg/L [pH_o 5.5]	5.31E+02 (±16%)	1.39E+03	0.38	3.72E-05
20-5-GR-001-S	21	0.736	2.1 mg/L [pH_o 5.6]	7.00E+02 (±15%)	1.81E+03	0.39	3.95E-05
21-5-GR-001-S	22	0.728	7.5 mg/L [pH_o 8.2]	4.49E+02 (±17%)	1.14E+03	0.39	4.09E-05
22-5-GR-001-S	23	0.733	2.8 mg/L [pH_o 5.6]	1.34E+03 (±17%)	3.32E+03	0.40	4.51E-05

Notes: * Result (± %2σ, propagated error), where %2σ = 100%* (2σ/Result)
** Estimated with use of isotopic specific activities
% – percent
σ – one standard deviation
$CaCO_3$ – calcite
g – gram(s)
GR – Grayford/Ryker
ID – identification
L – liter
µg-U/L – microgram(s) uranium per liter
mg/L – milligram(s) per liter
pCi/L – picoCuries per liter
pCi/µg-U – picoCuries per microgram of uranium
PGR – soil type Grayford/Ryker
pH_o – initial pH
U_{total} – total uranium

Table A1- 7. Summary for Leach Series 6-GR-001 U
Non-Scraped (As-Found) Penetrator (526.4-g), placed in PGR Soil (1000.1-g)

6-GR-001-U		PGR-001-U Leachate					
Sample ID	**Leach Interval**	**Leachate Volume (L)**	**Alkalinity (mg/L as $CaCO_3$) [Initial pH]**	**U_{total} (pCi/L ± %2σ) ***	**U_{total} (µg-U/L) ****	**U_{total} (pCi/µg-U)**	**Cumulative Mass Fraction Leached**
00-6-GR-001-U	1	0.672	17.0 mg/L [pH_o 6.7]	5.29E+02 (±12%)	3.49E+02	1.52	4.46E-07
01-6-GR-001-U	2	0.566	0.00 mg/L [pH_o 2.5]	1.07E+03 (±12%)	7.45E+02	1.43	1.25E-06
02-6-GR-001-U	3	0.644	3.3 mg/L [pH_o 6.2]	9.02E+01 (±14%)	1.91E+02	0.47	1.48E-06
03-6-GR-001-U	4	0.646	3.0 mg/L [pH_o 6.1]	3.71E+02 (±17%)	9.37E+02	0.40	2.63E-06
04-6-GR-001-U	5	0.652	3.4 mg/L [pH_o 5.8]	1.59E+03 (±15%)	4.00E+03	0.40	7.58E-06
05-6-GR-001-U	6	0.666	3.9 mg/L [pH_o 6.1]	1.40E+03 (±16%)	3.59E+03	0.39	1.21E-05
06-6-GR-001-U	7	0.681	2.7 mg/L [pH_o 5.8]	6.09E+02 (±15%)	1.58E+03	0.39	1.42E-05
07-6-GR-001-U	8	0.728	3.4 mg/L [pH_o 6.0]	1.62E+03 (±15%)	4.18E+03	0.39	1.99E-05
08-6-GR-001-U	9	0.697	2.7 mg/L [pH_o 5.9]	5.06E+02 (±16%)	1.33E+03	0.38	2.17E-05
09-6-GR-001-U	10	0.704	2.8 mg/L [pH_o 6.0]	2.81E+02 (±16%)	7.35E+02	0.38	2.27E-05
10-6-GR-001-U	11	0.727	2.2 mg/L [pH_o 5.6]	4.84E+02 (±16%)	1.25E+03	0.39	2.44E-05
11-6-GR-001-U	12	0.708	2.0 mg/L [pH_o 5.5]	2.35E+02 (±16%)	6.00E+02	0.39	2.52E-05
12-6-GR-001-U	13	0.710	1.6 mg/L [pH_o 5.8]	1.81E+02 (±17%)	4.75E+02	0.38	2.59E-05
13-6-GR-001-U	14	0.699	2.8 mg/L [pH_o 5.7]	5.66E+02 (±16%)	1.44E+03	0.39	2.78E-05
14-6-GR-001-U	15	0.704	2.3 mg/L [pH_o 5.8]	1.19E+02 (±16%)	3.02E+02	0.39	2.82E-05
15-6-GR-001-U	16	0.679	2.8 mg/L [pH_o 5.9]	3.28E+02 (±16%)	8.52E+02	0.39	2.93E-05
16-6-GR-001-U	17	0.699	2.0 mg/l [pH_o 5.5]	4.32E+02 (±17%)	1.11E+03	0.39	3.08E-05
17-6-GR-001-U	18	0.696	2.1 mg/L [pH_o 5.7]	2.11E+02 (±18%)	5.48E+02	0.39	3.15E-05
18-6-GR-001-U	19	0.706	2.0 mg/L [pH_o 5.5]	4.66E+02 (±16%)	1.21E+03	0.39	3.31E-05

6-GR-001-U		PGR-001-U Leachate					
Sample ID	**Leach Interval**	**Leachate Volume (L)**	**Alkalinity (mg/L as $CaCO_3$) [Initial pH]**	**U_{total} (pCi/L ± %2σ) ***	**U_{total} (µg-U/L) ****	**U_{total} (pCi/µg-U)**	**Cumulative Mass Fraction Leached**
19-6-GR-001-U	20	0.705	2.6 mg/L [pH_o 5.6]	4.01E+02 (±17%)	1.00E+03	0.40	3.44E-05
20-6-GR-001-U	21	0.715	2.2 mg/L [pH_o 5.6]	6.36E+02 (±15%)	1.60E+03	0.40	3.66E-05
21-6-GR-001-U	22	0.697	3.2 mg/L [pH_o 6.2]	3.48E+02 (±18%)	9.07E+02	0.38	3.78E-05
22-6-GR-001-U	23	0.697	2.8 mg/L [pH_o 5.7]	9.80E+02 (±17%)	2.59E+03	0.38	4.13E-05

Notes: * Result (± %2σ, propagated error), where %2σ = 100%* (2σ/Result)
** Estimated with use of isotopic specific activities
% – percent
σ – one standard deviation
$CaCO_3$ – calcite
g – gram(s)
GR – Grayford/Ryker
ID – identification
L – liter
µg-U/L – microgram(s) uranium per liter
mg/L – milligram(s) per liter
pCi/L – picoCuries per liter
pCi/µg-U – picoCuries per microgram of uranium
PGR – soil type Grayford/Ryker
pH_o – initial pH
U_{total} – total uranium

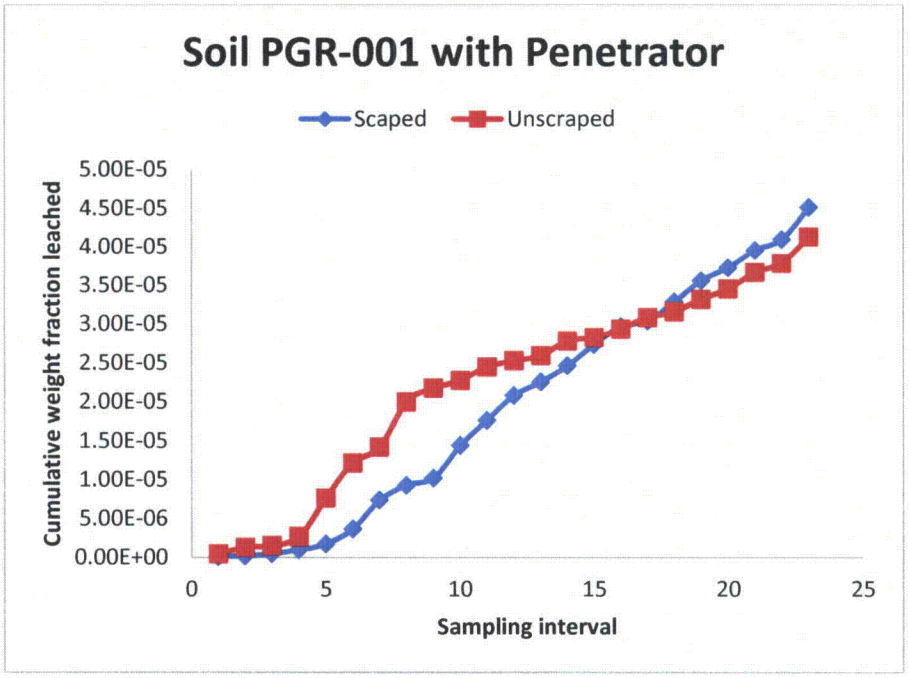

Notes: PGR – soil type Grayford/Ryker

Figure A1- 8. Estimates of Fractional Leaching of Uranium from Penetrators in Soil for Specimens in PGR-001 Soil.

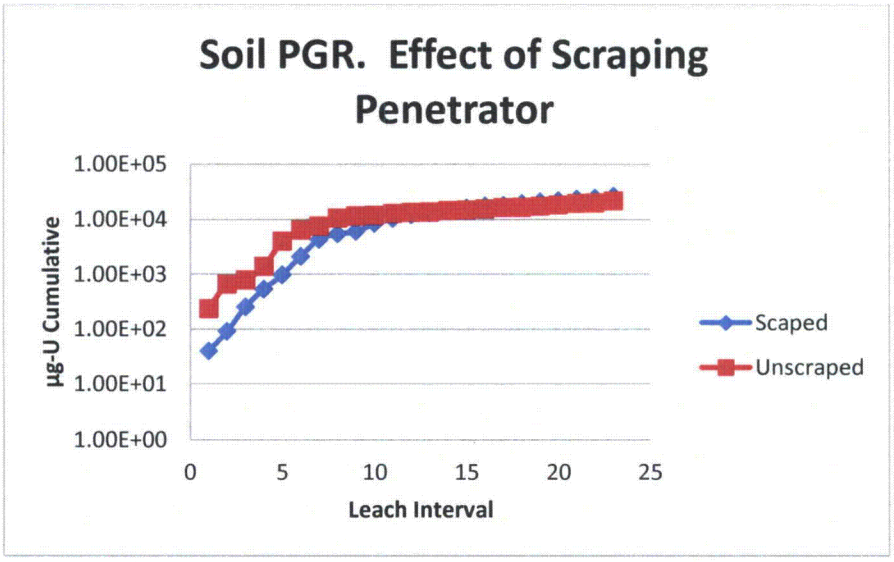

Notes: PGR – soil type Grayford/Ryker
µg-U – microgram(s) uranium

Figure A1- 9. Data as in Figure A1-8, but with Logarithmic Chart Ordinate (to Emphasize Data for Initial Leach Intervals).

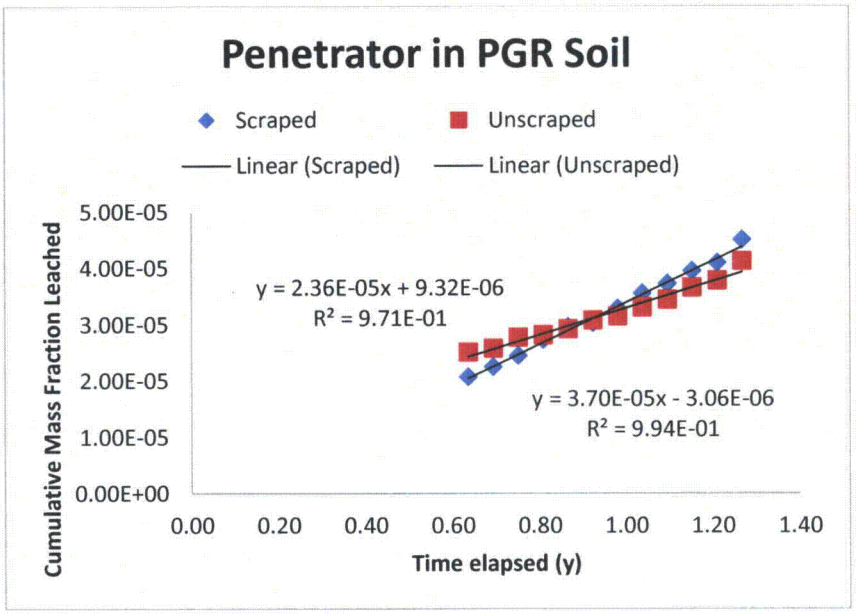

Notes: DU – depleted uranium
PGR – soil type Grayford/Ryker
R^2 – correlation coefficient squared
y – year(s)

Figure A1- 10. Steady-State Migration Rate of DU from Soil Containing Penetrator Dart into Collected Aqueous Leachate.

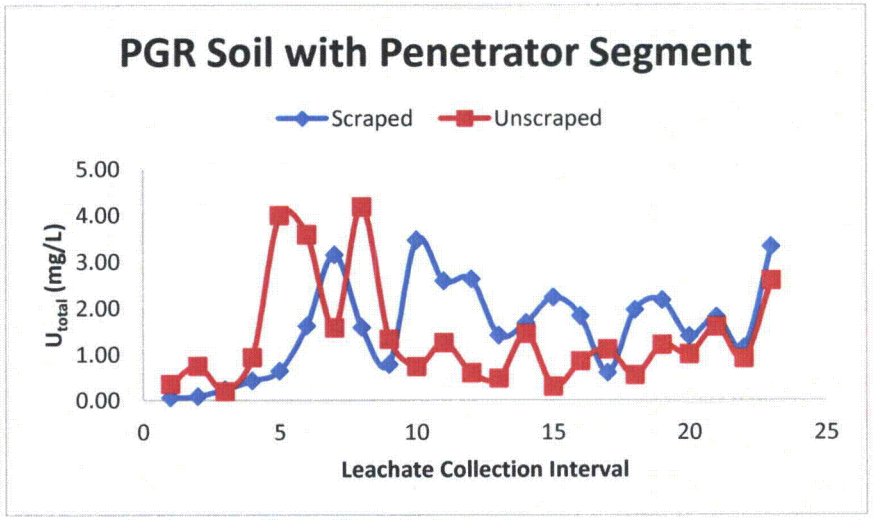

Notes: mg/L – milligram(s) per liter
PGR – soil type Grayford/Ryker
U_{total} – total uranium

Figure A1- 11. Estimates of Total Uranium *Concentration* in Aqueous Eluate by Collection Interval for Soil Type PGR

A2. EFFECT OF SOIL TYPE ON LEACHING FROM PENETRATOR

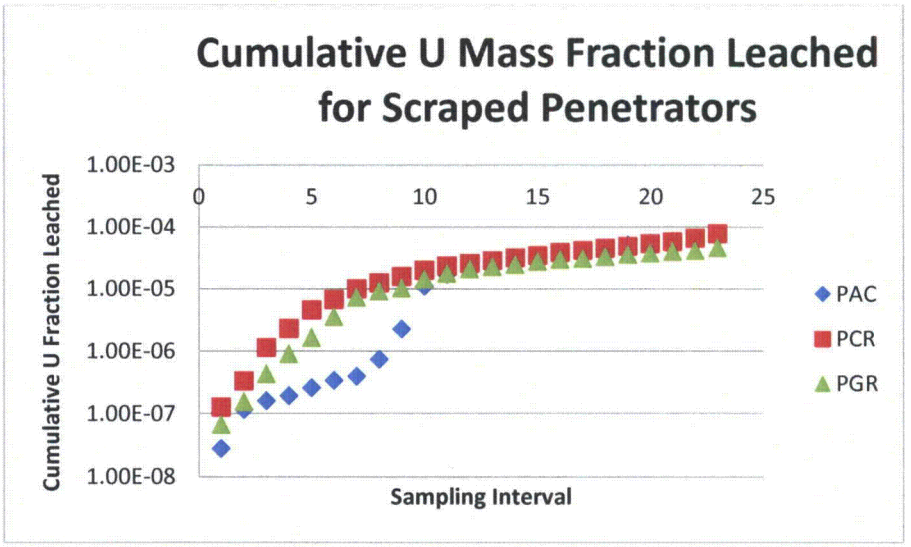

Notes: PAC – soil type Avonsburg/Cobbsfork
PCR – soil type Cincinnati/Rossmoyne
PGR – soil type Grayford/Ryker
U – uranium

Figure A1- 12. Effect of Soil Type on Leaching from (Scraped) Penetrator (Note Logarithmic Ordinate)

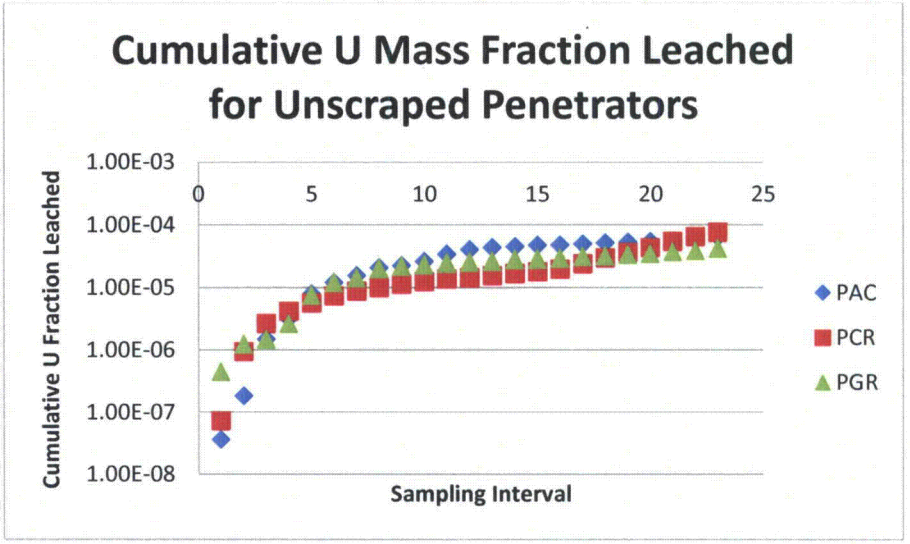

Notes: PAC – soil type Avonsburg/Cobbsfork
PCR – soil type Cincinnati/Rossmoyne
PGR – soil type Grayford/Ryker
U – uranium

Figure A1- 13. Effect of Soil Type on Leaching from (Unscraped) Penetrator (note logarithmic ordinate)

Table A1- 8. Summary for Leach Series 7-AC-005
No Penetrator; 1000.4-g soil

7-AC		PAC Leachate					
Sample ID	**Leach Interval**	**Leachate Volume (L)**	**Alkalinity (mg/L as $CaCO_3$) [Initial pH]**	**U_{total} (pCi/L ± %2σ) ***	**U_{total} (µg-U/L) ****	**U_{total} (pCi/µg-U)**	**Cumulative µg Leached**
00-7-AC	1	0.517	34.9 mg/L [pH_o 6.9]	1.15E+02 (±12%)	6.05E+01	1.90	3.13E+01
01-7-AC	2	0.626	2.6 mg/L [pH_o 6.0]	1.22E+01 (±16%)	2.09E+01	0.58	4.44E+01
02-7-AC	3	0.617	5.1 mg/L [pH_o 6.6]	2.53E+01 (±14%)	3.48E+01	0.73	6.59E+01
03-7-AC	4	0.630	4.9 mg/L [pH_o 6.4]	1.50E+01 (±15%)	2.41E+01	0.62	8.11E+01
04-7-AC	5	0.632	4.0 mg/L [pH_o 6.3]	3.88E+01 (±13%)	5.72E+01	0.68	1.17E+02
05-7-AC	6	0.647	4.7 mg/l [pH_o 6.4]	1.25E+01 (±17%)	3.01E+01	0.42	1.37E+02
06-7-AC	7	0.658	3.5 mg/L [pH_o 6.0]	1.41E+01 (±17%)	3.71E+01	0.38	1.61E+02
07-7-AC	8	0.694	2.9 mg/L [pH_o 6.2]	9.78E+00 (±21%)	2.45E+01	0.40	1.78E+02
08-7-AC	9	0.669	2.5 mg/L [pH_o 6.1]	5.07E+00 (±24%)	1.33E+01	0.38	1.87E+02
09-7-AC	10	0.691	2.8 mg/l [pH_o 6.1]	8.06E+00 (±21%)	1.97E+01	0.41	2.01E+02
10-7-AC	11	0.675	2.0 mg/l [pH_o 5.7]	5.29E+00 (±23%)	1.28E+01	0.41	2.09E+02
11-7-AC	12	0.683	2.7 mg/L [pH_o 5.9]	3.24E+00 (±27%)	7.70E+00	0.42	2.15E+02
12-7-AC	13	0.682	1.7 mg/L [pH_o 5.9]	5.64E+00 (±21%)	1.26E+01	0.45	2.23E+02
13-7-AC	14	0.678	2.8 mg/L [pH_o 6.0]	6.05E+00 (±22%)	1.29E+01	0.47	2.32E+02
14-7-AC	15	0.677	2.9 mg/L [pH_o 5.9]	5.55E+00 (±22%)	1.35E+01	0.41	2.41E+02
15-7-AC	16	0.675	3.0 mg/L [pH_o 5.9]	6.84E+00 (±23%)	1.71E+01	0.40	2.53E+02
16-7-AC	17	0.689	3.3 mg/L [pH_o 6.2]	7.46E+00 (±23%)	1.95E+01	0.38	2.66E+02
17-7-AC	18	0.701	2.5 mg/L [pH_o 6.0]	1.07E+01 (±36%)	2.30E+01	0.46	2.82E+02
18-7-AC	19	0.704	2.0 mg/L [pH_o 5.8]	4.46E+00 (±25%)	1.08E+01	0.41	2.90E+02

7-AC		PAC Leachate					
Sample ID	**Leach Interval**	**Leachate Volume (L)**	**Alkalinity (mg/L as $CaCO_3$) [Initial pH]**	**U_{total} (pCi/L ± %2σ) ***	**U_{total} (µg-U/L) ****	**U_{total} (pCi/µg-U)**	**Cumulative µg Leached**
19-7-AC	20	0.676	2.2 mg/L [pH_o 5.8]	4.90E+00	1.29E+01	0.38	2.98E+02
20-7-AC	21	0.682	2.2 mg/l [pH_o 5.8]	6.81E+00 (±21%)	1.74E+01	0.39	3.10E+02
21-7-AC	22	0.677	4.8 mg/L [pH_o 7.1]	6.60E+00 (±22%)	1.52E+01	0.43	3.21E+02
22-7-AC	23	0.685	2.4 mg/L [pH_o 5.9]	1.54E+01 (±69%)	2.67E+01	0.58	3.39E+02

Notes: * Result (± %2σ, propagated error), where %2σ = 100%* (2σ/Result)
** Estimated with use of isotopic specific activities
% – percent
σ – one standard deviation
$CaCO_3$ – calcite
g – gram(s)
AC – Avonsburg/Cobbsfork
ID – identification
L – liter
µg – microgram(s)
µg-U/L – microgram(s) uranium per liter
mg/L – milligram(s) per liter
pCi/L – picoCuries per liter
pCi/µg-U – picoCuries per microgram of uranium
PAR – soil type Avonsburg/Cobbsfork
pH_o – initial pH
U_{total} – total uranium

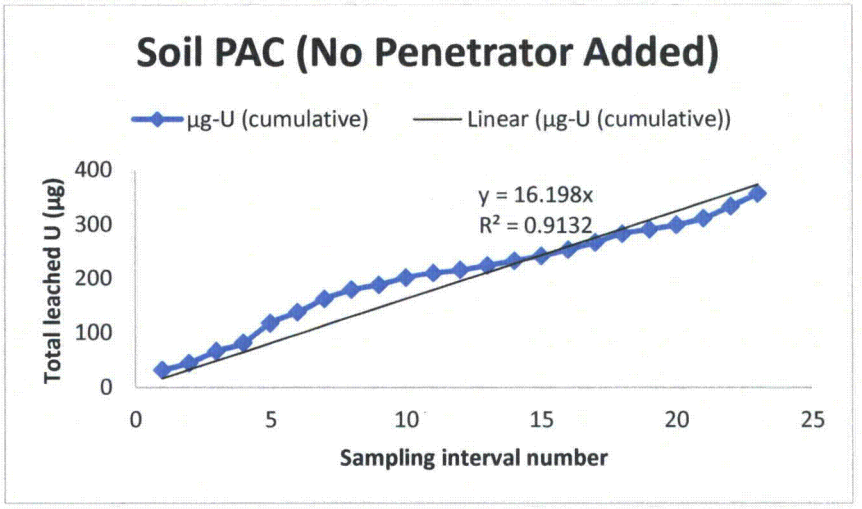

Notes: PAC – soil type Avonsburg/Cobbsfork
R^2 – correlation coefficient squared
µg-U – microgram(s) of uranium
U – uranium

Figure A1- 14. Estimates of Fractional Leaching of Uranium from PAC-001 Soil (No Penetrator Dart Segment Added).

For the duration of testing, the average uranium activity in the leachate is approximately 15 pCi/L (23 µg-U/L). The uranium in the soil without added penetrator dart appears to be impacted by both natural and depleted uranium.

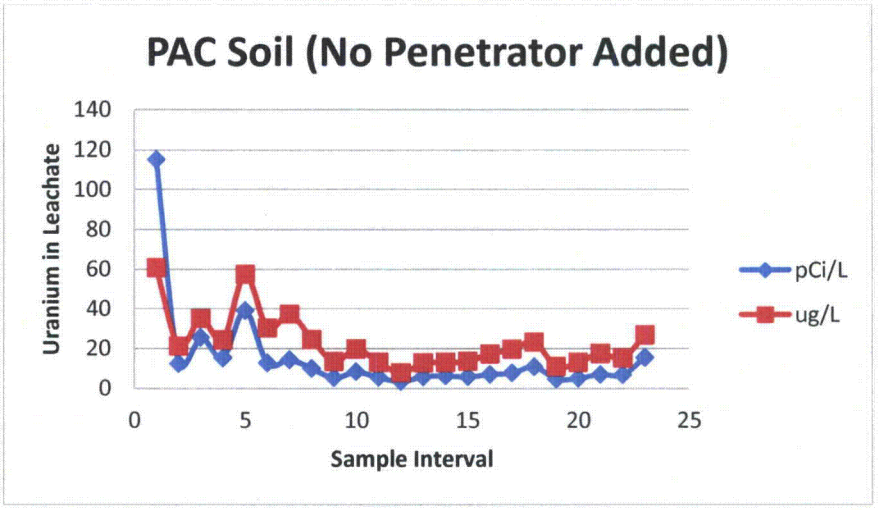

Notes: PAC – soil type Avonsburg/Cobbsfork
pCi/L – picoCurie(s) per liter
µg/L – microgram(s) per liter

Figure A1- 15. Total Uranium Estimates in Leachate from PAC-001 Soil (No Penetrator Dart Segment Added).

By sample interval #6, uranium activity in the leachate is consistently below 20 pCi/L. By Interval #8, the corresponding *concentration* estimates (μg-U/L) projected from the measured isotopic alpha activity data are consistently below the current (as of December 2003) EPA maximum contaminant level (MCL) criterion of 30 μg-U/L.

APPENDIX 2. PENETRATOR GEOMETRY AND "CORROSION RATE" ESTIMATES

Appendix 2. Penetrator Geometry and "Corrosion Rate" Estimates

Figure A2-1 illustrates a "typical" dart segment, with nominal diameter of 2.67-cm (greatest dimension).

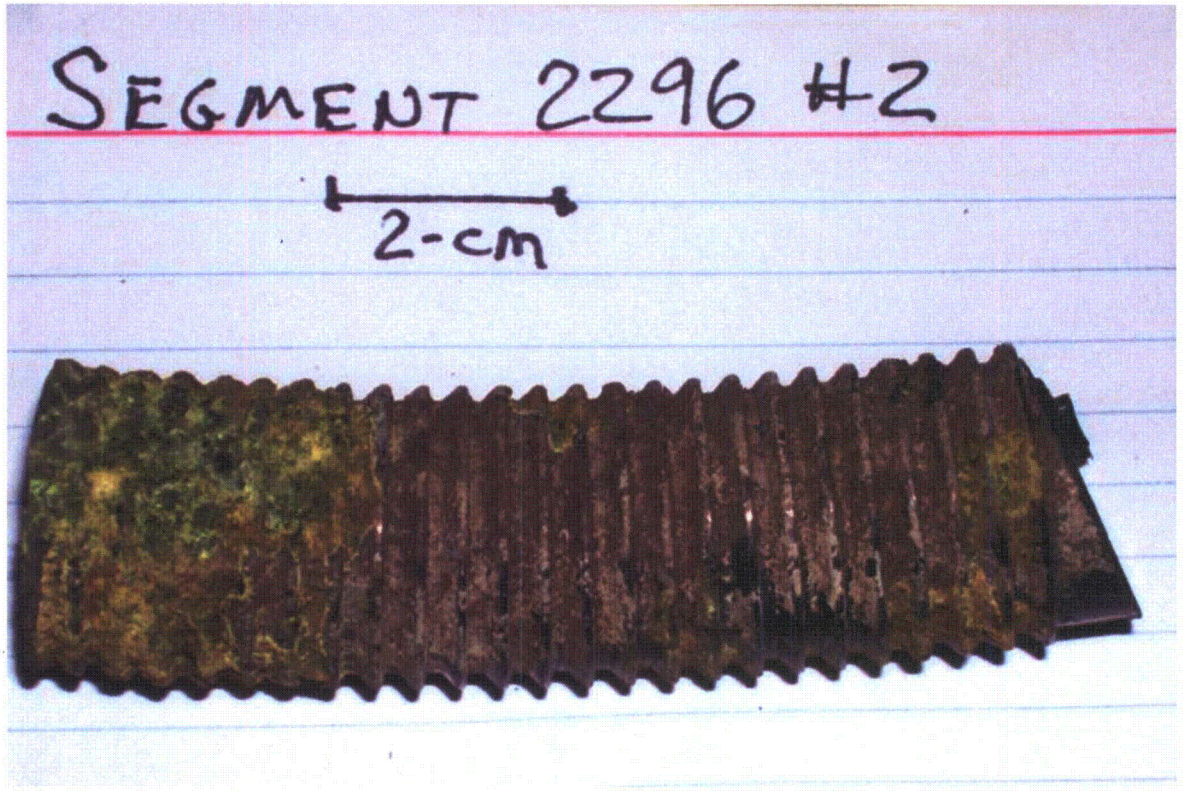

Notes: cm – centimeter
g –gram(s)

Figure A2- 1. Image of Dart Segment 2296-2 (577.5-g).

Using dimensions and geometries estimated from Figure A2-1 (using only the minimally corroded section), a *crude* estimate for the correlation between total simple geometric surface area and dart segment mass may be calculated:

$$\textbf{Surface area (}\textit{geometric}\textbf{, cm}^2\textbf{)} \sim \textbf{10+0.1*(mass, g)} \qquad \text{(A2-1)}$$

Where: ~ – approximately
cm^2 – square centimeter(s)
g – gram(s)

The empirical expression in (A2-1) does not include any additional roughness factor, to compensate between nominal geometric and actual surface area (i.e., it does not include estimates for adherent porous coatings or adhesions).

Data for nominal metal corrosion rate is typically normalized to the substrate surface area, and expressed in units such as g cm^{-2} y^{-1} (Handley-Sidhu et al., 2010; Hilton, 2000) (Equation A2-2).

$$\textbf{Corrosion Rate } (\mathbf{g\ cm^{-2}y^{-1}}) = \frac{\textbf{365 x Weight loss (g)}}{\textbf{Metal Surface Area } (\mathbf{cm^2}) \textbf{ x Time (days)}} \qquad \text{(A2-2)}$$

From Equation A2-1, the normalized metal corrosion rate (g $cm^{-2}y^{-1}$) is proportional to the metal release rate (gram(s) per day [g/d]) only after the soil column is completely saturated with the leached metal (no further retardation), and leaching rate approaches a steady-state.

Table A2-1 provides a crude estimate for geometric surface area for penetrator dart segments used in this study. Since dart mass changes minimally during the test period (Table 9 of main text), it may be assumed (for calculation purposes) that nominal dart geometric surface area also changes minimally (true surface area will be affected by the extent of surface corrosion).

Table A2- 1. Estimate of Test Dart Geometric Surface Areas

Cell Number	Initial Dart Mass (g)	Nominal Geometric Estimate * Surface Area (cm^2)
1	701.8	80.18
2	623.5	72.35
3	557.1	65.71
4	620.2	72.02
5	583.1	68.31
6	526.4	62.64

Notes: * From Equation A2-1
cm^2 – square centimeter(s)
g –gram(s)

Appendix 1 provides data for the mass of uranium that leaches from the penetrator dart segment through the associated soil layer (i.e., net metal release data). The *total* uranium metal lost, see Equation A2-2, cannot be determined until mass balance closure (i.e., until determination of the uranium hold-up in soil component and on the DU dart segment itself).

Figures A2-2 through A2-4 indicate that the steady-state release rate for total uranium in the leachate is of the order of 1E-4 g-U/d for dart segments with nominal surface area approximately 70-cm^2 (Table A2-1). From Equation A2-2, this yields an apparent "corrosion rate" about 5E-04 g $cm^{-2}y^{-1}$ (assuming that the test soil is essentially saturated with uranium by leach interval #10). Estimates are presented in Table A2-2; as noted previously, these estimates of "corrosion rate" do not account for the uranium that is effectively sequestered by relatively tenacious adherence to the dart surface. These qualified estimates may be compared to "corrosion rate" values compiled by Handley-Sidhu (Table A2-3). The present estimate of "effective" corrosion rate is very low, compared to estimates for (e.g.) oxic "field moist soil" (0.5 g $cm^{-2}y^{-1}$), and is more comparable to low corrosion rates noted for waterlogged media and/or

phosphate amended soil. This may suggest that the associated near-field soil is still significantly retarding uranium migration after about 1.3-y of laboratory weathering.

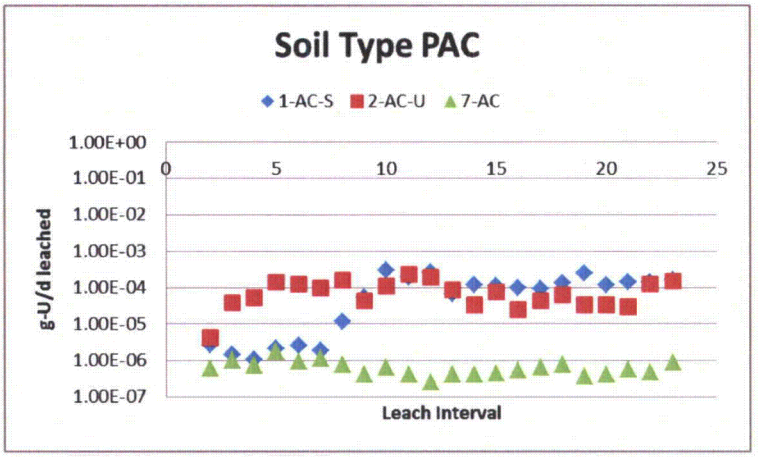

Notes: Δg-U/Δt – difference in grams(s) uranium per difference in time
AC –Avonsburg/Cobbsfork
g-U/d –gram(s) uranium per day
PAC – soil type Avonsburg/Cobbsfork

Figure A2- 2. Uranium Leached from Soil Type PAC (Δg-U/Δt).

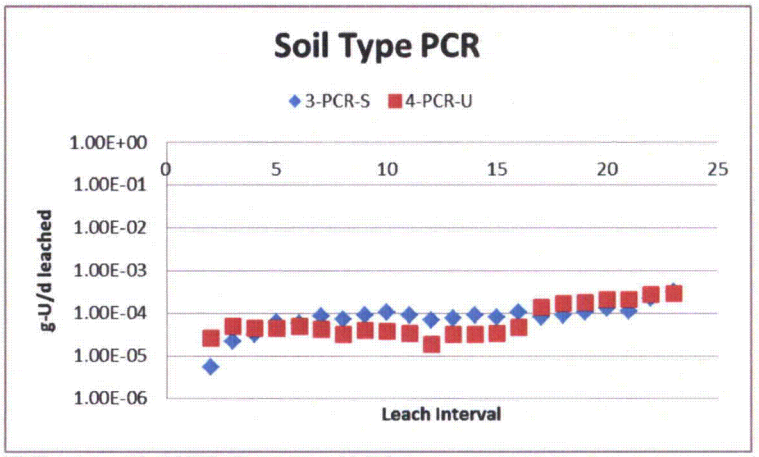

Notes: Δg-U/Δt – difference in grams(s) uranium per difference in time
CR – Cincinnati/Rossmoyne
g-U/d –gram(s) uranium per day
PCR – soil type Cincinnati/Rossmoyne

Figure A2- 3. Uranium Leached from Soil Type PCR (Δg-U/Δt).

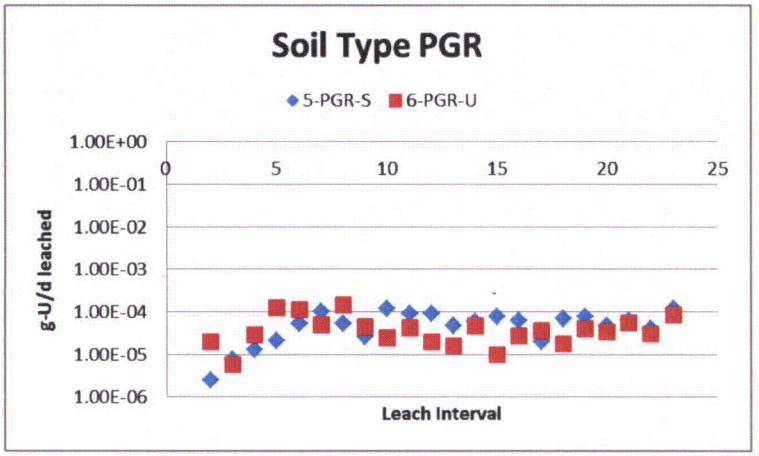

Notes: Δg-U/Δt – difference in grams(s) uranium per difference in time
g-U/d –gram(s) uranium per day
PGR – soil type Grayford/Ryker

Figure A2- 4. Uranium Leached from Soil Type PGR (Δg-U/Δt).

Table A2- 2. Estimates for Mean Release Rate and Nominal "Corrosion Rate" for JPG Data
(Leach intervals #10-23, elapsed time 211-463-d)

Cell ID	Release Rate (g-U/d)	Nominal "Corrosion Rate" * (g-U/(cm^{2}y))
1-AC-S	(1.55 ± 0.68)E-04	1.72E-02
2-AC-U	(0.86 ± 0.69)E-04	8.44E-03
3-CR-S	(1.21 ± 0.72)E-04	1.77E-02
4-CR-U	(1.24 ± 1.02)E-04	1.68E-02
5-GR-S	(0.69 ± 0.27)E-04	1.88E-02
6-GR-U	(0.35 ± 0.20)E-04	2.85E-02
7-AC (no dart)	(5.16 ± 1.69)E-07	N/A

Notes: * From Equation A2-1. Note that the nominal "corrosion rate" includes uranium hold-up in soil as well as the soluble uranium eluted with aqueous leachate.
AC –Avonsburg/Cobbsfork
CR – Cincinnati/Rossmoyne
g-U/(cm^{2}y) – gram(s) uranium per square centimeter year
g-U/d –gram(s) uranium per day
GR – soil type Grayford/Ryker
ID – identification
N/A – not applicable

Table A2- 3. Corrosion rates of DU-Ti alloy, as compiled by Handley-Sidhu et al. (2010).

Study	Environment	Geochemical Conditions	Rate ($g\ cm^{-2}y^{-1}$)	Comments	References
1	Air	Oxic	0.0012	Laboratory air (30 days)	Trzaskoma (1982)
2	H_2O	Oxic	0.072	Distilled water	Trzaskoma (1982)
3	3.5% NaCl	Oxic	0.40		Trzaskoma (1982)
4	5% NaCl	Oxic	1.5		McIntyre et al. (1988)
5	Seawater, Solway Firth	Oxic	2.6-3.1	In situ biogeochemical conditions and the level of physical disturbance were uncharacterised.	Toque and Baker (2007)
6	Marine sediment, Solway Firth	Not characterized	1.4-1.8	In situ biogeochemical conditions and the level of physical disturbance were uncharacterised.	Toque and Baker (2007)
7	Marine sediment microcosums simulating the Solway Firth	Progressively anoxic	0.056 ± 0.006	Salinities of 31.5 and 16.5; pH 6.4–8.0; 3.2% OC; CEC 4.0 meq/100 g and inorganic carbon 370 mg kg−1	Handley-Sidhu et al. (2009b)
8	Waterlogged sand (salinities of 31.5)	Nitrate-reducing	0.020 ± 0.003	(Salinity of 31.5; pH 7.6–7.9; 0.8% OC; CEC 1.3 meq/100 g and inorganic carbon 430 mg kg−1	Handley-Sidhu (2008)
9	Dune sand Eskmeals, Cumbria	Not characterized	0.080-0.17	pH 6.5–7.9	Toque and Baker (2006)
10	Dune sand simulating Eskmeals, Cumbria	Oxic	0.10 ± 0.01	pH 7.2–7.5; 0.8% OC; CEC 1.3 meq/100 g; inorganic carbon 430 mg kg−1 and sand moisture content of 13%	Handley-Sidhu et al (2009a)
11	Organic, clay-rich soil from Kirkcudbright	Not characterized	0.80-1.1	pH 5.8–6.0	Toque and Backer (2006)
12	Field-moist soil	Oxic	0.49 ± 0.06	pH 5.0–6.5; 12% OC; CEC 21 meq/100 g; inorganic carbon 80 mg kg−1 and soil moisture content of 22%	Handley-Sidhu et al (2009c)
13	Sandy-loamy and silty-loamy soil	Not characterized	0.19 ± 0.03	Two soils investigated; pH 5.6 and 5.7; 2.1% OC.	Schimmack et al. (2007)
14	Waterlogged soil	Nitrate-reducing	0.010-0.02*	pH 5.0 – 6.5; 12% OC; CEC 21 meq/100 g and inorganic carbon 80 mg kg^{-1}. *Corrosion ceased under anoxic conditions.	Handley-Sidhu et al (2009c)
15	Phosphate-fertilized waterlogged soil	Nitrate-reducing	0.00016-0.0044	Olsen phosphorus 27 – 45 mg kg^{-1}; pH 5.0 – 6.0; 12% OC; CEC 21 meq/100 g and inorganic carbon 80 mg kg^{-1}.	Unpublished;

Notes:
* Corrosion ceased under anoxic conditions.
% – percent
CEC – cation exchange capacity
DU – depleted uranium
$g\ cm^{-2}y^{-1}$ – gram(s) per centimeters squared year
H_2O – water
meq – milliequivalent of hydrogen
mg kg-1 – milligram(s) per kilogram
NaCl – sodium chloride
OC – organic carbon
Ti – titanium

APPENDIX 3. SOIL SAMPLE PROVENANCE

Appendix 3. Soil Sample Provenance

Soil specimens were held at the MCLinc facility for a long time duration, which encompassed delays in notice to proceed with different phases of the investigation and also the duration of active testing that was performed. Since soil storage conditions (including oxygen fugacity) may affect the activity of native microbial populations, we summarize these conditions in Table A3-1.

Table A3- 1. Soil Sample Provenance

Date	Action	Comment
10/22/2008	Field sampling event (SAIC COC JPG001-MCL)	Samples shipped with water ice (~0 °C)
10/23/2008	Receipt of bulk soil samples at MCLinc	Samples refrigerated (~6 °C)
5/28/2009	Initial notice to proceed from client	Samples refrigerated (~6 °C)
6/26/2009	Begin leach interval #1 (21-d cycle) *	Ambient (~23 °C) temperature
10/06/2010	Collect final leach interval #23	Total leach test duration ~ 480-d
6/08/2012	Remove soil from leach chambers and refrigerate soil cores	Prior static ambient (~23 °C) storage 611-d.
6/26/2013	Remove refrigerated soil cores for additional analysis	Refrigerated (~2 °C) storage 385-d
7/08/2013	Begin SE	

Notes: * Soil samples were stored refrigerated (approximately 6 °C) until shortly before the preparation of soil columns for use in accelerated leach testing.
~ – approximately
°C – degree(s) Celsius
COC – Chain of Custody
d - day
MCL – Materials and Chemistry Laboratory, Inc.
SAIC – Science Applications International Corporation
SE – sequential extraction

Note that the soil cores were stored in the test chambers at ambient laboratory temperature for 611-d between the completion of leach interval #23 (10/06/2010) and the date (6/08/2012) that the soils were removed from the test chamber, bagged and refrigerated (approximately 6 °C) for possible indefinite storage. During the interval of static ambient storage, the soil was maintained moist and there was some communication with ambient air (Figure A1-1). The ambient-stored soil cores maintained biological activity, as evinced by the flora illustrated in Figures A1-1 and A1-2.

Figure A3- 1. Soil Test Cells Photographed April 26, 2011 (During Static Ambient Storage).

Flora (algae) appear to have been established in the control and other cells. Note that the cells, containing drained soil, communicate with the ambient atmosphere via severed ¼ inch tubing, and that there is water condensate present in the chamber. Storage conditions thus likely approximate that of soil in the drained, near-surface vadose zone.

Figure A3- 2. Cell #7 Soil Core (Type PAC, Control), Photographed After Static Ambient Storage of 611-d.

Flora has been established at the surface of the control cell and also in several of the test specimens (notably in Soil type PAC, Cells #1 and 2).

APPENDIX 4. MCLINC PROCEDURE FOR MODIFIED TESSIER SEQUENTIAL EXTRACTION PROCEDURE

Materials and Chemistry Laboratory, Inc. (MCLinc)
2010 Highway 58, Suite 1000
Oak Ridge, Tennessee 37830-1702
(865) 576-4138 www.MCL-inc.com

Appendix 4. MCLinc Procedure for Modified Tessier Sequential Extraction Procedure

(Uncontrolled copy of MCLinc, Modified Tessier Sequential Extraction Procedure for 2.5-g Soil or Sediment Sample, MCL-7756, Appendix XX)

Code: MCL-7756
OPERATOR AIDS
Appendix XX
Effective: 12/10/2010

APPENDIX XX

MODIFIED TESSIER SEQUENTIAL EXTRACTION PROCEDURE FOR 2.5 GRAMS OF SOIL OR SEDIMENT SAMPLE

1. PURPOSE

The practical technique of choice for evaluating low-level radionuclide partitioning in soils and sediments is the sequential extraction approach.[1] This methodology applies to operationally-defined chemical treatments to selectively dissolve specific classes of macro-scale soil or sediment components. There is no general agreement on the solutions preferred for the extraction of various components in sediment or soils, due mostly to the matrix effects involved in heterogeneous chemical processes. The protocol below is based on the original method of Tessier et al. (1979), with minor modifications reflecting more recent literature evaluations.

2. SAMPLE RECEIPT AND PREPARATION

It is recommended that soil core samples be shipped overnight to Materials and Chemistry Laboratory, Inc. (MCLinc), packed with water ice to maintain the temperature at approximately 0 to 4 degrees Celcius (°C) to minimize potential constituent changes due to microbial activity. If analysis cannot be initiated on the day of receipt, core samples will be placed in a deep freeze and maintained at approximately -20 °C until testing can be performed (see, e.g., Hlavay et al., 2004). Unless specific contractual arrangements have been negotiated with the client, sample after thawing will not be excluded from exposure to the ambient atmosphere during sample processing; strict air-exclusion may minimize confounding sulfide-bound metals with their oxide-bound counterparts and may help preserve in-situ redox conditions for anoxic sediments (Rapin et al., 1986; Peltier, 2005). If air-exclusion is specified and commissioned by the client, then sample preparation and extraction must be performed in an oxygen-free environment (e.g., within a specially maintained anoxic glove box).

Sample size is dictated by the apparent sample homogeneity. If relatively large pebbles are first removed (e.g., with use of a #10 mesh standard screen, to remove particles greater than two millimeters in diameter), a sample size of approximately 2.5 grams (g) (dry weight equivalent) of blended soil may be used. (Record actual mass taken). If wet soil is used, the moisture content must be estimated with use of a separate sample, to permit interpretation of results expressed on a dry-weight basis.

The lack of suitable certified reference materials for use with this procedure has precluded intra-laboratory comparability of results and hence good quality control (QC). QC is thus the usual controls on analytical accuracy.

3. ACRONYMS

°C	degrees Celcius
cc	cubic centimeter(s)
$CaCO_3$	calcite

UNCONTROLLED
INFORMATIONAL USE ONLY

[1] http://physics.nist.gov/Divisions/Div846/Gp4/Environ/speciation.html

CBD reagent	citrate-bicarbonate-dithionite
CH_3COOH	acetic acid or acetate
CH_3COONa	sodium acetate
CO_2	carbon dioxide
EPA	U.S. Environmental Protection Agency
Fe	iron
FW	formula weight
g	gram(s)
h	hour(s)
H_2O	water (de-ionized)
H_2O_2	hydrogen peroxide
HCl	hydrochloric acid
HNO_3	nitric acid
ICP	inductively coupled plasma spectroscopy
L	liter(s)
MCLinc	Materials and Chemistry Laboratory, Inc.
min	minute(s)
µg/g	microgram(s) per gram
mg/Kg	milligram(s) per kilogram
mL	milliliter(s)
mol/L	mole(s) per liter
$MgCl_2$	magnesium chloride
NaOH	sodium hydroxide
$NH_4C_2H_3O_2$	ammonium acetate
NIOSH	National Institute for Occupational Safety and Health
OES	optical emission spectrometry
QC	quality control
RPM	revolutions per minute
TCLP	Toxicity Characteristic Leaching Procedure
U	uranium
V	volume
v/v	volume per volume

UNCONTROLLED
INFORMATIONAL USE ONLY

4. FRACTION 1: EXCHANGEABLE CATIONS (MAGNESIUM CHLORIDE, pH 7)

Short-term (e.g., 1 hour [h]) equilibration of soil with a near-neutral solution containing a relatively high concentration (e.g., 1 mole per liter [mol/L]) of electrolyte dissolves water-soluble salts and liberates readily exchangeable cations (by ion displacement). For the extraction of trace contaminants, Phillips and Chapple (1995) and also Tessier et al. (1979) favor use of a solution of 1 mol/L magnesium chloride ($MgCl_2$) (pH 7).

4.1. Extraction:

Reagent 1: For about 250 milliliters (mL) lixivant (extraction reagent), add 50.8-g $MgCl_2 \cdot 6H_2O$ (formula weight [FW] = 203.3) to approximately 200-mL de-ionized water; adjust pH value to approximately 7.0 with the use of dilute sodium hydroxide (NaOH) or hydrochloric acid (HCl) solution, then adjust to final volume (approximately 250-mL).

UNCONTROLLED
INFORMATIONAL USE ONLY

Dry soil, 2.5-g, is contacted with 20-mL of 1 mol/L $MgCl_2$ (pH 7) in a sealed 50 cubic centimeter (cc) centrifuge cone for 1-h at ambient temperature. (Optimum contact is provided by tumbling the sealed vial on a Toxicity Characteristic Leaching Procedure [TCLP] rotary extractor unit). Slurry is subsequently centrifuged at 4000 revolutions per minute (RPM) for 12 minutes (min) and then the supernate is taken to a labeled 50-mL volumetric flask. Solid residue is rinsed in another 10-mL aliquot of lixivant, and then clarified by centrifugation. The supernate is added to the labeled volumetric flask, and the contents diluted to final volume by addition of demineralized (de-ionized) water (H_2O).

5. FRACTION 2: CARBONATE-BOUND METALS (ACETATE REAGENT, pH 8.2)

Following the extraction of exchangeable cations, many researchers, including Phillips and Chapple (1995), have included an extraction using 6-h contact with slightly acidic 1 mol/L sodium acetate (CH_3COONa) (pH 5). This step is said to liberate the trace metal ions co-precipitated or otherwise occluded in calcite ($CaCO_3$) sediment deposits. Tessier et al (1979) prefer a variant reagent, in which the pH of the acetate solution is adjusted to 8.2; attack on silicate and sulfide minerals is said to be minimal with use of this reagent.

5.1. Extraction:

Reagent 2: For approximately 250-mL reagent, add about 15-g reagent grade acetic acid (CH_3COOH) to approximately 200-mL de-mineralized water. Adjust pH value to 8.2 by the gradual addition of NaOH, then add de-mineralized water to a final volume of 250-mL.

To the wet solid residue from Fraction 1, add 20-mL of 1 mol/L CH_3COONa (pH adjusted to a value of 8.2). Contact for 6-h at ambient temperature. The supernate is added to the labeled volumetric flask. Sample may be washed by the addition of another 10-mL aliquot of reagent, briefly re-suspending the solids, followed by centrifugation. Supernate is again added to the labeled volumetric flask and contents diluted to final volume by addition of demineralized water.

6. FRACTION 3: METALS ASSOCIATED WITH HYDROUS IRON AND MANGANESE OXIDES (HYDROXYLAMINE-ACETATE REAGENT)

(Hydroxylamine-Acetate Reagent)

Methods for leaching iron and manganese oxides involve a combination of reagents to reduce these metals to soluble Fe^{+2} and Mn^{+2} forms, respectively, and to keep these forms in solution at relatively high concentrations. The reagent preferred by Tessier et al. (1979) consists of 0.04 mol/L $NH_4OH{\cdot}HCl$ in 25 percent (volume per volume [v/v]) (CH_3COOH [pH 2]). The extraction of reducible iron and manganese oxides is said to be complete when soil is contacted with the reagent at 96 ± 3 °C for about 6-h with occasional agitation. The hydroxylamine reagent is said to be more effective than citrate-bicarbonate-dithionite (CBD reagent) for the dissolution of metal sulfide phases (Tessier et al., 1979).

6.1. Extraction: To the residue from Fraction 2, add 20-mL of 0.04 mol/L $NH_4OH{\cdot}HCl$ (FW = 71.5) in 25 percent (v/v) acetic acid (pH 2).

Reagent 3: For approximately 250-mL reagent: to approximately 150-mL of de-ionized water add 62.5-mL (65.5-g) metals-grade CH_3COOH, and then 0.715-g $NH_4OH{\cdot}HCl$. Mix well and

check pH value; adjust to pH 2 (if necessary) with use of dilute NaOH or HCl solution. Dilute to final volume (250-mL) with de-ionized water.

To the residue from Fraction 2, add 20-mL of 0.04 mol/L NH_4OH•HCl (FW = 71.5) in 25 percent (v/v) acetic acid (pH 2). *Caution*: for samples containing large amounts of carbonate minerals, carbon dioxide (CO_2) gas evolution may be excessive, causing bubbling and possible spewing (with loss of sample). If vigorous bubbling is observed upon initial addition of reagent, allow several minutes for degassing in an uncapped vessel before applying heat. The centrifuge cone is then capped loosely and the soil is contacted with the reagent by placing the cone and contents in a water bath (or dry heating bock) maintained at 96 ± 3 °C for about 6-h, with occasional agitation of the bottle and contents. After equilibration, the sample is centrifuged and the supernate is added to the labeled volumetric flask. Sample may be washed by the addition of another 10-mL aliquot of reagent, briefly re-suspending the solids, followed by centrifugation. Supernate is again added to the labeled volumetric flask and the contents diluted to final volume by addition of de-ionized water.

7. FRACTION 4: BOUND TO ORGANIC MATTER

Trace metals may be bound to various forms of organic matter: natural organic matter (notably humic and fulvic acids), microbes, detritus, coatings on mineral particles, etc. (Tessier et al., 1979). Phillips and Chapple (1995) treat the residue from Fraction 3 (above) with dilute (0.02 mol/L) nitric acid (HNO_3) with added hydrogen peroxide (H_2O_2) solution, heating the mixture to approximately 85°C for a total of 6-h.

7.1. Extraction:

Reagent 4A: Approximately 250-mL of lixivant is prepared by the addition of 100-mL of 0.02 mol/L HNO_3 to 150-mL of 30 percent H_2O_2. (Add dilute acid to the peroxide until the mixture pH value is adjusted to 2).

Reagent 4B: Acidic ammonium acetate solution is prepared as 3.2 mol/L (247 grams per liter [g/L]) ammonium acetate ($NH_4C_2H_3O_2$) in 20 percent (v/v) HNO_3.

The solid residue from Fraction 3 is extracted with 20-mL of acid peroxide solution (Reagent 4A). The solids are re-suspended in this solution, and the slurry heated to 85 ± 2 °C for 2-h with occasional shaking. Heating is continued for a total of 5-h, with additional increments of reagent added periodically as required to maintain slurry volume. The container and contents are allowed to cool to room temperature. Next, add 20-mL of acidic ammonium acetate solution (Reagent 4B), and shake the bottle and contents continuously for 0.5-h at room temperature. Centrifuge and collect the supernate into a labeled 50-mL volumetric flask. Sample may be washed by the addition of another 10-mL aliquot of ammonium acetate reagent (Reagent 4B), briefly re-suspending the solids, followed by centrifugation. Supernate is again added to the labeled volumetric flask and contents diluted to final volume by addition of demineralized water.

8. RESIDUAL FRACTION

Because the residual fraction is not considered to be available for release to the environment except on a geological time scale, it may not be necessary to quantitate this fraction unless the data is needed for mass balance closure. Total digestion is relatively difficult and expensive, and seldom used in environmental analysis. More commonly used strong, acid-based extractions such as U.S. Environmental Protection Agency (EPA) Method 3050B,"Acid Digestion of Sediments,

UNCONTROLLED
INFORMATIONAL USE ONLY

UNCONTROLLED
INFORMATIONAL USE ONLY

Sludges, and Soils," and Method 3051A, "Microwave Assisted Acid Digestion of Sediments, Sludges, Soils, and Oils," generally recover most of the available heavy metal content, but they cannot recover metals locked within a refractory silicate matrix. The proportion of residual metal may also be roughly estimated by mass balance, if an estimate of total constituent analysis is available for the original material. Optionally (as a QC check), the residue from Fraction 5 (above) can be extracted by the same methodology used to estimate the original soil constituent or contaminant inventory; this would thus represent a direct estimate of the residual fraction.

8.1. Extraction (As Total Environmentally Available Constituent)

A separate aliquot sample of test material is extracted with use of MCLinc standard operating procedure MCL-7746, "Acid Digestion for Metals," (based on EPA preparative Method 3050B as defined in SW-846). This estimate for each constituent of interest will represent the total environmentally available constituent. The results for metals analysis for each of the previous sequential extractions may be compared to the available inventory, computing a percentage extracted. Mass balance closure (original inventory less constituent extracted by Fractions 1 through 4) represents an indirect estimate of the residual fraction.

9. ANALYTICAL PROCEDURES

Analysis by inductively coupled plasma spectroscopy (ICP) may require digestion to destroy excess organic reagent (e.g., acetate [CH_3COOH]) and/or substantial dilution of the sample prior to analysis. Analysis will be for select dissolved metals (e.g., uranium [U] and iron [Fe], etc.) by ICP (with detection by optical emission spectroscopy, ICP-OES, MCL-7751, "Inductively Coupled Plasma-Atomic Emission Spectrometry [EPA Method 6010B]," or mass spectroscopy, ICP-MS, MCL-7768, "Inductively Coupled Plasma – Mass Spectrometry Element/Metals Sample Preparation and Analysis"), with appropriate analytical quality assurance (e.g., MCL-7751, based upon National Institute for Occupational Safety and Health [NIOSH] Method 7300, "Elements by ICP [Nitric/Perchloric Acid Ashing]," and EPA SW-846 Method 6010B). Due to the very high salt and organic acid concentrations in many lixiviates used, sample digestion (MCL-7752, "Acid Digesion of Aqueous Samples [EPA Method 3010A]," based on EPA SW-846 Method 3010A, "Acid Digestion of Aqueous Samples and Extracts for Total Metals for Analysis by FLAA or ICP Spectroscopy") and extensive dilution will be required prior to ICP analysis. This high salt content of the digested spent lixivant limits the sensitivity for trace elements (e.g., for U in soil, the reporting limit by ICP-OES will be 0.4 micrograms per gram [µg/g] for each of the extraction steps).

10. CALCULATIONS

The total mass of selected constituent extracted by each sequential leaching procedure is referenced to the original sample mass (Step 1), and is reported in units of milligrams per kilogram (mg/kg) or µg/g.

Constituent (µg/g) = (concentration, µg/L)*(Volume [V] in liters [L])/(original dry sample weight, g)

Concentration (µg/L) in the original extraction lixivant (corrected for any dilution factors required for analysis) is estimated by the ICP instrumentation. By the procedure above, V = 50-mL = 0.05-L.

APPENDIX 4. MCLINC PROCEDURE FOR MODIFIED TESSIER SEQUENTIAL EXTRACTION PROCEDURE

Characterization of Two sections of Sample JP-PAC-05 (2288) by Scanning Electron Microscopy with Associated Energy Dispersive Spectroscopy (EDS)

MCLinc Project EMP002105

Prepared for:

Joseph N. Skibinski, Program Manager for SAIC

Prepared by:
Robert J. Stevenson, Ph.D.
Materials and Chemistry Laboratory, Inc. (MCLinc)
2010 Highway 58, Suite 1000
Oak Ridge, Tennessee 37830-1702
(865) 576-4138 www.MCL-inc.com

Date Prepared: January 22, 2010

Robert J. Stevenson, Ph.D. _____ Date _____

Greg Wagner, Ph.D. _____ Date _____

CASE NARRATIVE

Sample Receipt

Twenty-four samples of uranium-containing material were received by Materials and Chemistry Laboratory, Inc. (MCLinc) on October 31, 2008 (under COC No. JPG004-MCL). One specimen, designated JP-PAC-005 (Figure 1), was selected for use in preparing polished cross-sections for examination. The polished cross-section sample sub-sample identifications are given below in Table 1.

Table 1. Sample Identification.

SAIC Number	MCLinc Number	Sub-sample Number
JP-PAC-005	08-2288	4
JP-PCR-005	08-2288	5

Experimental

Uranium is a very hard metal and is difficult to cut or machine. Cutting, grinding, filing, or machining under uncontrolled conditions may produce pyrophoric small particles that ignite on contact with air producing dangerous radioactive smoke. MCLinc subcontracted segmentation of the selected penetrator to a licensed facility (Manufacturing Sciences Corporation [1]) having experience in such segmentation of depleted uranium alloys.

Select segments of JP-PCR-005 sub-sample were embedded in epoxy and subsequently polished, to enable the segments to the examined in cross-section.

An optical stereomicroscope and a Hitachi S-4500 scanning electron microscope (SEM) with associated EDAX energy dispersive spectrometry (EDS) were used in this investigation.

SEM was used to collect images and the chemistry of areas on the polished samples. EDS analysis is based on characteristic x-rays that are produced by the beam/specimen interaction. The elements that can be analyzed using EDS are boron through uranium. Representative areas of the sample preparations were imaged with secondary electrons (SEI) and backscattered (BEI) and are included in the Figures. All EDS spectra are placed at the end of the text.

[1] Manufacturing Sciences Corporation (MSC) is licensed by the State of Tennessee under authority as an Agreement State as granted by the U.S. NRC (license number S-01046-L00). MSC is licensed to manufacture, store, transport and dispose of DU. (http://www.mfgsci.com/).

Results

Figure 1 illustrates Specimen JP-PAC-005 as received at MCLinc, before segmentation. Optical stereomicroscope images of prepared cross-sections are presented in Figures 2, 3, 7, 8, 12, 13, 23 and 24.

Data for Segment 08-2288-5 are presented in Figures 2 through 22; data for Segment 2288-5 are presented in Figures 23 through 31.

Conclusions

The optical stereomicroscope images of cut cross sections of weathered penetrator darts show corrosion products and alteration phases (uranium oxides) at the surface of the depleted uranium alloy. Under short wavelength (266 nm) ultraviolet light, the yellow-colored phases are strongly fluorescent, consistent with hydrated U^{6+} phase(s) such as schoepite (formally equivalent to $UO_3 \bullet nH_2O$). The gray-colored phases nearest the uranium alloy are not fluorescent, consistent with reduced or mixed-valent forms of uranium (e.g., UO_2 and U_3O_8).

In general, the yellow phases are found between the gray uranium oxide layers and (when present) the overlying soil minerals (brown).

SEM-EDS images at the interface between uranium allow and oxidation product(s) show that the adherent oxidation products are very fine grained (< 2 microns; see (e.g.) Figures 11) and 26). Note that he surface of uranium metal oxidizes rapidly in air, so that all EDS spectra show the presence of both U and O.

These observations may be compared to those of Mellini and Riccobono (2005),[2] who report that a depleted-uranium penetrator, shot in 1999 at Djakovica, Western Kosovo, and there collected in June 2001, showed evident alteration processes, perceivable as black and yellow coatings. X-ray diffraction (XRD) indicates that the black coating mostly consists of uraninite, UO_2, with possible presence of other more oxidized uranium forms, such as U_3O_8. The yellow material is reported to be mostly amorphous, with variable weak diffraction lines, due to minor embedded uraninite grains, or possibly to schoepite.

[2] Mellini, M. and Riccobono, R. (2005), "Chemical and mineralogical transformations caused by weathering in anti-tank DU penetrators ("the silver bullets") discharged during the Kosovo war," *Chemosphere*, **60** (9), 1246-1252.

Figure 1. As-Received Sample JP-PAC-05 (08-2288).[3] Segments from the more corroded end of the penetrator were prepared for examination in cross-section. The diameter of the segments is nominally ~ 2.67-cm (greatest dimension).

[3] From S. Travaglini, "Corrosion study of 24 penetrator samples: photographs of as-received samples," MCLinc Project EMP002105, November 17, 2008.

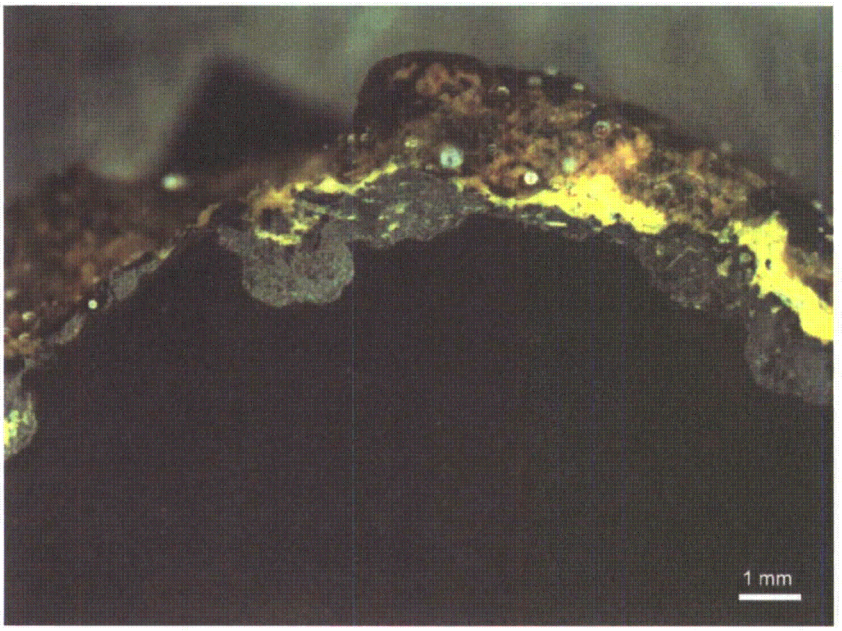

Figure 2. Stereomicroscope photomicrograph of the edge of sample 2288-4, area 1. Note the uranium metal in the lower half of the image and the oxidized uranium species adjacent to the metal.

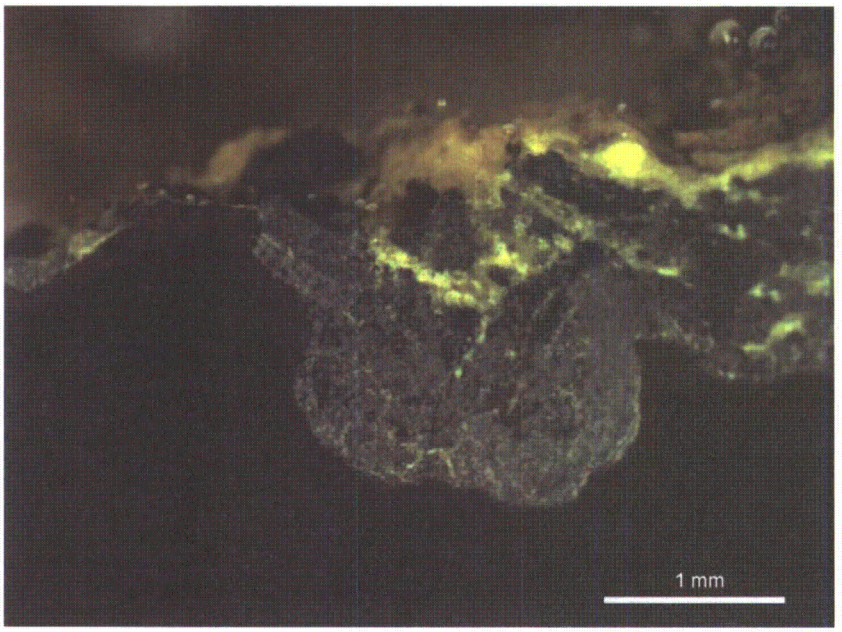

Figure 3. Stereomicroscope photomicrograph of the edge of sample 2288-4, area 1. This image area is from the center left of Figure 1.

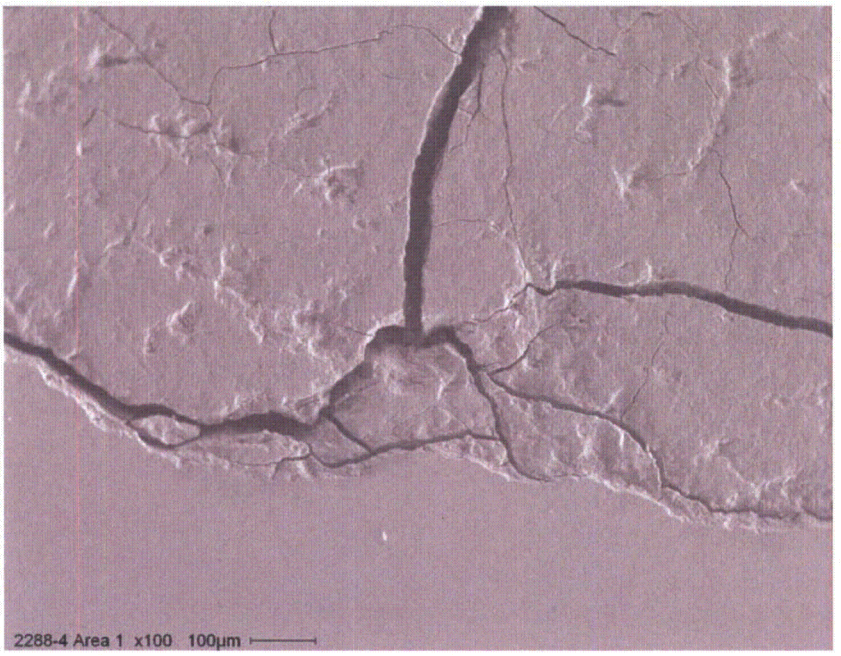

Figure 4. SEI photomicrograph of the uranium metal-oxide area of area 1 on sample 2288-4. This image area is from the lower center of Figure 3 (interface with gray area in optical microscopy Figures 2 and 3).

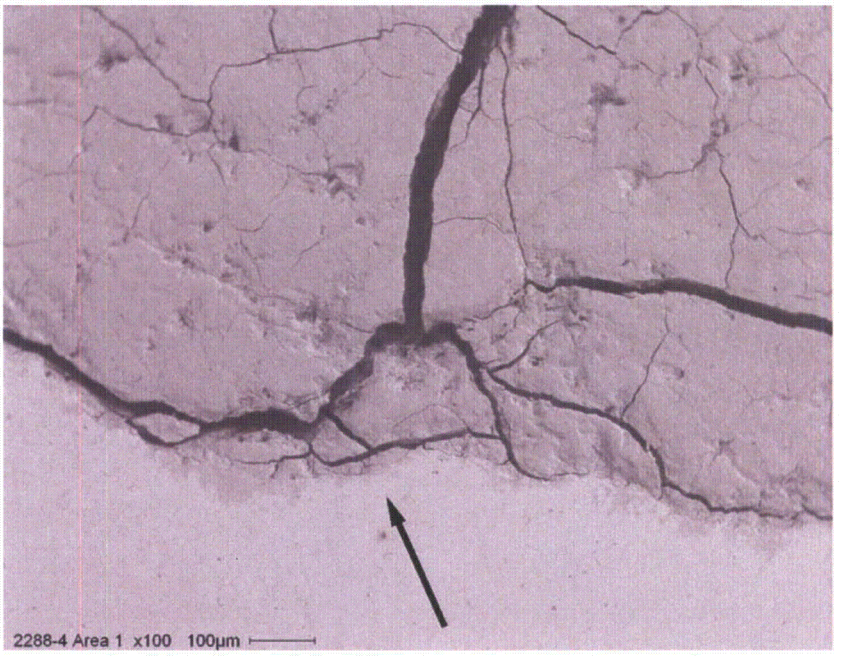

Figure 5. BEI photomicrograph of the uranium metal-oxide area of area 1 on sample 2288-4. This image area is the same as shown in Figure 4.

Figure 6. BEI photomicrograph of the uranium metal-oxide area of area 1 on sample 2288-4. This is an enlarged image from the area shown by the arrow in Figure 5.

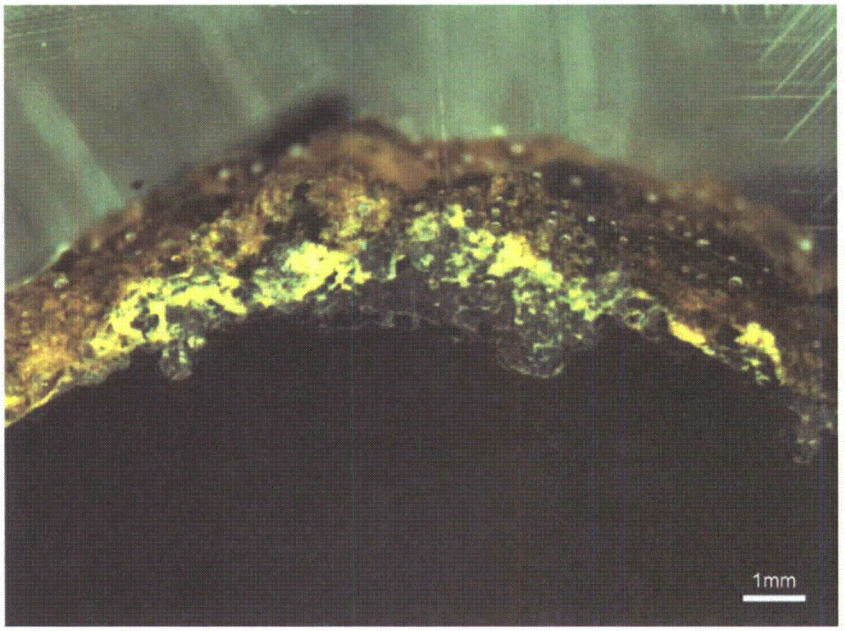

Figure 7. Stereomicroscope photomicrograph of the edge of sample 2288-4, area 2. Note the uranium metal in the lower half of the image and the oxidized uranium species adjacent to the metal.

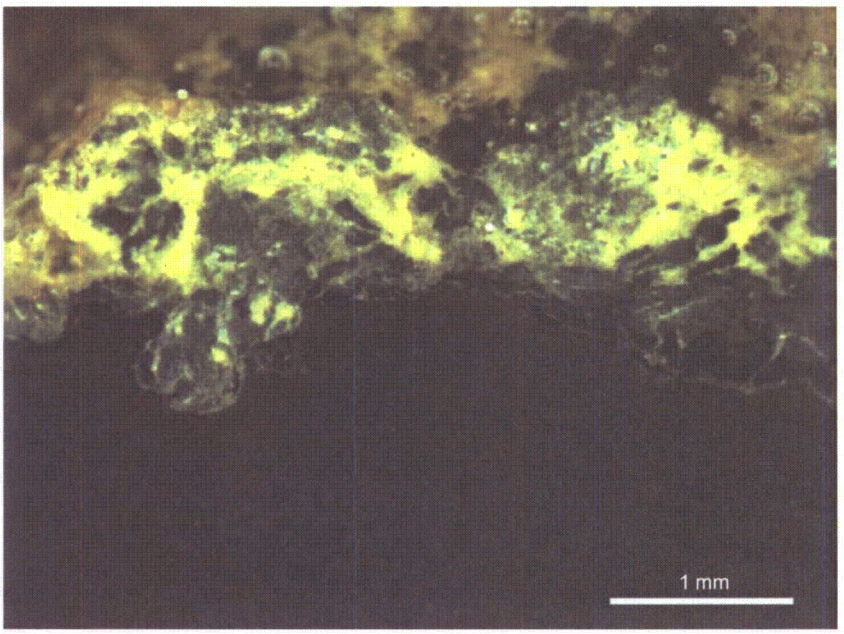

Figure 8. Stereomicroscope photomicrograph of the edge of sample 2288-4, area 2. This image area is from the center left of Figure 7.

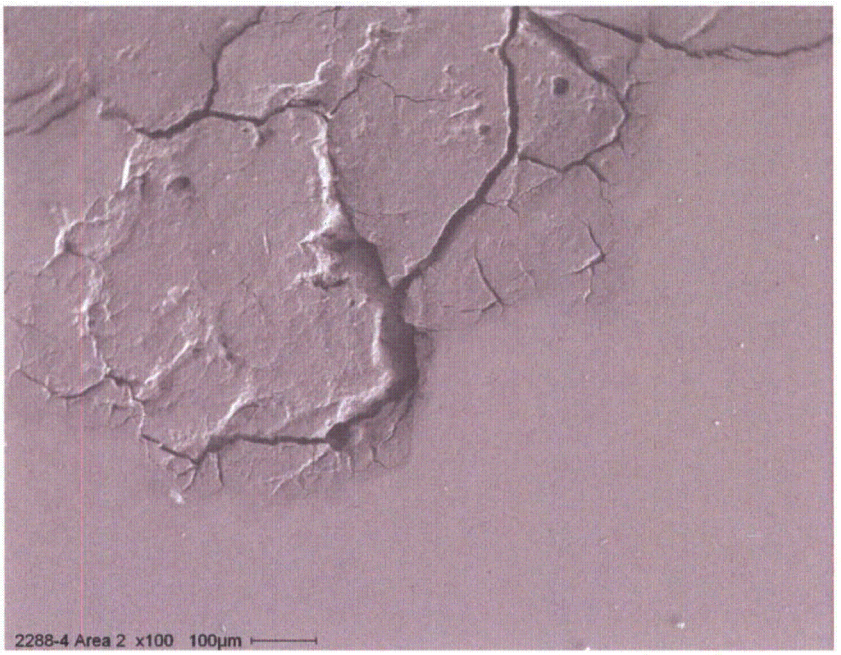

Figure 9. SEI photomicrograph of the uranium metal-oxide area of area 2 on sample 2288-4. This image area is from the center left of Figure 8.

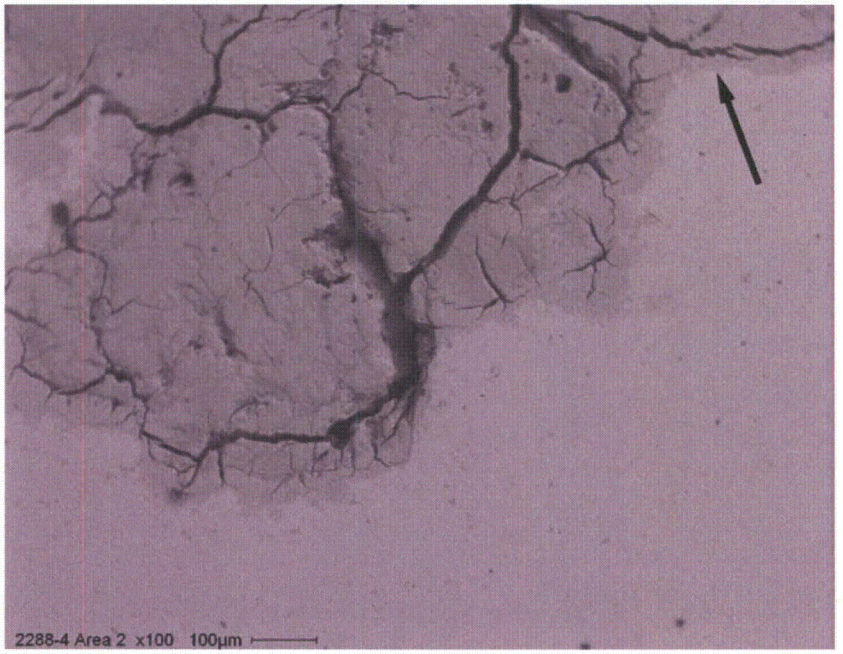

Figure 10. BEI photomicrograph of the uranium metal-oxide area of area 2 on sample 2288-4. This image area is the same as shown in Figure 9.

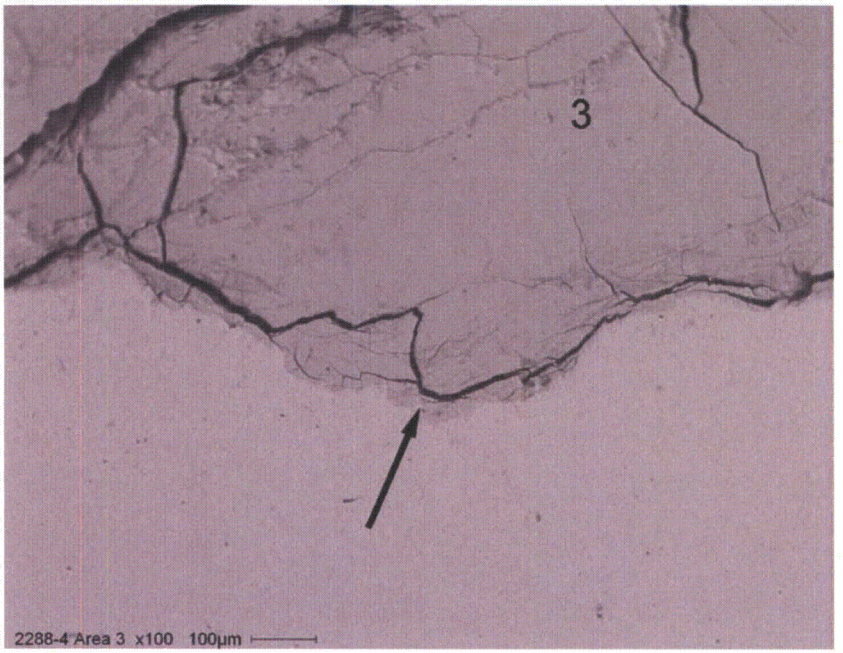

Figure 11. BEI photomicrograph of the uranium metal-oxide area of area 2 on sample 2288-4. This is an enlarged image from the area shown by the arrow in Figure 10. The EDS spectra of analysis areas 1 and 2 are shown in Figures 17 and 18, respectively.

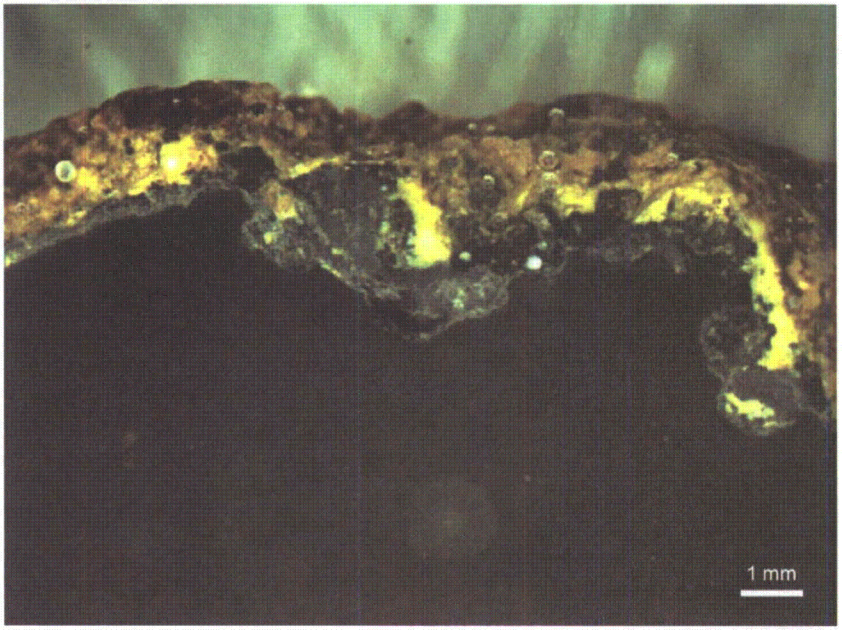

Figure 12. Stereomicroscope photomicrograph of the edge of sample 2288-4, area 3. Note the uranium metal in the lower half of the image and the oxidized uranium species adjacent to the metal.

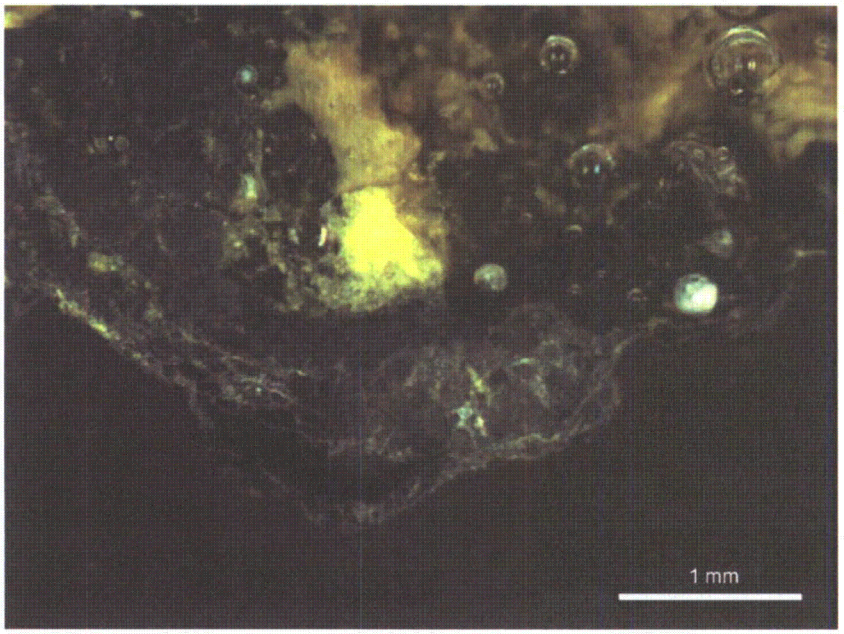

Figure 13. Stereomicroscope photomicrograph of the edge of sample 2288-4, area 3. This image area is from the center of Figure 11.

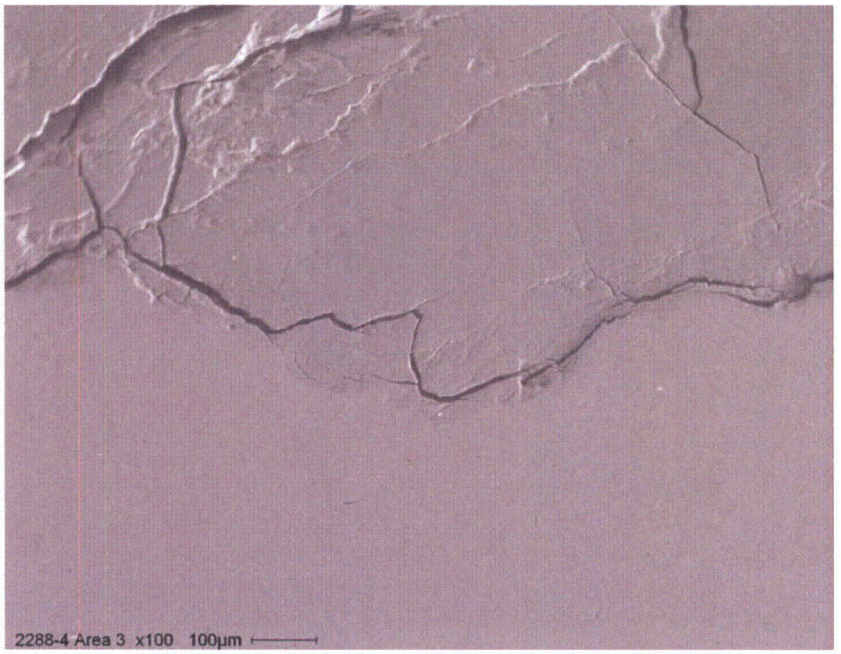

Figure 14. SEI photomicrograph of the uranium metal-oxide area of area 3 on sample 2288-4. This image area is from the lower center of Figure 13.

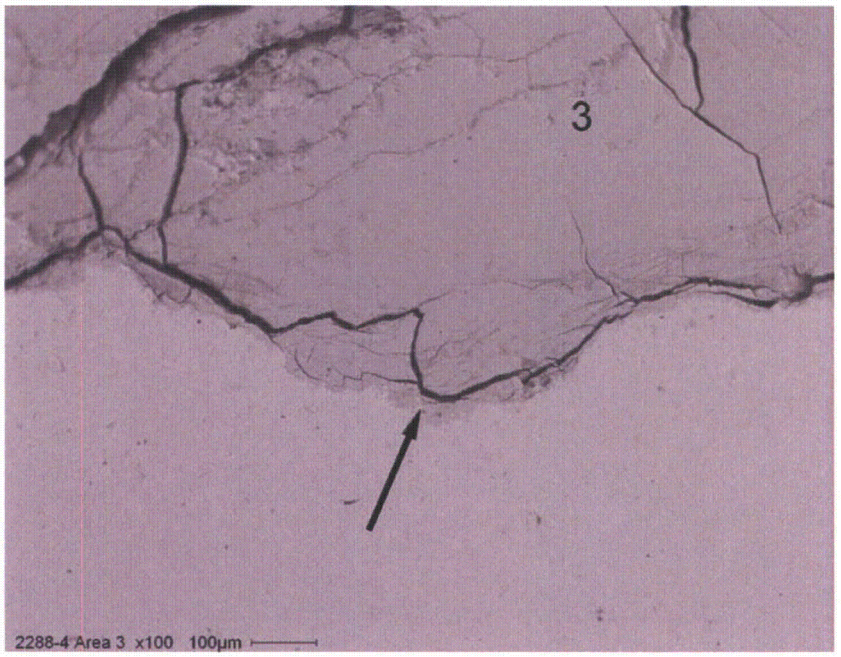

Figure 15. BEI photomicrograph of the uranium metal-oxide area of area 3 on sample 2288-4. This image area is the same as shown in Figure 14. The EDS spectrum of analysis area 3 is shown in Figure 19.

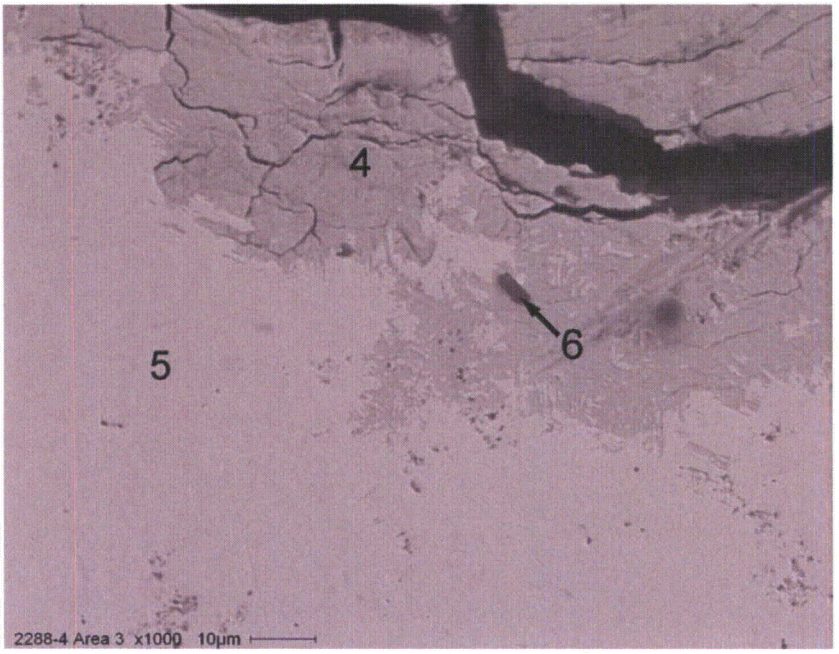

Figure 16. BEI photomicrograph of the uranium metal-oxide contact of area 3 on sample 2288-4. This is an enlarged image from the area shown by the arrow in Figure 15. The spectra of analysis areas 4 through 6 are shown in Figures 20 through 22, respectively.

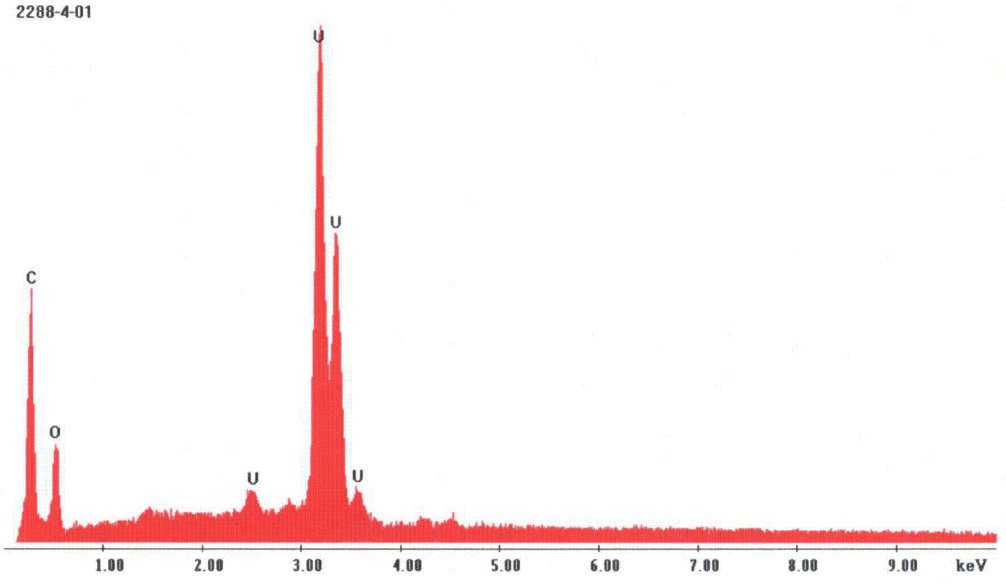

Figure 17. EDS spectrum of analysis area 1on Figure 10 of area 2 of sample 2288-4.

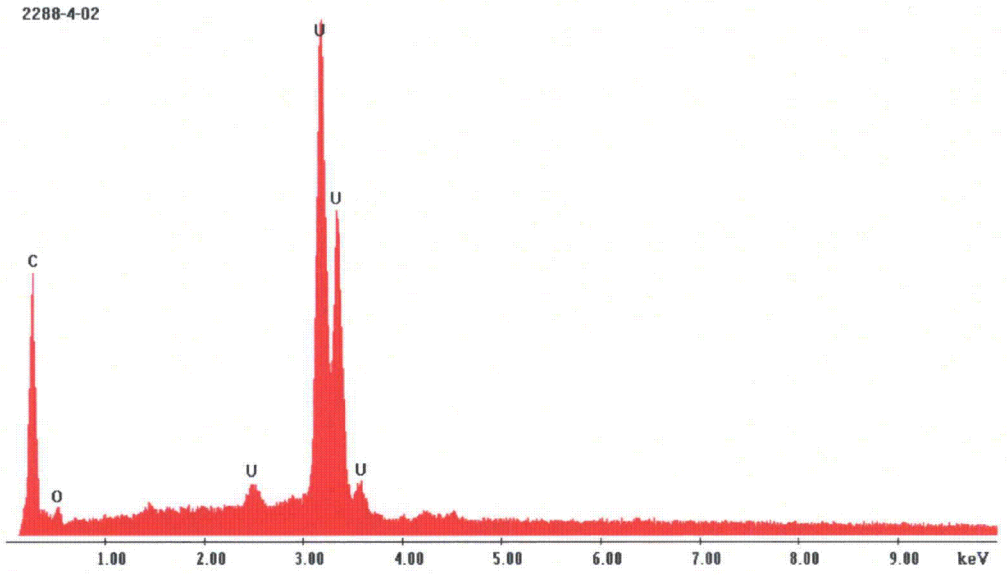

Figure 18. EDS spectrum of analysis area 2 on Figure 10 of area 2 of sample 2288-4.

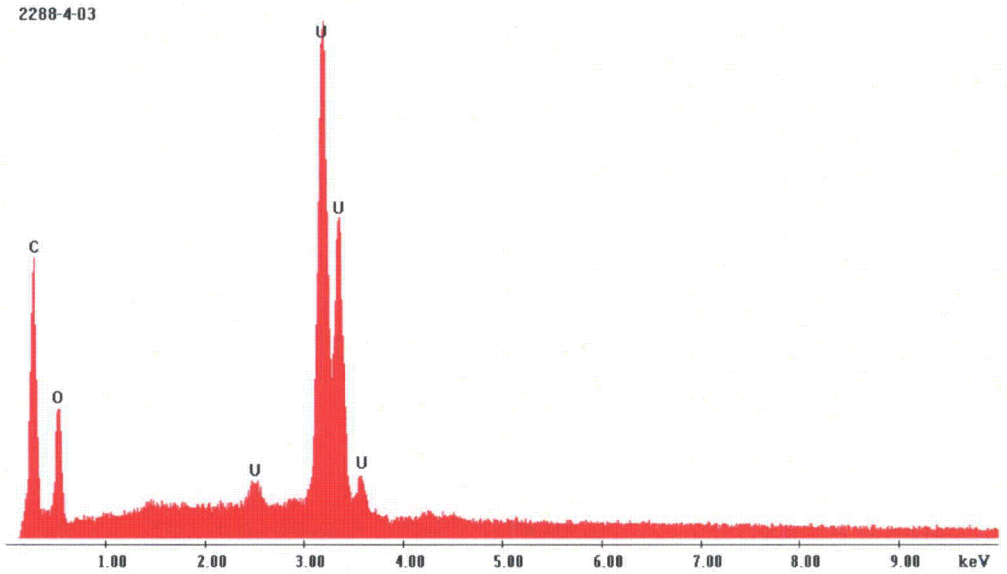

Figure 19. EDS spectrum of analysis area 3 on Figure 14 of area 3 of sample 2288-4.

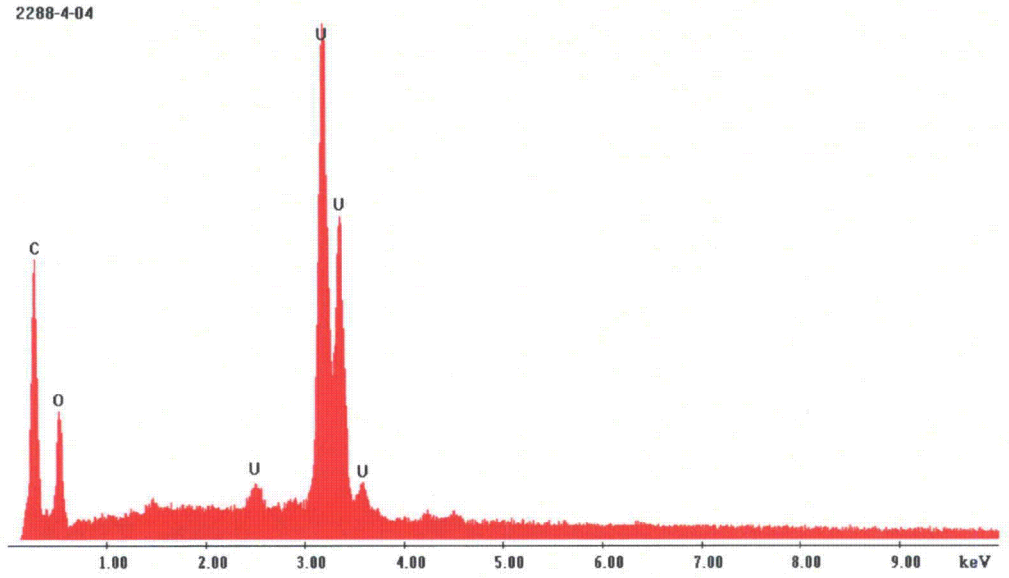

Figure 20. EDS spectrum of analysis area 4 on Figure 15 of area 3 of sample 2288-4.

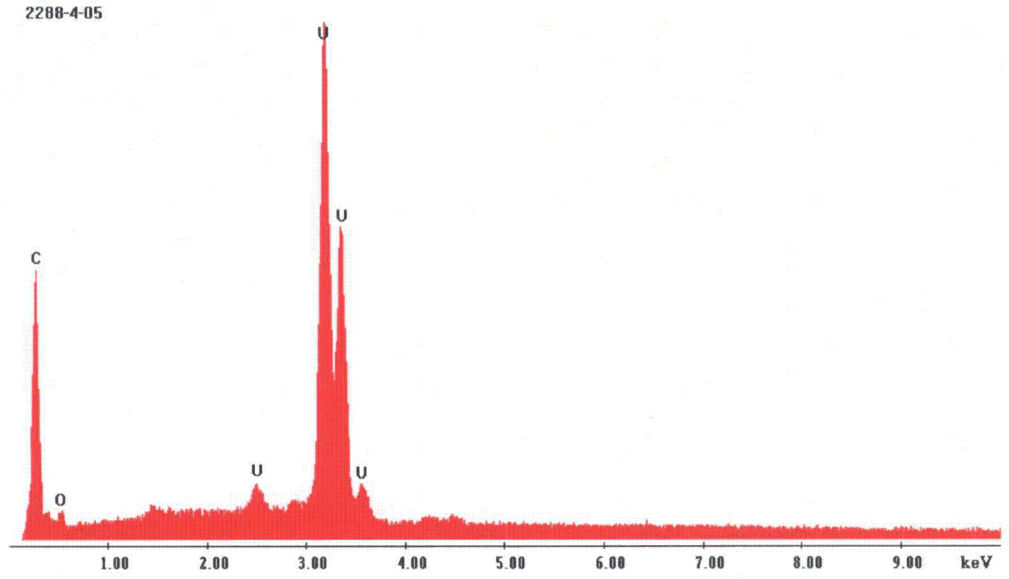

Figure 21. EDS spectrum of analysis area 5 on Figure 10 of area 3 of sample 2288-4.

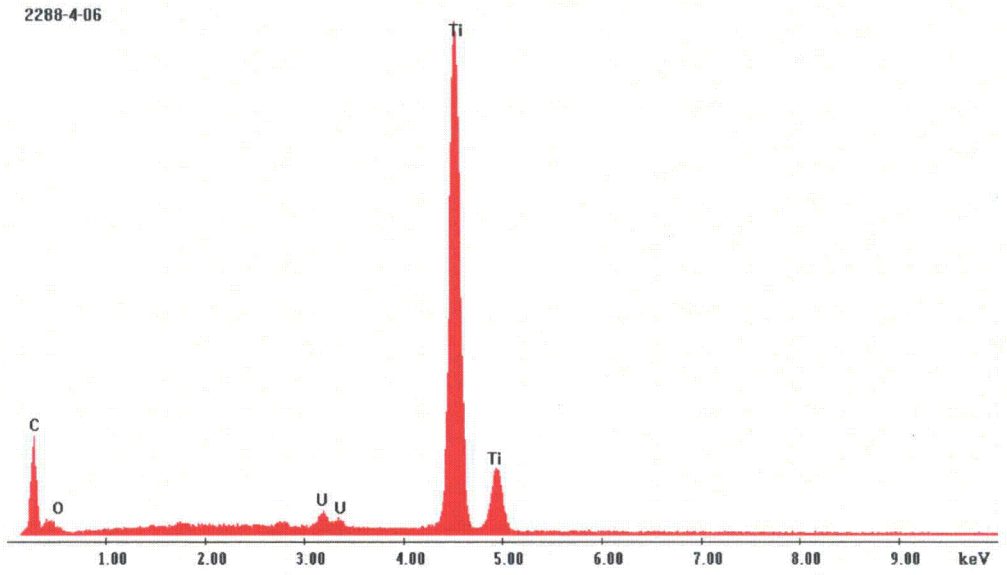

Figure 22. EDS spectrum of analysis area 6 on Figure 10 of area 3 of sample 2288-4.

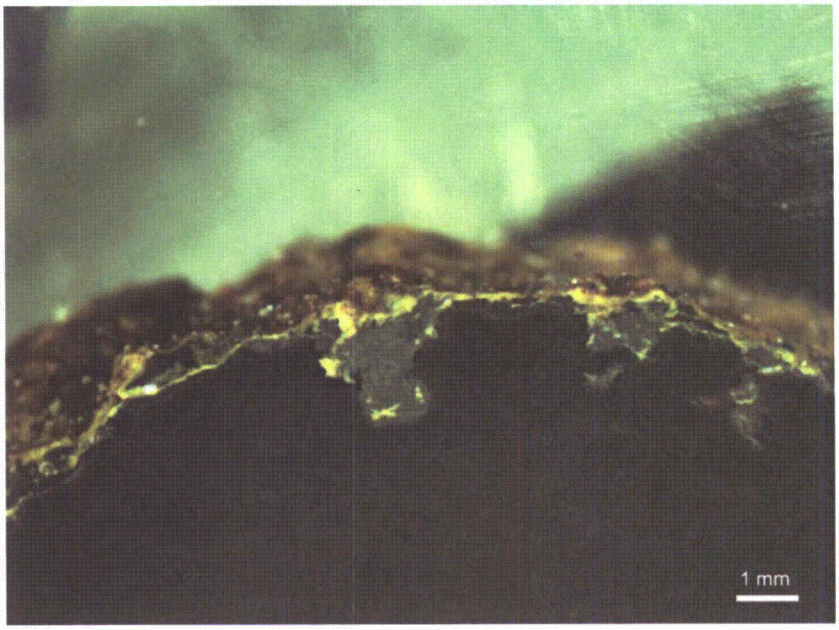

Figure 23. Stereomicroscope photomicrograph of the edge of sample 2288-5, area 1. Note the uranium metal in the lower half of the image and the oxidized uranium species coating adjacent to the metal.

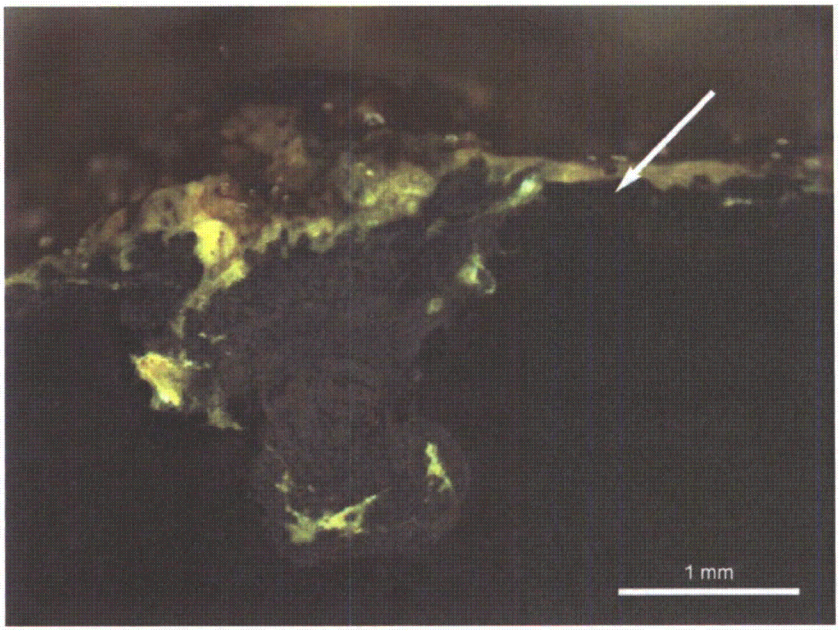

Figure 24. Stereomicroscope photomicrograph of the edge of sample 2288-5. This image area is from the center of Figure 23.

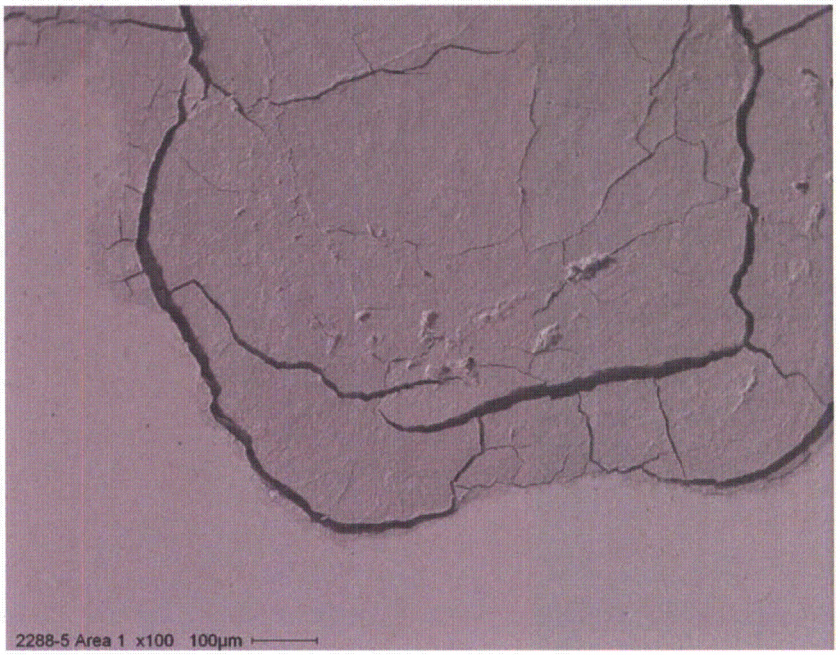

Figure 25. SEI photomicrograph of the uranium metal-oxide area of area 1 on sample 2288-5. This image area is from the lower center of Figure 24.

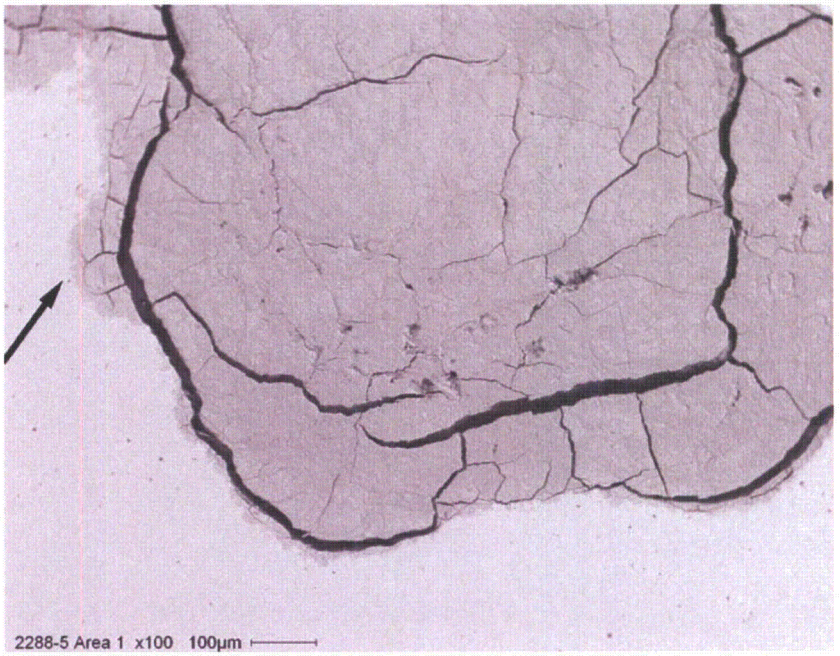

Figure 26. BEI photomicrograph of the uranium metal-oxide area of area 1 on sample 2288-5. This image area is the same as shown in Figure 25.

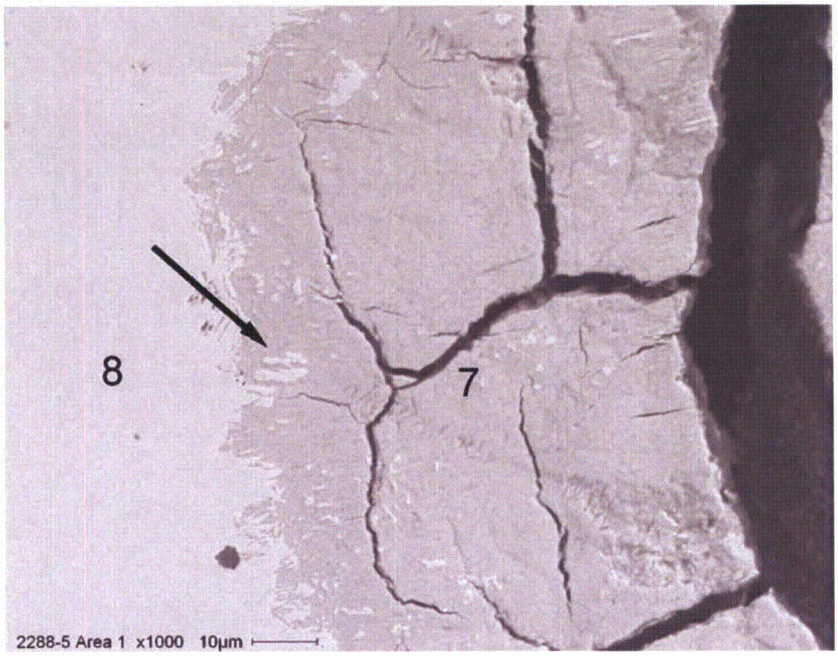

Figure 27. BEI photomicrograph of the uranium metal-oxide area of area 1 on sample 2288-5. This is an enlarged image from the area shown by the arrow in Figure 26. The spectra of analysis areas 7 and 8 are shown in Figures 29 and 30, respectively.

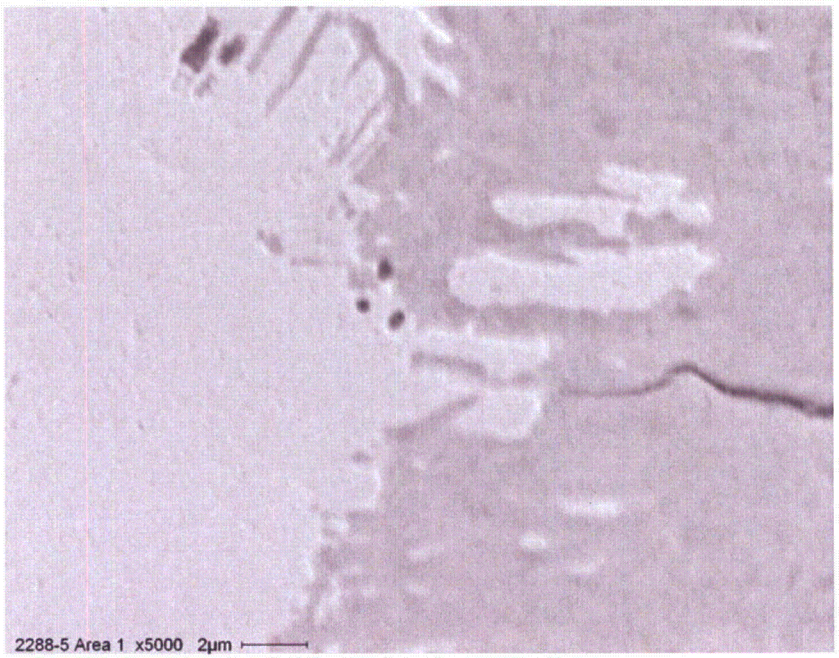

Figure 28. BEI photomicrograph of the uranium metal-oxide area of area 1 on sample 2288-5. This is an enlarged image from the area shown by the arrow in Figure 27.

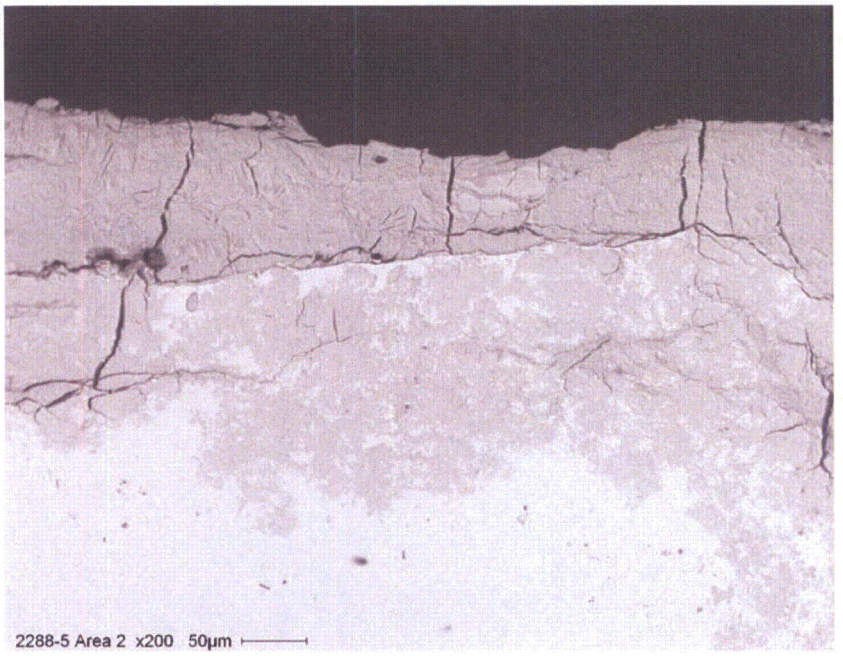

Figure 29. BEI photomicrograph of the metal-coating area of area 2 on sample 2288-5. This image area is from the upper right (arrow) of Figure 24.

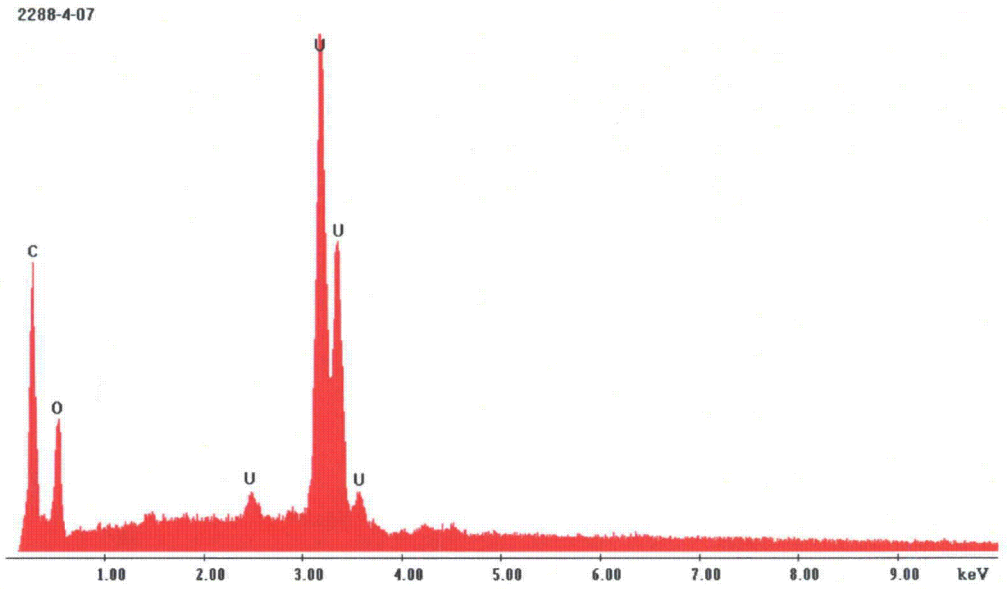

Figure 30. EDS spectrum of analysis area 7 on Figure 26 of area 1 of sample 2288-5.

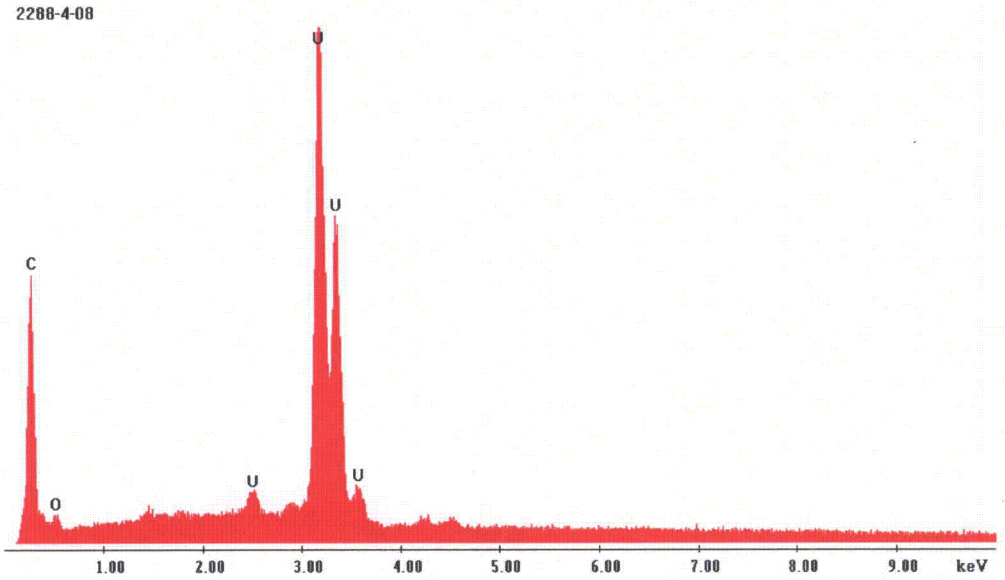

Figure 31. EDS spectrum of analysis area 7 on Figure 26 of area 1 of sample 2288-5.

MATERIALS & CHEMISTRY LABORATORY, INC.

"Linking Technology to Solutions"

Determination of Site-Specific Penetrator Weathering Rate and DU Migration Potential for Jefferson Proving Ground Site: Select Soil Properties and Sequential Extraction of DU-Exposed Soils

MCLinc Project SAI002726, Revision 1

SAIC Subcontract PO10147178

"Sequential Extraction Testing for Site Characterization Jefferson Proving Ground, Indiana"

Prepared for:

Joseph N. Skibinski, Program Manager for SAIC

Compiled by:
William D. Bostick, Ph.D.
Materials and Chemistry Laboratory, Inc. (MCLinc)
2010 Highway 58, Suite 1000
Oak Ridge, Tennessee 37830-1702
(865) 576-4138 www.MCL-inc.com

August, 2013

William Bostick	Date
Mike Tutor	Date
Mark Colberg	Date

Table of Contents

Table of Tables

Table of Figures

ACRONYMS

Δ	difference or change
°C	degrees Celcius
AC	Avonsburg/Cobbsfork
Al	aluminum
ASTM	American Society of Testing and Materials
$CaCl_2$	calcium chloride
$CaCO_3$	calcite
cm^2	square centimeter(s)
CO_2	carbon dioxide
COC	Chain of Custody
CR	Cincinnati/Rossmoyne
d	day(s)
DIW	de-ionized water
DoD	U.S. Department of Defense
DU	depleted uranium (approximately 0.2 weight percent isotope ^{235}U)
DUP	duplicate
EDS	energy dispersive spectrometer
EPA	U.S. Environmental Protection Agency
Fe	iron
g	gram(s)
g $cm^{-2}y^{-1}$	gram(s) per square centimeter year
GR	Grayford/Ryker
g-U	gram(s) uranium
ICP-MS	inductively coupled plasma with mass spectroscopic detection
ICP-OES	inductively coupled plasma – optical emission spectroscopy
ID	identification
JPG	Jefferson Proving Ground, Indiana
Kd	Partition Coefficient
kV	kilovolts
MCLinc	Materials and Chemistry Laboratory, Inc.
mg/Kg	milligrams(s) per kilogram
mg/L	milligram(s) per liter
mm	millimeter(s)
mm^2	square millimeter(s)
Mn	manganese
N	normal
NIST	National Institute of Standards and Technology
NRC	U.S. Nuclear Regulatory Commission
PAC	JPG soil type Avonsburg/Cobbsfork
pCi	picoCurie (unit of radioactivity)
PCR	JPG soil type Cincinnati/Rossmoyne

PGR	JPG soil type Grayford/Ryker
PZC	point of zero charge
redox	*red*uction-*ox*idation reactions
SAIC	Science Applications International Corporation
SE	sequential extraction (testing protocol)
SEM	scanning electron microscope
TC	total carbon
Ti	titanium
TOC	total organic carbon
U	uranium
^{235}U	uranium – 235
UO_2^{+2}	uranyl ion
$UO_3 \cdot 2H_2O$	schoepite
UXO	(conventional) unexploded ordinance
wt%	weight percent (percentage composition by mass)
y	year(s)

EXECUTIVE SUMMARY

Depleted uranium (DU) projectiles were tested at the Jefferson Proving Ground (JPG) in southeastern Indiana between 1983 and 1994. These tests were intended to be nondestructive in nature (i.e., without the formation of DU aerosol from striking hard targets), although some of the rounds may have partially fragmented upon impact. It is estimated that approximately 154,000 pounds (70,000 kilograms) of DU remain in the DU Impact Area (SAIC 2007). The DU Impact Area (approximately 2000 acres) is under U.S. Nuclear Regulatory Commission (NRC) license and is contaminated with both conventional unexploded ordinance (UXO) and DU.

Bostick et al. (2011) presented data from an accelerated weathering and leach test protocol (American Society of Testing and Materials [ASTM], Method D 5744) that used penetrator dart segments implanted in test cells containing the three prevalent site soil types. Twenty-three cycles (3 weeks each) of wet/dry exposure (1.3 years [y] total elapsed time) were performed, with collection of eluent from the drained soil after each cycle. The soil column eluent was analyzed for uranium (U) activity, which permitted estimation of an eluted U release rate. However, there was no assessment authorized at that time for the final drained soil.

This report examines the stored soil, less penetrator segment; the provenance of the stored soil is given in Appendix 1. Post-exposure soil was examined to determine basic mineralogy and major elemental composition, moisture content, pH, total carbon (TC) and total organic carbon (TOC) content. These soil parameters can affect near-field retention of sparingly-soluble U alteration products.

The environmentally-available inventory of DU was determined in the soils after retrieval of the dart segments. In terms of mass, total DU partitioned to drained liquid and retained soil was 0.26 ± 0.10 weight percent (wt.%) over 1.3-y of accelerated leaching, with soil-retention being dominant (with approximately 98 percent of the U inventory "lost" from the penetrator). With the soil inventory known, the overall DU corrosion rate under the test conditions is roughly estimated to be approximately (1.8 ± 0.6)E-2 grams per centimeter squared year ($g\text{-}cm^{-2}y^{-1}$). This estimate is well within the range of reported estimates for DU corrosion under field condition testing as tabulated by Handley-Sidhu et al. (2010).

Aliquots from the DU-exposed soil columns were subjected to modified Tessier sequential extraction (SE) procedure. The premise of the Tessier-type SE protocol is that a progressively more aggressive series of lixiviates are used to extract the soil matrix, in order to assess the risk of ground water contamination and the subsequent migration of contaminant into the environment. These SE methods recognize that total soil metal inventory is of limited use in understanding bioavailability or metal mobility, and that it is useful to estimate the amount of metal present in different solid-phase forms. Despite some drawbacks, the sequential extraction method can provide a valuable tool to distinguish among trace element fractions of different solubility related to mineral phases.

Uranium was found to be associated predominantly with the relatively more refractory "carbonate" and "hydrous metal oxide" (operationally-defined) geochemical fractions (*vide infra*). The soils contained plentiful iron (Fe), manganese (Mn), and aluminum (Al), which have mineral forms that can sorb and bind uranyl (UO_2^{2+}) ion (Krupka and Serne, 2002).

1. INTRODUCTION

The JPG in southeastern Indiana was established in 1941 as a proving ground for the test firing of a wide variety of munitions. DU projectiles were tested here between 1983 and 1994. These tests were intended to be nondestructive in nature (i.e., without the formation of DU aerosol from striking hard targets), although some of the rounds may have partially fragmented upon impact. It is estimated that approximately 154,000 pounds (70,000 kilograms) of DU remain in the DU Impact Area (SAIC 2007). The DU impact area (approximately 2000 acres) is under NRC license and is contaminated with both conventional UXO and DU.

Bostick et al. (2011) prepared an Interim Report[1] describing a long-term laboratory weathering procedure (based on ASTM D 5744) that (1) enhanced reaction-product transport in the aqueous leach of a solid sample, and (2) measured rates of weathering product release from a shallow soil column. That earlier investigation determined a release rate of DU partitioning from the soil column into the collected column aqueous eluate. The penetrator dart segments are shown to very slowly corrode, and the corrosion products subsequently partially dissolve and then leach through a thin soil column under the accelerated weathering test conditions. After 22 accelerated leach intervals, representing over one year of real-time leaching , the *maximum* cumulative mass fraction of DU draining from the shallow soil column with implanted penetrator segment is estimated to be less than or equal to 8E-05 (less than or equal to 0.008 percent, by mass). The *maximum* concentration of dissolved U in the soil column leachate toward the end of the testing period approaches approximately 10 milligrams per liter (mg/L) (approximately 4E+03 picoCuries per liter [pCi/L]), consistent with formation of schoepite (nominally $UO_3 \bullet 2H_2O$) as the solubility-limiting surface alteration product (Jang et al., 2006).

In order to compare the prior-obtained results to literature estimates for other published site-specific DU penetrator dissolution rates, the hold-up inventory for U bound to soil is needed. The prior investigation (Bostick et al. [2011]) did not include determination of total U inventory remaining in the soil columns at the termination of the accelerated weathering cycles and with the removal of the projectile segments that were present in the original test rig. The inventory of residual DU in the soil is an important parameter for DU mass balance estimates, allowing a better estimate for overall DU corrosion rate during the test interval, and also proving an estimate for near-field hold-up of DU in soil.

It was further proposed that MCLinc perform a modified Tessier SE protocol (MCL-7756, Appendix XX) on the same soils previously subjected to the accelerated leach tests, to obtain information on the tenacity (leach-resistance) of U held in soil components within the near-field of a DU projectile. The premise of the Tessier-type SE protocol is that a progressively more aggressive series of lixiviates are used to extract the soil matrix, in order to assess the risk of ground water contamination and the subsequent migration of contaminant into the environment.

In addition, in order to satisfy a regulator (NRC) request, we provide data for TOC, TC, and soil pH analysis on each of the soil samples tested during the sequential extraction testing (7 total plus 1

[1] EMP002105; currently in revision to incorporate information from the present investigation.

duplicate). TOC, TC, and soil pH analysis were completed in accordance with ASTM method D422-63, SW9060, and ASTM method D4972-01.

For reference, the sample identification and analysis matrix for this Project (SAI002726) is presented in Exhibit 1.

EXHIBIT 1. SAMPLE IDENTIFICATION AND ANALYSIS MATRIX

Project # SAI002726

Sample ID	MCL ID	Description	TOC	Tot Carbon	Extraction	SEM/EDS	pH	% moisture	Metals-OES U,Fe,Mn,Al	Metals-MS Iso U
E-1	13-1663	Cell #1 Soil	X	X	X	X	X	X	X	X
E-2	13-1664	Cell #2 Soil	X	X	X	X	X	X	X	X
E-3	13-1665	Cell #3 Soil	X	X	X	X	X	X	X	X
E-4	13-1666	Cell #4 Soil	X	X	X	X	X	X	X	X
E-5	13-1667	Cell #5 Soil	X	X	X	X	X	X	X	X
E-6	13-1668	Cell #6 Soil	X	X	X	X	X	X	X	X
E-7	13-1669	Cell #7 Soil	X	X	X	X	X	X	X	X
E-7-MS	13-1670	Cell #7 Spiked Soil			X				X	X
E-7-DUP	13-1674	Cell #7 Soil Duplicate	X	X						
S-1	13-1671	Soil Type PAC	X	X		X	X	X		
S-2	13-1672	Soil Type PCR	X	X		X	X	X		
S-3	13-1673	Soil Type PGR	X	X		X	X	X		
E-1-1	13-1675	Cell #1 Extraction #1							X	X
E-1-2	13-1676	Cell #1 Extraction #2							X	X
E-1-3	13-1677	Cell #1 Extraction #3							X	X
E-1-4	13-1678	Cell #1 Extraction #4							X	X
E-2-1	13-1679	Cell #2 Extraction #1							X	X
E-2-2	13-1680	Cell #2 Extraction #2							X	X
E-2-3	13-1681	Cell #2 Extraction #3							X	X
E-2-4	13-1682	Cell #2 Extraction #4							X	X
E-3-1	13-1683	Cell #3 Extraction #1							X	X
E-3-2	13-1684	Cell #3 Extraction #2							X	X
E-3-3	13-1685	Cell #3 Extraction #3							X	X
E-3-4	13-1686	Cell #3 Extraction #4							X	X
E-4-1	13-1687	Cell #4 Extraction #1							X	X
E-4-2	13-1688	Cell #4 Extraction #2							X	X
E-4-3	13-1689	Cell #4 Extraction #3							X	X
E-4-4	13-1690	Cell #4 Extraction #4							X	X
E-5-1	13-1691	Cell #5 Extraction #1							X	X
E-5-2	13-1692	Cell #5 Extraction #2							X	X
E-5-3	13-1693	Cell #5 Extraction #3							X	X
E-5-4	13-1694	Cell #5 Extraction #4							X	X
E-6-1	13-1695	Cell #6 Extraction #1							X	X
E-6-2	13-1696	Cell #6 Extraction #2							X	X
E-6-3	13-1697	Cell #6 Extraction #3							X	X
E-6-4	13-1698	Cell #6 Extraction #4							X	X
E-7-1	13-1699	Cell #7 Extraction #1							X	X
E-7-2	13-1700	Cell #7 Extraction #2							X	X
E-7-3	13-1701	Cell #7 Extraction #3							X	X
E-7-4	13-1702	Cell #7 Extraction #4							X	X
E-7-MS-1	13-1703	Cell #7 MS Extraction #1							X	X
E-7-MS-2	13-1704	Cell #7 MS Extraction #2							X	X
E-7-MS-3	13-1705	Cell #7 MS Extraction #3							X	X
E-7-MS-4	13-1706	Cell #7 MS Extraction #4							X	X

2. DU-EXPOSED SOIL

A geological description of the DU impact area soil types is given in SAIC (2007). The field data indicate that the somewhat poorly drained Avonburg series may be grouped together with the poorly drained Cobbsfork series for the purpose of interpretation and future site characterization sampling tasks. Combined, these two soil series would comprise approximately 55 percent of the DU Impact Area. The well-drained Cincinnati and Rossmoyne series also may be grouped together, since both have a fragipan subsurface diagnostic horizon, which tends to perch water during parts of the year, and this combination would account for another 32 percent of the DU Impact Area. The well-drained Grayford, Ryker, and somewhat poorly drained Holton series all have somewhat unique soil conditions and are proposed to be treated separately. Combined these series account for the remaining 13 percent of the DU Impact Area.

The original configuration of the soil test cells is presented in Table 1 (from Bostick et al. [2011], MCL Report EMP002105).

Table 1. Test Cell Preparation

Cell Number	Soil Type *	Penetrator Segment ID No. (location/condition)	Initial Mass of Soil (g)	Initial Mass of Penetrator (g)
1	PAC	JP-PAC-005 (AC/Scraped)	1,000.1	701.8
2	PAC	JP-PAC-005 (AC/Un-scraped)	1,001.4	623.5
3	PCR	JP-PCR-008 (CR/Scraped)	1,000.2	577.1
4	PCR	JP-PCR-008 (CR/Un-scraped)	1,000.3	620.2
5	PGR	JP-PGR-001 (GR/Scraped)	1,000.5	583.1
6	PGR	JP-PGR-001 (GR/Un-scraped)	1,000.1	526.4
7	PAC	No penetrator segment	1,000.4	

Notes:
* PAC = soil type Avonsburg/Cobbsfork; PCR = soil type Cincinnati/Rossmoyne, PGR = soil type Grayford/Ryker.
AC – Avonsburg/Cobbsfork
CR – Cincinnati/Rossmoyne
GR – Grayford/Ryker
g – gram(s)
ID – identification
JP – Jefferson Proving Ground

As described in Bostick et al. (2011) (MCLinc Report EMP002105), soil specimens and associated DU penetrator dart segments (described in Table 1) were subjected to 22 accelerated leach intervals, in accordance with ASTM D 5744; this testing represented over one year of real-time leaching. At the end of this test cycle, soil columns remained in standby condition while awaiting Project review of the Interim

Report (Bostick et al. [2011], MCLinc Report EMP002105), and/or requests for additional testing. The provenance of the soil specimens during this prolonged interval is given in Appendix 1.

Figure 1 illustrates a view into a soil column with inserted penetrator segment. Figure A-1., in Appendix 1, illustrates a representative soil test cell.

Figure 1. Top view of an embedded penetrator segment in Cell #1. Photographed after the drying cycle.

3. SOIL pH ESTIMATES

Soil pH value was estimated using ASTM D4972-01, *Standard Test Method for pH of Soils*. By this method, pH measurements were made in both water and a dilute (0.01 Normal [N]) calcium chloride ($CaCl_2$) solution (pH 5.15) because the calcium displaces some of the exchangeable aluminum. The low ionic strength counters the dilution effect on the exchange equilibrium by setting the salt concentration of the solution closer to that expected in the soil solution. The pH values obtained in the solution of $CaCl_2$ are slightly lower than those measured in water due to the release of more aluminum ions which then hydrolyzed. Therefore, both measurements are required to fully define the character of the soil pH. Data are summarized in Table 2 (for all specimens) are slightly acidic (pH 4.0 to 4.8), suggesting the occurrence of exchangeable Al and also minimal calcite ($CaCO_3$). High microbial respiration (producing weakly acidic dissolved carbon dioxide [CO_2]) can also contribute to soil acidity. McLean (1982) states that soil water in a pore containing 10 percent CO_2 in the gaseous state would be at a pH value of 4.45 if it is not buffered at a higher pH by the soil or neutralized by basic substances.

Table 2. Soil pH values

MCL ID	Soil Type *	Description	pH (in DIW)	pH (in 0.01 N $CaCl_2$)	Δ
13-1663	PAC	Cell #1 Soil	4.48	4.24	-0.24
13-1664	PAC	Cell #2 Soil	4.36	4.17	-0.19
13-1665	PAC	Cell #3 Soil	3.92	3.68	-0.24
13-1666	PCR	Cell #4 Soil	3.99	3.76	-0.23
13-1667	PCR	Cell #5 Soil	4.43	4.23	-0.2
13-1668	PGR	Cell #6 Soil	4.55	4.33	-0.22
13-1669	PGR	Cell #7 Soil	4.40	4.22	-0.18
13-1671	PAC	Soil Type PAC	4.79	4.49	-0.3
13-1672	PAC	Soil Type PCR	4.47	3.95	-0.52
13-1672-DUP	PCR	Soil Type PCR	4.46	3.91	-0.55
13-1673	PGR	Soil Type PGR	4.82	4.52	-0.3

Notes:
* PAC = soil type Avonsburg/Cobbsfork; PCR = soil type Cincinnati/Rossmoyne, PGR = soil type Grayford/Ryker.
Δ is the difference in pH vales estimated for soil contacted with DIW and with dilute $CaCl_2$ solution.
$CaCl_2$ – calcium chloride
DIW – deionized water equilibration
DUP – duplicate
ID – identification
N – Normal

Chen and Yiacoumi (2002) performed simulation calculations to show that DU mobilization from soil is a relatively slow process. Whenever possible, simulation results were compared with published experimental and field data. Precipitation, redox (*red*uction-*ox*idation reactions), and sorption reactions resulted in the immobilization of DU. Among these reactions, sorption played a major role, and the pH of soils was critical in the immobilization; higher pH in soils generally resulted in greater immobilization of DU.

Sorption of ions to mineral surfaces is strongly dependent upon the solution phase pH value, which affects the surface charge distribution on the sorptive substrate. As the pH value increases above the point of zero charge (pzc) for the substrate, the surface becomes more negatively charged and the sorption of cations generally increases. Conversely, sorption of anions is generally favored at pH values below the pzc of the substrate. For iron-containing minerals, the pzc is typically in the range of approximately 6 to 8.5 (Silva & Nitche, 1995).

Sorption by iron oxides of uranyl carbonate anions is strongly affected by solution pH value, with an optimum specific sorption occurring at pH values near 5.5 to 6.5 (Farrell et al., 1999), although removal of soluble U by all mechanisms (e.g., by sorption, ion-exchange and co-precipitation) may continue to be effective at elevated pH values. Barnett et al. (2002) had fair success modeling the sorption of soluble U to soil minerals, based upon a model independently developed for sorption of UO_2^{2+} to ferrihydrate; both

experimental data and theoretical prediction indicate maximum Variation in Partition Coefficient (Kd) values for UO_2^{2+} sorbed to soil minerals at pH values near 5 to 8.

4. SOIL MOISTURE ESTIMATES

Moisture in select soil samples was analyzed using MCLinc Operator Aid MCL-7756, Appendix MM, based on ASTM-D2216, *Standard Test Method for Laboratory Determination of Water (Moisture Content of Soil and Rock by Mass*. Results are summarized in Table 3.

Table 3. Soil Moisture Estimates

MCL ID	Soil Type *	Description	As-Prepared		As Retrieved (Drained) Soil		
			wet wt. (g)	Water wt.% (**)	wet wt. (g)	Water wt.%	Dry wt. (g)
13-1663	PAC	Cell #1 Soil	1000	13.3	1058	18.1	867
13-1664	PAC	Cell #2 Soil	1001	12.9	1047	16.7	872
13-1665	PCR	Cell #3 Soil	1000	14.1	1021	15.9	859
13-1666	PCR	Cell #4 Soil	1000	13.6	1020	15.3	864
13-1667	PGR	Cell #5 Soil	1000	15.1	998	14.9	849
13-1668	PGR	Cell #6 Soil	1000	14.8	1013	15.9	852
13-1669	PAC	Cell #7 Soil	1000	12.0	1089	19.2	880
13-1671	PAC	Background				2.6	
13-1672	PCR	Background				2.1	
13-1673	PGR	Background				9.0	

Notes:
* PAC = soil type Avonsburg/Cobbsfork; PCR = soil type Cincinnati/Rossmoyne, PGR = soil type Grayford/Ryker.
** Estimated value, based on the dry weight estimate from retrieved soil
% - percent
g – gram(s)
ID – identification
wt. – weight

5. TOC ESTIMATES

Aliquots of wet soil were submitted to GEL Laboratories, LLC[2] for analysis of TC and TOC, using U.S. Environmental Protection Agency (EPA), SW846 Method 9060. Results (summarized in Table 4) are reported on as-received basis (see Table 3 for moisture estimates).

Table 4. Total Carbon and Total Organic Carbon in Soil Samples

MCL Sample ID	Soil Type *	Description	TOC (mg/Kg)	TC (mg/Kg)	TOC/TC (%)
13-1663	PAC	Cell #1 Soil	6,780	8,520	80%
13-1664	PAC	Cell #2 Soil	6,900	9,130	76%
13-1665	PCR	Cell #3 Soil	6,970	10,100	69%
13-1666	PCR	Cell #4 Soil	4,860	9,340	52%
13-1667	PGR	Cell #5 Soil	8,400	8,940	94%
13-1668	PGR	Cell #6 Soil	8,380	9,630	87%
13-1669	PAC	Cell #7 Soil	7,690	7,850	98%
13-1669	PAC	Cell #7 Soil	6,110	7,990	76%
13-1671	PAC	Background	12,500	12,800	98%
13-1672	PCR	Background	9,030	10,700	84%
13-1673	PGR	Background	8,210	12,200	67%

Notes:
* PAC = soil type Avonsburg/Cobbsfork: PCR = soil type Cincinnati/Rossmoyne, PGR = soil type Grayford/Ryker.
% – percent
ID – identification
MCL – Materials and Chemistry Laboratory, Inc.
mg/Kg – milligram(s) per kilogram
TC – total carbon
TOC – total organic carbon

Soil organic carbon is the main source of energy for soil microorganisms. TOC contains contributions from soil microbial biomass, decomposing plant matter, stable "humus" from organic decomposition residues, etc. For the soils described in Table 4, TOC is the predominant form of carbon. Minerals, such as $CaCO_3$ and dolomite, are the principal inorganic carbonate species in most soils.

6. SOIL ANALYSIS

Soils were analyzed for major elements (greater than 1.0 weight percent) and minor elements (1.0 to 0.1 weight percent) using a scanning electron microscope (SEM) and associated energy dispersive spectrometer (EDS). Samples were prepared by grinding to a fine powder in a SPEX Mixer/Mill® for three minutes using tungsten carbide lined grinding vials and a tungsten carbide ball. Preliminary examination of the powdered original soils (13-1671, 13-1672, and 13-1673) with a polarized light

[2] GEL Laboratories, LLC, Charleston, SC, Work Order 329188, reported July 15, 2013.

microscope showed the samples to consist primarily of quartz (near 70 percent by volume) and clay with minor amounts of plagioclase feldspar, and heavy mineral phases (e.g. pyroxene, titanite, rutile and other oxides).

Small portions of the powdered samples were placed on carbon dots mounted on aluminum disks. The powder was compacted by hand and carbon coated. A JEOL 840 SEM and an EDAX genesis EDS system were used for analyses. Analyses were performed using a 20 kilovolt (kV) beam scanned over a 1.8 square millimeter (mm^2) area, and counted for a period of 200 seconds. Representative EDS spectra are shown in the figures below. Figure 2 is from Sample 13-1663, a post leach sample for soil type PAC. Figure 3 is from Sample 13-1671, an original, air dried sample of soil type PAC.

Results for all samples are reported as oxide equivalents in Table 5 below. These data represent averages of two analyses per sample and are normalized to 100 percent by weight. Carbon was not included since no carbonate was noted under polarized light microscopy.

Table 5. Weight percent of oxides in soils as determined by semiquantitative EDS analysis.

Oxides	Sample Numbers (in weight percent of oxides)									
	13-1663	13-1664	13-1665	13-1666	13-1337	13-1668	13-1669	13-1671	13-1672	13-1673
SiO_2	80.23	78.80	83.09	84.17	70.01	69.18	80.18	82.66	84.15	74.59
TiO_2	1.35	1.11	1.12	1.07	0.92	1.03	1.29	0.98	1.36	1.03
Al_2O_3	10.97	12.23	7.88	7.93	15.92	16.03	10.71	9.95	7.62	12.39
Fe_2O_3	4.19	4.21	4.45	3.64	8.28	8.92	4.47	3.40	3.55	7.12
MgO	0.55	0.59	0.38	0.35	0.94	1.03	0.50	0.49	0.38	0.75
CaO	0.44	0.59	0.27	0.28	0.53	0.52	0.45	0.40	0.29	0.60
K_2O	1.66	1.41	1.54	1.52	2.28	2.44	1.68	1.37	1.49	2.13
Na_2O	0.46	0.85	0.62	0.49	0.93	0.54	0.48	0.48	0.59	0.77
P_2O_5	0.08	0.11	0.05	0.07	0.09	0.09	0.04	0.08	0.06	0.12
SO_2	0.10	0.13	0.13	0.13	0.06	0.12	0.12	0.12	0.11	0.15
CuO	0.00	0.00	0.50	0.38	0.07	0.13	0.09	0.10	0.44	0.39
Total	100.0	100.0	100.0	100.0	100.0	100.0	100.0	100.0	100.0	100.0

Notes:
EDS – energy dispersive spectrometer

As a quality check two internal standards from the National Institute of Standards and Technology (NIST) were analyzed along with the samples; NIST 2704 (Buffalo River Sediment) and NIST 2711 (Montana Soil). The published analyses for both standards, as well as the results of two analyses from this study are shown in Table 6. Note that the results for analyses from this study and the published results do show some differences. The published analyses, given as weight percent elements, were recast to weight percent oxides and normalized to 100 percent. This was the same treatment used for the results reported in the study. As reported, the original analyses were not normalized to 100 percent. However, given the semiquantitative nature of the present study, the analyses compare favorably to the standards.

Table 6. Comparison of Standard Analyses.

Oxides	NIST Sample 2704 (Buffalo River Sediment) (in weight percent of oxides)			NIST Sample 2711 (Montana Soil) (in weight percent of oxides)		
	2704 published	2704-01	2704-02	2711 published	2711-01	2711-02
SiO_2	69.07	62.02	61.35	69.71	65.21	64.61
TiO_2	0.85	0.92	0.90	0.55	0.60	0.65
Al_2O_3	12.82	16.32	16.22	13.21	15.79	15.49
Fe_2O_3	6.52	9.26	9.85	4.42	5.55	6.14
MnO	0.00	0.13	0.11	0.88	0.30	ND
MgO	2.21	2.29	2.20	1.86	2.07	2.21
CaO	4.04	3.46	3.84	4.31	4.94	6.16
K_2O	2.67	3.36	3.44	3.16	3.30	3.54
Na_2O	0.82	0.61	0.67	1.65	1.96	1.20
SO_2	0.88	0.97	1.05	0.09	0.21	ND
CuO	0.12	0.25	0.29	0.15	ND	ND
Total	100	100	99.9	99.9	99.9	100

Notes:
NIST – National Institute of Standards and Technology

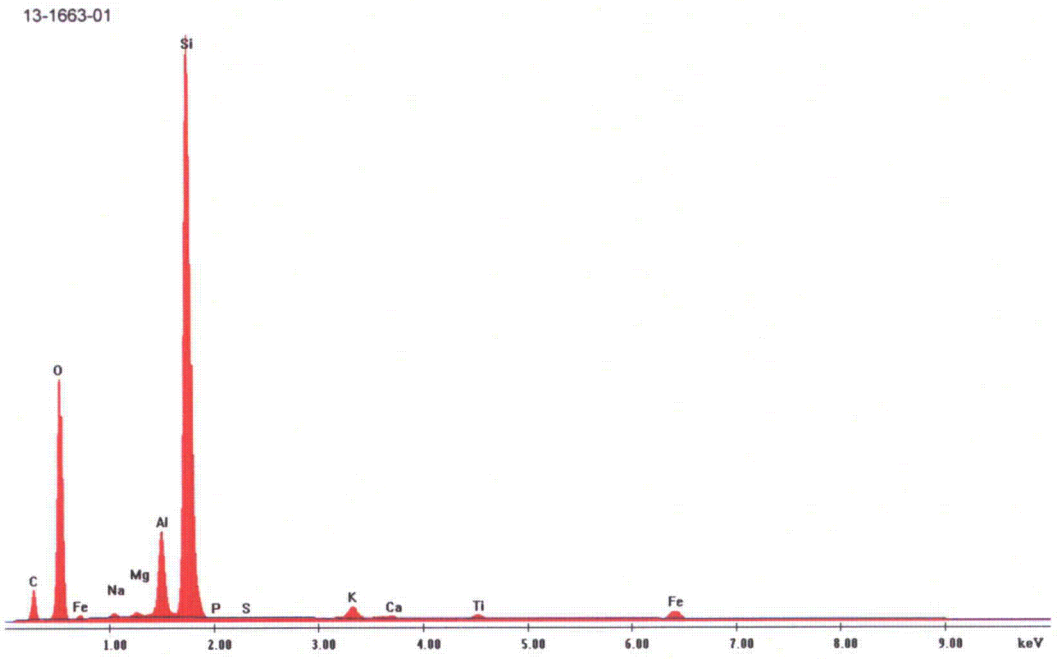

Figure 2. EDS spectra for sample 13-1663; post leach soil type PAC.

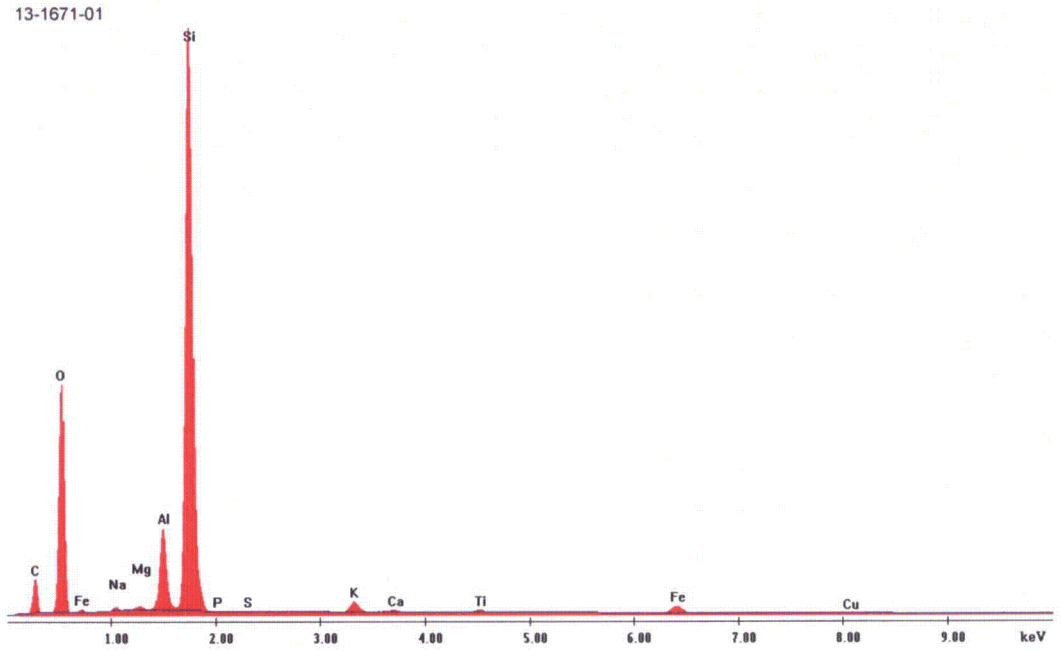

Figure 3. EDS spectra for sample 13-1671; original pre-leach soil type PAC.

7. SE OF SOIL SPECIMENS

7.1. Background

Often, the technique of choice for evaluating low-level radionuclide partitioning in soils and sediments is the SE approach. This methodology applies operationally-defined chemical treatments to selectively dissolve specific classes of macro-scale soil or sediment components (e.g., Tessier et al., 1979; Phillips and Chappelle, 1995). These methods recognize that total soil metal inventory is of limited use in understanding bioavailability or metal mobility, and that it is useful to estimate the amount of metal present in different solid-phase forms. Despite some drawbacks, the sequential extraction method can provide a valuable tool to distinguish among trace element fractions of different solubility related to mineral phases.

Many recent studies published in the technical literature have used a selected sequence of extractions from the soil matrix, with each successive lixivant solution increasing in its aggressiveness. The results of these sequential extractions (or "fractionation") often allow a comparison of how tenaciously different metal contaminants partition to different soil and sediment compositions. The partitioning of contaminants to different geochemical fractions is related to the contaminant speciation (or chemical form), as well as other physiochemical factors. Metals deemed least mobile in soil have a relatively small proportion of the total associated with the most readily accessible (or "exchangeable") fraction while having the greatest proportion associated with the most refractory (or "residual") fraction. Metals in the residual fraction are typically locked up within refractory crystalline mineral phases, and are not readily accessible to leach into the environment except on a geological time scale.

SE by modified Tessier protocol has attracted attention as an operational means to aid in the assessment for the potential risk of DU penetrator shards left in war zones, such as the Balkans and the Middle East (see, e.g., Oliver et al., 2008, and Radenković et al.).

Details of the modified Tessier SE procedure performed at MCLinc are presented in Appendix 2. The sequence of extractions, and the attributed geochemical components affected, is briefly described below:

Fraction 1: Exchangeable Cations (Magnesium Chloride lixiviate, pH approximately 7)

Fraction 2: Carbonate-Bound Metals (Acetate Reagent, pH approximately 8.2)

Fraction 3: Metals Associated With Hydrous Iron- and Manganese Oxides (Hydroxylamine-Acetate Reagent)

Fraction 4: Bound to Organic Matter (Acid and hydrogen peroxide reagent)

For the purpose of mass balance calculations, it is also necessary to determine the total environmentally-available metal inventory.

7.2. Total Environmentally-Available Metal (Extractable Inventory)

Aliquots of the selected soil samples (less than 2 millimeters [mm] size fraction) were extracted as described in MCL-7746, "Acid Digestion for Metals Based on EPA Method 3050B." This digestion

method (using strong nitric acid and hydrogen peroxide) recovers most of the environmentally available heavy metal content, but it does not recover metals locked within a refractory silicate matrix.

7.3. Residual Fraction

Because the residual fraction is not considered to be available for release to the environment except on a geological time scale, it may not be necessary to quantitate this fraction unless the data is needed for mass balance closure. Total digestion is relatively difficult and expensive, and seldom used in environmental analysis. More commonly used strong acid-based extractions such as EPA Methods 3050 and 3051 generally recover most of the available heavy metal content, but they cannot recover metals locked within a refractory silicate matrix. The proportion of residual metal may also be roughly estimated by mass balance, if an estimate of total constituent analysis is available for the original material. In the tabulations reported below, the residual fraction is defined as the computed difference between the total environmentally-available metal inventory and the sum of inventories from extraction Fractions 1 through 4.

7.4. Results

Inductively-coupled plasma – optical emission spectrometry (ICP-OES) is used to quantitate U and select metals in soil extract. MCLinc participates in the Mixed Analyte Performance Evaluation Program (MAPEP) to maintain certification in ICP-OES metals analyses. MAPEP evaluates the performance of the instrument, analysts, and laboratory providing proof the quality of the analyses are maintained. MCLinc's "Quality Assurance Plan," MCL-7701, meets the requirements of ISO/IEC 17025; ANSI/ASQC E4-1994; ASME NQA-1-2000; DOE, *Consolidated Audit Program Quality Systems for Analytical Services Revision 2.9*; 10 CFR 830.120; and *National Environmental Laboratory Accreditation Conference Standards*.

Inductively-coupled plasma – mass spectroscopy (ICP-MS) is used to determine the U enrichment (weight percent of uranium – 235 [^{235}U] isotope) in soil extracts. MCLinc also participates in the MAPEP for ICP-MS. For extracts derived from soil from Cells 1 through 6, previously contacted with DU, the average U enrichment was determined to be (0.198 ± 0.004) percent ^{235}U isotope, consistent with the expected composition of United States DU munitions.[3]

Cell #7 was prepared using PAC-type soil collected outside of the DU impact area. This soil and its extracts had no detectable U content. An aliquot of Cell #7 was used for purposes of preparing a matrix spike, by the addition of a small aliquot of natural U (0.71 percent ^{235}U isotope) as uranyl nitrate solution;

---

[3] The NRC defines DU as U in which the percentage of the ^{235}U isotope by weight is less than 0.711 percent (10 CFR 40.4). The military specifications designate that the DU used by U.S. Department of Defense (DoD) contain less than 0.3 percent ^{235}U (AEPI, 1995). In actuality, DoD uses only DU that contains approximately 0.2 percent ^{235}U (AEPI, 1995). [See URL: http://www.gulflink.osd.mil/library/randrep/du/mr1018.7.chap1.html]

leached aliquots from Cell #7-MS were determined to have an average U enrichment value (0.703 ± 0.006) percent ^{235}U isotope. The recovery of added U (at 248 mg/kg) was 110 percent.

Results for the extraction of select metals in the test soil cells are summarized in Tables 7 through 13, and are presented in graphical form in Figures 4 through 10. By the end of the accelerated soil leaching procedure, the drained soils leached in the presence of penetrator dart segments (Cells #1 through #6) were in contact with aqueous phase containing soluble U at approximately 10 mg/L, consistent with formation of schoepite (nominally $UO_3 \bullet 2H_2O$) as the solubility-limiting surface alteration product (Bostick et al., 2011). Thus, it is expected that the drained test soils from these cells would have a considerable inventory of exchangeable U, due to soluble U in the pore water. However, most of the test cell soils had the greatest proportion of U in the more-refractory so-called carbonate and hydrous oxide fractions, with the latter usually predominant. This is consistent with other investigations of U-contaminated soils.

The surface complexation reaction of uranyl with iron-containing minerals has been used as one means to model subsurface migration (Barnett et al., 2002; Payne and Waite, 1991; De Nero et al., 1999), used in conjunction with information on the site water chemistry and hydrology. The assessment of U bound to hydrous metal oxides is one component of the operationally-defined partitioning by the sequential extraction methodology.

For modeling the retardation of the mobility of UO_2^{2+} in soil matrix, the fraction operationally associated with hydrous metal oxides has generally been the dominant concern. However, the so-called "organic" geochemical compartment may also be important; for example, Oliver et al. (2006) used SE to identify the dominance of organic matter in controlling migration and bioavailability of DU in the near-field.

Table 7. SE of Cell #1 Soil (PAC)

MCLinc ID	Fraction	U *†		Mn *		Al *		Fe *	
		mg/Kg	%Total	mg/Kg	%Total	mg/Kg	%Total	mg/Kg	%Total
13-1675	Exchangeable	126	9%	14	6%	69	1%	4	0%
13-1676	Carbonate-Bound	439	30%	0.4	0%	6.3	0%	4	0%
13-1677	Hydrous Oxide	739	51%	137	63%	198	3%	1,060	16%
13-1678	Organic matter	80	6%	32	15%	777	13%	279	4%
(Calculated)	Residual	66	5%	34	16%	4800	82%	5333	80%
13-1663	Total	1,450	100%	217	100%	5,850	100%	6,680	100%

Notes: * Analysis of extracts by ICP-OES (inductively coupled plasma – optical emission spectroscopy)
† ICP-MS: Average wt.% ^{235}U isotope = (0.194 ± 0.004) – DU
% - percent
Al – aluminum
DU – depleted uranium
Fe – Iron
ICP-MS – inductively coupled plasma – mass spectroscopy
ID – identification
mg/Kg – milligram(s) per kilogram
Mn - manganese
PAC –soil type Avonsburg/Cobbsfork
SE – sequential extraction
U – uranium
^{235}U – uranium – 235
wt.% - weight percent

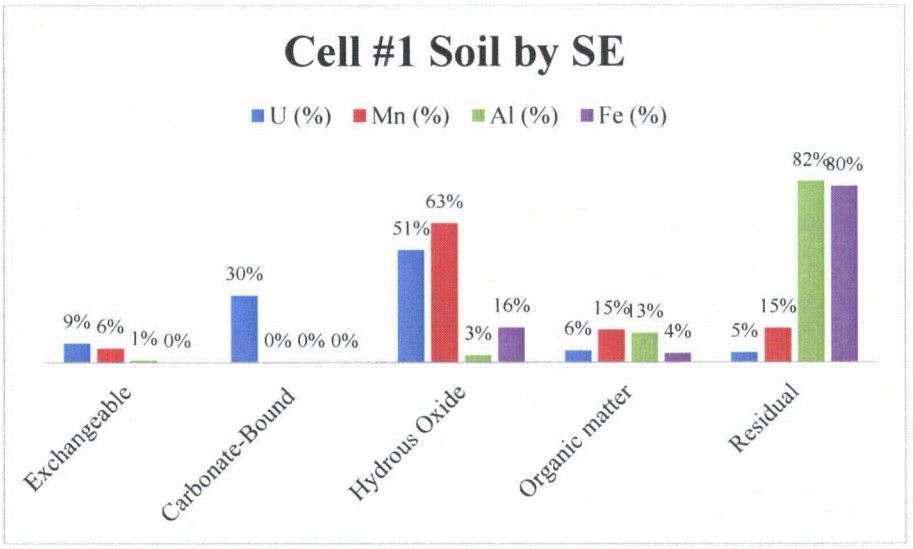

Figure 4. Partitioning of Select Metals to Aqueous SE Extract for Cell #1 Soil

Table 8. SE of Cell #2 Soil (PAC)

MCLinc ID	Fraction	U *†		Mn *		Al *		Fe *	
		mg/Kg	%Total	mg/Kg	%Total	mg/Kg	%Total	mg/Kg	%Total
13-1679	Exchangeable	34	4%	14	6%	81	1%	3.9	0%
13-1680	Carbonate-Bound	175	19%	0.4	0%	7	0%	3.9	0%
13-1681	Hydrous Oxide	324	36%	143	58%	226	4%	1,380	19%
13-1682	Organic matter	56	6%	35	14%	698	11%	283	4%
(Calculated)	Residual	313	35%	56	23%	5098	83%	5669	77%
13-1664	Total	902	100%	248	100%	6,110	100%	7,340	100%

Notes: * Analysis of extracts by ICP-OES (inductively coupled plasma – optical emission spectroscopy)
† ICP-MS: Average wt.% ^{235}U isotope = (0.193 ± 0.001) – DU
% - percent
Al – aluminum
DU – depleted uranium
Fe – Iron
ICP-MS – inductively coupled plasma – mass spectroscopy
ID – identification
mg/Kg – milligram(s) per kilogram
Mn - manganese
PAC –soil type Avonsburg/Cobbsfork
SE – sequential extraction
U – uranium
^{235}U – uranium – 235
wt.% - weight percent

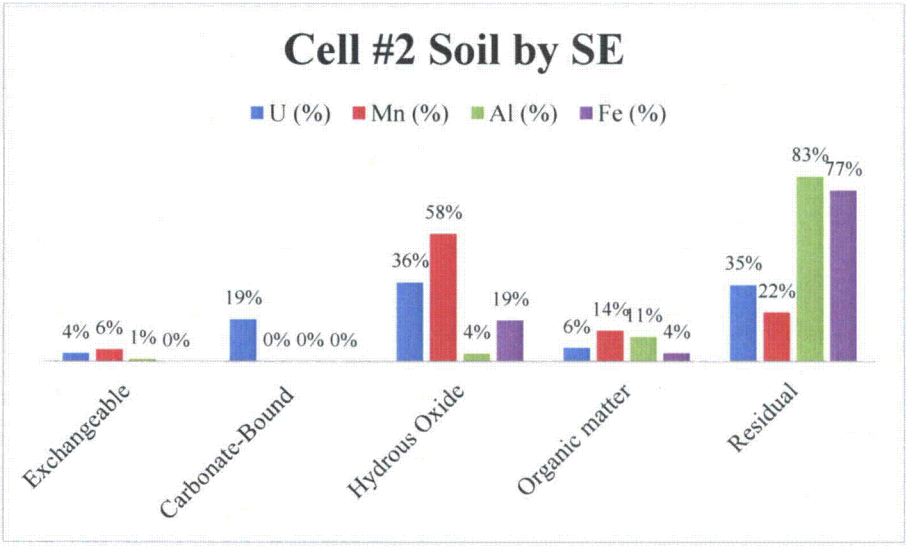

Figure 5. Partitioning of Select Metals to Aqueous SE Extract for Cell #2 Soil

Table 9. SE of Cell #3 Soil (PCR)

MCLinc ID	Fraction	U *†		Mn *		Al *		Fe *	
		mg/Kg	%Total	mg/Kg	%Total	mg/Kg	%Total	mg/Kg	%Total
13-1679	Exchangeable	211	13%	12	7%	175	4%	3.9	0%
13-1680	Carbonate-Bound	438	26%	0.4	0%	11	0%	3.9	0%
13-1681	Hydrous Oxide	115	7%	64	36%	160	4%	1,030	15%
13-1682	Organic matter	629	37%	25	14%	436	10%	345	5%
(Calculated)	Residual	287	17%	79	44%	3498	82%	5587	80%
13-1664	Total	1,680	100%	180	100%	4,280	100%	6,970	100%

Notes: * Analysis of extracts by ICP-OES (inductively coupled plasma – optical emission spectroscopy)
† ICP-MS: Average wt.% ^{235}U isotope = (0.200 ± 0.002) – DU
% - percent
Al – aluminum
DU – depleted uranium
Fe – Iron
ICP-MS – inductively coupled plasma – mass spectroscopy
ID – identification
mg/Kg – milligram(s) per kilogram
Mn - manganese
PCR –soil type Cincinnati/Rossmoyne
SE – sequential extraction
U – uranium
^{235}U – uranium – 235
wt.% - weight percent

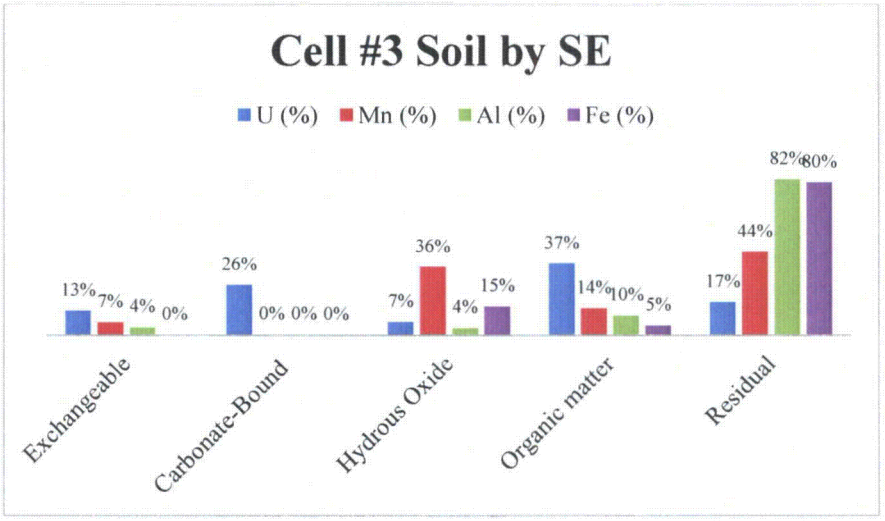

Figure 6. Partitioning of select metals to aqueous SE extract for Cell #3 Soil

Table 10. SE of Cell #4 Soil (PCR)

MCLinc ID	Fraction	U *†		Mn *		Al *		Fe *	
		mg/Kg	%Total	mg/Kg	%Total	mg/Kg	%Total	mg/Kg	%Total
13-1679	Exchangeable	212	11%	12	8%	170	4%	4	0%
13-1680	Carbonate-Bound	427	22%	0.4	0%	9	0%	4	0%
13-1681	Hydrous Oxide	629	32%	91	59%	181	4%	1,260	19%
13-1682	Organic matter	123	6%	21	14%	540	13%	338	5%
(Calculated)	Residual	569	29%	30	19%	3310	79%	5154	76%
13-1664	Total	1,960	100%	154	100%	4,210	100%	6,760	100%

Notes: * Analysis of extracts by ICP-OES (inductively coupled plasma – optical emission spectroscopy)
† ICP-MS: Average wt.% ^{235}U isotope = (0.198 ± 0.002) – DU
% - percent
Al – aluminum
DU – depleted uranium
Fe – Iron
ICP-MS – inductively coupled plasma – mass spectroscopy
ID – identification
mg/Kg – milligram(s) per kilogram
Mn - manganese
PCR –soil type Cincinnati/Rossmoyne
SE – sequential extraction
U – uranium
^{235}U – uranium – 235
wt.% - weight percent

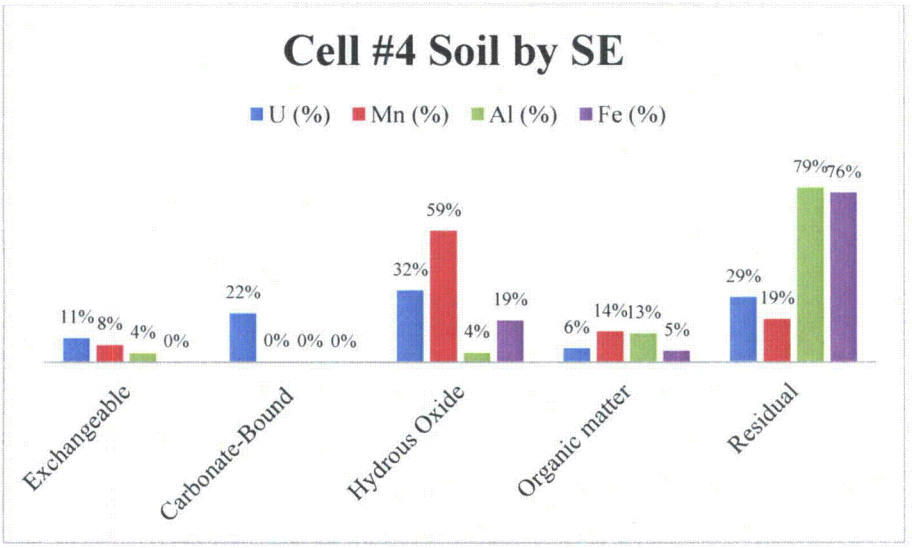

Figure 7. Partitioning of Select Metals to Aqueous SE Extract for Cell #4 Soil

Table 11. SE of Cell #5 Soil (PCR)

MCLinc ID	Fraction	U *†		Mn *		Al *		Fe *	
		mg/Kg	%Total	mg/Kg	%Total	mg/Kg	%Total	mg/Kg	%Total
13-1679	Exchangeable	140	10%	16	4%	159	2%	6.8	0%
13-1680	Carbonate-Bound	419	29%	0.4	0%	9	0%	3.9	0%
13-1681	Hydrous Oxide	712	48%	252	64%	369	4%	959	5%
13-1682	Organic matter	88	6%	49	12%	938	10%	174	1%
(Calculated)	Residual	111	8%	76	19%	7635	84%	18316	94%
13-1664	Total	1,470	100%	393	100%	9,110	100%	19460	100%

Notes: * Analysis of extracts by ICP-OES (inductively coupled plasma – optical emission spectroscopy)
† ICP-MS: Average wt.% ^{235}U isotope = (0.201 ± 0.004) – DU
% - percent
Al – aluminum
DU – depleted uranium
Fe – Iron
ICP-MS – inductively coupled plasma – mass spectroscopy
ID – identification
mg/Kg – milligram(s) per kilogram
Mn - manganese
PCR –soil type Cincinnati/Rossmoyne
SE – sequential extraction
U – uranium
^{235}U – uranium – 235
wt.% - weight percent

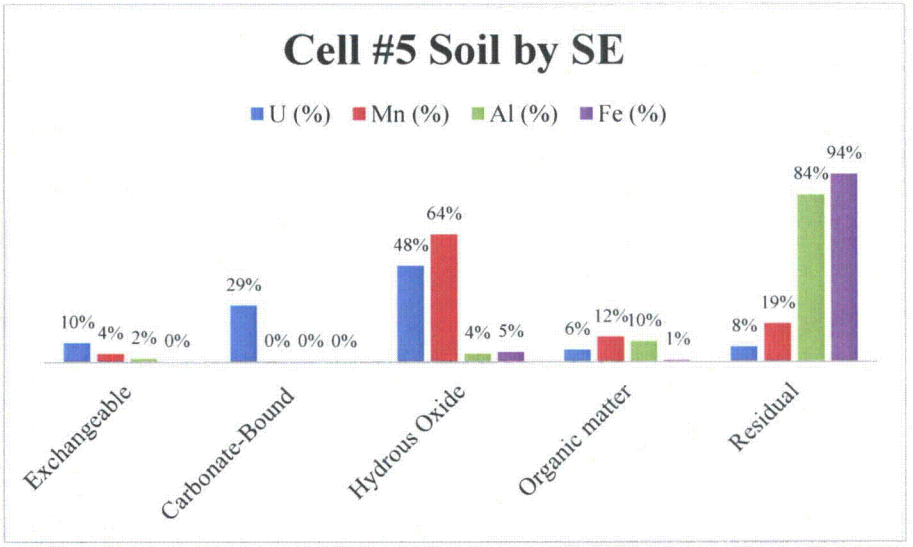

Figure 8. Partitioning of Select Metals to Aqueous SE Extract for Cell #5 Soil

Table 12. SE of Cell #6 Soil (PCR)

MCLinc ID	Fraction	U *†		Mn *		Al *		Fe *	
		mg/Kg	%Total	mg/Kg	%Total	mg/Kg	%Total	mg/Kg	%Total
13-1695	Exchangeable	133	5%	7	2%	111	1%	7.8	0%
13-1696	Carbonate-Bound	463	17%	0.4	0%	9	0%	4	0%
13-1697	Hydrous Oxide	982	36%	394	89%	463	5%	1,120	5%
13-1698	Organic matter	96	4%	98	22%	916	10%	177	1%
(Calculated)	Residual	1036	38%	-56	-13%	7701	84%	19081	94%
13-1667	Total	2,710	100%	444	100%	9,200	100%	20,390	100%

Notes: * Analysis of extracts by ICP-OES (inductively coupled plasma – optical emission spectroscopy)
† ICP-MS: Average wt.% ^{235}U isotope = (0.198 ± 0.003) – DU
% - percent
Al – aluminum
DU – depleted uranium
Fe – Iron
ICP-MS – inductively coupled plasma – mass spectroscopy
ID – identification
mg/Kg – milligram(s) per kilogram
Mn - manganese
PCR –soil type Cincinnati/Rossmoyne
SE – sequential extraction
U – uranium
^{235}U – uranium – 235
wt.% - weight percent

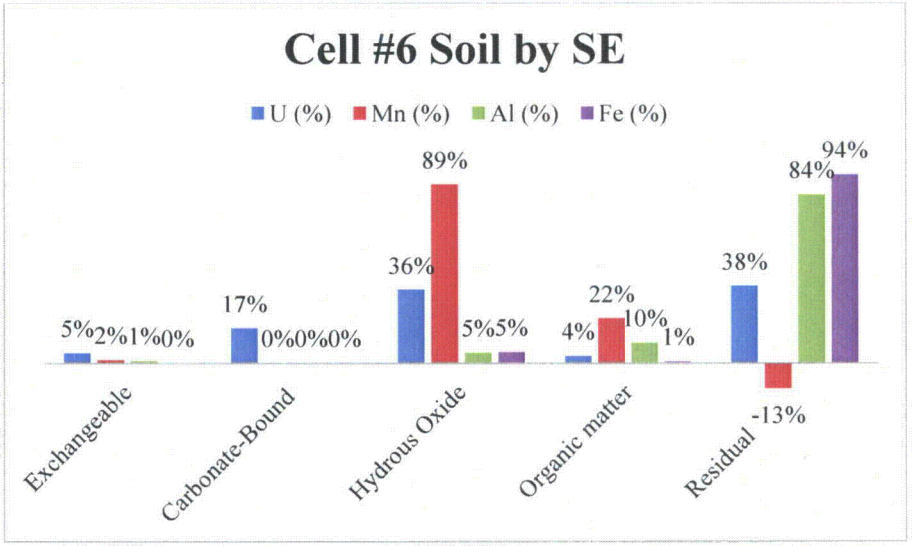

Figure 9. Partitioning of Select Metals to Aqueous SE Extract for Cell #6 Soil

Table 13. SE of Cell #7 Soil (7-PAC-MS)

MCLinc ID	Fraction	U *†		Mn *		Al *		Fe *	
		mg/Kg	%Total	mg/Kg	%Total	mg/Kg	%Total	mg/Kg	%Total
13-1695	Exchangeable	17	6%	20	9%	96	2%	3.9	0%
13-1696	Carbonate-Bound	86	32%	0.5	0%	10	0%	3.9	0%
13-1697	Hydrous Oxide	121	44%	136	62%	224	4%	1,360	19%
13-1698	Organic matter	18	7%	29	13%	678	12%	268	4%
(Calculated)	Residual	31	11%	33	15%	4502	82%	5634	77%
13-1667	Total	273	100%	218	100%	5,510	100%	7,270	100%

Notes: * Analysis of extracts by ICP-OES (inductively coupled plasma – optical emission spectroscopy)
† ICP-MS: Average wt.% ^{235}U isotope = (0.703 ± 0.0063) – U (natural)
% - percent
Al – aluminum
Fe – Iron
ICP-MS – inductively coupled plasma – mass spectroscopy
ID – identification
mg/Kg – milligram(s) per kilogram
Mn - manganese
MS – matrix spike
PCR –soil type Cincinnati/Rossmoyne
SE – sequential extraction
U – uranium
^{235}U – uranium – 235
wt.% - weight percent

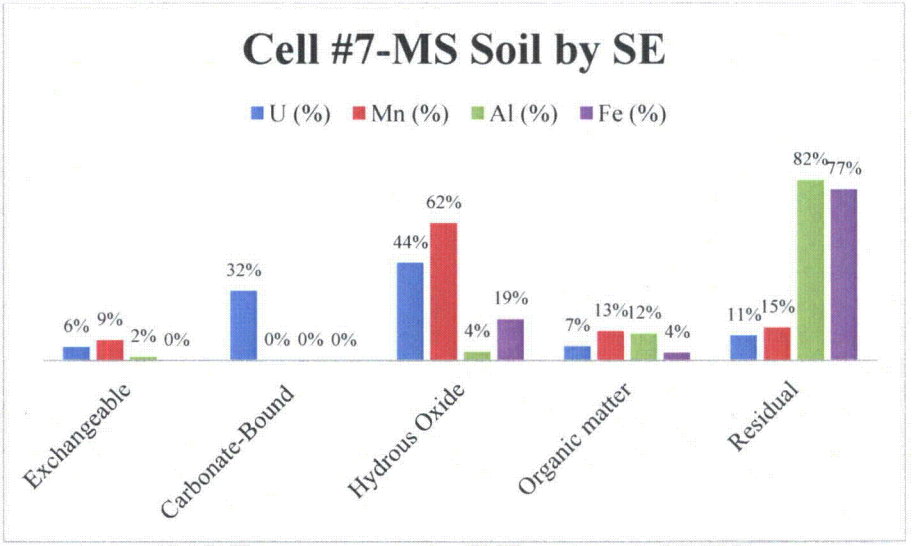

Figure 10. Partitioning of Select Metals to Aqueous SE Extract for Cell #7-MS Soil

8. MASS BALANCE SUMMARY – PERCENTAGES OF DU RETAINED IN SOIL AND ELUTED INTO COLLECTED WATER

Refer to Table 1 for the leach test logistics (i.e., original mass for as-received site soil and inserted penetrator dart segment). For the soil test columns with inserted penetrator dart segments (*viz.*, Cells #1 through #6), the *average* mass of DU partitioning to soil and water, referenced to the original mass of penetrator dart, is only on the order of approximately 0.26 percent after about 1.3-y of accelerated leaching (Table 14). Of this mass of DU "lost "from the dart specimen, about 98 percent is retained in the near-field soil, and about 2 percent is leached into the collected water (aqueous fraction).

Table 14. Partitioning of DU to Retained Soil and Eluted Aqueous Phases After 23 Cycles of Accelerated Leaching

MCL ID	Soil Type	Description	Penetrator	Original Mass Penetrator (g)	End of Test: Mass Balance for U Loss			
					Uranium Inventory (g)			Total % Mass Loss
					Aqueous	Soil	Total	
13-1663	PAC	Cell #1 Soil	Scraped	701.8	0.05	1.71	1.75	0.25%
13-1664	PAC	Cell #2 Soil	Unscraped	623.5	0.04	0.73	0.77	0.12%
13-1665	PCR	Cell #3 Soil	Scraped	577.1	0.04	1.43	1.47	0.26%
13-1666	PCR	Cell #4 Soil	Unscraped	620.2	0.04	1.49	1.54	0.25%
13-1667	PGR	Cell #5 Soil	Scraped	583.1	0.03	1.60	1.63	0.28%
13-1668	PGR	Cell #6 Soil	Unscraped	526.4	0.02	2.25	2.27	0.43%
13-1669	PAC	Cell #7 Soil	N/A	N/A	0.000	0.001	0.00	N/A
Average for Cells #1 through #6				605.4	0.04	1.54	1.57	0.26%

Notes: % - percent
g – gram(s)
ID – identification
MCL – Materials and Chemistry Laboratory, Inc.
mg/Kg – milligram(s) per kilogram
Mn - manganese
N/A – not applicable
PAC – soil type Avonsburg/Cobbsfork
PCR –soil type Cincinnati/Rossmoyne
PGR – soil type Grayford/Ryker
U – uranium

9. REVISED CORROSION RATE ESTIMATES

In the interim report for this project (Bostick et al., 2011), we estimated a release rate for DU partitioning to the aqueous eluate. With the data from Table 14, these estimates can be revised to reflect the DU partitioning to both residual soil and aqueous eluate.

Data for nominal metal corrosion rate is typically normalized to the substrate surface area, and expressed in units such as g cm^{-2} y^{-1} (Handley-Sidhu et al., 2010; Hilton, 2000) (Equation A3-2).

$$\textbf{Corrosion Rate } (\text{g cm}^{-2}\text{y}^{-1}) = \frac{\textbf{365 x Weight loss (g)}}{\textbf{Metal Surface Area (cm}^2\textbf{) x Time (days)}} \qquad (1)$$

Nominal geometric surface areas for the penetrator dart segment used are presented in interim report Bostick et al., Appendix A3. These estimated are used for the computations presented in Table 15.

Table 15. Esimates for DU Corrosion Rate Under Accelerated Leaching (Real Time Leach Duration is 1.3-y)

Cell Number	Original dart mass (g)	Penetrator Dart Preparation	Nominal Dart Surface Area (cm^2) *	Aqueous Eluent		Total (Soil + Aqueous)	
				g-U lost	Rate g $cm^{-2}y^{-1}$ **	g-U lost	Rate g-$cm^{-2}y^{-1}$ **
1	701.8	Scraped	80.18	0.05	4.64E-04	1.75	1.72E-02
2	623.5	Unscraped	72.35	0.04	4.33E-04	0.77	8.44E-03
3	557.1	Scraped	65.71	0.04	5.38E-04	1.47	1.77E-02
4	620.2	Unscraped	72.02	0.04	4.74E-04	1.54	1.68E-02
5	583.1	Scraped	68.31	0.03	3.03E-04	1.63	1.88E-02
6	526.4	Unscraped	62.64	0.02	2.73E-04	2.27	2.85E-02

Notes: * From Bostick et al (2011), Appendix, Table A3-1. (Nominal geometric surface area)
** Computed using equation (1).
cm^2 – centimeter squared
g $cm^{-2}y^{-1}$ – gram(s) per centimeter squared year
g – gram(s)
g-U – gram(s) uranium

From Table 15, the *nominal* average corrosion rate for DU penetrator dart segment, accounting for loss to residual soil and aqueous eluate, is approximately (1.8 ± 0.6)E-2 g-$cm^{-2}y^{-1}$. This estimate was computed using conservative estimates for the dart surface area and for the elapsed exposure time (i.e., accelerated leaching vs. field conditions).

In a recent review, Handley-Sidhu et al. (2010) compiled estimates for the corrosion rates of DU-titanium (Ti) alloy; their summary table is reproduced below as Table 16. In general, for DU weathered under non-marine geological conditions, reported corrosion rates ranged from approximately 0.01 g-$cm^{-2}y^{-1}$ (for waterlogged soil) to 0.8 g-$cm^{-2}y^{-1}$ (for organic clay-rich soil). Our crude estimates for DU corrosion in soils exposed to oxic wet/dry accelerated leach conditions (approximately 0.02 g $cm^{-2}y^{-1}$) is toward the lower end of this literature range.

Table 16. Corrosion Rates of DU-Ti alloy, as Compiled by Handley-Sidhu et al. (2010).

Study	Environment	Geochemical Conditions	Rate ($g\ cm^{-2}y^{-1}$)	Comments	References
1	Air	Oxic	0.0012	Laboratory air (30 days)	Trzaskoma (1982)
2	H_2O	Oxic	0.072	Distilled water	Trzaskoma (1982)
3	3.5% NaCl	Oxic	0.40		Trzaskoma (1982)
4	5% NaCl	Oxic	1.5		McIntyre et al. (1988)
5	Seawater, Solway Firth	Oxic	2.6-3.1	In situ biogeochemical conditions and the level of physical disturbance were uncharacterised.	Toque and Baker (2007)
6	Marine sediment, Solway Firth	Not characterized	1.4-1.8	In situ biogeochemical conditions and the level of physical disturbance were uncharacterised.	Toque and Baker (2007)
7	Marine sediment microcosums simulating the Solway Firth	Progressively anoxic	0.056 ± 0.006	Salinities of 31.5 and 16.5; pH 6.4–8.0; 3.2% OC; CEC 4.0 meq/100 g and inorganic carbon 370 mg kg−1	Handley-Sidhu et al. (2009b)
8	Waterlogged sand (salinities of 31.5)	Nitrate-reducing	0.020 ± 0.003	(Salinity of 31.5; pH 7.6–7.9; 0.8% OC; CEC 1.3 meq/100 g and inorganic carbon 430 mg kg−1	Handley-Sidhu (2008)
9	Dune sand Eskmeals, Cumbria	Not characterized	0.080-0.17	pH 6.5–7.9	Toque and Baker (2006)
10	Dune sand simulating Eskmeals, Cumbria	Oxic	0.10 ± 0.01	pH 7.2–7.5; 0.8% OC; CEC 1.3 meq/100 g; inorganic carbon 430 mg kg−1 and sand moisture content of 13%	Handley-Sidhu et al (2009a)
11	Organic, clay-rich soil from Kirkcudbright	Not characterized	0.80-1.1	pH 5.8–6.0	Toque and Backer (2006)
12	Field-moist soil	Oxic	0.49 ± 0.06	pH 5.0–6.5; 12% OC; CEC 21 meq/100 g; inorganic carbon 80 mg kg−1 and soil moisture content of 22%	Handley-Sidhu et al (2009c)
13	Sandy-loamy and silty-loamy soil	Not characterized	0.19 ± 0.03	Two soils investigated; pH 5.6 and 5.7; 2.1% OC.	Schimmack et al. (2007)
14	Waterlogged soil	Nitrate-reducing	0.010-0.02*	pH 5.0 – 6.5; 12% OC; CEC 21 meq/100 g and inorganic carbon 80 mg kg^{-1}. *Corrosion ceased under anoxic conditions.	Handley-Sidhu et al (2009c)
15	Phosphate-fertilized waterlogged soil	Nitrate-reducing	0.00016-0.0044	Olsen phosphorus 27 – 45 mg kg^{-1}; pH 5.0 – 6.0; 12% OC; CEC 21 meq/100 g and inorganic carbon 80 mg kg^{-1}.	Unpublished;

Notes:
* Corrosion ceased under anoxic conditions.
% – percent
CEC – cation exchange capacity
DU – depleted uranium
g $cm^{-2}y^{-1}$ – gram(s) per centimeters squared year
H_2O – water
meq – milliequivalent of hydrogen
mg kg-1 – milligram(s) per kilogram
NaCl – sodium chloride
OC – organic carbon
Ti – titanium

10. REFERENCES

AEPI, *Health and Environmental Consequences of Depleted Uranium Use in the U.S. Army,* technical report, Atlanta, Ga.: U.S. Army Environmental Policy Institute, June 1995.

Al-Saad, K.A.; M. A. Amr; A. Ismail and A. I. Helal, "Determination of depleted uranium in the presence of natural uranium in environmental soil samples by ICPMS after sequential extraction," *Journal of Environmental Chemistry and Ecotoxicology Vol. 2(4)*, pp. 60-66, May 2010 (Viewable at URL: http://www.academicjournals.org/jece/pdf/pdf2010/May/Al-Saad%20et%20al.pdf).

ANSI/ASQC E4-1994, *Specifications and Guidelines for Quality Systems for Environmental Data Collection and Environmental Technology Programs.*

ASME NQA-1-2000, Edition, *Quality Assurance Program Requirements for Nuclear Facilities,* Level 1.

ASTM, Method D2216, "Standard Test Method for Laboratory Determination of Water (Moisture Content of Soil and Rock by Mass."

ASTM, Method D422-63, "Standard Test Method for Particle-Size Analysis of Soils."

ASTM D4972-01, "Standard Test Method for pH of Soils" (http://www.astm.org/Standards/D4972.htm)

ASTM, Method D5744, "Accelerated Weathering of Solid materials Using a Modified Humidity Cell."

Barnett, M. O., Jardine, P. M., & Brooks, S. C. (2002). "U (VI) adsorption to heterogeneous subsurface media: Application of a surface complexation model." *Environ. Sci. Technol.*, 36(5), 937-942.

Bostick, W.D., G.J. Wagner, R.J. Stevenson, E.B. Mundy, *Estimation of Site-Specific Penetrator Weathering Rate and DU Migration for Jefferson Proving Ground Site*, MCLinc Report EMP002105, April 2011.

Chen, J.P., and S. Yiacoumi (2002), *Modeling of Depleted Uranium Transport in Subsurface Systems. Water, Air, & Soil Pollution, Volume 140*, Numbers 1-4 / October, 2002.

Del Nero, M., et al. (1999), "Sorption/Desorption Processes of Uranium in Clayey Samples of the Bangombe Natural Reactor Zone, Gabon," *Radiochim. Acta*, 87, 135-149.

Farrell (1999), W.D. Bostick, R.J. Jarabek, and J.N. Fiedor, "Effects of Water Chemistry on Uranium Removal from Groundwater using Zero Valent Iron Media," *Ground Water, 37(4)*, 618 (1999).

Handley-Sidhu S, Keith-Roach MJ, Lloyd JR, Vaughan DJ (2010), "A review of the environmental corrosion, fate and bioavailability of munitions grade depleted uranium," *Sci Total Environ 408(23):5690-700.*

Hilton, B.A., 2000, *Review of Oxidation Rates of DOE Spent Nuclear Fuel Part 1: Metallic Fuel,* ANL-00/24, Argonne National Laboratory, Idaho Falls, ID. (Viewable at: http://www.osti.gov/bridge/product.biblio.jsp?osti_id=775264).

Hlavay, J.; Prohaska, T.; Weisz, M.; Wenzel, W.W.; Stingeder, G.J. (2004). "Determination of Trace Elements Bound to Soils and Sediment Fractions," *Pure Appl. Chem.*, **76**(2), 415-442.

ISO/IEC 17025, *General Requirements for the Competence of Testing and Calibrations Laboratories*, 2005..

Jang, J-E, B.A. Dempsey & W.D. Burgos (2006), "Solubility of schoepite: comparison and selection of complexation constants for U(VI)," *Water Research* **40** 2738-2746.

Krupka, K.M.; Serne, R.J. (2002), *Geochemical Factors Affecting the Behavior of Antimony, Cobalt, Europium, Technetium, and Uranium in Vadose Sediments*, Report PNNL-14126. (Viewable at URL: http://www.pnl.gov/main/publications/external/technical_reports/PNNL-14126.pdf).

McLean, E.O. (1982), "Soil pH and Lime Requirement," Chapter 12 in A.L. Page (Editor), *Methods of Soil Analysis, Part 2: Chemical and Microbial Properties*, 2nd Ed., American Soc. Agronomy, Inc.

MCLinc, *Quality Assurance Plan*, MCL-7701

MCLinc, *Electron Microscopy Operation Guide*, MCL-7708.

MCLinc, *Acid Digestion for Metals Based on EPA Method 3050B*, MCL-7746.

MCLinc, *Inductively Coupled Plasma – Atomic Emission Spectrometry Metals Analysis*, MCL-7751.

MCLinc, *Acid Digestion of Aqueous Samples (EPA Method 3010A)*, MCL-7752.

MCLinc, *Modified Tessier Sequential Extraction Procedure for 2.5-g Soil or Sediment Sample*, MCL-7756, Appendix XX.

MCLinc, *Operator Aid for Determination of Water Content by Mass*, Operator Aid MCL-7756, Appendix MM.

MCLinc, *ICP-MS Element/Metal Sample Preparation and Analysis (Based upon EPA Method 6020A and EPA ORD Method 200.8)*, MCL-7768.

MCLinc, *Determination of Isotopic Ratios by ICP-MS.*, MCL-7769

Manaka, M.; Y. Seki, K. Okuzawa, H. Kamioka and Y Watanabe, (2007), "Natural attenuation of dissolved uranium within a small stream of central Japan," *Limnology*, Volume 8, Number 2, 143-153

Murakami, T. , Ohnuki, T., Isobe, H., Sato, T.: "Mobility of uranium during weathering," *American Mineralogist 82*, 888-899 (1997).

"National Environmental Laboratory Accreditation Conference Standards," Latest Approved Edition.

Oliver, I.W.; A.B. Mackenzie; R.M. Ellam; M.C. Graham and J.G. Farmer, "Determining the extent of depleted uranium contamination in soils at a weapons test site: An isotopic investigation," *Geochimica et Cosmochimica Acta*, Volume 70, Issue 18, Supplement 1, August-September 2006, Page A457.

Oliver, I.W.,, M. C. Graham, A. B. MacKenzie, R. M. Ellam and J. G. Farmer, "Distribution and partitioning of depleted uranium (DU) in soils at weapons test ranges – Investigations combining the BCR extraction scheme and isotopic analysis," *Chemosphere*, Volume 72, Issue 6, June 2008, Pages 932-939.

Payne, T.E.; P.L. Airey (2006), "Radionuclide migration at the Koongarra uranium deposit, Northern Australia – Lessons from the Alligator Rivers analogue project," *Physics and Chemistry of the Earth*, Parts A/B/C, Volume 31, Issues 10-14, 2006, Pages 572-586.

Payne, T.E.; Waite, T.D. (1991), "Surface Complexation Modeling of Uranium Sorption Data Obtained by Isotope Exchange Techniques," *Radiochim. Acta*, **52/53**, 487-493.

Phillips, I.; Chapple, L. (1995), "Assessment of a Heavy Metals-Contaminated Site Using Sequential Extraction, TCLP, and Risk Assessment Techniques," *J. Soil Contam.*, **4**, 311-325.

Radenković, R., D. Djordjević, J. Joksić, S. Djogo, P.Pfendt, and J. Raičević, "Uranium Mobility in Soils Contaminated with Depleted Uranium," *CEJOEM 2003*, Vol.9. No.4.: 327–331

SAIC (2007), Well Location Selection Report. "Depleted Uranium Impact Area Site Characterization: Soil Verification, Surface Water Gauge Installation, Fracture Trace Analysis, and Electrical Imaging Jefferson Proving Ground, Madison, Indiana," (NRC Staff Exh. 26; Viewable at URL: http://pbadupws.nrc.gov/docs/ML0731/ML073100034.pdf).

Silva, R. J., and H. Nitsche (1995), "Actinide Environmental Chemistry," *Radiochim. Acta*, 70/71, 377 .

Tessier, A., PG; C. Campbell; M. Bisson; "Sequential extraction procedure for the speciation of particulate trace metals," *Anal. Chem.*, **1979**, *51* (7), pp 844–851.

10 CFR 40.4,Title 10, Code of Federal Regulations (CFR), Chapter I – Energy, Part 40, Section 40.4, "Definitions."

10 CFR 830.120, Title 10, Code of Federal Regulations (CFR), Chapter I – Energy, Part, 830, Section 830.120, "Nuclear Safety Management, Quality Assurance Requirements, Scope."

U.S. Department of Energy, *Consolidated Audit Program Quality Systems for Analytical Services Revision 2.9,* May, 2013.

USEPA, Acid Digestion of Sediments, Sludges, and Soils, SW-846, Method 3050B

USEPA, Microwave Assisted Acid Digestion of Sediments, Sludges, Soils, and Oils, SW-846,Method 3051A.

USEPA, Total Organic Carbon (TOC) in Soil, SW-846 Method 9060

APPENDIX 1. SOIL SAMPLE PROVENANCE

Soil specimens were held at the MCLinc facility for a long time duration, which encompassed delays in notice to proceed with different phases of the investigation and also the duration of active testing that was performed. Since soil storage conditions (including oxygen fugacity) may affect the activity of native microbial populations, we summarize these conditions in Table A-1.

Table A- 1. Soil Sample Provenance

Date	Action	Comment
10/22/2008	Field sampling event (SAIC COC JPG001-MCL)	Samples shipped with water ice (0 °C)
10/23/2008	Receipt of bulk soil samples at MCLinc	Samples refrigerated (6 °C)
5/28/2009	Initial notice to proceed from client	Samples refrigerated (6 °C)
6/26/2009	Begin leach interval #1 (21-d cycle) *	Ambient (23 °C) temperature
10/06/2010	Collect final leach interval #23	Total leach test duration 480-d
6/08/2012	Remove soil from leach chambers and refrigerate soil cores	Prior static ambient (23 °C) storage 611-d.
6/26/2013	Remove refrigerated soil cores for additional analysis	Refrigerated (2 °C) storage 385-d
7/08/2013	Begin SE	

Notes:

* Soil samples were stored refrigerated (approximately 6 °C) until shortly before the preparation of soil columns for use in accelerated leach testing.
°C – degrees Celcius
COC – Chain of Custody
d - day(s)
MCL or MCLinc – Materials and Chemistry Laboratory, Inc.
SE – sequential extraction

Note that the soil cores were stored in the test chambers at ambient laboratory temperature for approximately 611-d between the completion of leach interval #23 (10/06/2010) and the date (6/08/2012) that the soils were removed from the test chamber, bagged and refrigerated (6 °C) for possible indefinite storage. During the interval of static ambient storage, the soil was maintained moist and there was some communication with ambient air (Figure A-1). The ambient-stored soil cores maintained biological activity, as evinced by the flora illustrated in Figures A-1 and A-2.

Figure A- 1. Soil test cells photographed April 26, 2011 (during static ambient storage).

Flora (algae) appear to have been established in the control and other cells. Note that the cells, containing drained soil, communicate with the ambient atmosphere via severed ¼-in tubing, and that there is water condensate present in the chamber. Storage conditions thus likely approximate that of soil in the drained, near-surface vadose zone.

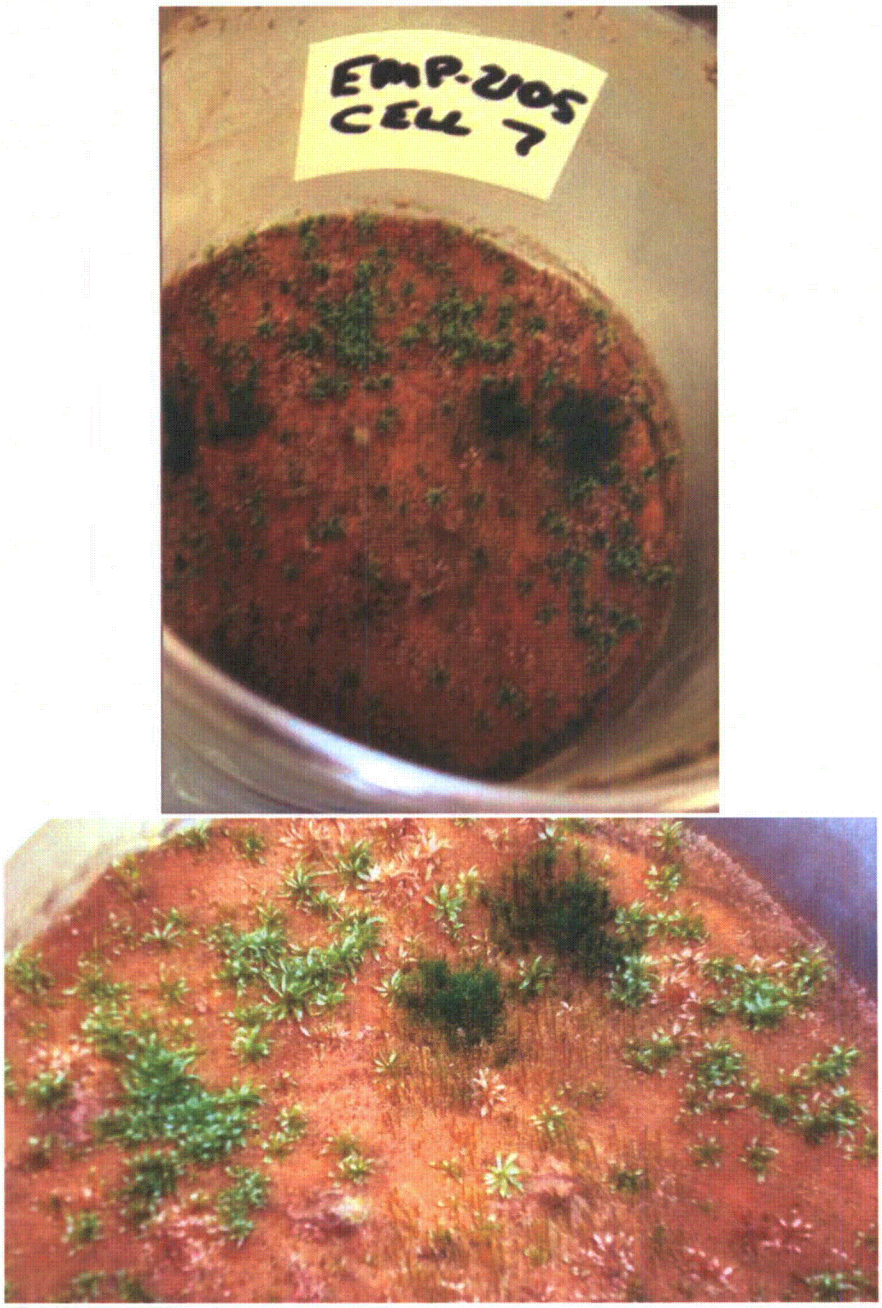

Figure A- 2. Cell #7 soil core (Type PAC, control), photographed after static ambient storage 611-d.

Flora has been established at the surface of the control cell and also in several of the test specimens (notably in Soil type PAC, Cells #1 and 2).

APPENDIX 2. MCLINC PROCEDURE FOR MODIFIED TESSIER SEQUENTIAL EXTRACTION PROCEDURE

(Uncontrolled copy of MCLinc, Modified Tessier Sequential Extraction Procedure for 2.5-g Soil or Sediment Sample, MCL-7756, Appendix XX)

Code: MCL-7756
OPERATOR AIDS
Appendix XX
Effective: 12/10/2010

APPENDIX XX

MODIFIED TESSIER SEQUENTIAL EXTRACTION PROCEDURE FOR 2.5 GRAMS OF SOIL OR SEDIMENT SAMPLE

1. PURPOSE

The practical technique of choice for evaluating low-level radionuclide partitioning in soils and sediments is the sequential extraction approach.[1] This methodology applies to operationally-defined chemical treatments to selectively dissolve specific classes of macro-scale soil or sediment components. There is no general agreement on the solutions preferred for the extraction of various components in sediment or soils, due mostly to the matrix effects involved in heterogeneous chemical processes. The protocol below is based on the original method of Tessier et al. (1979), with minor modifications reflecting more recent literature evaluations.

2. SAMPLE RECEIPT AND PREPARATION

It is recommended that soil core samples be shipped overnight to Materials and Chemistry Laboratory, Inc. (MCLinc), packed with water ice to maintain the temperature at approximately 0 to 4 degrees Celcius (°C) to minimize potential constituent changes due to microbial activity. If analysis cannot be initiated on the day of receipt, core samples will be placed in a deep freeze and maintained at approximately -20 °C until testing can be performed (see, e.g., Hlavay et al., 2004). Unless specific contractual arrangements have been negotiated with the client, sample after thawing will not be excluded from exposure to the ambient atmosphere during sample processing; strict air-exclusion may minimize confounding sulfide-bound metals with their oxide-bound counterparts and may help preserve in-situ redox conditions for anoxic sediments (Rapin et al., 1986; Peltier, 2005). If air-exclusion is specified and commissioned by the client, then sample preparation and extraction must be performed in an oxygen-free environment (e.g., within a specially maintained anoxic glove box).

Sample size is dictated by the apparent sample homogeneity. If relatively large pebbles are first removed (e.g., with use of a #10 mesh standard screen, to remove particles greater than two millimeters in diameter), a sample size of approximately 2.5 grams (g) (dry weight equivalent) of blended soil may be used. (Record actual mass taken). If wet soil is used, the moisture content must be estimated with use of a separate sample, to permit interpretation of results expressed on a dry-weight basis.

The lack of suitable certified reference materials for use with this procedure has precluded intra-laboratory comparability of results and hence good quality control (QC). QC is thus the usual controls on analytical accuracy.

3. ACRONYMS

°C	degrees Celcius
cc	cubic centimeter(s)
$CaCO_3$	calcite

UNCONTROLLED
INFORMATIONAL USE ONLY

[1] http://physics.nist.gov/Divisions/Div846/Gp4/Environ/speciation.html

CBD reagent	citrate-bicarbonate-dithionite
CH_3COOH	acetic acid or acetate
CH_3COONa	sodium acetate
CO_2	carbon dioxide
EPA	U.S. Environmental Protection Agency
Fe	iron
FW	formula weight
g	gram(s)
h	hour(s)
H_2O	water (de-ionized)
H_2O_2	hydrogen peroxide
HCl	hydrochloric acid
HNO_3	nitric acid
ICP	inductively coupled plasma spectroscopy
L	liter(s)
MCLinc	Materials and Chemistry Laboratory, Inc.
min	minute(s)
µg/g	microgram(s) per gram
mg/Kg	milligram(s) per kilogram
mL	milliliter(s)
mol/L	mole(s) per liter
$MgCl_2$	magnesium chloride
NaOH	sodium hydroxide
$NH_4C_2H_3O_2$	ammonium acetate
NIOSH	National Institute for Occupational Safety and Health
OES	optical emission spectrometry
QC	quality control
RPM	revolutions per minute
TCLP	Toxicity Characteristic Leaching Procedure
U	uranium
V	volume
v/v	volume per volume

UNCONTROLLED
INFORMATIONAL USE ONLY

4. FRACTION 1: EXCHANGEABLE CATIONS (MAGNESIUM CHLORIDE, pH 7)

Short-term (e.g., 1 hour [h]) equilibration of soil with a near-neutral solution containing a relatively high concentration (e.g., 1 mole per liter [mol/L]) of electrolyte dissolves water-soluble salts and liberates readily exchangeable cations (by ion displacement). For the extraction of trace contaminants, Phillips and Chapple (1995) and also Tessier et al. (1979) favor use of a solution of 1 mol/L magnesium chloride ($MgCl_2$) (pH 7).

4.1. Extraction:

Reagent 1: For about 250 milliliters (mL) lixivant (extraction reagent), add 50.8-g $MgCl_2 \cdot 6H_2O$ (formula weight [FW] = 203.3) to approximately 200-mL de-ionized water; adjust pH value to approximately 7.0 with the use of dilute sodium hydroxide (NaOH) or hydrochloric acid (HCl) solution, then adjust to final volume (approximately 250-mL).

UNCONTROLLED
INFORMATIONAL USE ONLY

Dry soil, 2.5-g, is contacted with 20-mL of 1 mol/L $MgCl_2$ (pH 7) in a sealed 50 cubic centimeter (cc) centrifuge cone for 1-h at ambient temperature. (Optimum contact is provided by tumbling the sealed vial on a Toxicity Characteristic Leaching Procedure [TCLP] rotary extractor unit). Slurry is subsequently centrifuged at 4000 revolutions per minute (RPM) for 12 minutes (min) and then the supernate is taken to a labeled 50-mL volumetric flask. Solid residue is rinsed in another 10-mL aliquot of lixivant, and then clarified by centrifugation. The supernate is added to the labeled volumetric flask, and the contents diluted to final volume by addition of demineralized (de-ionized) water (H_2O).

5. FRACTION 2: CARBONATE-BOUND METALS (ACETATE REAGENT, pH 8.2)

Following the extraction of exchangeable cations, many researchers, including Phillips and Chapple (1995), have included an extraction using 6-h contact with slightly acidic 1 mol/L sodium acetate (CH_3COONa) (pH 5). This step is said to liberate the trace metal ions co-precipitated or otherwise occluded in calcite ($CaCO_3$) sediment deposits. Tessier et al (1979) prefer a variant reagent, in which the pH of the acetate solution is adjusted to 8.2; attack on silicate and sulfide minerals is said to be minimal with use of this reagent.

5.1. Extraction:

Reagent 2: For approximately 250-mL reagent, add about 15-g reagent grade acetic acid (CH_3COOH) to approximately 200-mL de-mineralized water. Adjust pH value to 8.2 by the gradual addition of NaOH, then add de-mineralized water to a final volume of 250-mL.

To the wet solid residue from Fraction 1, add 20-mL of 1 mol/L CH_3COONa (pH adjusted to a value of 8.2). Contact for 6-h at ambient temperature. The supernate is added to the labeled volumetric flask. Sample may be washed by the addition of another 10-mL aliquot of reagent, briefly re-suspending the solids, followed by centrifugation. Supernate is again added to the labeled volumetric flask and contents diluted to final volume by addition of demineralized water.

6. FRACTION 3: METALS ASSOCIATED WITH HYDROUS IRON AND MANGANESE OXIDES (HYDROXYLAMINE-ACETATE REAGENT)

(Hydroxylamine-Acetate Reagent)

Methods for leaching iron and manganese oxides involve a combination of reagents to reduce these metals to soluble Fe^{+2} and Mn^{+2} forms, respectively, and to keep these forms in solution at relatively high concentrations. The reagent preferred by Tessier et al. (1979) consists of 0.04 mol/L $NH_4OH{\cdot}HCl$ in 25 percent (volume per volume [v/v]) (CH_3COOH [pH 2]). The extraction of reducible iron and manganese oxides is said to be complete when soil is contacted with the reagent at 96 ± 3 °C for about 6-h with occasional agitation. The hydroxylamine reagent is said to be more effective than citrate-bicarbonate-dithionite (CBD reagent) for the dissolution of metal sulfide phases (Tessier et al., 1979).

6.1. Extraction: To the residue from Fraction 2, add 20-mL of 0.04 mol/L $NH_4OH{\cdot}HCl$ (FW = 71.5) in 25 percent (v/v) acetic acid (pH 2).

Reagent 3: For approximately 250-mL reagent: to approximately 150-mL of de-ionized water add 62.5-mL (65.5-g) metals-grade CH_3COOH, and then 0.715-g $NH_4OH{\cdot}HCl$. Mix well and

UNCONTROLLED
INFORMATIONAL USE ONLY

check pH value; adjust to pH 2 (if necessary) with use of dilute NaOH or HCl solution. Dilute to final volume (250-mL) with de-ionized water.

To the residue from Fraction 2, add 20-mL of 0.04 mol/L NH_4OH•HCl (FW = 71.5) in 25 percent (v/v) acetic acid (pH 2). *Caution*: for samples containing large amounts of carbonate minerals, carbon dioxide (CO_2) gas evolution may be excessive, causing bubbling and possible spewing (with loss of sample). If vigorous bubbling is observed upon initial addition of reagent, allow several minutes for degassing in an uncapped vessel before applying heat. The centrifuge cone is then capped loosely and the soil is contacted with the reagent by placing the cone and contents in a water bath (or dry heating bock) maintained at 96 ± 3 °C for about 6-h, with occasional agitation of the bottle and contents. After equilibration, the sample is centrifuged and the supernate is added to the labeled volumetric flask. Sample may be washed by the addition of another 10-mL aliquot of reagent, briefly re-suspending the solids, followed by centrifugation. Supernate is again added to the labeled volumetric flask and the contents diluted to final volume by addition of de-ionized water.

7. FRACTION 4: BOUND TO ORGANIC MATTER

Trace metals may be bound to various forms of organic matter: natural organic matter (notably humic and fulvic acids), microbes, detritus, coatings on mineral particles, etc. (Tessier et al., 1979). Phillips and Chapple (1995) treat the residue from Fraction 3 (above) with dilute (0.02 mol/L) nitric acid (HNO_3) with added hydrogen peroxide (H_2O_2) solution, heating the mixture to approximately 85°C for a total of 6-h.

7.1. Extraction:

Reagent 4A: Approximately 250-mL of lixivant is prepared by the addition of 100-mL of 0.02 mol/L HNO_3 to 150-mL of 30 percent H_2O_2. (Add dilute acid to the peroxide until the mixture pH value is adjusted to 2).

Reagent 4B: Acidic ammonium acetate solution is prepared as 3.2 mol/L (247 grams per liter [g/L]) ammonium acetate ($NH_4C_2H_3O_2$) in 20 percent (v/v) HNO_3.

The solid residue from Fraction 3 is extracted with 20-mL of acid peroxide solution (Reagent 4A). The solids are re-suspended in this solution, and the slurry heated to 85 ± 2 °C for 2-h with occasional shaking. Heating is continued for a total of 5-h, with additional increments of reagent added periodically as required to maintain slurry volume. The container and contents are allowed to cool to room temperature. Next, add 20-mL of acidic ammonium acetate solution (Reagent 4B), and shake the bottle and contents continuously for 0.5-h at room temperature. Centrifuge and collect the supernate into a labeled 50-mL volumetric flask. Sample may be washed by the addition of another 10-mL aliquot of ammonium acetate reagent (Reagent 4B), briefly re-suspending the solids, followed by centrifugation. Supernate is again added to the labeled volumetric flask and contents diluted to final volume by addition of demineralized water.

8. RESIDUAL FRACTION

Because the residual fraction is not considered to be available for release to the environment except on a geological time scale, it may not be necessary to quantitate this fraction unless the data is needed for mass balance closure. Total digestion is relatively difficult and expensive, and seldom used in environmental analysis. More commonly used strong, acid-based extractions such as U.S. Environmental Protection Agency (EPA) Method 3050B,"Acid Digestion of Sediments,

UNCONTROLLED
INFORMATIONAL USE ONLY
Code: MCL-7756
OPERATOR AIDS
Appendix XX
Effective: 12/10/2010

Sludges, and Soils," and Method 3051A, "Microwave Assisted Acid Digestion of Sediments, Sludges, Soils, and Oils," generally recover most of the available heavy metal content, but they cannot recover metals locked within a refractory silicate matrix. The proportion of residual metal may also be roughly estimated by mass balance, if an estimate of total constituent analysis is available for the original material. Optionally (as a QC check), the residue from Fraction 5 (above) can be extracted by the same methodology used to estimate the original soil constituent or contaminant inventory; this would thus represent a direct estimate of the residual fraction.

8.1. Extraction (As Total Environmentally Available Constituent)

A separate aliquot sample of test material is extracted with use of MCLinc standard operating procedure MCL-7746, "Acid Digestion for Metals," (based on EPA preparative Method 3050B as defined in SW-846). This estimate for each constituent of interest will represent the total environmentally available constituent. The results for metals analysis for each of the previous sequential extractions may be compared to the available inventory, computing a percentage extracted. Mass balance closure (original inventory less constituent extracted by Fractions 1 through 4) represents an indirect estimate of the residual fraction.

9. ANALYTICAL PROCEDURES

Analysis by inductively coupled plasma spectroscopy (ICP) may require digestion to destroy excess organic reagent (e.g., acetate [CH_3COOH]) and/or substantial dilution of the sample prior to analysis. Analysis will be for select dissolved metals (e.g., uranium [U] and iron [Fe], etc.) by ICP (with detection by optical emission spectroscopy, ICP-OES, MCL-7751, "Inductively Coupled Plasma-Atomic Emission Spectrometry [EPA Method 6010B]," or mass spectroscopy, ICP-MS, MCL-7768, "Inductively Coupled Plasma – Mass Spectrometry Element/Metals Sample Preparation and Analysis"), with appropriate analytical quality assurance (e.g., MCL-7751, based upon National Institute for Occupational Safety and Health [NIOSH] Method 7300, "Elements by ICP [Nitric/Perchloric Acid Ashing]," and EPA SW-846 Method 6010B). Due to the very high salt and organic acid concentrations in many lixiviates used, sample digestion (MCL-7752, "Acid Digesion of Aqueous Samples [EPA Method 3010A]," based on EPA SW-846 Method 3010A, "Acid Digestion of Aqueous Samples and Extracts for Total Metals for Analysis by FLAA or ICP Spectroscopy") and extensive dilution will be required prior to ICP analysis. This high salt content of the digested spent lixivant limits the sensitivity for trace elements (e.g., for U in soil, the reporting limit by ICP-OES will be 0.4 micrograms per gram [µg/g] for each of the extraction steps).

10. CALCULATIONS

The total mass of selected constituent extracted by each sequential leaching procedure is referenced to the original sample mass (Step 1), and is reported in units of milligrams per kilogram (mg/kg) or µg/g.

Constituent (µg/g) = (concentration, µg/L)*(Volume [V] in liters [L])/(original dry sample weight, g)

Concentration (µg/L) in the original extraction lixivant (corrected for any dilution factors required for analysis) is estimated by the ICP instrumentation. By the procedure above, V = 50-mL = 0.05-L.

UNCONTROLLED
INFORMATIONAL USE ONLY

11. REFERENCES

Hlavay, J.; Prohaska, T.; Weisz, M.; Wenzel, W.W.; Stingeder, G.J. (2004). "Determination of Trace Elements Bound to Soils and Sediment Fractions," *Pure Appl. Chem.*, 76(2), 415-442.

MCL-7746, "Acid Digestion for Metals Based on EPA Method 3050B."

MCL-7751, "Inductively Coupled Plasma – Atomic Emission Spectroscopy Metals Analysis."

MCL-7752, "Acid Digestion of Aqueous Samples (EPA Method 3010A)."

MCL-7768, "Inductively Coupled Plasma – Mass Spectrometry Element/Metals Sample Preparation and Analysis."

National Institute for Occupational Safety and Health (NIOSH), NIOSH Manual of Analytical Methods (NMAM), Method 7300: Elements by ICP (Nitric/Perchloric Acid Ashing), Fourth Edition, Issue 3, March 15, 2003.

Peltier, E.; Dahl, A.L.; Gaillard, J.-F. (2005), "Metal Speciation in Anoxic Sediments: When Sulfides can be Construed as Oxides," *Environ. Sci. Technol.*, 39, 311-316.

Phillips, I.; Chapple, L. (1995), "Assessment of a Heavy Metals-Contaminated Site Using Sequential Extraction, TCLP, and Risk Assessment Techniques," *J. Soil Contam.*, 4, 311-325.

Rapin, F.; Tessier, A.; Campbell, P.G.C.; Carignan, R. (1986), "Potential artifacts in the determination of metal partitioning in sediments by a sequential extraction procedure," *Environ. Sci. Technol.*; 20(8), 836-840.

Tessier, A.; Campbell, P.G.C.; Bisson, M. (1979), "Sequential Extraction Procedure for the Speciation of Particulate Trace Metals," *Anal. Chem.*, 51, 844-851.

U.S. Environmental Protection Agency (EPA), "Test Methods for Evaluating Solid Waste, Physical/Chemical Methods," SW-846, Method 3050B: Acid Digestion of Sediments, Sludges, and Soils, latest edition.

U.S. Environmental Protection Agency (EPA), "Test Methods for Evaluating Solid Waste, Physical/Chemical Methods," SW-846, Method 3051A: Microwave Assisted Acid Digestion of Sediments, Sludges, Soils, and Oils, latest edition.

U.S. Environmental Protection Agency (EPA), "Test Methods for Evaluating Solid Waste, Physical/Chemical Methods," SW-846, Method 6010B: Inductively Coupled Plasma-Atomic Emission Spectrometry, latest edition.